

The role of polyadenylation in the induction of inflammatory genes

Raj Gandhi BSc & ARCS

Thesis submitted for the degree of Doctor of Philosophy

September 2016

Declaration

Except where acknowledged in the text, I declare that this thesis is my own work and is based on research that was undertaken by me in the School of Pharmacy, Faculty of Science, The University of Nottingham.

Acknowledgements

First and foremost, I give thanks to my primary supervisor Dr. Cornelia de Moor. She supported me at every step, always made time for me whenever I needed it, and was sympathetic during times of difficulty. I feel very, very fortunate to have been her student. I would also like to thank Dr. Catherine Jopling for her advice and Dr. Graeme Thorn for being so patient and giving me so much help in understanding the bioinformatics parts of my project. I am grateful to Dr. Anna Piccinini and Dr. Sadaf Ashraf for filling in huge gaps in my knowledge about inflammation and osteoarthritis, and to Dr. Sunir Malla for help with the TAIL-seq work. I thank Dr. Richa Singhanian and Kathryn Williams for proofreading.

Dr. Hannah Parker was my “big sister” in the lab from my first day, and I am very grateful for all her help and for her friendship. My project was made all the more enjoyable/bearable by the members of the Gene Regulation and RNA Biology group, especially Jialiang Lin, Kathryn Williams, Dr. Richa Singhanian, Aimée Parsons, Dan Smalley, and Hibah Al-Masmoum. Barbara Rampersad was a wonderful technician.

Mike Thomas, James Williamson, Will Hawley, Tom Upton, and Jamie Ware were some of the best of friends I could have hoped to make in Nottingham. Regularly meeting up for board games nights was instrumental in the maintenance of my sanity. I am thankful to Jess Beaver, my personal trainer and friend, through whom I discovered my hobby of fitness and formed goals that gave me a sense of purpose and meaning. Yes, my life is that sad. I give thanks to my girlfriend Janay Gibbons for helping me to keep my head screwed on towards the end when it started loosening.

Lastly, I am grateful to my parents and I thank my beloved siblings Vikram Gandhi, Krishna Gandhi, and Catherine Soskice-Gandhi for their love and support, especially through tough times.

Abstract

Polyadenylation is a universal step in the production of all metazoan mRNAs except histone mRNA. Despite being universal, previous experiments have implicated it in the regulation of inflammation. An inflammatory system using RAW 264.7 murine macrophage cells was established with bacterial lipopolysaccharide (LPS) used as a stimulus. After improving the poly(A) tail test (PAT) method of measuring poly(A) tail lengths, it was applied to inflammatory mRNAs during the inflammatory response. Poly(A) tail length was shown to vary over the course of the inflammatory response, and for *Tnf*, this was even true of initial poly(A) tail size, which is widely believed to be uniform for the majority of mRNAs. The adenosine analogue cordycepin (3'-deoxyadenosine) was shown to have anti-inflammatory effects on mRNA, in line with existing literature, and is likely to be the anti-inflammatory component of *Cordyceps militaris* ethanol extract. Inhibition of either import of cordycepin into cells or phosphorylation of cordycepin was sufficient to abolish its anti-inflammatory effects. Adenosine treatment led to repression of *I1b* mRNA, but did not repress other mRNAs tested that were cordycepin-sensitive. This suggests that cordycepin does not simply act by mimicking the effect of adenosine, and that the two compounds have distinct modes of action. Inhibiting deamination of cordycepin potentiated its effects. We also observed that pre-mRNA levels of inflammatory genes were decreased by cordycepin treatment, indicative of effects on transcription. Other groups have reported that cordycepin interferes with NF- κ B signalling. As NF- κ B is an important transcription factor for the induction of inflammatory genes, this would provide a basis for explaining our observation that cordycepin represses at the transcriptional level. However, we did not observe any changes in NF- κ B signalling, with degradation of I κ B α completely unimpeded by cordycepin treatment. Notably, cordycepin did shorten the *Tnf* poly(A) tail, and the

observed inhibition of polyadenylation is consistent with observations that cordycepin led to decreased efficiencies of mRNA 3' cleavage and transcription termination for *Tnf*. Such effects on polyadenylation and 3' processing of mRNA were hypothesised to particularly affect unstable mRNAs that depend on longer poly(A) tails for avoiding decay and/or mRNAs with a high rate of transcription. However, comparison of microarray data to data from RNA-seq of RNA from 4-thiouridine labelling experiments showed that cordycepin-sensitivity did not correlate with mRNA stability or transcription rate. Long noncoding RNAs (lncRNAs) were found to be enriched in cordycepin-treated cells. If some of those lncRNAs have regulatory roles in inflammation, cordycepin's effects may be mediated through them. Lastly, cordycepin significantly altered pain behaviour in a rat model of osteoarthritis (OA), supporting its continued use as a lead compound for exploration of new OA therapeutics.

Abstract.....	i
List of figures.....	vii
List of tables.....	xi
List of abbreviations.....	xii
1 Introduction	1
1.1 Polyadenylation	2
1.1.1 Mechanics of nuclear polyadenylation.....	2
1.1.2 Control of poly(A) tail length	5
1.1.3 Poly(A) polymerases and other types of polyadenylation.....	8
1.1.3.1 Cytoplasmic polyadenylation.....	10
1.1.3.2 Mitochondrial polyadenylation.....	12
1.1.4 Biological importance and role of the poly(A) tail.....	13
1.1.5 Alternative polyadenylation.....	17
1.1.6 Measuring poly(A) tails	17
1.2 Cordycepin	24
1.2.1 Cordycepin and transcription	24
1.2.2 Cordycepin and mTOR signalling	25
1.2.3 Cordycepin and polyadenylation	27
1.2.3.1 Polyadenylation and cordycepin’s mechanism.....	29
1.3 Inflammation.....	30
1.3.1 Inflammation and pain.....	31
1.3.2 Macrophages	32
1.3.2.1 Macrophage receptors and signalling.....	34
1.3.2.1.1 LPS signalling through TLR4	35
1.3.2.1.1.1 MyD88-dependent pathway.....	36
1.3.2.1.1.2 TRIF-dependent pathway	38
1.3.2.1.2 NF-κB signalling in inflammation	39
1.3.2.1.3 Regulation of inflammatory cytokine mRNA stability	42
1.3.3 Anti-inflammatory effects of cordycepin.....	45
1.4 Osteoarthritis – a therapeutic application of cordycepin?.....	47
1.5 Project aims and outcomes	51
2 Materials and methods.....	53

2.1	Cell work	53
2.1.1	Cell culture	53
2.1.2	Cell stimulation with lipopolysaccharide (LPS) and treatments with compounds	53
2.1.3	Preparation of fungal ethanol extracts for use in cell culture	54
2.1.3.1	Assessing cordycepin and 3' deoxyinosine concentration in fungal extracts by liquid chromatography/mass spectrometry (LC/MS) (performed by Wahyu Utami)	55
2.2	RNA work	56
2.2.1	RNA isolation.....	56
2.2.2	RNA isolation from nuclear and cytoplasmic fractions.....	57
2.2.3	4-thiouridine labelling for nascent mRNA capture performed by Richa Singhania	58
2.2.4	Reverse transcription quantitative PCR (RT-qPCR)	60
2.2.5	Microarray analysis (data analysis performed by Graeme Thorn)	63
2.2.6	Poly(A) tail measurement	64
2.2.7	High throughput poly(A) tail measurement: TAIL-seq.....	74
2.3	Protein work	80
2.3.1	Western blot analysis.....	80
2.4	Animal work	81
2.4.1	Rat osteoarthritis model pain behaviour assessment by James Burston	81
2.4.2	RNA isolation from rat synovia	81
3	Optimising and developing methodologies for poly(A) tail measurements.....	83
3.1	Deadenylation by oligo (dT)/RNase H treatment	83
3.2	Appraising different ligation strategies	86
3.3	Identifying artefacts.....	91
3.4	High-throughput poly(A) tail measurements – TAIL-seq	96
3.5	Discussion	104
4	Inflammation and polyadenylation in RAW 264.7 cells.....	105
4.1	Developing the inflammatory system.....	106
4.2	Time courses and poly(A) tails	108
4.3	Discussion	114

5	Cordycepin and macrophages	115
5.1	<i>Cordyceps</i> fungal extracts	116
5.2	Effects of purified cordycepin	118
5.3	Discussion	134
6	High-throughput analysis of cordycepin-treated RAW 264.7 cells.....	136
6.1	LPS and cordycepin treatments	136
6.2	Cordycepin sensitivity and mRNA kinetics.....	140
6.3	Cordycepin and long noncoding RNAs	141
6.4	Discussion	144
7	Cordycepin in a rat model of osteoarthritis.....	146
7.1	Pain behaviour – work done by James Burston.....	146
7.2	Analysing rat RNA	149
7.3	Discussion	152
8	Discussion and conclusions.....	153
8.1	Advances in poly(A) tail measurements	153
8.2	Polyadenylation in the inflammatory response.....	154
8.3	Mechanistic insight into cordycepin’s mode of action	155
8.4	High throughput analysis of cordycepin’s effects.....	159
8.5	Demonstrated therapeutic potential of cordycepin in osteoarthritis.....	161
9	Bibliography	164

List of figures

Chapter 1 - Introduction

Figure 1.1	The poly(A) tail allows for formation of the closed-loop complex which enhances recruitment of translation initiation factors	13
Figure 1.2	Life cycle of an mRNA	16
Figure 1.3	Schematic overview of the RNA ligation-mediated PAT procedure	20
Figure 1.4	Overview of the TAIL-seq library generation procedure	23
Figure 1.5	Chemical structure of cordycepin	25
Figure 1.6	Simplified PI3 kinase/Akt signalling pathway showing proposed interaction with cordycepin	26
Figure 1.7	TLR4 signalling through the MyD88 pathway	38
Figure 1.8	NF- κ B activation downstream of the MyD88 pathway following LPS binding to TLR4	40
Figure 1.9	Simplified p38 signalling pathway overview	43
Figure 1.10	Changes in knee physiology in osteoarthritis	49

Chapter 2 - Materials and methods

Figure 2.1	Mechanism of RNA ligation	67
Figure 2.2	Overview of sPAT ligation	70
Figure 2.3	Overview of the TAIL-seq library generation procedure	74

**Chapter 3 - Optimising and developing methodologies for poly(A) tail
measurements**

Figure 3.1	Incomplete deadenylation using NEB RNase H was addressed by increasing oligo (dT) and RNase H quantities	85
Figure 3.2	RL2 PAT yields more consistent results with a range of input RNA quantities, and more efficient cDNA generation	87
Figure 3.3	The L2T ligation improves sPAT compared to the T4 Rnl2 sPAT ligation	89
Figure 3.4	RL2-PAT results in greater efficiency of cDNA generation	90
Figure 3.5	An increase in PCR product:formamide ratio increases the prevalence of suspected multimeric bands	92
Figure 3.6	Artefactual species are multimers and can be removed through fully denaturing PAGE	94
Figure 3.7	Addition of oligo (dT) to PAT-PCR products can remove multimer species	95
Figure 3.8	Only unligated RA3 oligo is recovered after the streptavidin pulldown	97
Figure 3.9	Increasing RNase T1 digestion time results in shorter RNA fragments	102
Figure 3.10	Changing the 3' adapter ligation strategy and increasing the RNase T1 digest duration resulted in successful amplification of a library	103

Chapter 4 - Inflammation and polyadenylation in RAW 264.7 cells

- Figure 4.1** Serum withdrawal prior to LPS stimulation results in a more pronounced response 107
- Figure 4.2** LPS stimulation of RAW 264.7 cells induces expression of inflammatory genes 109
- Figure 4.3** Tnf and Cxcl2 poly(A) tails change in size over the course of their inductions by LPS 111
- Figure 4.4** Initial Tnf poly(A) tail size is variable 113

Chapter 5 - Cordycepin and macrophages

- Figure 5.1** Ethanol extracts from *C. militaris* and *O. sinensis* exhibited similar repressive effects to those of cordycepin 117
- Figure 5.2** Cordycepin represses inflammatory gene expression 119
- Figure 5.3** Administering cordycepin 10 minutes after LPS causes the same repression as a 1 hour pretreatment 121
- Figure 5.4** Cordycepin represses at the transcriptional level 122
- Figure 5.5** Pentostatin potentiates cordycepin's repressive effect on inflammatory gene expression 123
- Figure 5.6** Inhibiting import of cordycepin or its phosphorylation abrogates its repression of inflammatory genes 126
- Figure 5.7** Cordycepin effects can be persistent 128
- Figure 5.8** Cordycepin shortens the Tnf poly(A) tail 129
- Figure 5.9** Cordycepin causes defects in transcription termination and mRNA 3' cleavage 130

Figure 5.10	The effects of cordycepin on mRNA 3' processing are not shared by adenosine and are unlikely to be mediated extracellularly	132
Figure 5.11	I κ B α degradation is not prevented by cordycepin	133
Chapter 6 - High-throughput analysis of cordycepin-treated RAW 264.7 cells		
Figure 6.1	94 RNAs with a >2-fold increase after LPS treatment are >2-fold downregulated by cordycepin	139
Figure 6.2	Cordycepin sensitivity is independent of mRNA stability and transcription rate	141
Figure 6.3	lncRNAs are enriched in RNAs that are upregulated by cordycepin treatment	143
Chapter 7 - Cordycepin in a rat model of osteoarthritis		
Figure 7.1	Cordycepin alters pain behaviour in a rat osteoarthritic model	148
Figure 7.2	After killing the rat, the synovium must be quickly removed and chilled to avoid RNA degradation	150
Figure 7.3	No significant differences observed in assessed inflammatory gene mRNA levels in rat ipsilateral synovia between treatment groups	151
Figure 7.4	No global poly(A) tail length differences were observed between rat groups in ipsilateral synovial RNA samples	152

List of tables

Table 1.1	List of general polyadenylation factors thought to function in most cell types	3
Table 2.1	List of PAT primers	72
Table 2.2	List of TAIL-seq primers	78
Table 2.3	List of qPCR primers	79
Table 2.4	List of rat qPCR primers used	82
Table 3.1	The ligation used in the PAT workflow successfully generated cDNA for TAIL-seq	99
Table 5.1	<i>Cordyceps militaris</i> extract contains significant quantities of cordycepin while <i>Cordyceps sinensis</i> extract does not	117
Table 6.1	Immune and inflammatory GO terms are the most significantly enriched in genes downregulated by cordycepin	138

List of abbreviations

3' UTR	3' untranslated region
³²P-pCp	[5'- ³² P]Cytidine 3',5'-bis(phosphate)
4EBP1	eIF4E-binding protein
4SU	4-thiouridine
5' UTR	5' untranslated region
ADA	Adenosine deaminase
AMP	Adenosine monophosphate
AMPK	AMP-activated protein kinase
AP-1	Activator protein 1
APA	Alternative polyadenylation
ARE	AU-rich element
ARE-BP	ARE-binding protein
ASM	Airway smooth muscle
ATF2	Activating transcription factor 2
ATP	Adenosine triphosphate
BCP	Basic calcium phosphate
BDNF	Brain-derived neurotrophic factor
BM-MSC	Bone marrow mesenchymal stem cell
cAMP	Cyclic AMP
CBP	CREB binding protein
CDE	Constitutive decay element
cDNA	complementary DNA
CF I_{II}	Mammalian cleavage factor II
CF I_I	Mammalian cleavage factor I

CNS	Central nervous system
CPEB	Cytoplasmic polyadenylation element binding protein
CPPD	Calcium pyrophosphate dehydrate
CPSF	Cleavage and polyadenylation specificity factor
CREB	cAMP response element-binding protein
CstF	Cleavage stimulating factor
DAMP	Danger-associated molecular pattern
DEG	Differentially expressed gene
DMEM	Dulbecco's modified Eagle medium
DMSO	Dimethyl sulfoxide
dNTP	deoxynucleoside triphosphate
DTT	Dithiothreitol
EDTA	Ethylenediaminetetraacetic acid
EGF	Epidermal growth factor
EGTA	Ethylene glycol-bis(β -aminoethyl ether)-N,N,N',N'-tetraacetic acid
eIF4E	Eukaryotic translation initiation factor 4E
ERK	extracellular signal-regulated kinase
FBP	Foetal bovine serum
FLS	Fibroblast-like synoviocytes
FPKM	Fragments per kilobase per million mapped reads
GPI	Glycosylphosphatidylinositol
HEPES	4-(2-hydroxyethyl)-1-piperazineethanesulfonic acid
HMGB1	High mobility group box 1
HSC	Haematopoietic stem cell
IDD	Intervertebral disc degeneration

IFNγ	Interferon gamma
IKK	I κ B kinase
IL1R	IL-1 receptor, type I
IL-1β	Interleukin 1 beta
IP	Immunoprecipitation
IRAK	IL-1 receptor-associated kinase
IRF	Interferon regulatory factor
ITu	5-Iodotubericidin
IκBα	Nuclear factor of kappa light polypeptide gene enhancer in B-cells inhibitor, alpha
JNK	Jun N-terminal kinase
KSRP	KH-type splicing regulatory protein
LBP	Lipopolysaccharide binding protein
lncRNA	Long non-coding RNA
LPS	Lipopolysaccharide
MAP3K7	Mitogen-activated protein kinase kinase kinase 7
MAPK	Mitogen-activated protein kinase
MD-2	Myeloid differentiation protein 2
MEK	MAPK Erk kinase
MIA	Monosodium iodoacetate
MK2	MAPK-activated protein kinase 2
mRNA	Messenger RNA
mTOR	Mammalian target of Rapamycin
MyD88	Myeloid differentiation primary response gene 88
NBTI	S-(4-Nitrobenzyl)-6-thioinosine

ncPAP	Non-canonical poly(A) polymerase
NEMO	NF- κ B essential modulator
NF-κB	Nuclear factor kappa-light-chain-enhancer of activated B cells
NGF	Neural growth factor
NLS	Nuclear localisation signal
NMDA	N-methyl-D-aspartate
NMDAR	NMDA receptor
NOD2	Nucleotide-binding oligomerisation domain-containing protein 2
NP	Nucleus pulposus
NPM1	Nucleophosmin
OA	Osteoarthritis
PABP	Poly(A) binding protein
PAMP	Pathogen-associated molecular pattern
PAP	Poly(A) polymerase
PARN	Poly(A) ribonuclease
PAT	Poly(A) tail test
PBE	Pumilio binding element
PBS	Phosphate-buffered saline
PCR	Polymerase chain reaction
PEG	Polyethylene glycol
PGE2	Prostaglandin E ₂
PI3-kinase	Phosphoinositide 3-kinase
PKAc	Catalytic subunit of protein kinase A
PLE	Poly(A) limiting element
PMSF	Phenylmethylsulfonyl fluoride

PNK	Polynucleotide kinase
PP2A	Protein phosphatase 2A
PRR	Pattern recognition receptor
PTM	Post-translational modification
PUM2	Pumilio
PWT	Paw withdrawal threshold
RHD	Rel homology domain
RIG-I	Retinoic acid-inducible gene 1
RIP1	Receptor-interacting protein 1
RNAP II	RNA polymerase II
ROS	Reactive oxygen species
rRNA	Ribosomal RNA
RT-qPCR	Reverse transcription quantitative PCR
SAPK	Stress-activated protein kinase
SARM	Sterile α and HEAT-Armadillo motifs-containing protein
SDS	Sodium dodecyl sulfate
SDS-PAGE	SDS-polyacrylamide gel electrophoresis
TAD	Transactivation domain
TAK1	Transforming growth factor β -activated kinase 1
TANK	TRAF family member-associated NF- κ B activator
TBE	Tris/Borate/EDTA
TBK1	TANK binding kinase 1
TGF-β1	Transforming growth factor beta 1
TIF-I	Transcription Initiation Factor I
TIR	Toll/IL1R homology

TIRAP	TIR domain-containing adapter protein
TLR	Toll-like receptor
TNF	Tumour necrosis factor
TNFR1	TNF receptor-1
TRAF6	TNF receptor-associated factor 6
TRAM	TRIF-related adapter molecule
TRAMP complex	Trf4p/Air2p/Mtr4p polyadenylation complex
TRIF	TIR domain-containing adapter inducing IFN- β
tRNA	Transfer RNA
TTP	Tristetraprolin
U2AF	U2 auxiliary factor
UBC13	Ubiquitin-conjugating enzyme 13
UBF	Upstream binding factor
UEV1A	Ubiquitin-conjugating enzyme variant 1 isoform A

1 Introduction

There are many forms of gene regulation at the epigenetic, transcriptional, and post-transcriptional levels. One of the key steps in posttranscriptional gene regulation is the 3' processing of mRNA. It is an integral step in the production of a mature eukaryotic mRNA transcript. It involves cleavage of the mRNA 20-40 nt downstream of a poly(A) signal in the 3' UTR, followed by the addition of a poly(A) tail at the point of cleavage (Proudfoot 2011). This happens for all metazoan mRNAs with the exception of histone mRNA. The poly(A) tail facilitates export of transcripts from the nucleus, aids mRNA association with factors that promote translation initiation, and serves a protective role for the mRNA (Matthew Brook and Gray 2012; Burgess et al. 2010; Kahvejian et al. 2005). While mRNA 3' processing is a universal process, it was recently suggested that it may have a specific role in regulating inflammation (Kondrashov et al. 2012). Inflammation is a key part of the innate mammalian immune system, mediating host defence against pathogenic threats and responding to tissue damage. It must be carefully regulated in order to respond sufficiently to resolve threats and damage, but not be so active that it causes collateral damage to the host. In the case of the latter, inflammatory diseases result (Barnes et al. 2010; Karin 2006; Puntmann, Taylor, and Mayr 2011; Hummasti and Hotamisligil 2010). Cordycepin, an adenosine analogue, is a polyadenylation inhibitor derived from caterpillar fungi prized in Far Eastern traditional medicine. Cordycepin is said to have anti-inflammatory properties (among many others), and this has been shown both in cell culture systems as well as animal disease models (X. Yang et al. 2015; H. Kim et al. 2011; Rottenberg et al. 2005; H. G. Kim et al. 2006; Shin, Lee, et al. 2009; Y. Li et al. 2016). Briefly, this project aimed to investigate the role of polyadenylation in the inflammatory response, and to gain insight into how cordycepin's anti-inflammatory

effects are mediated – whether through inhibition of polyadenylation or through other mechanisms.

1.1 Polyadenylation

1.1.1 Mechanics of nuclear polyadenylation

In metazoan gene expression, 3' cleavage and polyadenylation of pre-mRNA at the end of transcription is a critical step. With the exception of histone mRNA, it occurs for all transcribed mRNAs. Sequences in the 3' UTR are recognised and bound by various processing factors following which a cleavage reaction occurs, yielding two fragments. The 5' fragment yielded is polyadenylated immediately 3' of the site of cleavage, i.e. a chain of adenosine phosphate residues (the poly(A) tail), is added to produce the mature mRNA molecule. The 3' fragment of the cleavage reaction is degraded (Proudfoot 2011; Kuehner, Pearson, and Moore 2011). While there is variation e.g. between yeast and metazoan systems, there is significant similarity and homology between proteins that participate in the process (Shatkin and Manley 2000; Zhao, Hyman, and Moore 1999). Here, I will describe the metazoan system.

Polyadenylation is governed by *cis*-elements in the 3'UTR which interact with a host of *trans*-acting factors that facilitate the cleavage and polyadenylation reactions (Tian and Graber 2012). These factors, summarised in **Table 1.1**, include the cleavage and polyadenylation specificity factor (CPSF), cleavage factors I_m and II_m (CF I_m and CF II_m, respectively), cleavage stimulating factor (CstF), Symplekin, WDR33, FIP1L1, and a poly (A) polymerase (PAP). In cases for which commonly used names differ from official HUGO gene nomenclature, I will use the official names, but both sets of names are shown in **Table 1.1**.

A consensus hexamer, most commonly AAUAAA, is found some 15-30 nt upstream of the cleavage site in the mRNA 3' UTR. This sequence is recognised by WDR33 and

CPSF4 (Chan et al. 2014; Schönemann et al. 2014), and not by CPSF1, as previously thought (Keller et al. 1991; Murthy and Manley 1995). An upstream element (usually UGUA) associates with CF Im (Q. Yang, Gilmartin, and Doublie 2011), and a U/GU-rich element located 20-40 nt downstream of the cleavage site associates with CstF (Takagaki and Manley 1997; Perez Canadillas et al. 2003; Beyer, Dandekar, and Keller 1997). Symplekin is thought to serve as a scaffolding protein that links CstF and CPSF (Takagaki and Manley 2000). Two constituent proteins of CF IIm, CLP1 and PCF11, were found to be present in the 3' processing complex at very low levels (substoichiometric) compared to CPSF, CstF, and CF Im (Shi et al. 2009).

Protein Name	Other names
CPSF complex	
CPSF1	CPSF160
CPSF2	CPSF100
CPSF3	CPSF73
CPSF4	CPSF30
FIP1L1	hFip1
CstF complex	
CSTF1	CstF50
CSTF2	CstF64
CSTF3	CstF77
CF Im complex	
CPSF6	CF Im 68
CPSF7	CF Im 59
NUDT21	Cf Im 25; CPSF5
CF IIm complex	
PCF11	hPcf11
CLP1	hClp1
Other Known Polyadenylation Factors	
SYMPK	Symplekin
PAPOLG	PAP- γ
PAPOLA	PAP- α
PABPC1	
PABPC4	
PABPN1	
WDR33	

Table 1.1. List of general polyadenylation factors thought to function in most cell types. Official HGNC names for *Homo sapiens* are given in the first column, synonyms are given in the second column. Table adapted from (Shi et al. 2009)

Addition of antibodies against CLP1 to HeLa nuclear extracts reduced cleavage activity, but not polyadenylation activity (de Vries et al. 2000). Together, these findings suggest that Cf IIm may transiently associate with the rest of the 3' processing machinery to stimulate cleavage activity, possibly by linking CPSF and CF Im (de Vries et al. 2000). The exonuclease Xrn2 degrades the 3' product after mRNA cleavage, resulting in transcriptional termination (West, Gromak, and Proudfoot 2004). Further data from HeLa cells demonstrates roles for PCF11 in mediating efficient transcription termination and degradation of the 3' cleavage product (West and Proudfoot 2008). In mammals, a distal G-rich auxiliary downstream element has also been identified, although it is not clear which factor(s) it interacts with. Lastly, most cleavage sites have a CA dinucleotide immediately 5' of the cleavage site (with mRNA being cleaved immediately after the A). This dinucleotide sequence can be clinically relevant e.g. in the case of the human prothrombin gene. The prothrombin mRNA 3' UTR has a CG dinucleotide, rather than the more common CA, which has been shown to result in a lower efficiency of cleavage *in vitro* (F. Chen, MacDonald, and Wilusf 1995). In ~1-2% of the Caucasian population the CG dinucleotide is mutated to CA, and is thought to be a cause of thrombophilia experienced by individuals with the mutation (Poort et al. 1996; Cattaneo et al. 1999). In these cases, the processing of the prothrombin mRNA is enhanced, as seen in cell culture conditions and transgenic mice (Gehring et al. 2001; Danckwardt et al. 2004; Kuwahara, Kurachi, and Kurachi 2004). The resulting increase in prothrombin expression (at the level of both mRNA and protein) provided the basis for a model to explain the contribution of the mutation to the pathogenesis of thrombophilia.

While CPSF3 was reported to be the endonuclease that performs the cleavage (Mandel et al. 2006), it seems both CPSF3 and CPSF2 contribute to endonucleolytic activity (Kolev et al. 2008). Upon cleavage of the mRNA, a poly(A) polymerase

processively adds adenosine phosphate residues to form the poly(A) tail, typically thought to be 200-250 nt in length. The polyadenylation reaction is stimulated by FIP1L1 (Kaufmann et al. 2004). There are a number of canonical and non-canonical poly(A) polymerases (ncPAPs), which are discussed in **section 1.1.3**. PABPN1, a poly(A) binding protein (PABP), stimulates poly(A) tail extension and is thought to have a role in controlling its length (Kuhn et al. 2009). Nucleophosmin (NPM1) deposition on the poly(A) tail is also involved in poly(A) tail length control, with NPM1 knockdown resulting in hyperadenylation of mRNA in HeLa cells (Sagawa et al. 2011).

1.1.2 Control of poly(A) tail length

It is generally thought that a new mRNA is made in the nucleus with a poly(A) tail of 200-250 nt. The mechanism proposed for the control of the length involves interactions between CPSF, the poly(A) polymerase (PAP) doing the polyadenylation, and PABPN1 (Kuhn et al. 2009). Initially, binding of PABPN1 to the nascent poly(A) tail and of CPSF to the poly(A) signal allows them to stimulate PAP activity. However, once the critical length is reached (~250 nt), PABPN1 then disrupts stimulation of PAP by CPSF, and so PABPN1 is proposed to perform the role of measuring and limiting the length of the poly(A) tail. PABPN1 has also been shown to have a role in splicing. While splicing is generally understood to occur co-transcriptionally (Tilgner et al. 2012; Carrillo Oesterreich, Preibisch, and Neugebauer 2010; Khodor et al. 2011; Ameur et al. 2011), some splicing occurs following polyadenylation. In human cells, PABPN1 depletion decreased the splicing efficiency of a subset of pre-mRNAs that undergo splicing after polyadenylation (Muniz, Davidson, and West 2015). Knockdown of PAPOLA and PAPOLG also decreased the splicing efficiency, even for a synthetic construct whose cleavage and polyadenylation did not depend on cellular machinery i.e. the poly(A) polymerases' role in facilitating splicing was independent

of the process of polyadenylation. IP experiments also showed PABPN1 depletion reduced association of splicing factors with terminal introns.

The RNA binding protein ZC3H14 is important in neural function (Pak et al. 2011) and also has a role in controlling poly(A) tail lengths (Kelly et al. 2014). In mouse neuroblastoma cells, depletion of Pabpn1 led to shortening of total poly(A) tail length, while depletion of ZC3H14 led to longer poly(A) tails. Adult survival of flies lacking Nab2 (orthologue of ZC3H14) was very low, but those that did survive exhibited defects in development and locomotion. These could be rescued by neuron-specific transgenic expression of human ZC3H14, indicating an evolutionarily conserved role of this RNA binding protein. In yeast, the PABPs Pab2 and Nab2 have opposing roles in the nuclear decay of pre-mRNA (Grenier St-Sauveur et al. 2013). Pab2 facilitates exosomal degradation of pre-mRNA while Nab2 impedes it, affording the pre-mRNA more time to complete posttranscriptional splicing, 'escape' the Pab2-mediated exosomal decay, and be exported into the cytoplasm. Thus, nuclear PABPs can influence poly(A) tail length but can also serve other roles in regulating gene expression.

While the 250 nt length in animals is generally accepted as the initial poly(A) tail size of a newly transcribed mRNA, there appear to be a few exceptions to the rule.

Mammalian histone mRNA completely lacks a poly(A) tail (Marzluff, Wagner, and Duronio 2008; Marzluff 2005). eNOS mRNA in endothelial cells has been shown to be differentially polyadenylated in the nucleus in response to certain stimuli (Weber et al. 2005; Kosmidou et al. 2007). Under basal conditions, eNOS mRNA has a short poly(A) tail of <25 nt, but in response to statins or laminar shear stress, the mRNA is synthesised with a much longer poly(A) tail. The longer eNOS poly(A) tail is accompanied by greater mRNA half-life, greater representation of the mRNA in

higher polysome fractions (suggestive of increased translational activity), and greater mRNA levels in the cytoplasm (Weber et al. 2005; Kosmidou et al. 2007).

A *cis* element termed the poly(A) limiting element (PLE) was found in the terminal exon of a number of mRNAs whose initial poly(A) tail sizes were discrete and limited to <20 nt (Das Gupta et al. 1998; Gu, Das Gupta, and Schoenberg 1999). The PLE was originally identified in *Xenopus* albumin pre-mRNA, but placing the PLE-containing part of the mRNA into a β -globin reporter construct transfected into mouse fibroblasts produced β -globin mRNA with <20 nt poly(A) tails, indicating conservation of the limiting mechanism between species (Das Gupta et al. 1998). Other mRNAs with PLE sequences and <20 nt poly(A) tails include transferrin and HIV-EP2, and removal of the PLE sequence in reporter constructs led to mRNAs with long poly(A) tails (Gu, Das Gupta, and Schoenberg 1999). It was later found that U2 auxiliary factor (U2AF) binds to the PLE and has a role in modulating poly(A) tail length control by the PLE (Gu and Schoenberg 2003). Interestingly, it was found that the PLE increases mRNA levels in the cytoplasm by enhancing the efficiency of mRNA 3' processing in reporter constructs. PLE-containing RNA was cleaved in HeLa nuclear extract 80% faster than control RNA (J. Peng, Murray, and Schoenberg 2005). Furthermore, PLE-containing β -globin mRNA with a short tail <20 nt was shown to be as stable as non-PLE-containing β -globin mRNA with a poly(A) tail size of 100-200 nt. These β -globin reporter constructs had the last part of the terminal exon removed and a synthetic polyadenylation element added at this point. Thus, regulatory elements in the β -globin 3' UTR (which confer considerable mRNA stability (Peixeiro et al. 2011)) would not be present, and therefore would not be able to influence the stability of the mRNA produced.

1.1.3 Poly(A) polymerases and other types of polyadenylation

In humans, 8 poly(A) polymerase (PAP) enzymes have been identified. The three canonical PAP enzymes are PAP α , PAP β , and PAP γ (PAPOLA, PAPOLB, and PAPOLG respectively), with PAPOLA and PAPOLG thought to be the two main enzymes involved in nuclear polyadenylation of mRNA. Non-canonical PAPs (ncPAPs) include MTPAP (mitochondrial PAP), TUT1 (STAR-PAP), PAPD4 (GLD2), PAPD5 (GLD4), and PAPD7. Canonical PAPs are nuclear enzymes, as are some ncPAPs. However, a number of ncPAPs perform roles outside of the nucleus. Additionally, some ncPAPs also have terminal nucleotidyl transferase activity that is not limited to addition of adenosines. PAPD4 is a cytoplasmic PAP with importance in germline development and synaptic plasticity in a number of species (Sartain et al. 2011; Kwak et al. 2008; Rouhana et al. 2005; Benoit et al. 2008; Barnard et al. 2004). MTPAP is the only known mitochondrial PAP, and polyadenylates mitochondrial RNAs. PAPD5 polyadenylates aberrant pre-rRNA to bring about its degradation (Shcherbik et al. 2010), uridylylates histone mRNA to bring about its degradation (Mullen and Marzluff 2008), and performs 3' oligoadenylation for snoRNAs with possible implications for their stability (Berndt et al. 2012). PAPD5 is also implicated in the regulation of TP53 (p53) mRNA levels and protein expression (Burns and Richter 2008), which might be a cytoplasmic role (more on this in **section 1.1.3.1**). In yeast, the Trf4p/Air2p/Mtr4p polyadenylation (TRAMP) complex is a nuclear surveillance complex that serves to polyadenylate aberrant nuclear transcripts, leading to their exosomal degradation (Wyers et al. 2005; Vaňáčová et al. 2005; LaCava et al. 2005). This role of polyadenylation (performed by Trf4p – a non-canonical PAP and orthologue of PAPD5) appears to be more in line with polyadenylation's prokaryotic origins, in which it promotes degradation. In mammals, a TRAMP-like complex includes PAPD5, demonstrating evolutionary conservation of the decay mechanism and a role for this

non-canonical PAP (Sudo et al. 2016; Shcherbik et al. 2010). It should be noted, however, that the phenomenon of polyadenylation in the nucleus to mediate exosomal decay of aberrant transcripts is not exclusively performed by ncPAPs. Work in human cells has revealed an exosomal nuclear decay pathway in which PAP α and PAP γ (canonical PAPs), together with PABPN1 and exosomal subunits, perform this role (Bresson and Conrad 2013). Since these poly(A) polymerases appear to have multiple roles, it is conceivable that these depend on binding partners. It was noted that this decay pathway did not affect efficiently exported RNAs. A model could therefore be constructed wherein the coupling of 3' processing to nuclear export takes RNAs away from the polyadenylation-dependent degradative nuclear environment, and into the cytoplasm where the poly(A) tail serves other roles. A subset of long noncoding RNAs (lncRNAs) were among those found to be subject to this PABPN1-involved, polyadenylation-dependent turnover (Beaulieu et al. 2012). Further work is required for characterisation of PAPD7.

A cytoplasmic role of Trf4-1 for promoting decay in *Drosophila* was recently reported (Harnisch et al. 2016). 3' mRNA decay intermediates were found to have terminal oligoadenylations i.e. the mRNA had already experienced some 3' decay such that its 3' end was upstream of the poly(A) site, but then non-template As had been added to this end. These modifications were due to the cytoplasmic activity of Trf4-1, and knockdown of Trf4-1 and the Dcp2 decapping enzyme led to a significant accumulation of 3' decay intermediates of Dcp2 knockdown alone, illustrating the role of Trf4-1 in promoting decay. Some ncPAPs are capable of performing 3' end uridylation of mRNA, and are thus classed as terminal nucleotidyl transferases (TUTs) (Lim et al. 2014; Kwak and Wickens 2007; Rissland, Mikulasova, and Norbury 2007; Martin and Keller 2007). Terminal uridylation of mRNA is another modification that can influence cytoplasmic mRNA decay. In yeast and mammalian systems, it

promotes decay (Slevin et al. 2014; Malecki et al. 2013), while it may have the opposite function in *Arabidopsis* (Sement et al. 2013). Uridylation can occur after the poly(A) tail, with shorter tails being better substrates for uridylation than longer tails (Lim et al. 2014). Non-polyadenylated mRNAs like siRNA-directed cleavage products and histone mRNA decay intermediates can also be uridylated (Slevin et al. 2014; Shen and Goodman 2004).

1.1.3.1 *Cytoplasmic polyadenylation*

Polyadenylation can occur in the cytoplasm for mRNAs that have already been transcribed and exported from the nucleus via the process of cytoplasmic polyadenylation. Generally, the role of cytoplasmic polyadenylation is to 'activate' translation of certain mRNAs that are stored in the cytoplasm in a repressed state with a short poly(A) tail (Weill et al. 2012; Villalba, Coll, and Gebauer 2011). For an mRNA to be regulated in this way, it would have to (after export from the nucleus) recruit deadenylases and factors that repress translation, be stored in the cytoplasm, and then be recognised by cytoplasmic polyadenylation machinery. This process is governed by interplay between *cis* elements in the 3' UTR and *trans*-acting factors (Charlesworth, Meijer, and de Moor 2013). These include the same poly(A) signal as is used in nuclear polyadenylation (recognised by cytoplasmic CPSF complex), the cytoplasmic polyadenylation element (CPE) (recognised by CPE binding proteins (CPEBs)), and the Pumilio binding element (PBE) (bound by Pumilio (PUM2)).

Cytoplasmic polyadenylation was originally found in germ cell and embryonic development across a number of different species, and is known to play crucial roles in these processes (Sartain et al. 2011; Luitjens et al. 2000; Wilt 1973; Fox, Sheets, and Wickens 1989; Standart and Dale 1993; Vassalli et al. 1989; Lim et al. 2016).

However, cytoplasmic polyadenylation has also been found to play roles in somatic cells, with the nervous system being one example. *N*-methyl-D-aspartate (NMDA) is an agonist for the NMDA receptor (NMDAR). NMDAR is thought to be important in synaptic plasticity and memory (F. Li and Tsien 2009). Treating mammalian neurons with NMDA led to a rapid increase in poly(A) tail size of NR2A mRNA. This increase was reduced by PAPD4 depletion, and NMDA treatment promoted phosphorylation of CPEB and dissociation of poly(A) ribonuclease (PARN) – these are both events associated with the transition from a repressed to activated state of mRNAs regulated by cytoplasmic polyadenylation. Additionally, PAPD4 has been shown to be important in *Drosophila* for long-term memory (Kwak et al. 2008), and Orb2 (*Drosophila* somatic CPEB) is required for asymmetric cell division during neurogenesis (Hafer et al. 2011).

Cytoplasmic polyadenylation is also important in the regulation of cell cycle. In HeLa cells, total mRNA and mRNA with short poly(A) tails were separated into fractions for cells in S phase and cells in G2/M phase (Novoa et al. 2010). The ratio of total to short poly(A) tail for each mRNA was then evaluated and compared between cells from the two different phases. Hundreds of mRNAs displayed a change in this ratio, and polyadenylation of some of these transcripts was affected by knockdown of CPEB1 and CPEB4. A more recent study in HeLa cells compared differentially expressed genes (DEGs) between S and M phases (J.-E. Park et al. 2016). A small set of key cell cycle regulators, including CDK1, experienced a significant decrease in poly(A) tail length in M phase, with coincident translational repression. However, this group represented just 8 genes out of the 777 DEGs, suggesting greater importance of polyadenylation-independent regulation of gene expression in the cell cycle. In mouse primary fibroblasts, cells' ability to enter senescence was prevented by knockdown or ablation of CPEB1 (Groisman et al. 2006; Burns and Richter 2008).

Additionally, translational activation of TP53 (p53) – a master cell cycle regulator and tumour suppressor – mRNA was found to be dependent on CPEB1, and knockdown of CPEB1 led to TP53 mRNA with short poly(A) tails. PAPD5 was found to be associated with CPEB1 and TP53 mRNA, and knockdown of PAPD5 reduced TP53 mRNA polyadenylation and protein expression (Burns and Richter 2008). Taken together, these data implicate cytoplasmic polyadenylation in the regulation of the cell cycle and specifically TP53 mRNA.

The nuclear factor kappa-light-chain-enhancer of activated B cells (NF- κ B) is an important transcription factor in the process of inflammation (see **sections 1.3.2.1.1** and **1.3.2.1.3**). A kinase upstream of NF- κ B activation is mitogen-activated protein kinase kinase kinase 7 (**MAP3K7** or **TAK1**). TAK1 has been shown to be regulated by CPEB, with CPEB-depleted macrophages displaying elevated production of pro-inflammatory cytokines (Ivshina et al. 2015). In this way, CPEB plays an important role in the control of the inflammatory response, although polyadenylation was not implicated in the study.

1.1.3.2 Mitochondrial polyadenylation

In mammals, mitochondrial RNAs are produced as polycistronic RNAs that are then processed by endoribonucleases to yield separate, intronless mRNAs. For several mitochondrial mRNAs, this cleavage leaves a 3' end with an incomplete stop codon, with either a terminal UA or just U (S. Anderson et al. 1981). For these mRNAs, polyadenylation, performed by MTPAP, completes the UAA stop codon (Nagaike et al. 2005). A homozygous MTPAP mutation (N478D) in fibroblasts led to loss of polyadenylation but retention of oligoadenylation (Wilson et al. 2014). The enzyme was shown to have severely compromised polyadenylation activity *in vitro*. Fibroblasts with the mutation displayed a reduction in protein synthesis, and

reduction in levels of oxidative phosphorylation complexes I and IV. The loss of mitochondrial transcript polyadenylation and decreased levels of oxidative phosphorylation complexes I and IV was rescued by overexpression of wild-type MTPAP. So mitochondrial polyadenylation is an important posttranscriptional regulatory mechanism, and its dysregulation can lead to decreased mitochondrial protein synthesis and reduction in respiratory chain complexes.

1.1.4 Biological importance and role of the poly(A) tail

PABPs, through binding the poly(A) tail, perform a number of biologically important roles. Normally, they facilitate export of mRNAs from the nucleus. However, PABPN1 can also enhance the decay of some hyperadenylated mRNAs that are not efficiently exported.

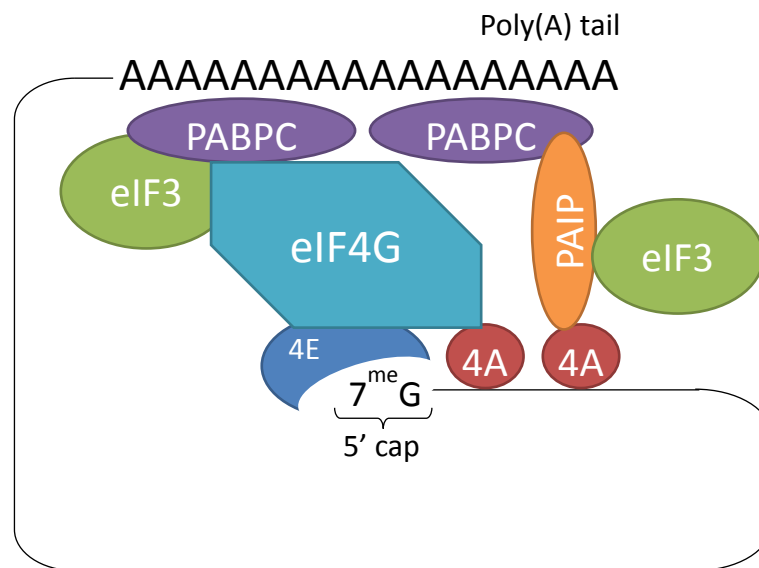


Figure 1.1. The poly(A) tail allows for formation of the closed-loop complex which enhances recruitment of translation initiation factors.

Adapted from Charlesworth et al. 2013

mRNAs are generally bound by the cytoplasmic poly(A) binding protein, PABPC1, on the poly(A) tail, while the 5' cap is bound by eIF4E, as part of the cap binding complex, comprising eIF4E, eIF4G, and eIF4A (Mangus et al. 2003). Interactions between eIF4G and PABP facilitate formation of the closed-loop complex (**Figure 1.1**). This complex is important for the formation of ribosomal initiation complexes (Kahvejian et al. 2005).

Most eukaryotic mRNA degradation is thought to require shortening of the poly(A) tail (deadenylation) by deadenylase complexes (PAN2-PAN3, Ccr4-Not) to some critical length, whereupon the mRNA then becomes susceptible either to decapping (i.e. hydrolytic removal of the mRNA 5' cap structure) followed by 5'-3' exonucleolytic decay (C.-Y. A. Chen and Shyu 2011), or exosomal decay in the 3'-5' direction. Some mRNAs contain regulatory *cis* elements that increase deadenylation and decay rates. AU-rich elements are a well-studied example of such sequences, and are found in many mRNAs encoding growth factors and inflammatory mediators (P. Anderson 2010; Stumpo, Lai, and Blackshear 2010; Khabar 2010). The AU-rich sequence UUAUUUUAU, for example, is bound by tristetraprolin (TTP) in TNF mRNA and mediates instability (Stoecklin et al. 2004; Mahtani et al. 2001) – see **section 1.3.2.1.3** for more detail. This sequence also appears to play a role in TNF translational repression (Han, Brown, and Beutler 1990; Kontoyiannis et al. 1999), discussed more in **section 1.3.2.1.1.1**.

Data from TAIL-seq, a high throughput poly(A) tail analysis technique, revealed that poly(A) tail length correlated positively with mRNA half-life (Chang et al. 2014).

However, it did not correlate with ribosome binding. Rather, data suggested that a very short or no poly(A) tail was detrimental for translation, but beyond a critical length of ~25 nt, further increases in poly(A) tail size had no bearing on translation.

High throughput analysis in *Arabidopsis* showed a modest negative correlation between poly(A) tail length and mRNA half-life (Kappel et al. 2015). Data yielded from PAL-seq, a similar technique to TAIL-seq, found either weak negative or variable correlations between poly(A) tail length and mRNA half-life in 3T3, HeLa, and yeast (Subtelny et al. 2014). PAL-seq data also showed that a strong positive correlation between poly(A) tail length and translational efficiency *did* exist for cells in early developmental stages, but not for cells that had passed this phase. This fits with existing knowledge that non-polyadenylated, maternally-derived mRNAs in *Xenopus* oocytes can be translationally unmasked and activated by cytoplasmic polyadenylation. It should be noted, however, that in these cases, translational efficiency was inferred from ribosome binding i.e. translation initiation. Changes in the rate of translation elongation are not considered, so these correlations rest on the assumption that translation elongation is constant and independent of poly(A) tail length changes, which may not be the case. A third, similar recently published technique, PAT-seq, found little or no correlation between mean poly(A) tail length for a given mRNA and its read count or protein abundance (Harrison et al. 2015).

In an *in vitro* decay system, it was shown that PABP depletion led to a several-fold increase in the decay rate of mRNAs (Bernstein, Peltz, and Ross 1989). This could be rescued by addition of exogenous PABP, and the decay rate of non-polyadenylated RNA was independent of the presence of PABP. Thus, the poly(A) tail and PABP, together, have a protective role, and it could be the case that the closed-loop complex reduces accessibility of the mRNA ends to decay machinery. However, the relationship between PABP and mRNA turnover is more complex than that, as it can also promote deadenylation and therefore decay, via TOB1 recruitment (Ezzeddine, Chen, and Shyu 2012). In summary, the poly(A) tail, through interaction with PABP, is important for nuclear export, translation, and mRNA lifetime.

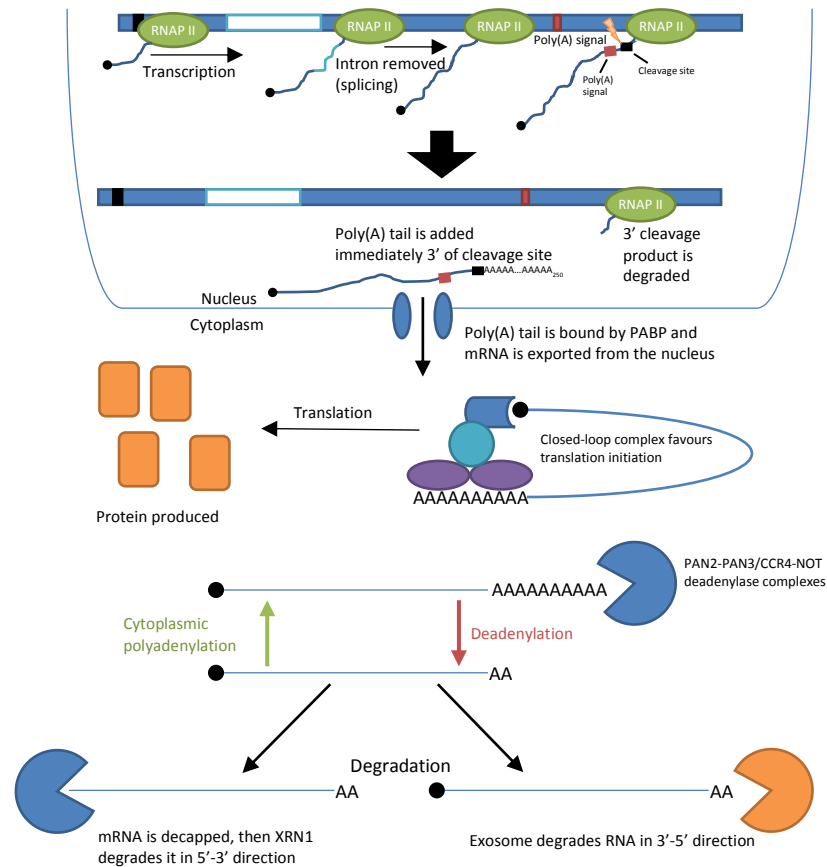


Figure 1.2. Life cycle of an mRNA. As RNA polymerase II (RNAP II) transcribes the DNA, the nascent mRNA is subject to splicing. The poly(A) signal and nearby *cis* elements are recognised by mRNA 3' processing machinery that cleaves the mRNA and polyadenylates the 5' fragment. The 3' product is degraded. The poly(A) tail is bound by poly(A) binding protein (PABP) and the mRNA is exported from the nucleus where it can adopt the closed-loop formation, favouring translation. The poly(A) tail can be removed by deadenylation and restored through cytoplasmic polyadenylation. Once shortened beyond a critical length, it is subject to degradation either by decapping and 5'-3' exonucleolytic decay by XRN1, or by 3'-5' exosomal decay.

1.1.5 Alternative polyadenylation

Some mRNAs have multiple poly(A) sites, and so cleavage and polyadenylation can take place at different sites to yield different products. This process is termed alternative polyadenylation (APA), of which there are four main types:

1. APA at tandem 3' UTR sites
2. APA at alternative terminal exons
3. APA at intronic sites
4. APA at exonic CDS sites

APA at tandem 3' UTR sites (1) produces mRNAs that vary solely in the length of their 3' UTR, but are otherwise identical. The other three types of APA produce mRNAs which differ in both coding and 3' UTR sequences. APA at alternative terminal exons (2), while termed APA, is a result of alternative splicing, which determines the terminal exon of the transcript. APA at cryptic poly(A) site in an intron or exon (3 and 4) can lead to production of truncated protein isoforms with altered coding and 3' UTR sequence.

Research has implicated APA and its regulation in cancer (Xia et al. 2014; Mayr et al. 2009; Sandberg et al. 2008). Specifically, this generally involves a switch to proximal poly(A) sites, resulting in shorter 3' UTRs which lack regulatory sequences e.g. miRNA binding sites for negative regulation. APA is also found to be important in the immune system, with T-cell activation leading to global 3'UTR shortening (Gruber et al. 2014). APA changes are also relevant in the activation of macrophages (Shell et al. 2005), and PTGS2 (COX2) regulation (Cornett and Lutz 2014; Hall-Pogar et al. 2007).

1.1.6 Measuring poly(A) tails

Given the importance of poly(A) tails, tools and techniques have been developed in order to study them and assess length. However, accurately studying poly(A) tail

length is not a simple task. If comparing full length mRNAs, differences in poly(A) tail sizes can be difficult to detect, given that these would be on a much smaller scale relative to the entire length of the mRNA. Traditional replication-based sequencing methods are not suitable for use in determining poly(A) tail lengths due to problems with slippage on homopolymeric sequences (Viguera et al. 2001; Clarke et al. 2001). Briefly described below are some of the commonly used methods, which include northern blotting, poly(A) tail test (PAT), and 3' end labelling.

Northern blotting:

- 1) A DNA probe that anneals at a known position of the 3' UTR of the mRNA of interest (e.g. 300 nt upstream of the cleavage site) is allowed to hybridise to the RNA. RNase H treatment will then cleave at the site of hybridisation between RNA and the DNA probe, yielding fragments whose lengths are equal to 300 nt (distance between where the probe annealed and the cleavage site) plus the length of the poly(A) tail (which may vary across a range in the pool of mRNAs).
- 2) The above is done, but, in addition to the specific oligo, oligo (dT) is added to the reaction, and so the poly(A) tail is removed. The product of the RNase H treatment should just be 300 nt. Only a single product should be produced (since the region of variable size – the poly(A) tail – has been removed).
- 3) Cleavage products are cleaned up, run on a gel and visualised by northern blotting. The difference in size between the polyadenylated and deadenylated samples corresponds to the length of the poly(A) tail.

This method has the advantage of specificity, but requires the use of radiation, high starting input of RNA, and lacks sensitivity, with mRNAs of low abundance being difficult to detect using this method. Also, the image quality is inferior to that of

agarose gels (see below), and the oligo (dT) has the potential to anneal to A-rich tracts instead of the poly(A) tail, leading to cleavage at an unintended location.

Poly(A) test (PAT):

There are a number of different PCR-based poly(A) test (PAT) methods, including RACE-PAT, ePAT, sPAT, and Klenow PAT, of which some are described in a recent review (Jalkanen, Coleman, and Wilusz 2014). The one described here is **RNA**

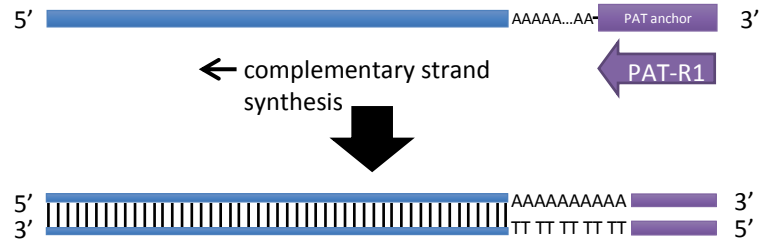
ligation-mediated PAT (Figure 1.3):

- 1) RNA is prepared in duplicate – one set is subjected to an RNase H/oligo (dT) treatment to remove poly(A) tails (deadenylated sample). The other set is untreated, and so retains poly(A) tails of mRNAs (non-deadenylated sample).
- 2) RNA has a DNA adapter ligated to its 3' end ("PAT anchor").
- 3) An oligo complementary to the PAT anchor ("PAT-R1") is used to perform a specific reverse-transcription reaction to synthesise cDNA from all RNA to which the PAT anchor was successfully ligated.
- 4) A PCR reaction is done, using a forward primer that anneals in the 3'UTR (at a known location), and PAT-R1 as the reverse primer. The PCR product length will be equal to the sum of the distance between the forward primer priming site and the cleavage site; the length of the poly(A) tail (for non-deadenylated samples); and the length of the ligated PAT anchor sequence. Deadenylated samples should give rise to a single PCR product.
- 5) PCR products are run on an agarose gel and visualised under UV by EtBr or SYBR Safe stain. The difference in size between deadenylated and non-deadenylated samples corresponds to the size of the poly(A) tail.

Step one: ligation



Step two: reverse transcription to cDNA



Step three: PCR

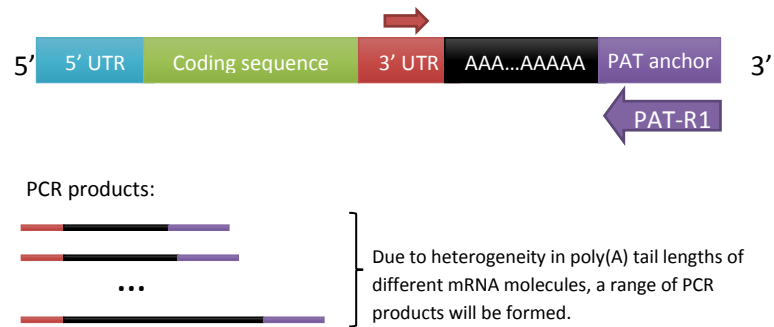


Figure 1.3. Schematic overview of the RNA ligation-mediated

PAT procedure. A 3'-blocked adapter ("PAT anchor") is ligated to

the 3' ends of RNA. Reverse transcription is done using a primer complementary to PAT anchor (PAT-R1) to generate PAT cDNA.

PCR is performed using a forward primer that anneals to the 3' UTR of the gene of interest, and PAT-R1 as the reverse primer.

The PCR products are analysed on an agarose gel.

This technique is more sensitive than northern blotting due to the amplification involved in the PCR, and does not require the use of radiation. The image quality obtained on the agarose gel is superior to that of a northern gel. However, high input RNA quantities are still required, especially if oligo (dT)/RNase H treatment is to be done, and the use of PCR can lead to artefacts and off-target amplification.

3' End-labelling

- 1) A radioactive pCp base is ligated to the 3' end of total RNA.
- 2) A cocktail of RNases digests all RNA that is not poly(A).
- 3) Free poly(A) tails are then run on a long TBE-urea PAGE gel, and then placed in a cassette with a phosphorimaging screen at -80°C for up to a week.
- 4) The screen is then imaged on the phosphorimager.

This technique allows for the measurement of global poly(A) tail sizes within a sample. It requires a much lower input quantity of RNA than the other two methods, but is a long process and uses radiation. No information on the poly(A) tails of individual mRNAs is obtained, unless a purification step is performed on the RNA to isolate a specific mRNA (Schoenberg et al. 1989). This requires a very high starting quantity of RNA, however, and use of the technique is limited to highly abundant mRNAs.

The methods discussed have their advantages and disadvantages. Our group primarily uses PAT and 3' end-labelling, results and optimisation of which can be found in later sections. A significant limitation of these methods is that they do not yield high-throughput genome-wide data. PAT can only be done for a single mRNA i.e. one forward primer per tube. 3' end labelling only provides a single result – the entire mix of poly(A) tails in a sample, with no way of separating the data into which poly(A) tails came from which mRNAs. Simply using RNA-seq is not an option, as

homopolymeric sequences result in slippage of the DNA polymerase, leading to misalignment and replication errors (Viguera et al. 2001; Clarke et al. 2001).

During the course of my project, other groups developed and published novel techniques for this very purpose of high-throughput poly(A) tail measurement. TAIL-seq, whose methodology is described briefly in **Figure 1.4**, requires a very large input quantity of RNA, but yields genome-wide distribution of poly(A) tail sizes within an RNA sample.

Other high throughput techniques exist including PAL-seq, PAT-seq, and mTAIL-seq (Harrison et al. 2015; Subtelny et al. 2014; Lim et al. 2016). These techniques use either a splint oligo with T bases (to anneal to poly(A) tails) for 3' adapter ligation, or a similar oligo with T bases which serves as the template to extend the 3' end of the mRNA to which it is annealed. In either case, this results in biasing towards polyadenylated mRNAs, and so mRNAs that are deadenylated or have non-A terminal modifications such as uridylation or guanylation will not be represented in the library. PAL-seq requires non-conventional use of the Illumina instrument in such a way that voids the manufacturer guarantee. While PAT-seq provides information on gene expression, poly(A) site usage, and changes in poly(A) tail length distribution, it does not yield data on actual poly(A) tail size. TAIL-seq has limitations of its own, but none of the above apply to it.

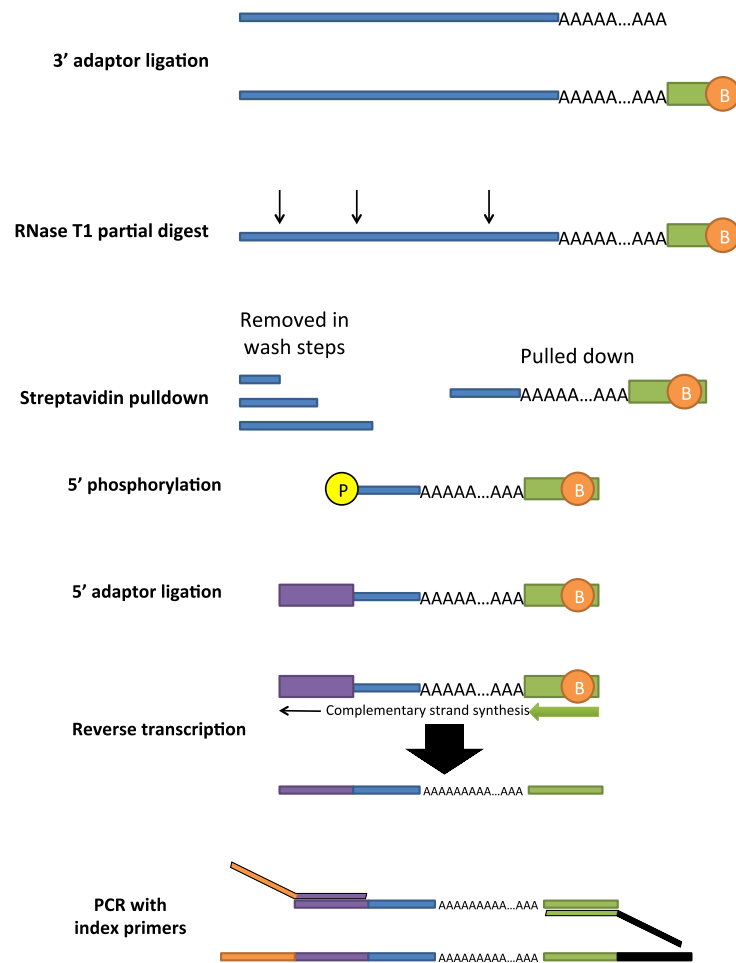


Figure 1.4. Overview of the TAIL-seq library generation procedure. Total RNA is subjected to two rRNA-removal steps and then has a biotinylated adaptor ligated to the 3' end of RNAs. This is then subjected to a partial RNase T1 digest, following which the 3'-most fragment of all digested RNAs (which has the biotinylated sequence) is purified by streptavidin pulldown, 5'-phosphorylated, and run on a gel for size selection (300-1000 nt). This size-selected, 5'-phosphorylated RNA then has the 5' adaptor ligated and is reverse transcribed to cDNA. PCR is then done using primers that have overhanging index sequences.

1.2 Cordycepin

Cordycepin (3'-deoxyadenosine) is an adenosine analogue that lacks the 3' hydroxyl group (**Figure 1.5**), and therefore functions as a chain terminator if phosphorylated and incorporated into a growing polynucleotide chain. It is extracted from parasitic caterpillar fungi that have been used in Far Eastern traditional medicine for treating a range of ailments, with its purported benefits including anti-inflammatory, anti-diabetic, anti-cancer, and anti-obesity properties, among others (Jeong et al. 2010b; Takahashi et al. 2012; S.-J. Lee et al. 2010). Over the last two decades, evidence has started to emerge to support the potential therapeutic benefits of both purified cordycepin itself, and extracts prepared from the entire fungus.

1.2.1 Cordycepin and transcription

As an adenosine analogue, it is conceivable that cordycepin triphosphate could be used by RNA polymerase II in place of ATP, thereby terminating transcription. Indeed, this was found to occur *in vitro* (Desrosiers et al. 1976; Shigeura and Boxer 1964), but data from cells were at odds with these findings. Incubation of HeLa cells with cordycepin revealed that pre-mRNA levels (produced by RNA polymerase II) were not significantly affected by cordycepin, suggesting that transcription is unaffected (Siev, Weinberg, and Penman 1969; Penman, Rosbash, and Penman 1970). More recently, it was confirmed that cordycepin indeed does not affect the transcription of housekeeping mRNAs in tissue culture (Kondrashov et al. 2012). Therefore, cordycepin is not an inhibitor of mRNA transcription in intact cells.

Previous data also showed that 45S pre-rRNA (produced by RNA polymerase I) was significantly decreased in cordycepin-treated cells, at concentrations of cordycepin that had no effect on pre-mRNA. To attempt to explain these findings, which were not limited to HeLa cells, the sensitivity of both RNA polymerases I and II were

compared *in vitro* (Desrosiers et al. 1976). However, both enzymes were determined to be sensitive to cordycepin with similar kinetic values obtained for both. The varying effects of cordycepin on the production of different RNA types could therefore not be ascribed to the intrinsic susceptibility of the polymerases. More recent findings on the effects of cordycepin on signal transduction suggest that the sensitivity of RNA pol I to cordycepin may be mediated by effects on signal transduction.

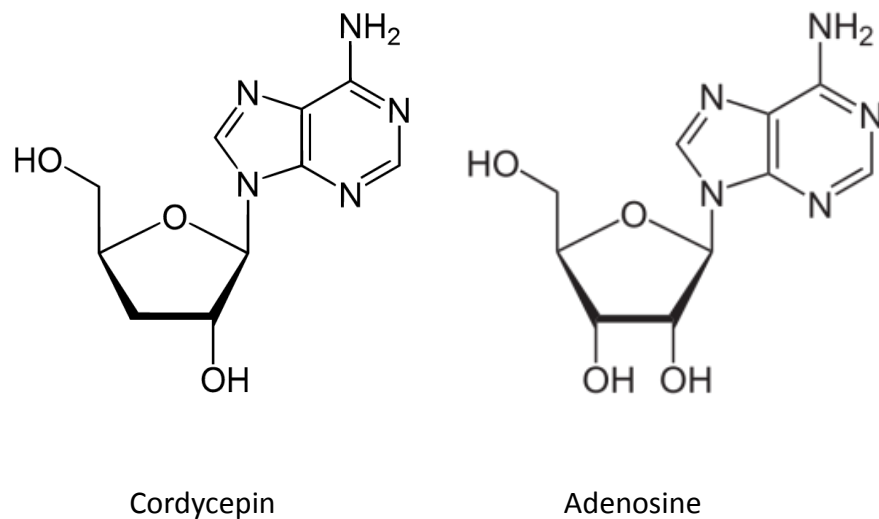


Figure 1.5. Chemical structure of cordycepin. The only difference between the structure of adenosine and cordycepin is the absence of the 3' hydroxyl group in cordycepin. This property would make it a chain terminator, if incorporated into a growing polynucleotide strand.

1.2.2 Cordycepin and mTOR signalling

As mentioned, cordycepin treatment in HeLa cells led to decreased levels of pre-rRNA. It should be noted that this reduction was accompanied by a decrease in tRNA levels. In more recent years, cordycepin has been found to inhibit mammalian target of rapamycin (mTOR) signalling (Wong et al. 2010). A simplified overview of mTOR signalling, and cordycepin's proposed involvement, is shown in **Figure 1.6**.

Cordycepin was found to activate AMP-activated protein kinase (AMPK) and cause dephosphorylation of eIF4E-binding protein (4EBP1). Dephosphorylated 4EBP1 binds eIF4E, thereby inhibiting its binding to the mRNA 5' cap structure to initiate translation. mTORC1 phosphorylates 4EBP1 to relieve this repression and facilitate translation initiation. This was blocked by cordycepin.

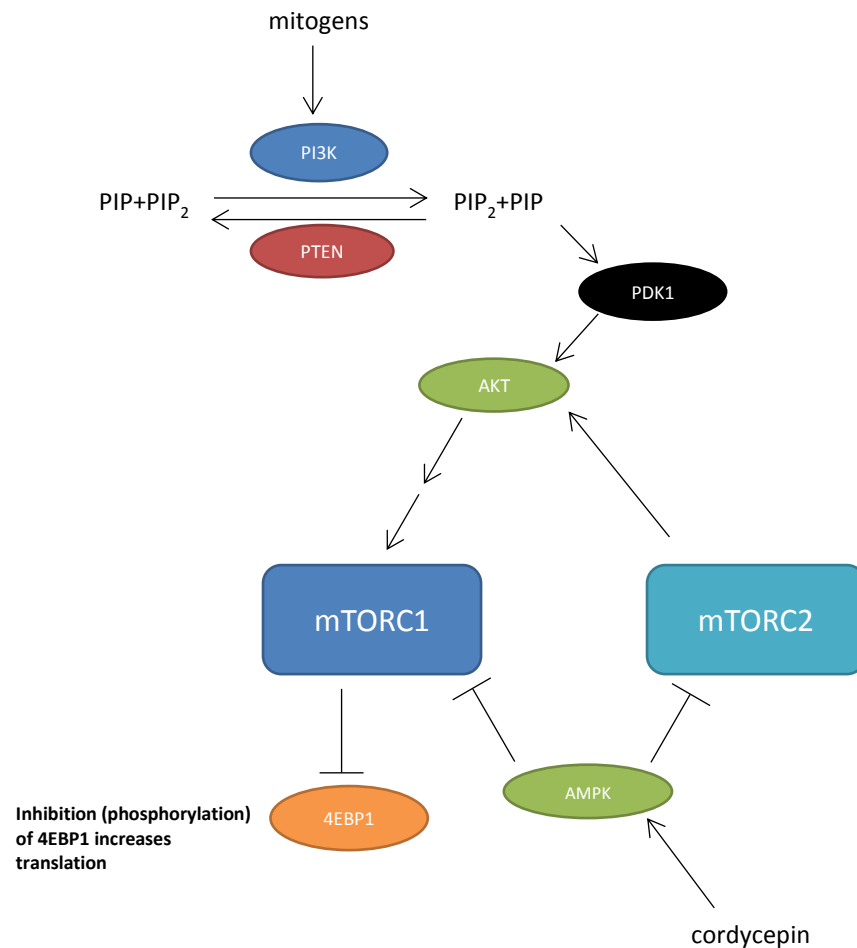


Figure 1.6. Simplified PI3 kinase/Akt signalling pathway showing proposed interaction with cordycepin. Cordycepin appears to inhibit mTOR signalling via activation of AMPK, but the detailed mechanism by which this occurs is unknown. See references for more detail (Memmott and Dennis 2009; Huang and Manning 2009; Wong et al. 2010).

mTOR signalling plays a role in the activities of RNA polymerases I and III (Mayer and Grummt 2006). Initiation of transcription by Pol I is dependent upon Transcription Initiation Factor I (TIF-I) A, TIF-IB/SL1, and Upstream Binding Factor (UBF). Signalling through the mTOR pathway leads to phosphorylation of UBF and TIF-IA, enabling their association with Pol I. Inhibition of mTOR signalling leads to both inactivation of TIF-IA and partial nuclear exclusion. Therefore, reduced Pol I transcription through inhibition of mTOR signalling provides a plausible model to account for the previously observed reduction in pre-rRNA. The same can apply for the observation of decreased tRNA levels, following cordycepin treatment. Pol III is responsible for production of tRNA, and mTOR signalling is also involved in its activity. In yeast, the TOR inhibitor rapamycin was shown to decrease Pol III activity, which was determined to occur through the negative regulator Maf1 (Zaragoza et al. 1998; Oficjalska-Pham et al. 2006). Maf1 represses Pol III activity when in a dephosphorylated state. Rapamycin treatment leads to dephosphorylation of Maf1, which results in its accumulation in the nucleus and facilitates repression of Pol III. This phenomenon was later found to be true in humans, as well, with mTORC1 directly phosphorylating human MAF1 (which represses Pol III in a hypophosphorylated state, as in yeast) (Michels et al. 2010; Shor et al. 2010). To summarise, reduction in levels of pre-rRNA and tRNA, but not pre-mRNA, following cordycepin treatment could be explained by its more recently discovered inhibitory effects on mTOR signalling.

1.2.3 Cordycepin and polyadenylation

As mentioned above, cordycepin does not inhibit transcription in cells (Penman, Rosbash, and Penman 1970; Siev, Weinberg, and Penman 1969). It was, however, shown to be an efficient chain terminator of polyadenylation (Rose, Bell, and Jacob 1977). Its status as a known polyadenylation inhibitor was exploited in several

studies for studying mRNA 3' processing. Through the use of cordycepin triphosphate for *in vitro* polyadenylation reactions, insight was gained into the cleavage and polyadenylation of mRNA (Ryner and Manley 1987; Zarkower et al. 1986), and it was also determined that a complex exists that recognises the poly(A) signal and is required for cleavage and polyadenylation (Zarkower and Wickens 1987). This study also found that this complex is normally transient but becomes stabilised when associated with cleaved RNA with a cordycepin-terminated tail. Another study made the same observation, noting that this stabilisation of the complex was observed both with cordycepin and non-hydrolysable ATP analogues (Zhang and Cole 1987). With *in vitro* effects well established, data from a number of cell types show reduced poly(A) tail size following cordycepin treatment, confirming that effects on polyadenylation are present (Ioannidis et al. 1999; Kondrashov et al. 2012; Wong et al. 2010).

Since polyadenylation is required for nearly all mRNAs, it is surprising that inhibiting this process can cause a specific reduction in the expression of inflammatory genes (Kondrashov et al. 2012). In human primary airway smooth muscle (ASM) cells treated with tumour necrosis factor (TNF), inflammatory gene expression measured by RT-qPCR was greatly increased. Pretreatment of the cells with cordycepin resulted in a much lower degree of induction in the mRNA levels of such genes, while housekeeping mRNA levels were unaffected. Other adenosine analogues were tested in place of cordycepin, and only the one that was also known to be a polyadenylation chain terminator was able to replicate its effects. In addition, knocking down poly(A) polymerase α (PAPOLA) also reduced the expression of inflammatory genes.

1.2.3.1 Polyadenylation and cordycepin's mechanism

Removal of the poly(A) tail is often the first and rate-limiting step in the process of mRNA decay (C.-Y. A. Chen and Shyu 2011), and many inflammatory mRNAs are inherently unstable owing to regulatory sequences in their 3' UTRs (P. Anderson 2010; Stumpo, Lai, and Blackshear 2010). Therefore, if cordycepin inhibits polyadenylation (thus shortening or even removing the rate-limiting step of deadenylation), it could be hypothesised that intrinsically unstable mRNAs (like those produced from inflammatory genes) would be particularly sensitive. This model provides an explanation for the specificity of cordycepin's effects in reducing the induction of inflammatory genes (Kondrashov et al. 2012).

Another model can be formed around the observation that cordycepin arrests the cleavage complex *in vitro* (Zarkower and Wickens 1987). In stabilising the 3' processing complex, cordycepin-terminated RNAs may be sequestering the constituent factors, thereby preventing proper processing of other transcripts. This hypothesis is further supported by the finding that cordycepin caused transcription termination defects – a sign of decreased pre-mRNA cleavage efficiency (Luo, Johnson, and Bentley 2006; West, Proudfoot, and Dye 2008; Richard and Manley 2009). For genes being induced (e.g. inflammatory genes in response to an inflammatory stimulus), mRNA production could be hampered by a reduced availability of 3' processing factors if they have high processing factor requirements. Such requirements could either be due to suboptimal *cis* elements around the poly(A) site; or simply because transcription becomes so fast that very many factors are required to process the large number of nascent transcripts. Additionally, there is evidence to show that proper mRNA 3' processing is required for efficient recycling of transcription factors to the promoter to initiate the next round of transcription (Mapendano et al. 2010). By interfering with 3' processing, cordycepin

may inhibit transcription of affected genes. In this way, cordycepin could specifically inhibit the induction of any genes for which rapid transcriptional increase is required (e.g. inflammatory genes in response to a pro-inflammatory stimulus (Kondrashov et al. 2012)). Housekeeping genes, on the other hand, may have a transcription rate that is sufficiently low to not be limited by the availability of 3' processing factors or inefficient recycling of transcription factors.

The above represents just three possible explanations of how cordycepin could affect gene expression by inhibiting polyadenylation. As discussed in **section 1.1.3**, poly(A) polymerases are diverse in their functions and polyadenylation is a varied process. With polyadenylation existing in nuclear, cytoplasmic, and mitochondrial forms, cordycepin may have multiple effects. Additionally, it may affect polyadenylation in the context of nuclear polyadenylation-mediated decay. Indeed, treatment of human cells with cordycepin led to nuclear accumulation of stable transcripts with shorter tails that, under control conditions, are hyperadenylated and degraded (Bresson and Conrad 2013).

1.3 Inflammation

Inflammation is a response of the innate immune system to infection and tissue injury. The term refers to a complex biological process whose purpose is to defend the host by eliminating invading pathogens, repairing damaged tissues, and restoring homeostasis. A number of cell types are involved, but I will focus specifically on macrophages, since studies have found this cell type to be sensitive to cordycepin (H. G. Kim et al. 2006; Shin, Lee, et al. 2009).

Inflammation is tightly controlled with large regulatory networks in place. There needs to be a sufficient degree of inflammation to deal with the harmful stimulus, but not so much that the inflammation causes collateral damage to the host.

Improper regulation of inflammation is known to give rise to a host of diseases and conditions, including rheumatoid arthritis, asthma, and Crohn's disease (Barnes et al. 2010; Bradley 2008; Suzuki and Yamamoto 2015).

1.3.1 Inflammation and pain

The process of inflammation is also tied to the sensation of pain (Kidd and Urban 2001). Nociception is the response of specific sensory neurons (nociceptors) to noxious stimuli, generally resulting in pain sensation. In normal tissues, the feeling of pain generally has to do with the nature of the stimulus. However, in inflamed tissue, pain can arise spontaneously without an external stimulus. When there is an external stimulus, pain in inflamed tissues can be enhanced (hyperalgesia), and pain can even result from innocuous stimuli that do not result in pain in normal tissue (allodynia). There are a number of ways in which inflammation results in pain sensation, some of which I will briefly describe. Tissue injury results in the release of inflammatory mediators of which some can activate peripheral nociceptors directly e.g. bradykinin, while others, e.g. neural growth factor (NGF), activate inflammatory cells and trigger the release of pain-inducing (algogenic) agents. Furthermore, release of inflammatory mediators recruits cells of the immune system that, in turn, release more inflammatory mediators and further contribute to the establishment of an inflammatory environment. Inflammation in peripheral tissues can also lead to the phenomenon of central sensitisation in the spinal dorsal horn, whereby changes, including altered neurotransmitter production, result in increased excitability of CNS neurons and persistent pain. Finally, neurotrophic growth factors, including NGF and brain-derived neurotrophic factor (BDNF), are produced in greater quantities during inflammation (Woolf et al. 1997; Cho et al. 1997). These play roles in central sensitisation, and cause hyperalgesia (through directly activating nociceptors and also indirectly through activation of mast cells) (Kerr et al. 1999; Lewin, Rueff, and

Mendell 1994; Aloe and Levi-Montalcini 1977). In short, inflammation is closely linked to pain sensation.

1.3.2 Macrophages

Macrophages are white blood cells derived through the myeloid lineage from haematopoietic stem cells (HSCs). They are mononuclear, and often defined by their capacity for phagocytosis. They play roles in host defence against tissue injury and infection, as well as tissue repair and homeostasis (Wynn, Chawla, and Pollard 2013). Macrophages are found in all tissues. Formerly, macrophages were thought to arise predominantly from recruitment of circulating monocytes in the blood and their subsequent differentiation into macrophages (van Furth and Cohn 1968). However, it has more recently been found that the majority of tissue-resident macrophages originate during embryonic development (Epelman, Lavine, Beaudin, et al. 2014; Hashimoto et al. 2013; Epelman, Lavine, Randolph, et al. 2014). During inflammation, circulating monocytes that are recruited to tissues and differentiated into macrophages may behave differently to embryonically-derived tissue-resident macrophages. For instance, in cardiac tissue, embryonic macrophages seem to serve a more reparative role while macrophages derived from HSCs are more inflammatory in nature (De Wit et al. 2003; Epelman, Lavine, Randolph, et al. 2014; Aurora et al. 2014).

Definition and classification of macrophages becomes difficult when considering the specialisation of tissue-resident macrophages in distinct anatomical sites and the fact that macrophages are remarkably plastic cells. They are involved in the induction as well as the resolution of inflammation, and can change their activity and gene expression programmes to exhibit different phenotypes depending on the microenvironmental context and the specific stimuli that they encounter. Indeed,

transcriptional profiling of tissue-resident macrophages from different organs done through the Immunological Genome Project revealed highly diverse profiles (Gautier et al. 2012). For this reason, it can be dangerous to think of them as a single cell type. Rather, macrophages are cells that are capable of occupying a large range of biological states depending on a number of factors (Hume 2015).

Macrophages are thought to be activated in two ways. Classical activation produces the M₁ macrophage subtype, and alternative activation produces the M₂ activated subtype (which has the M_{2a}, M_{2b}, and M_{2c} subcategories) (Italiani and Boraschi 2014; Laskin 2009). M₁ macrophages are activated by signals including lipopolysaccharide (LPS) and TNF (following priming by IFN γ (IFNG)), have a pro-inflammatory phenotype, and are associated with tissue destruction. Factors produced by M₁ macrophages include reactive oxygen/nitrogen species, TNF, IL-1, IL-6, and chemokines. They also have increased cell surface MHC class II expression through which they display antigens to helper T cells, thereby playing a role in adaptive immunity. M₂ macrophages, which are activated by signals including IL-4, IL-13, and transforming growth factor beta 1 (TGF- β 1, TGFB1), generally have a more anti-inflammatory phenotype, and are associated with wound healing and tissue repair. Factors produced by M₂ macrophages include IL-10, TGF β , and epidermal growth factor (EGF). These classifications, which have been greatly simplified, here, can be useful. However, it should be remembered that macrophages, in an organism-wide context, are too complex and diverse to fit into these two categories and macrophage biologists are working on a common framework for macrophage-activation nomenclature (Murray et al. 2014).

1.3.2.1 *Macrophage receptors and signalling*

Macrophages can sense infection and sterile tissue damage, and, in response, mediate inflammatory processes to remove the threat and restore homeostasis.

Pattern recognition receptors (**PRRs**) recognise particular molecular structures that broadly fit into two categories: pathogen-associated molecular patterns (**PAMPs**) and damage-associated molecular patterns (**DAMPs**). Examples of macrophage PRRs include Toll-like receptors (**TLRs**), capable of interacting with PAMPs and DAMPs, retinoic acid-inducible gene 1 (**RIG-I**) which detects viral dsRNA, and nucleotide-binding oligomerisation domain-containing protein 2 (**NOD2**) which detects the muramyl dipeptide structure found in certain bacteria (Hayden, West, and Ghosh 2006).

PAMPs represent molecular structures that are unique to pathogens and are subject to surveillance by the innate immune system of the host via PRRs (Tang et al. 2012). They are therefore exogenous signals. Examples include LPS (more detail in **section 1.3.2.1.1**) and flagellin (part of the bacterial flagellum).

DAMPs, by contrast, are the host's own endogenous molecular structures whose detection by PRRs signals danger and damage (Piccinini et al. 2010). Some DAMPs are intracellular molecules that are normally absent from the extracellular environment, and therefore are not 'seen' by extracellular PRRs (Tang et al. 2012). As a result of cellular stress or tissue injury, or cell necrosis, such DAMPs are released into the extracellular space where they can be recognised by extracellular PRRs and elicit sterile inflammation (G. Y. Chen and Nuñez 2010). Examples of DAMPs include mitochondrial DNA, nuclear proteins, and histones. While DAMPs have roles in immunity and tissue repair, excessive levels of DAMPs are implicated in diseases. The DAMP high mobility group box 1 (HMGB1) is present at elevated

concentrations in the serum and plasma of patients with sepsis (H. Wang et al. 1999). Antibodies against HMGB1 increased the survival of septic mice, suggestive of a causal relationship.

1.3.2.1.1 LPS signalling through TLR4

Lipopolysaccharide (LPS) is an archetypal PAMP found on the surface of gram-negative bacteria. It can trigger the innate immune system through the TLR4 receptor. TLR4 requires carriers and co-receptors to recognise LPS. In the extracellular space, LPS interacts with the soluble, shuttle protein LPS-binding protein (LBP). LBP in the bloodstream forms a complex with LPS (Jack et al. 1997) and transfers monomeric units of LPS to CD14 (a co-receptor of TLR4 expressed in immune cells) (Wright et al. 1990). CD14 – a GPI-anchored cell surface protein (which also exists in a soluble form) – facilitates the transfer of LPS to the TLR4/MD-2 receptor complex. The importance of LBP and CD14 is illustrated in mouse studies – deficiency in either protein led to a shift in sensitivity to LPS by 2-3 orders of magnitude (Haziot et al. 1996; Moore et al. 2000; Wurfel and Wright 1997), and LBP was essential for a rapid inflammatory response to LPS challenge or gram-negative bacterial infection (Jack et al. 1997). MD-2 is a soluble protein, which forms part of the receptor complex with TLR4. It can exist in soluble form (and bind LPS), or in a pre-formed complex with TLR4 (as described above). LPS binding occurs with a higher affinity for the TLR4-MD-2 complex than for soluble MD-2 alone (Akashi et al. 2003). The TLR4-MD-2-LPS complex forms a dimer, as confirmed by a crystal structure (B. S. Park et al. 2009). Downstream signalling is mediated through the intracellular Toll/IL1R homology (**TIR**) domain of TLR4, involving the recruitment of adapter proteins. These adapter proteins include myeloid differentiation primary response gene 88 (**MyD88**), TIR domain-containing adapter protein (**TIRAP**), TIR domain-containing adapter inducing IFN- β (**TRIF**), TRIF-related adapter molecule

(**TRAM**), and sterile α and HEAT-Armadillo motifs-containing protein (**SARM**). TLR4 is the only TLR member able to activate both the MyD88-dependent and TRIF-dependent pathways.

1.3.2.1.1.1 MyD88-dependent pathway

The MyD88-dependent pathway (**Figure 1.7**) leads to activation of transcription factors such as nuclear factor kappa-light-chain-enhancer of activated B cells (**NF- κ B**) and activator protein 1 (**AP1**). Three mitogen-activated protein kinases (**MAPKs**) are phosphorylated in the MyD88-dependent pathway. These are **p38**, c-Jun N-terminal kinase (**JNK**), and extracellular signal-regulated kinase 1/2 (**ERK 1/2**). Pro-inflammatory cytokines are induced by this pathway.

Following recognition of TLR4 as described above, MyD88 and TIRAP are recruited to the intracellular domain of TLR4. This leads to the recruitment of IL-1 receptor-associated kinase (**IRAK**) 4 and 1, and TNF receptor-associated factor 6 (**TRAF-6**). TRAF-6, in complex with ubiquitin-conjugating enzyme 13 (**UBC13**) and ubiquitin-conjugating enzyme variant 1 isoform A (**UEV1A**) activates mitogen-activated protein kinase kinase kinase 7 (**MAP3K7** aka **TAK1**). TAK1 activates I κ B kinase (**IKK**), which phosphorylates inhibitor of kappa B alpha (**I κ B α**), leading to its dissociation from NF- κ B, ubiquitination and proteasomal degradation, allowing nuclear translocation of NF- κ B. TAK1 also activates mitogen activated protein kinase (MAPK) pathways, namely **JNK**, **p38**, and **ERK 1/2**, all of which contribute to the inflammatory process. A conserved sequence UUAUUUUAU is found in the 3' UTR of a number of human and murine inflammatory mRNAs including TNF (Caput et al. 1986). As mentioned in **section 1.1.4**, this sequence is bound by TTP and mediates instability of the TNF mRNA. The role of TTP in regulating TNF mRNA stability is discussed in **section 1.3.2.1.3**. This sequence mediates translational repression, and

derepression occurs in response to endotoxin (LPS) (Han, Brown, and Beutler 1990). Dexamethasone specifically inhibits LPS-induced JNK activity in macrophages and led to decreased TNF production, but no change in TNF mRNA accumulation (Swantek, Cobb, and Geppert 1997). Overexpression of MAPK10 (**JNK3**, Stress activated protein kinase beta (**SAPKβ**)) was able to overcome the dexamethasone-mediated translational repression of TNF. A kinase-dead mutant of JNK3 mimicked the effect of dexamethasone, with no translational derepression of TNF observed after LPS stimulation (while TNF mRNA accumulation was unaffected). These data highlight an important role of JNK signalling in facilitating the inflammatory response. p38 phosphorylates and activates several transcription factors, including activating transcription factor 2 (**ATF2**), and a number of downstream kinases including MAP kinase activated protein kinase 2 (MAPKAPK2) (**MK2**) (Guha and Mackman 2001). The role of p38-induced MK2 activation in inflammation is discussed in **section 1.3.2.1.3**. Experiments done in monocytes show that inhibition of MAPK Erk kinase (**MEK**), which phosphorylates ERK 1/2, led to a decrease in LPS-induced production of a number of inflammatory cytokines including TNF and IL-1β (Scherle et al. 1998). Activation of the MAPK pathways also contributes to pro-inflammatory gene activation through the induction of the transcription factor AP-1.

In addition to the above, the MyD88 pathway also involves induction of IκBζ and interferon regulatory factor 5 (**IRF5**). IκBζ is a member of the IκB family that is localised in the nucleus. It is important for the induction of the pro-inflammatory cytokine IL-6 (Yamamoto et al. 2004), the antimicrobial protein LCN2 (Kohda, Yamazaki, and Sumimoto 2016), and also the anti-inflammatory cytokine IL-10 (Hörber et al. 2016). IRF5, which interacts with and appears to be activated by MyD88 and TRAF-6, is important for the induction of TNF, IL-6, and IL-12B (Takaoka et al. 2005).

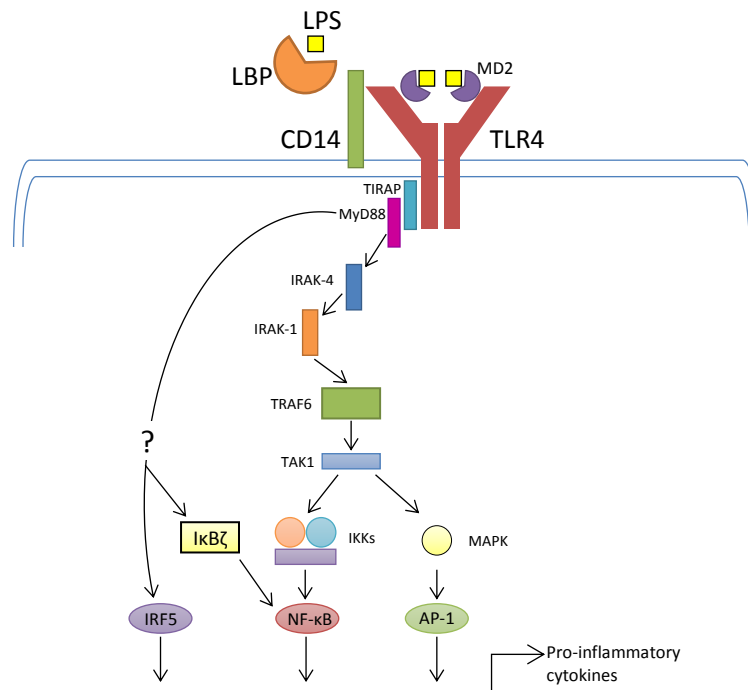


Figure 1.7 TLR4 signalling through the MyD88 pathway.

Following LPS stimulation, signalling through TLR4 via the MyD88 pathway culminates in the induction of pro-inflammatory cytokines with activation of NF- κ B, AP-1 and IRF5.

Figure taken and adapted from (Lu, Yeh, and Ohashi 2008).

1.3.2.1.1.2 TRIF-dependent pathway

TLR4 activation of the TRIF-dependent (or MyD88-independent) pathway occurs later when the receptor is endocytosed and trafficked to the endosome, where the TIR domain of TLR4 forms a complex with other adapter molecules such as TRIF and TRAM (Kagan et al. 2008). The activation of this pathway is responsible for the late-phase activation of NF- κ B and MAPKs and the production of inflammatory cytokines and Type I interferons, which serve roles in the host response to bacterial and viral infections (Perry et al. 2005). Transcriptional activation of Type I interferons is accomplished through joint action of IRF3 (which is phosphorylated in the pathway) and NF- κ B.

The TRAM and TRIF adapters are recruited and TRIF is able to interact with receptor-interacting protein 1 (**RIP1**). RIP 1 mediates the late-phase activation of NF- κ B and MAPKs (Cusson-Hermance et al. 2005; Ofengeim and Yuan 2013). In addition to NF- κ B and MAPKs, IRF3 is activated (T. Kawai et al. 2001). This occurs through TRAF-3, which can associate with TRAF family member-associated NF- κ B activator (**TANK**), TANK binding kinase 1 (**TBK1**) and **IKKi** (Oganesyan et al. 2006). Once activated, IRF3 and NF- κ B activate transcription of target genes, including Type I interferons (Moynagh 2005).

Endotoxin stimulation of MyD88-deficient macrophages still activates MAPKs and NF- κ B, albeit with delayed kinetics (Taro Kawai et al. 1999), ostensibly through the TRIF-dependent pathway. However, such macrophages did not experience an induction of pro-inflammatory cytokine production following LPS challenge. This suggests that, aside from NF- κ B and MAPK activation, other MyD88-dependent events are prerequisites for the induction of inflammatory gene expression.

1.3.2.1.2 NF- κ B signalling in inflammation

The NF- κ B transcription factor family comprises five members (Oeckinghaus and Ghosh 2009):

- p105 (produced from NFKB1 gene), which is constitutively processed to p50
- p100 (produced from NFKB2 gene), which is processed to p52 under tight control
- p65 (aka RelA, produced from RELA gene)
- RelB (produced from RELB gene)
- c-Rel (produced from REL gene)

Heterodimers and homodimers of this family constitute NF- κ B transcription factors that are able to bind to the NF- κ B consensus binding sequence and regulate gene

expression by either activating or repressing transcription. NF- κ B-responsive genes are numerous and diverse, but many are pro-inflammatory, and so NF- κ B is an important mediator in the inflammatory process and a potential therapeutic target. Target genes whose expression is driven by NF- κ B include TNF, IL-1, and IL-6 (Oeckinghaus and Ghosh 2009). A lack of proper control in NF- κ B signalling can give rise to disease (Courtois and Gilmore 2006; Ben-Neriah and Karin 2011).

Signals that activate NF- κ B include PAMPs e.g. LPS through TLR4 (see **section 1.3.2.1.1**), DAMPs e.g. HMGB1 through TLR4 (S. Kim et al. 2013), and cytokines e.g. TNF through TNF receptor-1 (**TNFR1**) (Wajant and Scheurich 2011) or IL-1 β through IL-1 receptor, type I (**IL1R**). The NF- κ B pathway downstream of TLR4 signalling is shown in **Figure 1.8**. As mentioned in previous sections, NF- κ B is kept inactive in the cytoplasm by members of the I κ B family (May and Ghosh 1997; Whiteside and Israël 1997). I κ B family members have ankyrin repeats that allow them to bind the N-terminal Rel homology domain (**RHD**) of NF- κ B family members. In binding NF- κ B, I κ Bs can mask the nuclear localisation signal (**NLS**), thereby excluding NF- κ B from the nucleus (and target genes).

Nuclear vs cytoplasmic localisation only represents one level of control, however. NF- κ B is also regulated through modulation of its capacity to bind DNA and its transcriptional activity (Guan, Hou, and Ricciardi 2005). NF- κ B proteins can be subjected to several post-translational modifications (PTMs) that can affect these properties (Karin and Ben-Neriah 2000; Christian, Smith, and Carmody 2016). All NF- κ B proteins have an N-terminal RHD. p65, c-Rel, and RelB all have a C-terminal transactivation domain (**TAD**), also. p105 and p100 (the precursors from which p50 and p52 are formed, respectively) have an N-terminal RHD, and also ankyrin repeats closer to the C-terminus that give the proteins an inhibitory I κ B-like function in the cytoplasm. This inhibitory action is lost upon processing of p105 and p100 to p50 and p52 which retain only the N-terminal RHD. p50 and p52 have DNA-binding activity, but do not have a TAD. As such, they function as transcriptional repressors when homodimeric (Bohuslav et al. 1998; Guan, Hou, and Ricciardi 2005).]

Phosphorylation at S276 in p65 is one of the best studied examples of NF- κ B regulation by phosphorylation. The catalytic subunit of protein kinase A (**PKAc**) is kept in an inactive cytoplasmic complex with I κ B α and p65 (Zhong et al. 1997).

Signals that lead to I κ B degradation then allow PKAc to phosphorylate p65 at S276. This modification both promotes interaction of p65 with the p300/CBP (cAMP response element-binding protein (CREB) binding protein) coactivators, thus enhancing transcriptional activity, and also leads to acetylation at K310 which also increases transcriptional activity (Zhong et al. 1998; L.-F. Chen et al. 2005). IL-1 β stimulation in liver cancer cells led to PI 3-kinase-dependent phosphorylation and transactivation of p65 (Sizemore, Leung, and Stark 1999). Inhibition of PI 3-kinase decreased p65 phosphorylation and caused a decrease in NF- κ B-dependent gene expression with no effect on I κ B degradation, NF- κ B nuclear translocation, or even NF- κ B binding to DNA. This demonstrates the importance of PTMs as an independent modulator of NF- κ B activity.

1.3.2.1.3 Regulation of inflammatory cytokine mRNA stability

A number of mRNAs involved in the immune response and inflammation such as TNF and prostaglandin-endoperoxide synthase 2 (**PTGS2** or **COX-2**) contain AU-rich elements (AREs) in their 3' UTRs (P. Anderson 2008; Caput et al. 1986; Tudor et al. 2009). ARE sequences can confer instability upon the mRNA through interactions with ARE-binding proteins (ARE-BPs) that promote its turnover. One such protein is tristetraprolin (TTP), which binds its targets and mediates their rapid decay through recruitment of Not1 and Caf1 deadenylase subunits (Brooks and Blackshear 2013). Xrn1 exonuclease and decapping complex proteins and the exosome are also possibly recruited (Hau et al. 2007). Under normal, unstimulated conditions, TTP causes the rapid degradation of its ARE-containing target mRNAs, and so those mRNA levels are kept low. The amount of ARE content in inflammatory genes' 3' UTRs is said to direct the course and kinetics of the inflammatory response, as genes are expressed in three distinct temporal phases (Hao and Baltimore 2009). mRNAs expressed earlier had greater ARE content, while those expressed in later phases

had less. In this study by Hao & Baltimore, it is interesting to note that using TNF as a stimulus in fibroblasts had little or no effect on the measured half-lives of mRNAs with high ARE content. Using LPS to stimulate bone marrow derived macrophages, however, resulted in a marked increase in the stability of such mRNAs. It may be, therefore, that regulation at the level of mRNA stability in inflammation is dependent on the cell type (or possibly just the stimulus).

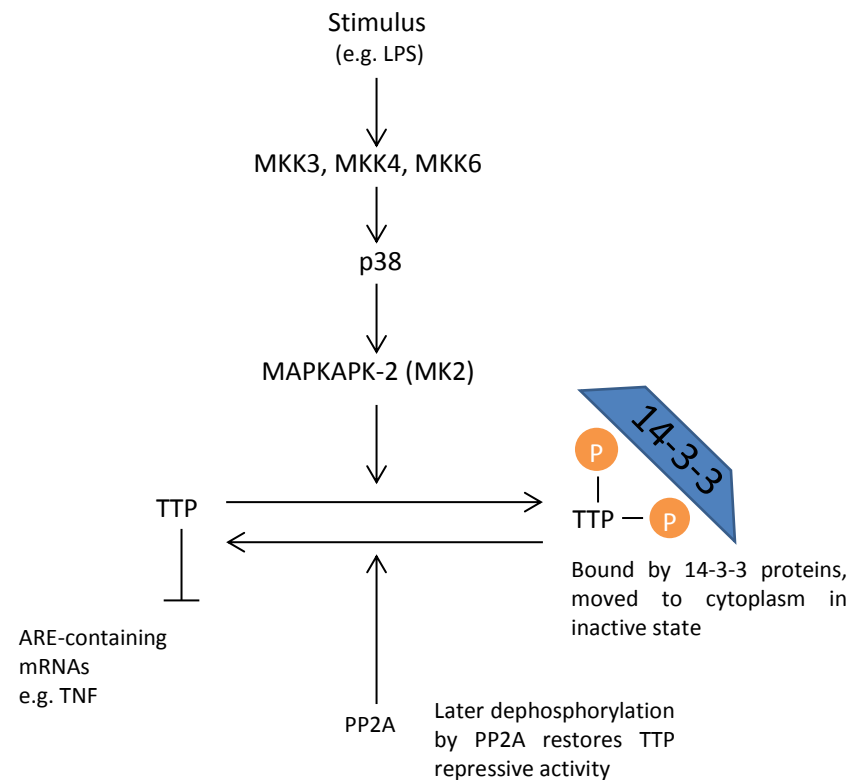


Figure 1.9. Simplified p38 signaling pathway overview. p38 activation leads to phosphorylation of TTP via MAP kinase activated protein kinase 2 (MAPKAPK-2) (MK2). Phosphorylated TTP is bound by 14-3-3 proteins and localises in the cytoplasm but remains inactive, unable to destabilise mRNAs like TNF with AREs in their 3' UTR, allowing such mRNAs to accumulate. Phosphorylated TTP can later be dephosphorylated by protein phosphatase 2A (PP2A) whereupon it regains its ability to destabilise ARE-containing mRNAs. This contributes to the decline in the levels of such mRNAs.

TNF is a key pro-inflammatory cytokine in the inflammatory response, and plays a large role in rheumatoid arthritis – evidence of this is provided by the fact that many successful therapies for rheumatoid arthritis target TNF (Brennan et al. 1989; P. C. Taylor, Taylor, and Feldmann 2009). A number of its effects are mediated through the activation of NF- κ B-dependent gene expression through I κ B degradation as described in the previous section. TNF contains AREs in its 3' UTR, and so levels are kept low by TTP in unstimulated cells. The role of TTP in regulating TNF mRNA levels is shown by TTP deficiency in a mouse model. These mice develop a syndrome whose symptoms include inflammatory arthritis, dermatitis, and autoimmunity, and TNF levels are found to be higher, with mRNA half-life being increased (Carballo 1998). Administration of antibodies against TNF to mice prevents the onset of nearly all symptoms (G. A. Taylor et al. 1996). Other 3' elements are also responsible for TNF mRNA dynamics, such as the constitutive decay element (CDE), which is bound by Roquin and Roquin2, which recruit the Ccr4-Caf1-Not deadenylase complex to the mRNA (Leppek et al. 2013).

The p38 MAP kinase pathway (**Figure 1.9**), activated by signals including LPS, causes phosphorylation of TTP by MAP kinase activated protein kinase 2 (**MAPKAPK2** or **MK2**) (Chrestensen et al. 2004). In this first phase of p38-TTP interplay, the phosphorylated TTP is bound by 14-3-3 proteins and becomes localised in the cytoplasm (M. Brook et al. 2006; Johnson et al. 2002). In this form, it is inactive and no longer able to repress ARE-containing mRNAs like TNF (Stoecklin et al. 2004), resulting in a rapid accumulation of such mRNAs. Phosphorylation of TTP by MK2 inhibits its ability to recruit the CAF1 deadenylase complex and deadenylate ARE-containing mRNAs (Marchese et al. 2010). In a second phase, the phosphatase PP2A, which competes with 14-3-3 proteins for phosphorylated TTP, dephosphorylates TTP (L. Sun et al. 2006). At this point, TTP regains its capacity to destabilise ARE-

containing mRNAs and is already localised in the cytoplasm to perform this role. In this phase, levels of ARE-containing mRNAs decline as part of the resolution of inflammation. TTP dynamics in p38 signalling is discussed in depth in this review (Sandler et al. 2008). In addition to regulation of TNF mRNA described above, the mRNA of other pro-inflammatory mediators including PTGS2, IL-10, IL-6, and IL-1 α is also stabilised by p38 through inhibition of TTP-mediated decay (Tudor et al. 2009). IL-1 β mRNA is also subject to ARE-mediated regulation. Like TNF mRNA, it is a target of TTP, with TTP destabilising it. TTP-deficient dendritic cells displayed elevated levels of IL-1 β mRNA compared to wild type dendritic cells, both with and without LPS stimulation (Bros et al. 2010). Stability of IL-1 β mRNA is increased, along with that of several other ARE-containing mRNAs, by p38 signalling (Frevel et al. 2003). KH-type splicing regulatory protein (KSRP) is an ARE-binding protein that promotes mRNA decay (Chou et al. 2006). Astrocytes from KSRP null mice displayed increased levels of IL-1 β mRNA both with and without stimulation by TNF, and also an increase in mRNA stability compared to astrocytes from wild type control mice (X. Li et al. 2012).

1.3.3 Anti-inflammatory effects of cordycepin

A number of studies have shown that cordycepin has anti-inflammatory effects in cells (H. Kim et al. 2011; Jeong et al. 2010b; Shin, Moon, et al. 2009; Y. Li et al. 2016; Kondrashov et al. 2012; Shin, Lee, et al. 2009). In a system of ASM cells stimulated with TNF, cordycepin did not prevent degradation of I κ B or translocation of NF- κ B into the nucleus (Kondrashov et al. 2012). In RAW 264.7 cells, a murine macrophage cell line, NF- κ B nuclear translocation was reduced by cordycepin (H. G. Kim et al. 2006). In HEK 293 cells, NF- κ B nuclear translocation was not prevented by cordycepin, but, at higher concentrations, NF- κ B DNA binding and transcriptional

activities were reduced (Ren et al. 2012). Another group examined rat nucleus pulposus (NP) cells in the context of intervertebral disc degeneration (IDD) (Y. Li et al. 2016). IDD is thought to be a contributing factor to the development of low back pain, and a strong pro-inflammatory environment provided by NP cells is heavily implicated in IDD. Treatment of NP cells with LPS increased expression and production of a number of cytokines, which was reduced by cordycepin treatment. In these cells, phosphorylation of I κ B α and p65 was decreased by cordycepin. It was noted that cordycepin did not affect MAPK signalling, however.

The therapeutic potential suggested by these studies has been tested *in vivo* in animal models of disease. In a study in which mice were infected with *Trypanosoma brucei*, a reduction in cerebral inflammation and pro-inflammatory cytokine levels in the brain was observed upon cordycepin treatment (Vodnala et al. 2009). Anti-inflammatory activity of cordycepin has also been observed in several other animal models of disease, including lung injury, cerebral ischemia/reperfusion injury, and asthma (X. Yang et al. 2015; M. Chen et al. 2012; H. Kim et al. 2011; Cheng et al. 2011).

In a study of nociception in rats, rats had a range of inflammatory mediators injected into their spines a week prior to administration of the hyperalgesic agent prostaglandin E₂ (PGE₂). The enhancement of pain sensation caused by the inflammatory mediators was significantly relieved by administration of cordycepin (Ferrari et al. 2015).

Microglia are brain-resident macrophages and play an important role in CNS repair and homeostasis (Gehrmann, Matsumoto, and Kreutzberg 1995). Their overactivity and increased production of inflammatory mediators is implicated in the progression of neurodegenerative diseases (González-Scarano and Baltuch 1999; Heneka et al.

2015; Liu and Hong 2003). Mounting evidence supporting a role for brain inflammation in Alzheimer's disease has led to significant interest in targeting inflammation to treat the disease (Heneka et al. 2015). Murine microglia stimulated with LPS exhibited increased production of inflammatory mediators, and typical signalling events including increased phosphorylation of p38, ERK1/2, and JNK MAP kinases; I κ B degradation; and NF- κ B (p65) translocation to the nucleus (Jeong et al. 2010a). Pretreatment of cells with cordycepin prior to addition of LPS, compared to LPS alone, resulted in decreased production of inflammatory mediators, reduced phosphorylation of aforementioned MAP kinases, stabilisation of I κ B, and nuclear exclusion of NF- κ B (measured both by Western blotting and immunocytochemistry). A more recent study made similar observations (Jie Peng et al. 2015). With *in vivo* work already showing that cordycepin protected against cerebral ischaemia/reperfusion injury (Cheng et al. 2011), these findings in microglia further support the therapeutic potential of cordycepin for neurodegenerative conditions.

1.4 Osteoarthritis – a therapeutic application of cordycepin?

Osteoarthritis (OA) is a joint disease that affects about a third of the population over the age of 45 in England. It is characterised by a number of hallmark features that include cartilage damage, synovial inflammation, and bone changes. The breakdown of articular cartilage results from the degradation of extracellular matrix by chondrocytes. OA is largely thought of as a non-inflammatory disorder. However, research has shown that inflammation is an integral component of OA progression contributing to the development of its symptoms (Berenbaum 2013). The inflamed synovium (synovitis) releases pro-inflammatory cytokines that can lead to further cartilage degradation. OA is characterised by an increase in anabolic activity in the subchondral bone. Osteoblastic (bone forming) and osteoclastic (bone degrading)

activities become unbalanced and increased bone deposition results in sclerosis of the subchondral bone (bone beneath the articular cartilage) and formation of osteophytes. Osteophytes (new bone formation) appear at the joint margins, subchondral bone thickens, joint capsule enlarges, mild synovitis and effusion are also observed (Johnston 1997; Sunita Suri and Walsh 2012; Wenham and Conaghan 2010). It remains yet to be confirmed whether subchondral bone sclerosis is a cause or consequence of cartilage loss in OA. The increased thickness and density of the subchondral bone and osteophyte formation may be a result of a disordered repair process to increase joint stability. An overview of these changes in the joint physiology is shown in **Figure 1.10**.

Articular cartilage is found at the junction between two or more bones. It functions as a shock absorber and facilitates movement at the joint. In the case of a healthy joint, articular cartilage is neither innervated nor does it have a blood supply, while the adjacent bone, on the other hand, has both a blood supply and nerves. It has been shown that blood vessels grow up from the subchondral bone, breaching the tidemark (a transitional zone which marks the division between articular cartilage and calcified cartilage above the subchondral bone) and invading the normally aneural and avascular articular cartilage in OA (Walsh et al. 2010; S. Suri et al. 2007). The route by which they do this is usually within the vascular channels that extend up from the subchondral bone marrow spaces through the calcified cartilage and into the non-calcified articular cartilage. The separation between bone and cartilage is thus lost and both nerves and blood vessels invade the cartilage from the bone, leading to joint pain.

Chondrocytes are the only cell types found in the articular cartilage. These cells are normally responsible for maintaining the cartilage by balancing matrix production

and degradation. In OA, the chondrocytes become hypertrophic and this balance is shifted towards matrix degradation, resulting in a reduction of cartilage, and chondrocytes also die by apoptosis (van der Kraan and van den Berg 2012; Akkiraju and Nohe 2015). In some cases, the cartilage is completely lost, leaving only bone on either side of the joint margin.

The subchondral bone, i.e. the layer of bone directly under the cartilage, undergoes

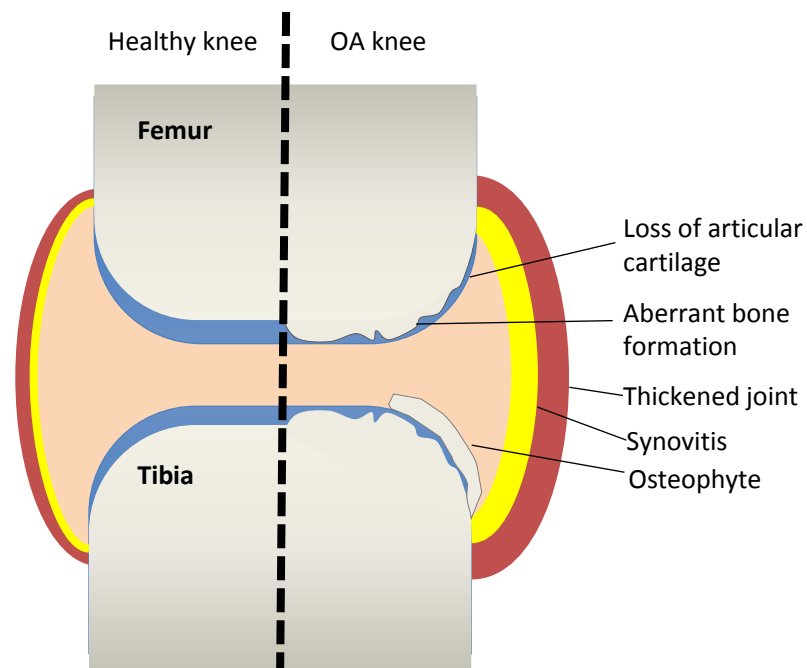


Figure 1.10. Changes in knee physiology in osteoarthritis.

notable remodelling in OA. Normal bone structure is in part maintained through the balance of osteoclasts (bone-degrading cells) and osteoblasts (bone-producing cells). In OA, the balance is disturbed, leading to aberrant bone structure (Sunita Suri and Walsh 2012). Osteophytes are also a common occurrence in OA. These are protrusions of bone that form along joint margins, and can contribute to the disease progression through malalignment of the bones at the joint (Felson et al. 2005).

The synovium encases the synovial fluid within the synovial cavity. This provides the nutrients and external factors required for maintenance of the cartilage.

Inflammation of the synovium (synovitis) is one of the hallmark features of OA

(Haywood et al. 2003). Synovial inflammation contributes to the disease in part through the activity of synovial macrophages and fibroblast-like synoviocytes (FLS). While the degree of inflammation can vary between patients, pro-inflammatory cytokines such as TNF and IL-1 β produced by synovial macrophages can promote degradation of the cartilage (Rahmati, Mobasheri, and Mozafari 2016). Macrophages in the synovial lining also have a role in the formation of osteophytes (Blom et al. 2004). FLS cells can also promote a pro-inflammatory environment that leads to cartilage destruction (A. R. Sun et al. 2016; Philp, Davis, and Jones 2016). In OA, synovial fluid may contain calcium pyrophosphate dehydrate (CPPD) crystals which are capable of activating the NLRP3 inflammasome in macrophages which, following caspase-1 proteolytic activation, enhances IL-1 β and IL-18 secretion (Jin et al. 2011). Basic calcium phosphate (BCP) crystals, which can also be found in OA synovial fluid, have been shown to induce IL-1 β secretion by macrophages through the NLRP3 inflammasome *in vitro*.

Together, the changes in subchondral bone, cartilage, and the synovium contribute to the pain associated with OA and the progression of the disease. Given that inflammation plays a part in the destruction of the cartilage, cordycepin may have therapeutic benefit in reducing pain in OA patients. In human chondrocytes from OA patients, IL-1 β -driven increases in proinflammatory cytokine production were inhibited by cordycepin pretreatment (Ying et al. 2014), and degradation of I κ B by IL-1 β was also prevented by cordycepin in these cells. Cordycepin was also able to inhibit the impairment of osteogenesis (bone formation) by oxidative stress in bone marrow mesenchymal stem cells (BM-MSCs) (F. Wang et al. 2015). Reactive oxygen species (ROS) are important in the differentiation of osteoclasts (N. K. Lee et al. 2005). Consistent with its role in opposing the effects of oxidative stress in BM-

MSCs, cordycepin was found to scavenge ROS generation and inhibit osteoclastogenesis (Dou et al. 2016).

1.5 Project aims and outcomes

The aim of my PhD project was twofold: to investigate the role of polyadenylation in the inflammatory response, and to gain insight into how cordycepin's anti-inflammatory effects were mediated. This was to be measured in RAW 264.7 macrophages, using LPS as a stimulus to induce an inflammatory response. Addition of LPS to RAW 264.7 cells did, indeed, result in increased inflammatory gene expression measured over a 2 hour period after addition of LPS. Adding cordycepin either 1 hour before LPS or 10 minutes after LPS led to a pronounced decrease in inflammatory mRNA levels (for both mature transcripts and pre-mRNA). This was confirmed on a genome-wide scale through microarray and cluster analysis. It was found that *Tnf* mRNA (whose levels are >100-fold increased following LPS treatment) experiences an increase in poly(A) tail size following LPS treatment, while housekeeper mRNA poly(A) tail size is unaffected. Performing this experiment with the nuclear fraction, to assess initial poly(A) tail size of newly synthesised mRNA, also showed an increase in *Tnf* poly(A) tail size, indicating that nuclear polyadenylation may be dynamic in the inflammatory response. The *Tnf* poly(A) tail size increase is noticeably reduced in the presence of cordycepin. Inhibition of cordycepin's import into the cell or its phosphorylation abrogated its anti-inflammatory effects. Taken together, these data suggest that, in a macrophage system, polyadenylation is dynamic in response to an inflammatory stimulus, and that cordycepin has specific anti-inflammatory effects that it elicits intracellularly, possibly through effects on polyadenylation. These data support the case for cordycepin as a potential therapeutic for diseases in which inflammation is involved.

Work done by James Burston (with whom I collaborated) in a rat model of osteoarthritis showed that cordycepin reduced pain behaviour associated with OA, but I was unable to see changes in inflammatory cytokine mRNA in the synovium. This suggests these mRNAs are not the therapeutic target in this case, or at least not in that tissue. However, the effects on pain behaviour still add weight to the therapeutic potential of cordycepin.

2 Materials and methods

2.1 Cell work

2.1.1 Cell culture

RAW 264.7 mouse macrophage cells were cultured in Dulbecco's Modified Eagle Medium (DMEM) (Sigma, cat no 6429) supplemented with 10% foetal bovine serum (FBS) (Sigma, cat no F9665-500ml). Cells were split into fresh flasks whenever they reached ~80% confluence. All experiments were done on cells between passage 20 and 40.

NIH-3T3 mouse fibroblasts were cultured in DMEM supplemented with 10% newborn calf serum (NBCS). For serum induction experiments, 10^6 cells were seeded in 10 cm plates (TPP, cat no 93100), then had medium changed to DMEM + 0.5% NBCS after 24 hours. 24 hours after this change of medium, cells were stimulated with addition of 10% NBCS. The experiment using NIH-3T3 cells from which data is presented in this thesis (**Figure 3.7**) was performed by Cornelia de Moor.

2.1.2 Cell stimulation with lipopolysaccharide (LPS) and treatments with compounds

RAW 264.7 cells were seeded into 15 cm plates (TPP, cat no 93150) 10 cm plates (TPP, cat no 93100), 6 cm plates (TPP, cat no 93060), 6-well plates (TPP, cat no 92006), or 12-well plates (TPP, cat no 92012). Seeding densities ranged from 2×10^3 - 6×10^4 cells/cm². 24 hours after seeding, the medium was aspirated, cells were washed in the same volume of phosphate-buffered saline (PBS) as the medium, and then DMEM + 0.5% FBS was added. ~24 hours after this, the experiment would take

place, with LPS (Sigma, cat no L6761) being added at a final concentration of 1 µg/ml for the desired duration. For some experiments, the LPS was added ~24 hours after seeding, without any change of medium.

For samples that were to be treated with cordycepin (≥98% pure) from *Cordyceps militaris* (Sigma, C3394), the cordycepin dissolved in DMSO (stock concentration 20 mM) was added to all plates (20µM final concentration unless otherwise indicated) 1 hour before, at the same time as, or 10 minutes after the addition of LPS to any plate. Fungal extracts (preparation described below) were treated as 1000-fold concentrated stocks, and so were added at 1/1000 of the volume of medium in which the cells were seeded. Pentostatin (Sigma, cat no SML0508) was added at the same time as cordycepin at 1nM concentration. Adenosine (Sigma, cat no A4036) was added at the same time and concentration as cordycepin. The adenosine transporter inhibitor S-(4-Nitrobenzyl)-6-thioinosine (NBTI) (Sigma, cat no N127) and the adenosine kinase inhibitor 5-Iodotubericidin (ITu) (Sigma, cat no I100) were added 15 minutes prior to cordycepin treatment.

2.1.3 Preparation of fungal ethanol extracts for use in cell culture

Cordyceps militaris fungi were from Hainan SHUNTIAN Biological Technology Co Ltd; *Ophiocordyceps sinensis* tablets (500 mg biomass per tablet) were from Mycology Research Laboratories Ltd; and *Pleurotus ostreatus*, *Agaricus bisporus*, and *Flammulina velutipes* were purchased from Sainsbury's supermarket. The fungus or starting material was ground and 1g dissolved in 20 ml ethanol. This suspension was then placed on a tube roller for 1 hour and then allowed to stand for 15 minutes. Supernatant was then divided into several 2 ml tubes, which were centrifuged at 10,000 g at 4°C for 30 minutes. Supernatant was pooled and filtered in a laminar flow hood for sterility. This sterile mix was then divided into several tubes (500 µl

per tube) and spun in a vacuum concentrator until dry. Once all the ethanol had evaporated, 25 µl of DMSO was added to each tube, thoroughly mixed, and then all liquid was combined to obtain a single, homogeneous mixture. This was divided into aliquots and stored at -20°C for further use.

2.1.3.1 Assessing cordycepin and 3' deoxyinosine concentration in fungal extracts by liquid chromatography/mass spectrometry (LC/MS) (performed by Wahyu Utami)

LC/MS analysis was performed by Wahyu Utami – the method described below is taken from her PhD thesis (Utami Wahyu 2015):

“Analyses of samples were carried out on an Agilent 1100 HPLC system (Agilent, Santa Clara, CA, USA) with auto sampler maintained at 8°C. Separations were achieved on a Luna C-18, 3 µm (2 × 150 mm) column with Security Guard (4 × 2 mm) (Phenomenex, Macclesfield, UK) at 40°C. The standards and the samples were eluted using a gradient mobile phase containing of 5 mM DMHA in water:methanol (95:5 v/v) (A), and 5 mM DMHA in methanol: water (80:20 v/v) (B). Mobile phase A was adjusted to pH 7 using acetic acid. The gradient condition was: 0-5 min, 10-20% B; 5-10 min, 20-28 % B; 10-22, 28-40 % B; 22-25, 40-10 % B; 25-35 min, 10 % B. The volume of sample injected to the column was 5 µL. The flow rate was set at 200 µL/min.

MS data were acquired on Waters Quattro Ultima triple quadrupole mass spectrometer (Waters, Milford, MA, USA) in negative electrospray ionisation (ESI) mode. Source temperature was at 125°C, with nitrogen as drying and nebulising gas and argon as collision gas. Multiple reactions monitoring (MRM) scan was used with dwell time 0.1 s. The MS system and data were processed by Waters MassLynx™ Software.”

2.1.4 Statistical tests for comparing cell treatments

Statistical tests were performed using GraphPad Prism version 6 for Windows (GraphPad Software, La Jolla California USA). 2-way ANOVA was performed with means between different conditions compared to each other within each group. For **Figure 5.5**, this means comparing the mean values for 0 nM pentostatin to the mean values for 1 nM pentostatin within each separate cordycepin concentration tested. For **Figure 5.9**, it means comparing the mean values for both C+10 and C-60 to the control mean (DMSO) within each separate timepoint. Default options were left unchanged, and recommended tests were used following the ANOVA. For **Figure 5.5**, the recommended test was Sidak's multiple comparisons test, and for **Figure 5.9**, it was Dunnett's multiple comparisons test.

2.2 RNA work

2.2.1 RNA isolation

At the end of any experiment, cells were harvested as follows:

Cells in 10cm/15cm plates	Cells in 6-well or 12-well plate
<ul style="list-style-type: none">Put plates on ice, aspirate medium from cells, and wash twice with ice-cold PBS (Oxoid, cat no BR0014G)	
<ul style="list-style-type: none">Add 5 ml ice-cold PBS and scrape cells using cell scraper (Greiner Bio-One, cat no 541070)	<ul style="list-style-type: none">Add lysis buffer from RNA isolation kit* directly to cells on plate, then transfer lysate to fresh tube
<ul style="list-style-type: none">Transfer cell suspension to fresh 15 ml tube and spin at 775 g for 2 minutes	
<ul style="list-style-type: none">Aspirate supernatant and add lysis buffer from RNA isolation kit* to cell pellet	

RNA was then isolated from the lysates using an RNA isolation kit, following manufacturer's protocol (except DNase treatment was done for 1 hour rather than 15 minutes), and stored at -20°C. *All experiments done before November 2015 used the NucleoSpin RNA kit (Macherey Nagel, cat no 740955), while experiments done thereafter used the ReliaPrep™ kit (Promega, cat no Z6012). The two kits performed equally well in our experience – the switch was made purely due to the ReliaPrep™ kit being cheaper.

2.2.2 RNA isolation from nuclear and cytoplasmic fractions

Fractionation experiments were done using a 15 cm plate for each timepoint. At the end of the experiment, cells were washed twice with ice-cold PBS, and then scraped in 5 ml ice-cold PBS with a cell lifter (Corning, cat no 07-200-364). All centrifugation was done at 4°C. The cell suspension was spun at 700 g for 5 minutes, the supernatant was discarded, and the pellet resuspended in 1 ml PBS. This suspension was centrifuged at 500 g for 5 minutes and supernatant was discarded. The pellet was resuspended in 400 µl of buffer A (10 mM HEPES pH 7.9, 10 mM KCl, 0.1 mM EDTA, 0.1 mM EGTA, 1 mM DTT, 0.5 mM PMSF) and incubated on ice for 15 minutes. 25 µl of 10% NP-40 was then added to the suspension which was vortexed for 10 seconds and placed on ice for 5 minutes. This mix was then centrifuged at 16,000 g for 1 minute, resulting in pelleted nuclei and a cytoplasmic supernatant. Approximately 60% of the supernatant was collected in a new tube (in order to avoid nuclear contamination by trying to collect all of the supernatant), and had an equal volume of 100% isopropanol added. This was then centrifuged at 16,000 g for 30 minutes. While spinning, the remaining supernatant was discarded, and the nuclear pellet was washed three times with 400 µl buffer A to remove remaining cytoplasmic material. When the cytoplasmic centrifugation was complete,

supernatant was aspirated yielding a cytoplasmic pellet. Cytoplasmic and nuclear pellets then had the appropriate amount of lysis buffer added from the RNA isolation kit. For the NucleoSpin kit, the lysis buffer volume used was 350 μ l. For the ReliaPrep™ kit, the volume used was 100 μ l for up to 5×10^5 cells, 250 μ l for 5×10^5 - 2×10^6 cells, and 500 μ l for any more than that. RNA was isolated from lysates following the manufacturer's protocol but with a 1 hour DNase treatment rather than the stated 15 minutes. Once eluted from the isolation kit, nuclear RNA was subjected to another DNase digestion using TURBO™ DNase (Ambion™, cat no AM2238), following manufacturer's protocol. RNA was then extracted by a phenol/chloroform extraction and precipitated with ethanol and sodium acetate. After washing and redissolving the nuclear pellet, cytoplasmic and nuclear RNA isolation was complete. Fractionation was validated by RT-qPCR to check for enrichment of pre-mRNA in the nuclear RNA sample.

2.2.3 4-thiouridine labelling for nascent mRNA capture performed by Richa Singhania

Labelling transcripts in the cells: 250 μ M 4-thiouridine (4SU) was added to RAW 264.7 cells 15 minutes before harvesting the cells.

To harvest, cells were placed on ice, washed twice with ice-cold PBS, and immediately lysed with 10 ml TriPure reagent and transferred to a fresh tube. 4SU-labelled yeast RNA was added at this point as a spike-in for later analysis purposes (see below). 2 ml chloroform/isoamyl alcohol (24:1) was added and the tube was incubated on ice for 10 minutes before being centrifuged at $>18,000$ g for 10 minutes. The top aqueous layer was removed and subject to an ethanol/sodium acetate precipitation, after which the pellet was redissolved in water, subjected to a TURBO DNase treatment following manufacturer's protocol.

Biotinylating 4-thiouridine labelled RNA: DNase-treated RNA, having been cleaned up, was then heated at 65°C for 5 minutes before being placed on ice. The following were then added (final concentrations are indicated) to the RNA for a final volume of 400 µl per 40 µg RNA: Tris-HCl pH 7.4 (10 mM), EDTA (1 mM), EZ-Link™ HPDP-Biotin (0.2 mg/ml) (Thermo, cat no 21341). This was then rotated at room temperature in the dark for 1 hour and 30 minutes, after which an equal volume of chloroform/isoamyl alcohol (24:1) was added and the aqueous phase was then collected using MaXtract column (Qiagen, cat no 129046). RNA was precipitated using isopropanol and NaCl, and pellet redissolved in water.

Fractionating the RNA: Streptavidin paramagnetic beads (Promega, cat no Z5482) were pipetted into a tube (200 µl per 70 µg RNA), placed into a magnetic rack, and the buffer was replaced with 200 µl of fresh MPG buffer (1M NaCl, 10 mM EDTA, 100 mM Tris-HCl pH 7.4). A known quantity of thiouridine-labelled RNA from *S. pombe* was added to the total RNA as a spike-in for data analysis purposes later (see below). RNA was heated at 65°C for 10 minutes, and then added to the beads and rotated at room temperature for at least 20 minutes. The tube was then placed on the magnetic rack – biotinylated nucleic acids are bound to the beads, while non-labelled RNA is contained in the supernatant. Supernatant (unlabelled fraction) was transferred to a fresh tube and kept on ice. Beads were washed for 5 minutes with 750 µl MPG buffer four times. The fourth wash was collected as a control fraction which should be free of RNA. 100 µl of 0.1 M DTT was added to the beads and rotated for 10 minutes to elute the bound, labelled RNA. The tube was placed onto the rack and supernatant (labelled RNA) collected in a fresh tube on ice. This was repeated and the second labelled RNA elution pooled with the first.

Final cleanup: the unlabeled fraction was precipitated with ethanol and sodium acetate and then redissolved in water. The labelled fraction was purified using RNeasy MinElute cleanup kit (Qiagen, cat no 74204).

Yeast spike-in and analysis: fixed amounts of 4SU-labelled RNA isolated from *S. pombe* were added to the cell lysate in TriPure reagent prior to isolating total RNA and performing the fractionation, as mentioned previously. RNA samples were then sent for RNAseq on the NextSeq platform. Raw reads from the sequencer then had adapter sequences and low quality base calls trimmed. Remaining reads were mapped to the joined mouse and *S. pombe* genomes – the best matches were returned and ambiguous mappings were discarded. For both the 4SU-labelled RNA and the total RNA, the number of reads mapping to features in the genome was counted. In order to compare the numbers of transcripts between 4SU-labelled and total RNA samples, the numbers must be adjusted so that they are on the same scale. This was accomplished using the *S. pombe* RNA spike in – since this was of a known, fixed amount, the fraction of 4SU-labelled RNA relative to the total could be calculated. The resulting scaling factor was used to scale the fragments per kilobase per million mapped reads (FPKM) values of the 4SU-labelled fraction. The FPKM values could then be used to calculate transcription rates (4SU-labelled FPKM) and decay rates (4SU-labelled FPKM divided by total FPKM).

2.2.4 Reverse transcription quantitative PCR (RT-qPCR)

RNA was reverse transcribed to cDNA using SuperScript™ III reverse transcriptase (Invitrogen, cat no 18080-044). For each sample, 500 ng of RNA was used with 120 ng of random hexamers (Invitrogen, cat no 48190-011), 0.5 mM dNTP mix (nucleotides supplied in separate tubes from Thermo, cat no R0182), 1x first strand buffer (supplied with kit), 5 mM DTT, and 0.5 µl of SuperScript™ III enzyme, in total

volume of 20 μ l. Incubations were done as per the protocol. At the end of the reaction, 180 μ l of water was added to dilute the cDNA 10-fold. The cDNA could then be used as template for qPCR.

In later experiments, SuperScript™ IV (Invitrogen, cat no 18090050) was used. Reaction was performed as above, but first strand buffer was replaced with SSIV buffer. Incubations were done as per manufacturer's protocol.

Earlier qPCR was done on an Agilent MX3005P qPCR machine (Agilent, cat no 401513-64000), while later work was done on a Qiagen Rotor-Gene Q qPCR machine (Qiagen, cat no 9001560).

MX3005P

qPCR was done using Promega SYBR Green GoTaq® qPCR master mix (Promega, A6002). Reactions were done in a volume of 20 µl with 4 µl of cDNA, a final primer concentration of 0.25 µM, and 1X GoTaq® qPCR master mix. PCR programme:

10 mins at 95°C

30 seconds at 95°C
30 seconds at 58°C
30 seconds at 72°C

} ×50

60 seconds at 95°C
30 seconds at 55°C
30 seconds at 95°C

} This is the dissociation
curve analysis segment

Options selected in the MxPro software, when setting up the above programme:

SYBR Green with dissociation curve, 'SYBR' box ticked.

Rotor-Gene Q

Reactions were done with 2 µl of cDNA, a final primer concentration of 1 µM, and 1X GoTaq® qPCR master mix in 10 µl total reaction volume. PCR programme:

5 mins at 95°C

10 seconds at 95°C
20 seconds at 60°C
20 seconds at 72°C

} ×40

Melt segment (default)

Gain optimisation was performed at 60°C at start of run, and before melt.

qPCR data were analysed using the $2^{-\Delta\Delta Ct}$ method.

2.2.5 Microarray analysis (data analysis performed by Graeme Thorn)

RNA was analysed from RAW 264.7 cells exposed to four treatment conditions (full details are given below): LPS stimulated and unstimulated cells both with and without a cordycepin pre-treatment (cells that were not pre-treated with cordycepin were pre-treated with DMSO instead).

Four wells of a 6-well plate were seeded with RAW 264.7 cells in DMEM + 10% FBS. Cells were washed and medium replaced with DMEM + 0.5% FBS after 24 hours. A further 24 hours later, one pair of wells had DMSO added, and the other pair of wells had 20 μ M cordycepin added. After a 60 minute incubation, two wells (one DMSO-treated well and one cordycepin-treated well) had LPS added at 1 μ g/ml. Nothing was added to the other two wells. 60 minutes later, all cells were lysed and RNA extracted as described in **section 2.2.1**. To summarise, cells were pre-treated with DMSO or cordycepin and then either stimulated with LPS or not. Cell conditions were named 'D0', 'D60', 'C0', and 'C60' – D means DMSO pre-treated, C means cordycepin pre-treated, 0 means NOT stimulated with LPS, 60 means LPS-stimulated.

This experiment was performed in biological quadruplicate (16 RNA samples in total), and these were then analysed on a SurePrint G3 Mouse Gene Expression 8x60K microarray kit (Agilent, cat no G4852A). Each slide for the microarray has 8 array slots. As we had 16 samples, 2 slides were used with 2 biological replicates on each.

Raw data were processed using limma (Ritchie et al. 2015) and affy R packages to read the data directly from the microarrays. Each individual microarray was then normalised using the 'qspline' option which matches the quantiles of intensities for each microarray. Estimates of measurement errors were taken from replicate arrays

using an empirical Bayes procedure, which calculates an estimated error based on duplicates on individual arrays. Probes for which intensity was greater than the background + error estimate were retained, while probes for which this criterion was not met were marked as “not above background”. Differences between the mean values were calculated between pairs of conditions: D0 vs D60, C0 vs D0, and C60 vs D60. Individual tests were performed if difference between conditions was significantly non-zero. P-values were corrected from individual p-values by Bonferroni procedure: p-values were multiplied by the number of comparisons made between conditions and capped at a maximum value of 1 (corrected p-val = $\max(1, p\text{-val} * \#\text{tests})$).

Gene ontology (GO) analysis for lists of genes generated from microarray data was performed using DAVID (<https://david.ncifcrf.gov>). The list of genes was uploaded to DAVID functional annotation tool along with a background list (containing all measurable genes on the microarray chip). The proportion of genes within a GO term out of the total number of genes in the list of interest was compared to the proportion of genes within the same GO term in the background list. The ratio between these two proportions represents the fold enrichment. The test for significance is based on Fisher’s exact test with p-values then adjusted by Bonferroni procedure (the raw p-value is multiplied by the number of comparisons being made) to correct for multiple comparisons.

2.2.6 Poly(A) tail measurement

3’ end labelling using [5'-³²P]Cytidine 3',5'-bis(phosphate) (³²P-pCp) and RNA ligase was performed as described (Minvielle-Sebastia et al. 1991). Briefly, ³²P-pCp was

ligated to the 3' end of total RNA, following which the RNA and ligase mixture was subjected to RNase and proteinase K treatment to digest the enzyme and all non-poly(A) RNA. A phenol/chloroform extraction and ethanol precipitation was done to then purify the remaining non-digested RNA (just poly(A) tails). These RNA samples were then run on a TBE-urea PAGE gel. The gel was then placed in a cassette with a phosphor screen and incubated at -80°C for 3-5 days before being imaged on a GE Storm 825 phosphorimager.

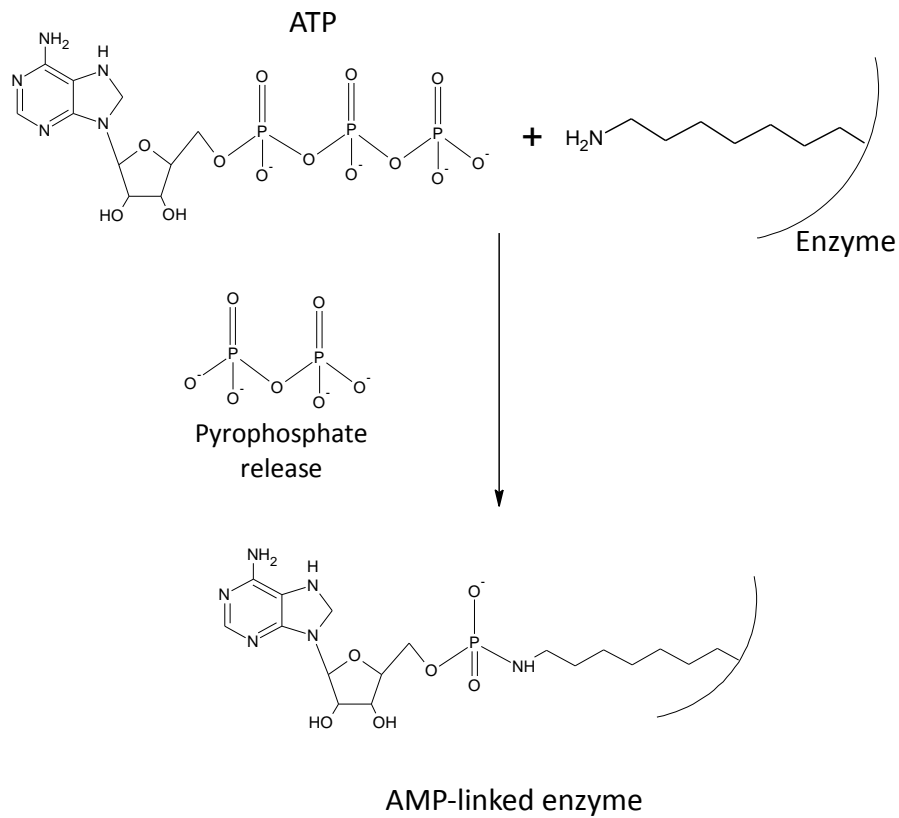
The poly(A) tail test (PAT) assay is done to assess poly(A) tail length. 3 different types of PAT were used – RL1-PAT, RL2-PAT, and sPAT (I/T). RL1-PAT was an older method that was supplanted by RL2-PAT. sPAT (I/T) was tested against RL2-PAT for potential improvements, but was found to be an inferior method, and so RL2-PAT was kept as the method in use.

For **RL1-PAT**, the 3'-blocked anchor oligo ('PAT-R1 anchor') was ligated to the 3' end of an RNA sample. 50 pmol of anchor and 2 µg of RNA were combined in an 8 µl volume. This mix was incubated for 5 minutes at 65°C, and then had 10 units of T4 RNA ligase 1 (NEB, cat no M0204S) added together with the supplied reaction buffer for a final concentration of 1X. The ligation mix was incubated at 37°C for 2 hours, then 15 minutes at 65°C to heat inactivate the enzyme. After this, reverse transcription was done directly on the resulting mix using SuperScript III. Reaction was done using 1 µM PAT-R1 (complementary to the ligated anchor oligo), 0.2 mM dNTP mix, 1x first strand buffer, 5 mM DTT, and 1 µl of SuperScript™ III enzyme, in total volume of 50 µl. Incubations done as per manufacturer's protocol.

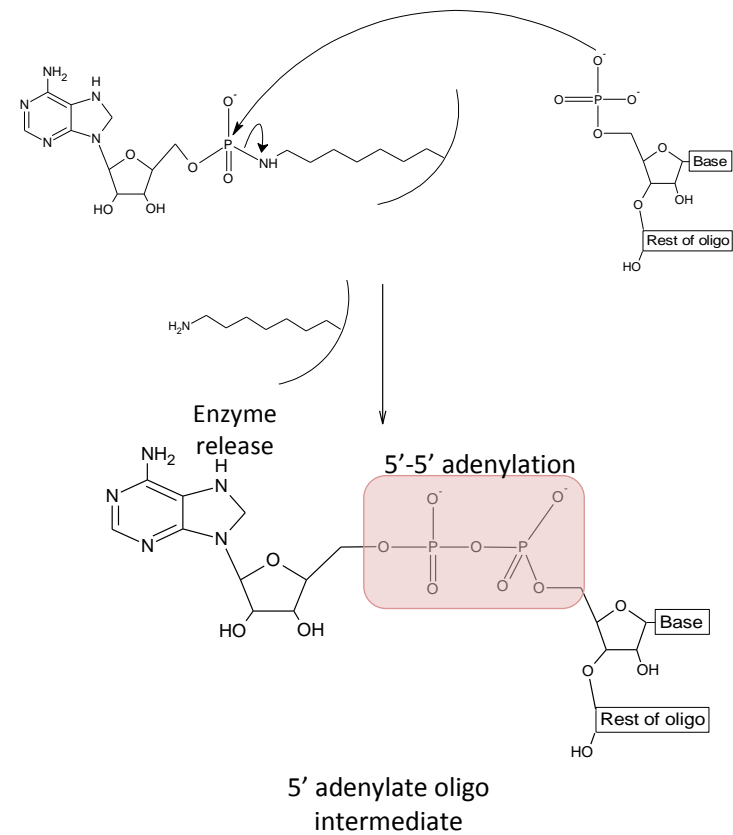
During the ligation, the oligo receives a 5'-5' adenylation (catalysed by the enzyme using ATP in the reaction buffer) to form an intermediate species (**Figure 2.1**). T4 RNA ligase 1 used in RL1-PAT is capable of generating this intermediate, which can

then be ligated to the 3' end of an acceptor RNA molecule. For **RL2-PAT**, T4 RNA ligase 2 truncated KQ (NEB, cat no M0373S) was used, which is incapable of generating the intermediate. It requires the donor oligo to already have the modification made. The enzyme can only ligate the pre-formed intermediate to an acceptor RNA molecule. The 5'-5' adenylation can be done using Mth RNA ligase from the 5' DNA adenylation kit (NEB, cat no E2610S), or oligos can be ordered with this modification already made. Since T4 RNA ligase 2 truncated KQ requires its substrates to be 5'-5' adenylated already, and is incapable of ligating 5'-phosphorylated substrates (Ho et al. 2004; Ho and Shuman 2002), endogenous RNA cannot supply the 5' end for the RL2-PAT ligation reaction and endogenous RNAs are not ligated to each other by this enzyme. Additionally, RL2-PAT ligation is ATP-independent. The ligation reaction used in RL2-PAT will be referred to as L2T.

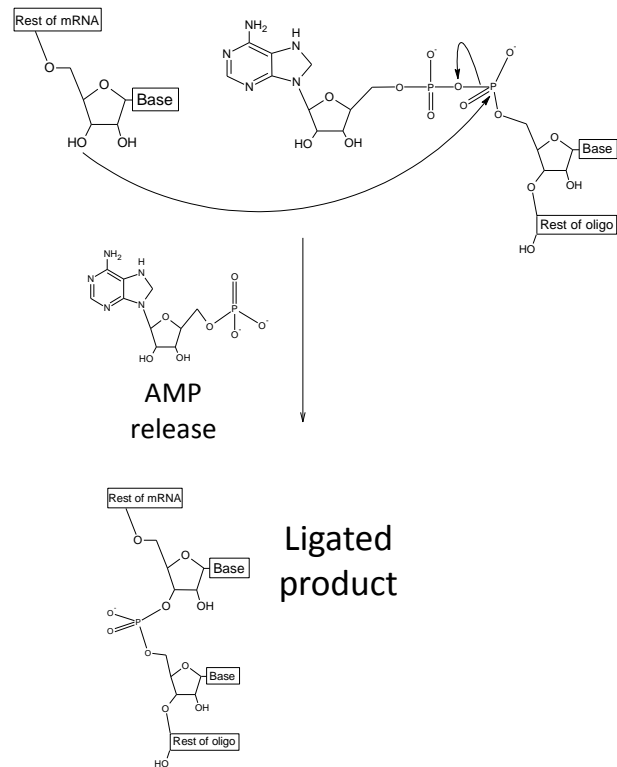
Step one – linking AMP to the ligase enzyme



Step two – transfer of AMP from the enzyme to the 5' phosphate of the donor oligo



Step three – formation of phosphodiester bond between the donor oligo 5' end and acceptor oligo (or mRNA) 3' hydroxyl group



Enzyme	Step 1	Step 2	Step 3
T4 RNA ligase 1	✓	✓	✓
Mth RNA ligase	✓	✓	✗
T4 RNA ligase 2	✓	✓	✓
T4 RNA ligase 2 truncated (KQ)	✗	✗	✓

Figure 2.1. Mechanism of RNA ligation. The ligation of an ssRNA or ssDNA oligo to ssRNA is completed in 3 steps. The table shows the ability of different enzymes to perform each step. An ssRNA donor oligo is depicted here, but is mechanistically interchangeable with ssDNA.

When assessing RL2-PAT as an alternative to RL1-PAT, Mth RNA ligase was used to perform the 5'-5' adenylation on the PAT-R1 anchor oligo. After determining that RL2-PAT was superior to RL1-PAT, a new anchor was ordered with the modification already made. This anchor was termed 'PAT-R1 anchor oligo (L2T)' (**Table 2.1**). The RL2 ligation was performed using 0.5 µg RNA, 20 pmol 5'-rApp PAT anchor oligo, 15% PEG 8000, and 10 units T4 RNA ligase 2 truncated KQ, with 1X supplied buffer in a 20 µl reaction volume. Note that this ligation is done in the absence of ATP. The ligation mix was incubated at 16°C overnight, following which a reverse transcription was done in the same way as is done for RL1-PAT, but all quantities were doubled, since the ligation mix volume for RL2-PAT is double that of RL1-PAT.

Splint mediated PAT (sPAT) involves the use of a DNA 'splint' oligo, which is supposed to contribute to the sensitivity and accuracy of the assay. An overview of the ligation used in sPAT is shown in **Figure 2.2**. It uses a 3'-blocked RNA anchor oligo (whereas RL1-PAT and RL2-PAT both use a DNA anchor oligo) and a DNA splint which has a 5' sequence complementary to the anchor followed by a string of T bases, designed to base pair to the poly(A) tail of mRNA. The splint, RNA sample, and the RNA anchor are mixed, heated, and then gradually cooled to room temperature. Under these conditions, the RNA anchor first base pairs to the splint. The non-paired T bases of the splint in this RNA-DNA hybrid then serve to guide the splint to the 3' ends of mRNA, by base pairing with the last A bases in poly(A) tails. At this point, T4 RNA ligase 2 is added, which repairs nicks in double-stranded RNA. This is not the same enzyme as that used in RL2-PAT (T4 RNA ligase 2 truncated). T4 RNA ligase 2 ligates 5'-phosphorylated oligos and can perform all steps of the ligation process (**Figure 2.1**). Once the ligation incubation is complete, the ligation mix is subjected to a DNase I treatment to remove the DNA splint. The ligated RNA is then cleaned up

by a phenol/chloroform extraction and ethanol precipitation, whereupon it can be reverse transcribed to PAT cDNA and used for PCR.

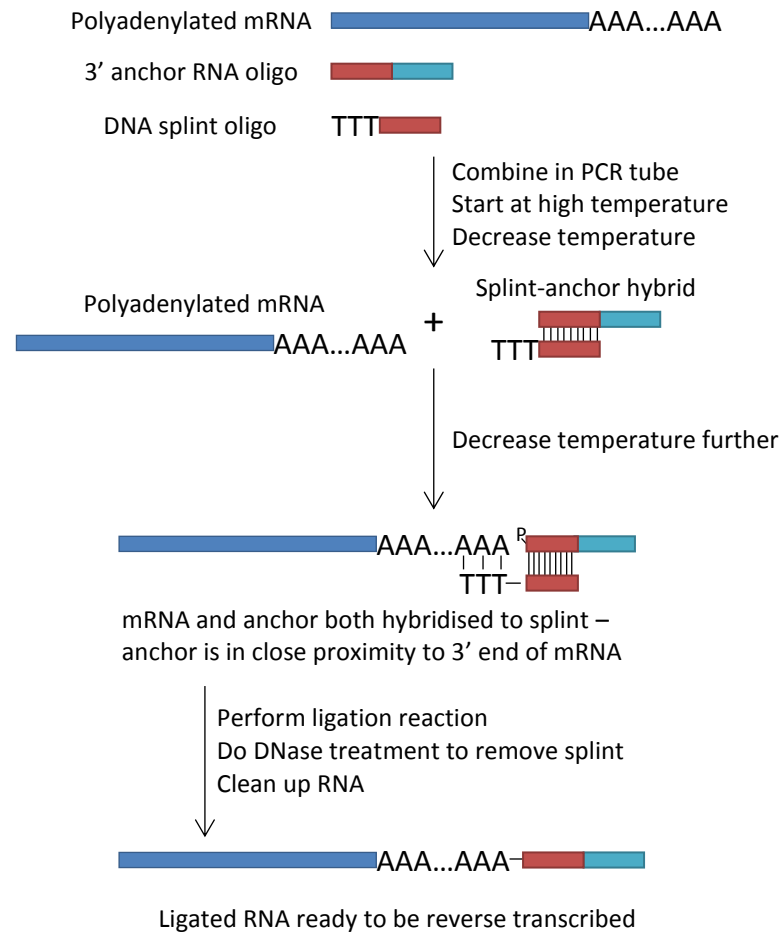


Figure 2.2. Overview of sPAT ligation. Total RNA is mixed with a 3'-blocked RNA anchor oligo and a splint. The splint has a 3' stretch of T bases that are complementary to the poly(A) tail, and a 5' stretch (red) that is complementary to part of the anchor oligo. After an initial melt phase in the thermocycler, the temperature is cooled enough to favour hybridisation between the splint and anchor only. The temperature is then cooled enough to favour hybridisation between the splint's T stretch and poly(A) tails. The splint thus guides the anchor to the 3' ends of mRNAs. The ligation reaction is then performed, a DNase treatment done to remove the splint, and the RNA is cleaned up, whereupon reverse transcription and PCR can be done as in RL1-PAT.

The version of sPAT we tested deviated from the published protocol (Minasaki, Rudel, and Eckmann 2014). The RNA oligo sequence was adapted so that we could use our existing PAT-R1 primer to do the reverse transcription and PCR. The DNA splint sequence was modified to be complementary to our modified RNA oligo. In addition to a DNA splint with a stretch of T bases, a second splint was designed in which the T bases were replaced with an equal number of inosine bases. This was in order to avoid biasing against mRNAs with terminal uridylation. sPAT using the oligo (dT) splint is abbreviated to sPAT (T) and sPAT using the oligo(dI) splint is abbreviated to sPAT (I). The last change made was to not only perform the ligation as it was done in the original publication, but also to test sPAT with the L2T ligation method. Written below is the method using the L2T ligation. For the original sPAT ligation, details are in the original publication.

1 µg of RNA was mixed with 20 pmol DNA splint and 3 pmol anchor in a 10 µl volume. This was then heated to 70°C for 5 minutes, then 60°C for 5 minutes, then 42°C for 5 minutes, then 25°C for 5 minutes, and then held at 15°C. This programme should favour first the hybridisation of the splint to the anchor, and then the hybridisation of the overhanging splint-anchor hybrid to the 3' end of mRNA. 10 units of T4 RNA ligase 2 truncated KQ was then added to the mix, with 1X reaction buffer and 15% PEG 8000 in a total reaction volume of 20 µl, and this was incubated overnight at 15°C. Following this, the ligation mix was subjected to a DNase digestion using TURBO™ DNase (Ambion™, cat no AM2238), following manufacturer's protocol, to remove the DNA splint. Following DNase treatment, the mix was subjected to a phenol/chloroform extraction and ethanol precipitation. The RNA pellet was redissolved in 20 µl water, and then subjected to reverse transcription using SuperScript III, in the same way as is done for RL2-PAT.

For all PAT types, once the reverse transcription was complete, the PCR step was done in the same way, using GoTaq G2 polymerase (Promega, cat no M7801). Reactions were done in a 50 µl volume with 1 µl PAT cDNA, 1X supplied buffer, 1.5 mM MgCl₂, 0.2 mM dNTP mix, 0.4 µM forward PAT primer, 0.4 µM reverse PAT primer (PAT-R1), and 1.25 units of GoTaq G2 polymerase. PCR programme: 5 minutes initial denaturation at 95°C, followed by 40 cycles of 1 minute at 95°C, 1 minute at 58°C, and 2 minutes at 72°C, and ending with a 10 minute final extension at 72°C. PCR products were then run on an agarose gel pre-stained with SYBR Safe (Invitrogen™, cat no S33102) at 4V/cm for 2.5-3 hours.

Gene name	Primer name	Sequence (5'-3')	Expected deadenylated product size/bp
Cxcl2	Cxcl2 PAT 1	TGGGGGTGGGGACAAATAGA	339
Fosb	Fosb 3F1	ATTGACTCCATAGCCCTCAC	189
Rpl28	Rpl28 3F1	GCCACTTCTTATGTGAGGAC	259
Tnf	TNF PAT 1	CTCTACCTTGTTGCCTCCTCTT	215
-	PAT-R1 anchor (RL1)	GGTCACCTTGATCTGAAGC-NH ₂	-
-	PAT-R1 anchor (L2T)	/rApp/GGTCACCTTGATCTGAAG/ddC/	-
-	sPAT anchor	/5Phos/GGUCACCUUGAUCUGAAGC-NH ₂	-
-	sPAT I splint	TCAGATCAAGGTGACCCCCCCCC-NH ₂	-
-	sPAT T splint	TCAGATCAAGGTGACCTTTTTTTTT-NH ₂	-
-	PAT-R1	GCTTCAGATCAAGGTGACCTTTTT	-

Table 2.1. List of PAT primers. Note sPAT anchor is entirely RNA. All other primers are DNA. Expected PCR product sizes resulting from PAT using cDNA synthesised from deadenylated RNA samples is shown.

After imaging the agarose gels on a Chemidoc XRS UV transilluminator (Biorad, cat no 1708265), the image was analysed using Quantity One 1-D analysis software (Biorad, cat no 1709602). Lanes in the image were framed and scanned, yielding a plot of physical distance migrated vs intensity for each lane, including one empty lane to measure background intensity. These data were exported and processed in Microsoft Excel as described below.

Firstly, physical distance was plotted against the \log_2 (base pairs) of the DNA fragments in the ladder (100 bp ladder, NEB cat no N3231S). Since the ladder fragments are of defined sizes, they can be used to derive a relationship between physical distance migrated and DNA length (bp). A fourth order polynomial trendline was fitted to the plot of physical distance vs \log_2 (base pairs) for the ladder lane. The equation of the trendline was then used to convert physical distance migrated to DNA length (bp). Note that this was only done within the range of the data available i.e. the smallest and largest fragment sizes in the ladder (100 bp and 1517 bp respectively). All data points outside this range were removed.

Secondly, the column representing background intensity values down the lane were subtracted from the intensity values for all sample lanes. The resulting background-corrected intensity values were then all divided by their corresponding DNA size (bp) to account for the fact that longer DNA molecules will produce a stronger signal.

Lastly, these intensity values in each lane were divided by the average intensity value of their respective lanes. This was done in order to normalise the data and be able to plot them on the same scale (in case more product was loaded in one lane compared to another). These were the final values to plot on the y-axis as 'relative frequency'. The x-axis values at this point are 'DNA size (bp)'. By subtracting the expected deadenylated PAT product size (**Table 2.1**) for whichever primer was used

from the DNA size (bp) values, the resulting x-values represent poly(A) tail length (bp). Thus, the final plot of poly(A) tail length vs relative frequency is obtained.

2.2.7 High throughput poly(A) tail measurement: TAIL-seq

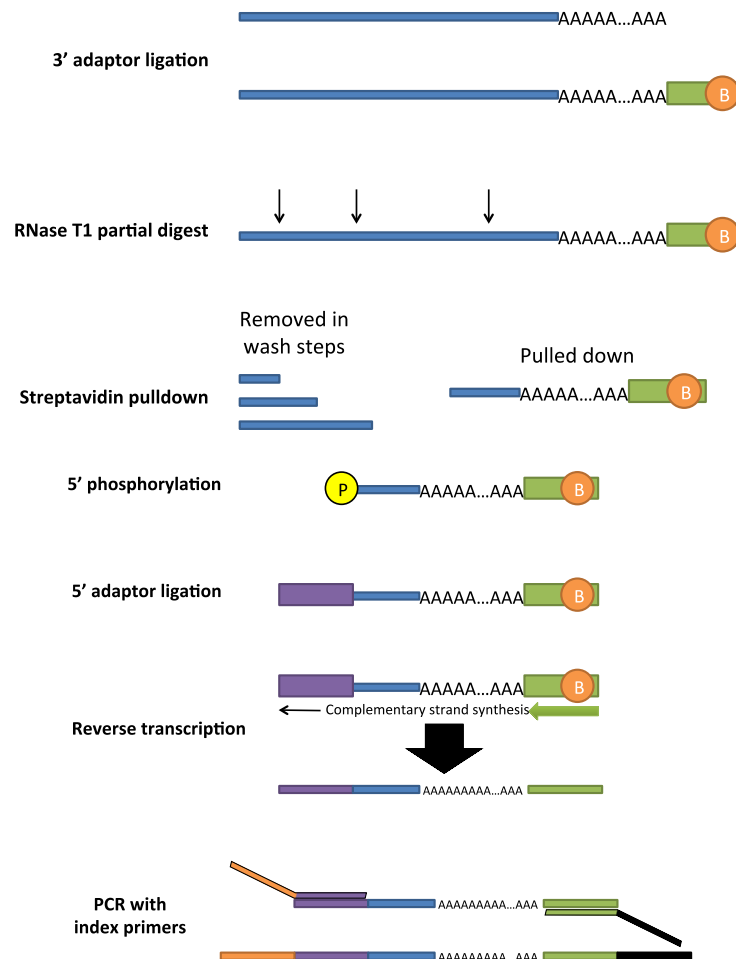


Figure 2.3. Overview of the TAIL-seq library generation procedure. Total RNA is subjected to 2 rRNA-removal steps and then has a biotinylated adaptor ligated to the 3' end of RNAs. This is then subjected to a partial RNase T1 digest, following which the 3'-most fragment of all digested RNAs (which has the biotinylated sequence) is purified by streptavidin pulldown, 5'-phosphorylated, and run on a gel for size selection (300-1000 nt). This size-selected, 5'-phosphorylated RNA then has the 5' adaptor ligated and is reverse transcribed to cDNA. PCR is then done using primers that have overhanging index sequences.

TAIL-seq, originally developed by the Kim lab (Chang et al. 2014), allows for a global assessment of poly(A) tail lengths. An overview of the process is shown in **Figure 2.3**. Work was done to establish a working protocol for this technique, since the original group's protocol was not producing results, in our experience. Below is the method we used, deviations from the original protocol are indicated.

rRNA depletion: 50 µg of total RNA was subjected to 2 rounds of rRNA depletion using Ribo-Zero Gold kit (MRZH11124C, Epicentre) following manufacturer's protocol with 10 µl rRNA removal solution used per round. 50 µg exceeds the capacity of the rRNA removal solution, which is why 2 rounds are used.

3' adapter ligation: After redissolving the RNA (now rRNA-depleted), the biotinylated 3' adapter (RA3_biotin4) was ligated to the 3' ends of all the RNA using T4 RNA ligase 2 truncated KQ, 20 pmol of the adapter, and 15% PEG 8000 in a 20 µl reaction volume. The ligation was done at 16°C overnight. This step differs from the original protocol, which used T4 RNA ligase 2 truncated (NEB, cat no M0242S), 10 pmol of the 3' adapter, no PEG 8000, a 10 µl reaction volume and the ligation temperature profile was 28°C for 1 hour, 25°C for 6 hours, 22°C for 6 hours, and then hold at 4°C.

Partial digestion: Following the ligation, the RNase T1 (Ambion, cat no AM2283) partial digest was done by assembling the 3' adapter ligated RNA in 100 µl reaction volume with 1X sequencing buffer (supplied with kit). This mixture was incubated at 50°C for 5 minutes then paused at 22°C, at which point 2 µl of RNase T1 was added. This digestion mixture was incubated at 22°C for 5 minutes in the original protocol, which we found to be insufficient, so we increased the duration (discussed in **section 3.4**). After the digestion, precipitation/inactivation buffer was added to the mixture

and RNA was precipitated following manufacturer's instructions and redissolved in 50 µl water.

Optimisation of the duration of the RNase T1 treatment (discussed in **section 3.4**) involved the use of synthetic RNA as a substrate. The synthetic RNA used ('T3CAT-xxsB1-M2') was produced by *in vitro* transcription from a construct containing the chloramphenicol acetyltransferase gene under the control of a T3 promoter. Further details are available in the methods section of the publication for which it was made (de Moor and Richter 1999).

Biotin/streptavidin pulldown, 5'-phosphorylation, and size selection: The 3' most RNA fragments were purified using Dynabeads M-280 Streptavidin (Invitrogen, cat no 11206D). 50 µl of Dynabeads were used per 10 pmol biotinylated oligo. Manufacturer's protocol was used up until the bead washing following binding of RNA to beads. At this point, a PNK (polynucleotide kinase) reaction was done while the RNA was still bound to the beads to phosphorylate the 5' ends of the RNAs. This was done by preparing a 50 µl mix containing 2 µl of T4 PNK (NEB, cat no M0201S), 1X PNK buffer (50 mM Tris-Cl pH 7.4, 10 mM MgCl₂, 0.5% NP-40), and 0.4 mM ATP. This mix was then mixed with the beads and incubated at 37°C for 30 minutes. Note that the PNK buffer is NOT the buffer supplied with the kit. Following the PNK reaction, the beads were washed twice with 100 µl PNK buffer, and then had 13 µl of RNA loading dye (95% formamide, 10 mM Tris-HCl) added. This was mixed, heated at 95°C for 3 minutes, placed on the magnetic rack, and supernatant immediately collected. This elution step was repeated and the two 13 µl elution volumes pooled. Eluted RNA was then run on a TBE-urea PAGE gel and stained with SYBR gold (Invitrogen, cat no S-11494). A size selection was done by cutting the gel between 300 nt and 1000 nt (in the original protocol, this was 450-1500 nt), placing

the gel slice into a gel breaker tube (IST engineering, cat no 3388-100) stacked into a 2 ml centrifuge tube and centrifuging at >16,000 g for 5 minutes. In the original protocol, the size selection was At the end of this, 800 µl of 0.3 M NaCl solution was added to the gel slice debris and rotated overnight at 4°C. The following day, the gel debris suspension in NaCl was divided between 2 Spin-X columns (Corning, cat no 8162) and centrifuged at >16,000 g for 5 minutes. The flow through was then precipitated with 2-3 volumes of 100% ethanol and 0.3 M sodium acetate. The pellet was redissolved in 4.2 µl water.

5' adapter ligation: This RNA (now with the 3' adapter in place, and 5'-phosphorylated) then had the 5' adapter ligated. T4 RNA ligase 1 (NEB, cat no M0204S) was used for this with 0.8 µl of the enzyme, 1mM ATP, 1X T4 RNA ligase buffer (supplied with kit) and 5 pmol of the 5' adapter (RA5) in an 8 µl reaction volume. In the original protocol, the temperature profile for the ligation incubation was 28°C for 1 hour, 25°C for 6 hours, 22°C for 6 hours, and hold at 4°C. We changed this to a single incubation temperature of 16°C overnight.

Reverse transcription (RT): The RNA was reverse transcribed using SuperScript III (Invitrogen, cat no 18080093). Manufacturer's protocol was followed using 4 pmol of the reverse transcription primer (RTP).

PCR: When the library is generated, the fewest cycles that results in successful amplification should be used – this is because amplification becomes non-linear at higher cycle numbers. A small-scale PCR at several different cycle numbers was performed to find out what the ideal number of cycles was. PCR was done using Phusion polymerase (Thermo, cat no F-530L), RP1 forward primer, and RPI X reverse primer (where X denotes. The reaction was done in a 4 µl volume with 0.4 µl of RT

product, 0.2 mM dNTP mix, 0.5 μ M primers and 0.04 μ l of enzyme. 13-21 cycles were used with the following cycling conditions:

98°C	30s	13-19 cycles
98°C	10s	
60°C	30s	
72°C	45s	
72°C	5 min	

After running the PCR products on the gel to determine what the lowest cycle number was that resulted in amplification, this number of cycles was used for a full-scale PCR. The same cycling conditions were used as above, the volumes were all scaled up by a factor of 12.5 so that the reaction volume was 50 μ l.

Purification of DNA library: Once the PCR was complete, the library was purified by AMPure XP beads (Beckman Coulter, cat no A63880) following manufacturer's protocol.

Primer name	Primer sequence (5'-3')
RNA 5' Adapter (RA5)	GUUCAGAGUUCUACAGUCCGACGAUC
RNA 3' Adapter (RA3 biotin 4)	/5App/CTGACNNNNNNNNNNNNNNNTGGAATTCTCG GGTGCCAAGGC/iBiodT//iBiodT//3ddC/
RNA RT Primer (RTP)	GCCTTGGCACCCGAGAATTCCA
RNA PCR Primer (RP1)	AATGATACGGCGACCACCGAGATCTACACGTTTCAGAGT TCTACAGTCCGA
RNA PCR Index Primers (RPIX)	Any of Illumina's proprietary TruSeq small RNA RNA PCR index primers between RPI 1 and RPI12

Table 2.2. List of TAIL-seq primers.

Gene	Primer name	Sequence (5'-3')
Acod1	Irg1-F1	ACTCCTGAGCCAGTTACCCT
	Irg1-R1	CTGTGACAGACTTGAGCATCAT
Acod1 (unspliced)	un Irg-F	TTCTCCA CTCCACGCATCA
	un Irg1-R	CAGAAACTTGGACGCAGCAG
Cxcl2	Cxcl2-F	TGAACAAAGGCAAGGCTAACTG
	Cxcl2-R	ACATCAGGTACGATCCAGGC
Gapdh	Mouse GAPDH F	AAGAAGGTGGTGAAGCAGGC
	Mouse GAPDH R	ATCGAAGGTGGAAGAGTGGG
Hprt	Mouse HPRT F	GGTGTCTAGTCCTGTGGCC
	Mouse HPRT R	AGTGCAAATCAAAAGTCTGGGG
Il1b	Mouse Il1b-F1	AGATGAAGGGCTGCTTCCAAA
	Mouse Il1b-R1	GGAAGGTCCACGGGAAAGAC
Ptgs2	Ptgs2 F	GGTTCACCCGAGGACTGGGC
	Ptgs2 R	GGGGGATACACCTCTCCACCAAT
Rpl28	Rpl28 Fw	TACAGCACGGAGCCAAATAA
	Rpl28 Rev	ACGGTCTTGCGGTGAATTAG
Rpl28 (unspliced)	Rpl28 Fw2	CATCGTGACACCTATTCCC
	Rpl28 Rev	ACGGTCTTGCGGTGAATTAG
Rpl28 (unterminated)	Rpl28 Rdthr 500 F1	ACATTCTGGTGGGTGTCAGC
	Rpl28 Rdthr 500 R1	TCTAAGGTCAGCAATTCACACTGA
Rpl28 (uncleaved)	Rpl28 PAS F1	ACACGCCCGAAGCAATAAAG
	Rpl28 PAS R1	CAACCCTCACTCCAGATGAACA
Tnf	TNF Fw1	CTATGGCCCAGACCCTCACA
	TNF Rv1	CCACTTGGTGGTTGCTACGA
Tnf (unspliced)	Mouse un Tnf-F1	ACACTGACTCAATCCTCCCC
	Mouse un Tnf-R1	AGCCTTGTCCTTGAAGAGA
Tnf (unterminated)	Tnf Rdthr 750 F1	ATCCAAGCCTGCATATGTGATTA
	Tnf Rdthr 750 R1	TATTGAGGTGGGTGGATTGGAAA
Tnf (uncleaved)	Tnf PAS F1	TTTTGTCCACGGGGTCTT
	Tnf PAS R1	GGGAGCCGTGACTGTAATCG

Table 2.3. List of qPCR primers. Primers are stacked as pairs. The top primer in each stack is the forward primer, the bottom is the reverse.

2.3 Protein work

2.3.1 Western blot analysis

At the end of the experiment, cells were placed on ice and washed twice with chilled PBS, and then scraped in 5 ml PBS with a cell lifter (Corning, cat no 07-200-364). This cell suspension was then centrifuged at 10,000 g for 1 minute at 4°C. The supernatant was discarded and the pellet resuspended in 500 µl ice-cold PBS, centrifuged as above, and supernatant discarded. To this pellet, 125 µl of ice-cold lysis buffer (1xPBS, 0.5% Igepal, 0.5% deoxycholate, 0.05% SDS, 1 mM β-glycerophosphate, 1 mM Na₃VO₄, 1 mM PMSF) was added, and pipetted up and down. This was centrifuged at 20,000 g for 10 minutes at 4°C and supernatant collected in a new tube. 10 µl of the supernatant was used for determining protein concentration by Bradford assay, and the rest had 3X SDS-PAGE loading buffer (0.2 M Tris-HCl pH 6.8, 9%SDS, 30% glycerol, 2.1 M β-mercaptoethanol, 0.0125% bromophenol blue) added for a final concentration of 1X. 45 µg of protein in 1X SDS-PAGE loading buffer was loaded per well on a 1mm 12% minigel (8.6cm × 6.8cm). After running the gel, proteins were blotted onto a PVDF membrane (Thermo, cat no 88518). Membrane was rinsed twice with TBST (10 mM Tris/HCl, 150mM NaCl, 0.05% Tween 20), incubated for 1 hour at room temperature while rocking in TBST containing 5% milk, rinsed three times with TBST, and then sealed in a small pouch with the primary antibody in milk. Primary antibodies used were mouse anti-IκBα (Cell signalling technology, cat no 4814) and mouse anti-symplekin (BD Biosciences, cat no 610644). This was then incubated for 1 hour at room temperature, with the pouch regularly rubbed to mix. The blot was then removed, rinsed three times with TBST, and then incubated with polyclonal goat anti-mouse secondary antibody (Dako, cat no P0447) in milk for 1 hour at room temperature in another small, sealed

pouch. The blot was then recovered, rinsed three times with TBST, and incubated for 20 minutes in TBST on a rocker at room temperature. Chemiluminescence solution (GE, cat no RPN2106) was prepared and, after placing the blot onto a glass plate (protein side up), pipetted onto the blot just enough to cover the surface. After approximately 5 minutes, the blot was imaged on the LAS-4000 imager (GE, discontinued, cat no 28-9558-10).

2.4 Animal work

2.4.1 Rat osteoarthritis model pain behaviour assessment by James Burston

The monosodium iodoacetate (MIA) model of osteoarthritis was used. On day 0, animals had either saline (one group) or MIA (two groups) injected into the knee of one hind leg. One MIA group had cordycepin mixed with food at 2 mg/kg every other day over the course of the experiment while the other MIA group and the saline group had DMSO (vehicle) mixed with food, instead. Pain behaviour was assessed on a number of days during this period, measured as weight bearing asymmetry between hind legs, and paw withdrawal thresholds when paws were pressed with Von Frey filaments of increasing force until the animal withdrew its paw. On day 14 post injection, animals were killed and tissues obtained for later use.

2.4.2 RNA isolation from rat synovia

A number of strategies were attempted to isolate RNA from synovia (discussed in results). The method that worked was the use of TRI Reagent (Sigma, cat no T9424) at 2 ml per 50 mg tissue. TRI Reagent was added to the synovium in a tube and immediately processed using a rotor-stator homogeniser for 15-30 seconds at room temperature, until a homogeneous suspension was obtained. The homogenates

were incubated at room temperature for 5 minutes after which 0.2 ml of 1-bromo-3-chloropropane was added per 1 ml of monophasic lysis reagent. Samples were mixed by shaking and then centrifuged at 10,000 g for 15 minutes at 4°C. The aqueous layer was then transferred to a fresh tube and subjected to an isopropanol/sodium acetate precipitation. Pellet was redissolved in water.

Gene	Primer name	Sequence (5'-3')
Actb	Actb-F	AGGCCATGTACGTAGCCATCCA
	Actb-R	TCTCCGGAGTCCATCACAATG
Il1b	Il1b-F	CACCTCTCAAGCAGAGCACAG
	Il1b-R	GGGTTCCATGGTGAAGTCAAC
Tnf	Rat Tnf-F	CCAGGAGAAAGTCAGCCTCCT
	Rat Tnf-R	TCATACCAGGGCTTGAGCTCA
Ptgs2	Cox2-F	GGCACAAATATGATGTTCGCA
	Cox2-R	CCTCGCTTCTGATCTGTCTTGA

Table 2.4. List of rat qPCR primers used. Primers are stacked as pairs. The top primer in each stack is the forward primer, the bottom is the reverse.

3 Optimising and developing methodologies for poly(A) tail measurements

The poly(A) tail test (PAT) offers a means for assessment of the distribution of poly(A) tail sizes for a specific mRNA within an RNA sample. There are several varieties of the PAT method, but the types that this chapter is concerned with all include ligation of an oligonucleotide adapter to the 3' end of RNA, reverse transcription to generate cDNA, and PCR using primers that flank the poly(A) tail.

The method that was in use in our research group when this project began was RNA ligation-mediated PAT (RL1-PAT) (Rassa et al. 2000). RL1-PAT requires a large input quantity of RNA, which was not always possible for samples with low yields. I sought to make improvements to RL1-PAT, as it was. Additionally, RL1-PAT was compared to two alternative PAT methods in case they offered superiority – RL2-PAT and splint-mediated PAT (sPAT) (Minasaki, Rudel, and Eckmann 2014).

Lastly, in collaboration with the Deep seq facility at the University of Nottingham, we attempted to establish the recently published TAIL-seq method for high-throughput poly(A) tail analysis (Chang et al. 2014).

3.1 Deadenylation by oligo (dT)/RNase H treatment

To determine if the correct product is amplified, RNA samples are used that have been subjected to an oligo (dT)/RNase H treatment to remove poly(A) tails. This should result in all PAT cDNAs that get amplified having a uniform poly(A) tail size close to zero. This means a single band will be observed on the gel, or 2 or more discrete, distinct bands in the case of alternative polyadenylation. Doing the oligo (dT)/RNase H treatment is therefore essential for testing new primers (to check that the expected deadenylated product is being amplified, and not an off-target product). In the event that different PAT products are yielded from different RNA

samples, repeating PAT on the samples' deadenylated counterparts should yield the same product(s) as 1 or more discrete, distinct band(s), thus proving that differences observed are exclusively due to poly(A) tail size differences. For this reason, the oligo (dT)/RNase H treatment is a crucial part of the PAT methodology.

After switching supplier of RNase H from Promega to NEB, our lab group was experiencing incomplete, unsatisfactory deadenylation with the oligo (dT)/RNase H treatment (**Figure 3.1A**). I tested multiple different permutations of the treatment to see if this could be rectified to yield complete deadenylation (**Figure 3.1B**). The treatments were all carried out under the same conditions, with the only differences being the quantity of oligo (dT) and RNase H enzyme used. Using 4 µg of oligo (dT) and 5U of enzyme consistently yielded properly deadenylated RNA, and so this combination of concentrations was adopted. The lowest combination of oligo (dT) and enzyme concentration (2 µg and 2.5 U respectively) appears to result in the same degree of deadenylation as using 4 µg of oligo (dT) and 5 U of enzyme in **Figure 3.1B**. However, such results were not consistent in further experiments, whereas 4 µg of oligo (dT) and 5 U of RNase H reliably caused deadenylation. Unexpectedly, the result of using 4 µg of oligo (dT) and 2.5 U of enzyme was less deadenylation than for the lowest combination of concentrations. This was probably an anomalous result.

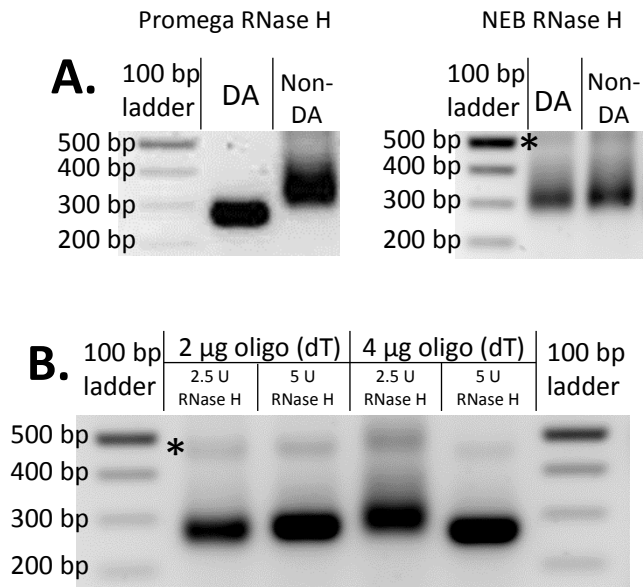


Figure 3.1 Incomplete deadenylation using NEB RNase H was addressed by increasing oligo (dT) and RNase H quantities. RL1 PAT was performed using the Rpl28 3F1 primer with various cDNA samples and PAT products were run on agarose gels. (A) DA and non-DA denote deadenylated and non-deadenylated PAT cDNA of RNA isolated from unstimulated RAW 264.7 cells. The deadenylation was performed using Promega or NEB RNase H (1.5 U of enzyme, 2 µg oligo (dT)). (B) NEB RNase H deadenylation was performed on RNA from RAW 264.7 cells stimulated with LPS at 1 µg/ml for 30 minutes using a range of different oligo (dT) and NEB RNase H quantities. * indicates artefactual bands.

Deadenylated Rpl28 product size: 259 bp

3.2 Appraising different ligation strategies

As part of the PAT optimisation, different ligation strategies were used and compared to each other. I compared RL1-PAT, which uses the T4 RNA ligase 1 enzyme, to RL2-PAT, which uses the T4 RNA ligase 2 truncated enzyme. The ligation in the RL2-PAT workflow is referred to as L2T. The sPAT method was also tested both with the original ligation and using the L2T ligation. Full details are in section **2.2.6**.

In order to see whether RL2-PAT offered advantages over the RL1-PAT method in use, reactions were incubated in parallel with 3 different input RNA quantities (2 µg, 1 µg, and 0.5 µg). PAT anchor was 5'-adenylated using a 5' DNA adenylation kit prior to use in the RL2-PAT workflow, while the normal, unaltered, PAT anchor (5'-phosphorylated) was used for RL1. Following the ligation step, the reverse transcription was done in the same way, but all volumes were doubled for RL2-PAT, since the ligation reaction volume was double that of RL1-PAT. PAT-PCR was then done in exactly the same way for both, with 1 µl of cDNA. RL2-PAT was found to yield consistent PAT products across the 3 different input RNA quantities, while the distribution of PAT products generated with RL1-PAT appeared to vary between the different input RNA quantities (**Figure 3.2A**). qPCR on all the PAT cDNA samples was performed, and demonstrated that cDNA generation was consistent for RL2-PAT for all input RNA quantities used (**Figure 3.2B**). This consistency was not seen for RL1-PAT, which also yielded considerably less cDNA than RL2-PAT, suggesting better ligation efficiency with L2T. Taken together, these data indicate that using the L2T ligation represents a significant improvement of the PAT method over the RL1 method that had been in use before. For this reason, RL2-PAT using L2T ligation replaced the RL1-PAT procedure, and a new PAT anchor oligo was ordered with the 5'-5' adenylation modification already made.

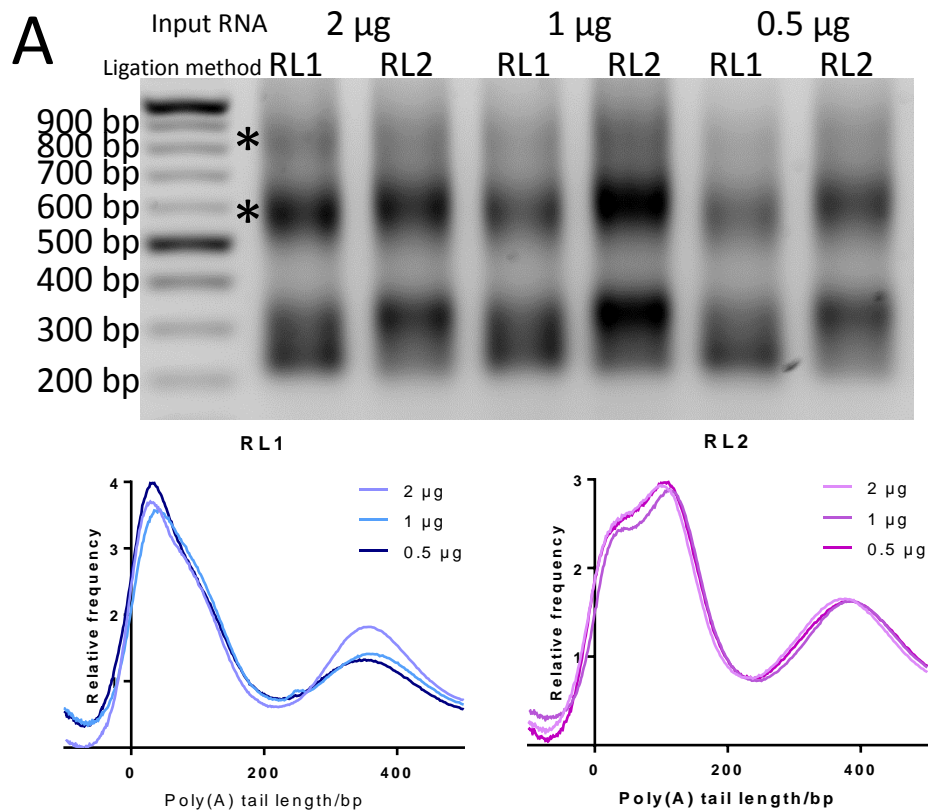


Figure 3.2. RL2 PAT yields more

consistent results with a range of

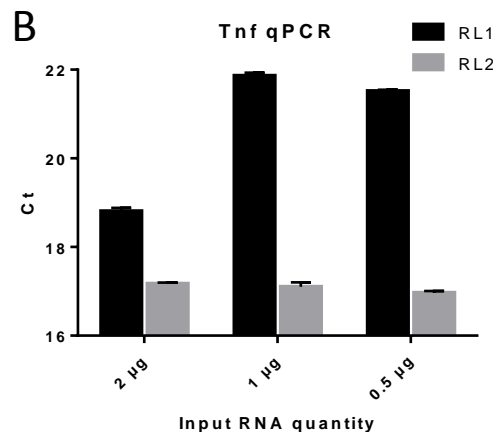
input RNA quantities, and more

efficient cDNA generation. (A) RL1

and RL2 PAT tests were performed

for Tnf using RNA from RAW 264.7

cells stimulated with LPS at 1 μ g/ml



for 30 minutes. Three input RNA quantities were used (2 μ g, 1 μ g, and 0.5 μ g)

for each ligation method (RL1 and RL2). PAT products were run on an agarose

gel. The gel image was scanned using Quantity One software and profiles

represented graphically. * indicates artefactual bands. (B) The PAT cDNA

samples were also subjected to qPCR for Tnf, and the raw Ct value was

measured. qPCR was performed on the Qiagen Rotor-Gene Q platform. Error

bars represent standard deviations across three technical replicates.

Deadenylated Tnf product size: 215 bp

After implementing the RL2 ligation in the PAT procedure, the sPAT method was published, which was tested against our newly adopted RL2-PAT method. In order to see if a combination of splint ligation and the ligation method used in RL2-PAT ligation could improve the ligation efficiency even further, the RNA anchor oligo was subjected to a 5'-5' adenylation step prior to use in some samples i.e. sPAT using RL2 ligation with 5'-5' adenyated RNA anchor instead of the standard sPAT using T4 RNA ligase 2 with 5'-phosphorylated RNA anchor. sPAT using the RL2 ligation method will be referred to as **L2T sPAT**, while standard sPAT using T4 RNA ligase 2 with 5'-phosphorylated RNA anchor will be referred to as **T4 Rnl2 sPAT**.

Both types of sPAT were done (L2T and T4 Rnl2), and the gel image (**Figure 3.3**) shows that the L2T method produced a stronger signal. It was later noted that the DNase treatment had been accidentally omitted in this experiment, and so it was repeated alongside RL2-PAT for direct comparison. However, having observed that L2T ligation appeared to improve sPAT, we only compared RL2-PAT to L2T sPAT – T4 Rnl2 sPAT was not included in the experiment. RL2-PAT produced results that were either similar to those for L2T sPAT or showed higher signal (**Figure 3.4**). qPCR was done on RL2-PAT and L2T sPAT cDNAs for a number of mRNAs across a range of different levels of abundance. RL2-PAT consistently resulted in a greater efficiency of cDNA generation (**Figure 3.4**). It was thus concluded that RL2-PAT was superior to L2T sPAT, and so the method was retained.

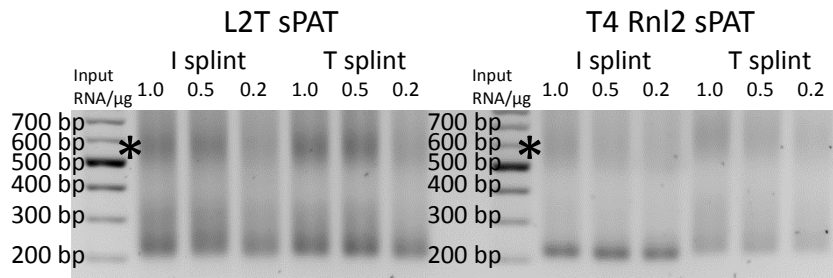


Figure 3.3. The L2T ligation improves sPAT compared to the T4

Rnl2 sPAT ligation. sPAT protocol was followed with two different

ligation strategies: the L2T ligation with a 5'-5' adenylated RNA

anchor oligo (L2T sPAT) or the standard sPAT ligation using T4 RNA

ligase 2 with 5'-phosphorylated RNA anchor oligo (T4 Rnl2 sPAT).

Both the I and T splints were used with 3 different input quantities

of RNA: 1 µg, 0.5 µg, and 0.2 µg. RNA was from RAW 264.7 cells that

had been stimulated for 30 minutes with LPS at 1 µg/ml. PAT

products (Tnf) were run on an agarose gel. Note that the DNase

treatment was forgotten. * indicates artefactual bands.

Deadenylated Tnf product size: 215 bp

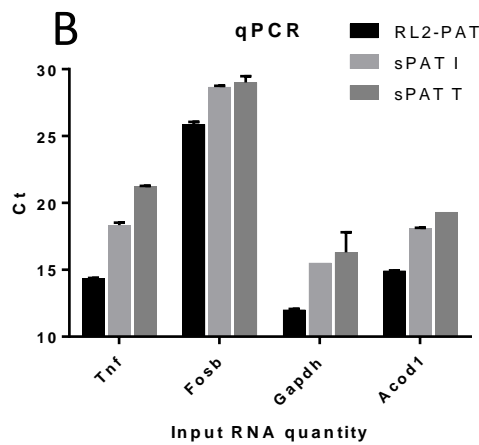
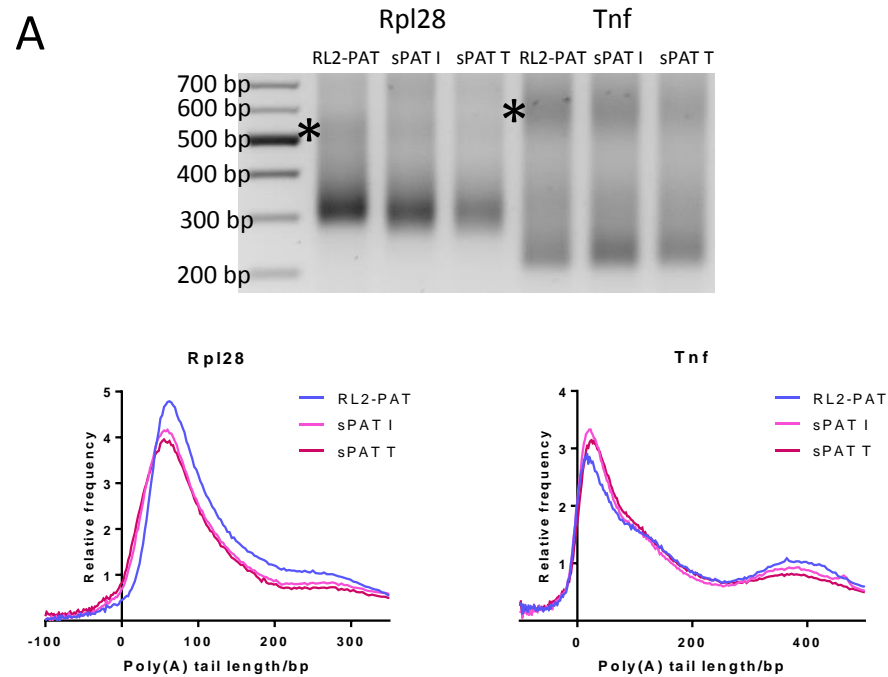


Figure 3.4. RL2-PAT results in greater efficiency of cDNA generation. (A) PAT

was performed for Tnf using RNA from RAW 264.7 cells stimulated with LPS at 1 μ g/ml for 30 minutes with three distinct methodologies: RL2-PAT, L2T sPAT using an oligo (dT) splint (sPAT T),

and L2T sPAT using an oligo(dI) splint. PAT products were run on an agarose gel. The gel image was scanned using Quantity One software and profiles represented graphically. (B) The PAT cDNA samples were subjected to qPCR for 4 genes of varying abundance levels, and the raw Ct values were plotted on a graph. qPCR was done on the Qiagen Rotor-Gene Q platform. Error bars represent standard deviations across three technical replicates.

Deadenylated product sizes – Rpl28: 259 bp. Tnf: 215 bp.

3.3 Identifying artefacts

Very large, unexpected, PAT products are routinely observed when running the products on agarose gels, in addition to the products that appear around the expected size (**Figure 3.7**). Possible explanations for the presence of these unexpected species were that they were products with very large poly(A) tails, products with a downstream poly(A) site (i.e. alternative polyadenylation) and therefore longer 3' UTR, or some sort of artefactual species. If these higher bands are due to alternative polyadenylation, then doing PAT on the samples' deadenylated counterparts should yield a correspondingly large deadenylated PAT product in addition to the expected one. However, this is generally not observed (e.g. **Figure 3.1A**), and so this was unlikely. If the higher bands represented some sort of artefact formed through secondary structure, then running them on a gel under denaturing conditions should remove them. I attempted this by mixing different quantities of a PAT product with formamide buffer (49.5% final concentration for all samples loaded), heating, and running on a TBE-urea PAGE gel (**Figure 3.5**). This was done for 2 different PAT products (*Rpl28* and *Tnf*), and the relative proportion of the higher bands increased with increasing PAT product being loaded, even though it was the exact same PAT product for each of the 3 quantities loaded. This was highly suggestive of the higher band representing an artefact whose formation was favoured by increasing concentration of the product.

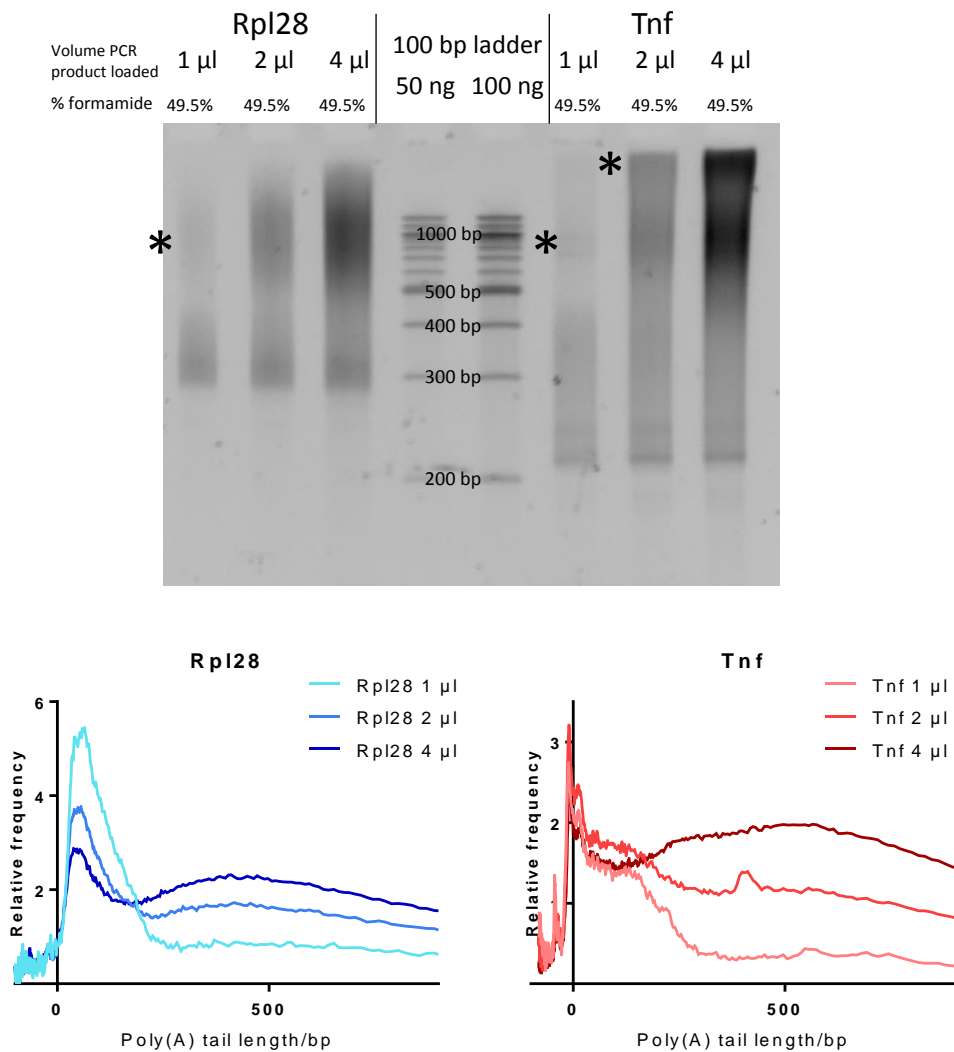


Figure 3.5. An increase in PCR product:formamide ratio increases the prevalence of suspected multimeric bands. RL2-PAT was performed for Rpl28 and Tnf using RNA from RAW 264.7 cells stimulated with LPS at 1 μ g/ml for 30 minutes. PAT products were run on a TBE-urea PAGE gel. Samples were in 49.5% formamide buffer and were heated at 90 $^{\circ}$ C for >10 minutes then placed on ice prior to loading and running. Gel images were scanned using Quantity One software and profiles represented graphically. * indicates artefactual bands.

Deadenylated product sizes – Rpl28: 259 bp. Tnf: 215 bp.

I ran those same products, again, on a TBE-urea PAGE gel, but with only 1 μ l of PAT product loaded in 90% formamide buffer, and with heated running buffer in the electrophoresis tank to maximise the denaturing potential of the system. Doing this completely removed the appearance of the higher bands which were observed on agarose and when using 49.5% formamide buffer on TBE-urea PAGE (**Figures 3.5 and 3.6**). A working model for the formation of these higher bands was conceived (**Figure 3.7B**), wherein the repetitive melting and reannealing in later stages of PCR leads to mispairing of strands with different poly(A)/poly(T) lengths, and looping out of excess A or T bases. Loops of excess A can then facilitate base pairing with loops of excess T from other mismatched duplexes to form a multimeric artefact. This model is consistent with the findings of an experiment in which oligo (dT) was able to remove higher bands. PAT cDNA from serum-stimulated NIH-3T3 cells were used for PAT to amplify Fosb – PAT for this mRNA in this cell type routinely results in higher bands. PAT products then had varying quantities of oligo (dT) added, were heated at 95°C, and then were run on an agarose gel. The gel photo and graphical scan show that the addition of oligo (dT) leads to disappearance of the higher bands (**Figure 3.7A**). Ostensibly this occurs by ‘titrating’ A loops, preventing their association with T loops.

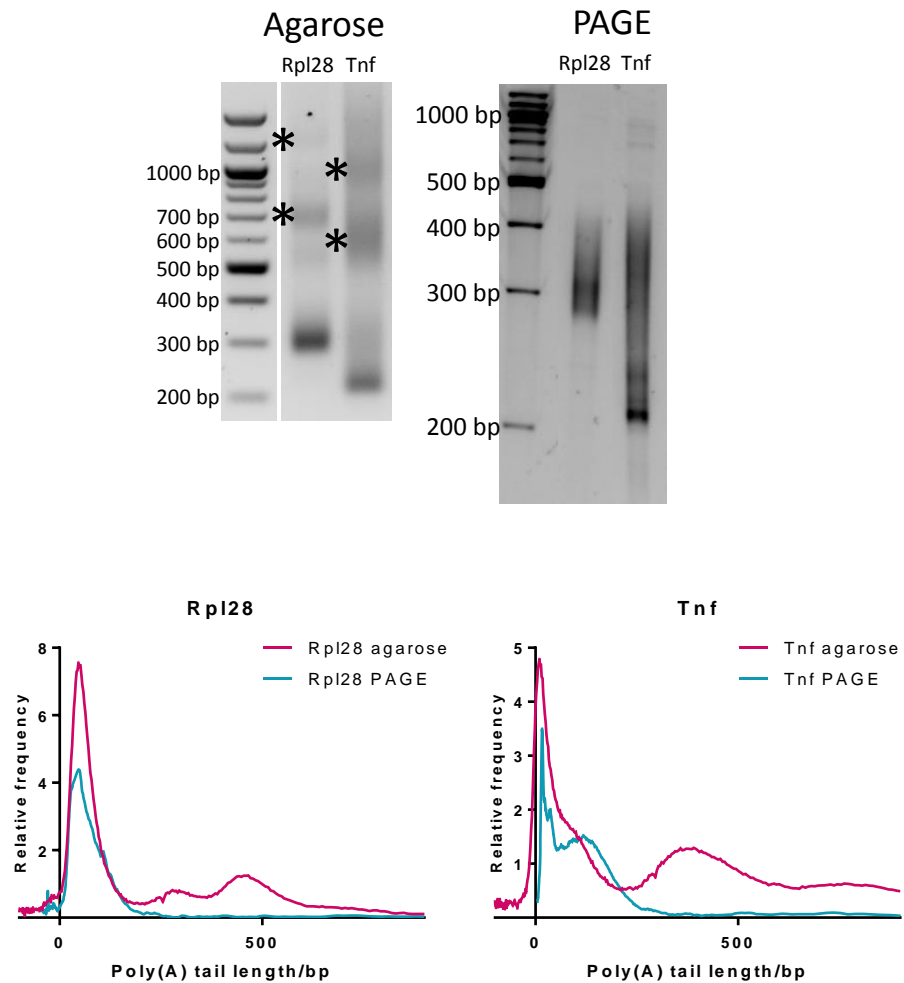


Figure 3.6. Artefactual species are multimers and can be removed through fully denaturing PAGE. RL2-PAT was performed for Rpl28 and Tnf using RNA from RAW 264.7 cells stimulated with LPS at 1 $\mu\text{g}/\text{ml}$ for 30 minutes. PAT products were run on an agarose gel, and on a TBE-urea PAGE gel. For PAGE, samples were in 95% formamide buffer, TBE in the gel tank was heated to 50 $^{\circ}\text{C}$ prior to running, and samples (in formamide buffer) were heated at 90 $^{\circ}\text{C}$ for >10 minutes immediately prior to loading and running. Gel images were scanned using Quantity One software and profiles represented graphically. * indicates artefactual bands.

Deadenlyated product sizes – Rpl28: 259 bp. Tnf: 215 bp.

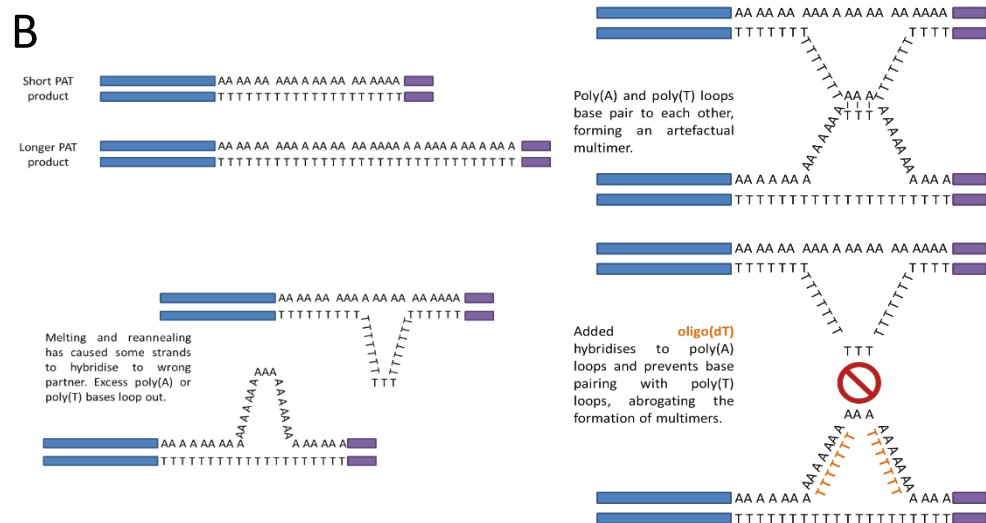
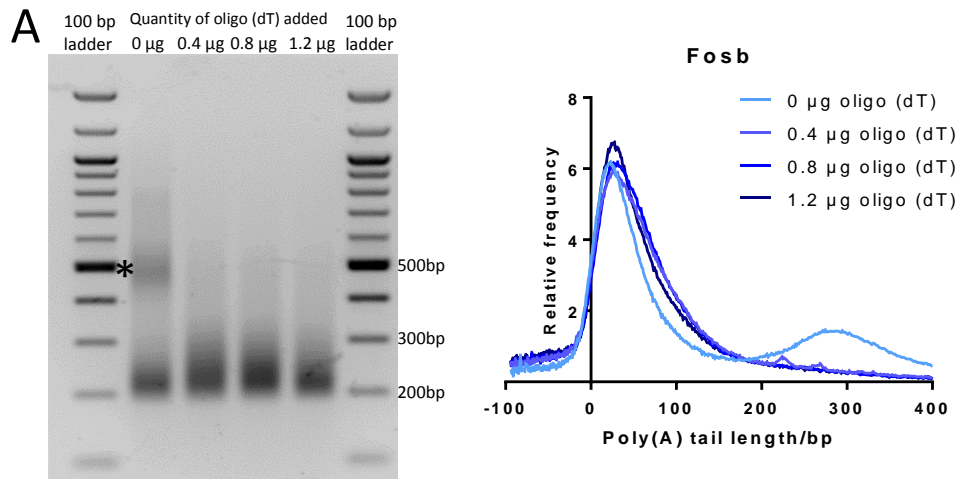


Figure 3.7. Addition of oligo (dT) to PAT-PCR products can remove multimer species. (A) RL2 PAT was performed for *Fosb* on RNA samples from NIH-3T3 cells stimulated with DMEM + 10% NBCS for 110 minutes (following a 24 hour incubation in DMEM + 0.5% NBCS). 15 µl of PAT-PCR products were mixed with the indicated amount of oligo (dT), heated at 95° C for 10 minutes then placed on ice prior to loading and running. Gel images were scanned using Quantity One software and profiles represented graphically. * indicates artefactual bands. (B) Working model for formation of the PAT multimer species.

Deadenylated *Fosb* product size: 189 bp.

3.4 High-throughput poly(A) tail measurements – TAIL-seq

TAIL-seq is a method that allows for the high-throughput measurement of poly(A) tail lengths, and other 3' terminal modifications, within an RNA sample. We sought to establish the technique within our group in conjunction with the Nottingham deep sequencing facility. However multiple attempts to follow the TAIL-seq protocol (provided by Narry Kim's group) failed to generate a library, and so we tried to troubleshoot the procedure by assessing how well individual steps within the protocol were working. An overview of the process is shown in **Figure 2.3**.

By the point of eluting RNA from the streptavidin beads, the expected RNA recovered would be the 3'-most fragment yielded from the partial RNase T1 digest with the biotinylated 3' adapter (RA3_biotin4) ligated to its 3' end, and phosphorylated at its 5' end (since a PNK reaction is performed on the beads after the wash steps and before eluting). As shown in **Figure 3.8**, only the unligated 3' adapter (RA3_biotin4) was being recovered following the streptavidin pulldown. The RA3_biotin4 oligo can be seen in the ligation mix along with the rRNA-depleted NIH 3T3 RNA – this indicates that at least some of the oligo did not ligate to the NIH 3T3 RNA. If the ligation had been successful, I would have expected the bands for the rRNA-depleted NIH 3T3 RNA to shift up between the two lanes on the gel (before and after ligation). The RA3_biotin4 adapter is 45 nt in length, and the ladder shows clear separation of the 30 nt and 50 nt RNA fragments, and so a 45 nt change in RNA length should be clearly observable, at least around this lower part of the gel. This suggests a possible failure of the 3' adapter ligation. Moreover, only a single band is observed on the gel after the streptavidin pulldown, corresponding to the RA3_biotin4 oligo. This strongly suggests that the 3' adapter ligation did indeed fail,

since ligation products would have otherwise been recovered in the pulldown (irrespective of whether the RNase T1 digest had been successful or not).

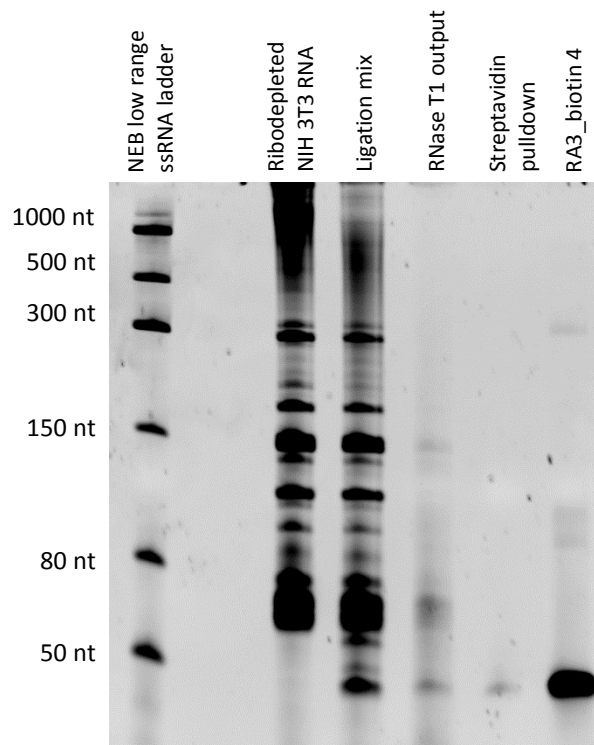


Figure 3.8. Only unligated RA3 oligo is recovered after the streptavidin pulldown. Total RNA from unstimulated NIH 3T3 cells was isolated and subjected to rRNA removal. The resulting ribodepleted RNA was then used for the 3' adapter ('RA3 oligo') ligation step, following original protocol (T4 RNA ligase 2 truncated, 10 pmol of the 3' adaptor, no PEG 8000, a 10 μ l reaction volume, 28°C for 1 hour, 25°C for 6 hours, 22°C for 6 hours, and then hold at 4°C). Once the ligation step was complete, the RNA was subjected to a partial RNase T1 digest (5' digestion time), and a streptavidin pulldown performed. A PNK reaction was completed prior to eluting bound RNA from the streptavidin beads. Samples of RNA from multiple points in this procedure were run on a TBE-urea PAGE gel alongside the 3' adapter ('RA3_biotin4') alone.

Our PAT protocol uses a very similar ligation step under different conditions that works well, so we sought to compare the efficiencies of the TAIL-seq ligation versus the L2T ligation used in the RL2-PAT method (see **section 2.2.6** for details). After doing the ligation in both ways, the RNA ligation mixes were divided into two halves – one half was reverse transcribed using random hexamers, while the other was reverse transcribed using the “RT primer” (primer complementary to the 3’ adapter). Using random hexamers was expected to produce similar amounts of cDNA for all RNA ligation mixes, while reverse transcription (RT) using the RT primer would depend on the efficiency of the ligation. Comparison of the ratio of the Ct value for the two RT methods will give an indication of how well the ligation has worked between the different ligation methods.

Surprisingly, the Ct values for the TAIL-seq ligation method and random hexamer RT were very high (**Table 3.1**). As a result, I was not able to directly compare the ligation efficiencies, but, since I obtained reasonable Ct values from all cDNAs made from our PAT ligation method, we elected to use this method for the TAIL-seq, also.

RT method used	Input RNA quantity	Gapdh (high abundance)		Tnf (mid-high abundance)		Fosb (low abundance)	
		L2T	TAIL-seq	L2T	TAIL-seq	L2T	TAIL-seq
Random hexamers	3 µg	14.02	35.08	19.37	No Ct	29.71	No Ct
	0.5 µg	18.62	32.34	23.60	No Ct	33.47	No Ct
RT primer (RTP)	3 µg	16.28	23.46	23.97	30.42	No Ct	No Ct
	0.5 µg	20.29	34.06	28.34	No Ct	No Ct	No Ct

Table 3.1. The ligation used in the PAT workflow successfully generated cDNA for TAIL-seq. 3 µg or 0.5 µg of total RNA from unstimulated RAW 264.7 cells had RA3_biotin4 3' adapter ligated to the 3' end of RNA in one of two ways: T4 RNA ligase 2 truncated KQ, 20 pmol of RA3_biotin4, and 15% PEG 8000 in a 20 µl reaction volume incubated overnight at 16°C overnight ('L2T'); or T4 RNA ligase 2 truncated, 10 pmol of RA3_biotin4, and no PEG 8000 in a 10 µl reaction volume incubated at 28°C for 1 hour, 25°C for 6 hours, 22°C for 6 hours, and then held at 4°C ('TAIL-seq'). Ligation mixes were then reverse transcribed using either random hexamers or the RT primer specific to RA3_biotin4 (the ligated 3' adapter). qPCR was done in technical triplicate for each reverse transcription mix for Gapdh, Tnf, and Fosb. Average Ct values are shown.

Following the RNase T1 partial digest, bands from the NIH-3T3 RNA are clearly visible (**Figure 3.8**). The quantity of RNA run on the gel at this point was very low compared to that of the previous two lanes, and so the signal is faint, but the bands between 50 nt and 80 nt, as well as the band just under 150 nt, can be observed at the same size as in the previous two lanes (undigested sample), possibly indicating limited digestion. For deep sequencing using Illumina technology, longer fragments of nucleic acids (>1,000 nt) experience a decreased efficiency of amplification during the process of cluster generation relative to that of shorter fragments (Quail et al. 2009). This can lead to an underestimation of longer fragments compared to shorter ones, since shorter ones will amplify more efficiently and result in proportionately more reads. For this reason, we wanted to ensure the digestion was not limited and sought to optimise it by testing different digestion durations. Using multiple aliquots of NIH-3T3 RNA that had been subjected to rRNA removal (the normal substrate for the RNase T1 partial digest step) to test multiple digestion durations was not viable, since the rRNA removal reactions were very expensive. For this reason, we used a synthetic RNA ('T3CAT-xxsB1-M2', henceforth referred to simply as 'synthetic RNA') as a substrate, instead, since this was expendable RNA from older work that was no longer required. The synthetic RNA was ~800 nt in length.

The RNase T1 enzyme cleaves single-stranded RNA after G residues, and so poly(A) tails are impervious to RNase T1 digestion. Therefore, in order to avoid the problem mentioned above (longer fragments that do not amplify efficiently during cluster generation), we aimed to ensure that the RNase T1 would cleave non-poly(A) RNA approximately every 400 nt. In this way, the fragments obtained after the ligation and RNase T1 digestion would have a length amounting to ~400 nt plus the length of their poly(A) tails. This would allow for even RNAs with long poly(A) tails (>250 nt) to

still fall below the 1,000 nt limit (after RNase T1 digestion). For our synthetic RNA (~800 nt total size), we aimed to achieve an extent of digestion which yields a distribution of products with a peak around 400 nt. **Figure 3.9** shows that a 10' RNase T1 treatment of the synthetic RNA yielded a spread of products, with most RNA appearing to fall in the range of 300 nt to ~800 nt (just below the undigested 0' control). The 30' digestion duration resulted in a greater degree of digestion than the 10' duration. Compared to the 10' digestion, no significant amount of RNA is observed above the 500 nt band, RNA between 300 nt and 500 nt is fainter, and more RNA appears below the 300 nt band. For the 60' RNase T1 digestion, the longest RNA fragments yielded are below the 300 nt band – a much greater extent of digestion than desired. The 10' digestion was not quite extensive enough (significant signal observed just under the undigested RNA band), and the 30' digestion appeared to be slightly too extensive (significantly fainter signal observed between 300 nt and 500 nt marker bands and more intense smear of shorter products below the 300 nt band compare to the 10' digestion). Ultimately, a digestion duration of 15' was chosen for the workflow.

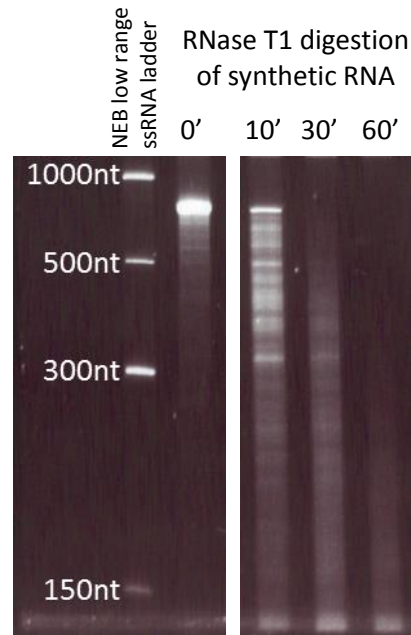


Figure 3.9. Increasing RNase T1 digestion time results in shorter RNA fragments. 3 μg of synthetic RNA produced from *in vitro* transcription was subjected to RNase T1 digestion for the indicated durations and run on a TBE-urea PAGE gel.

Our attempt to generate a library for TAIL-seq using the original ligation strategy and RNase T1 duration was unsuccessful, as shown in **Figure 3.10A** – the only product observed in the small-scale PCR is a band is observed below the 100 bp marker band, possibly due to primer dimer. After implementing the L2T ligation (to ligate the RA3_biotin4 3' adapter to the end of rRNA-depleted NIH-3T3 RNA) and the 15' RNase T1 digestion in the TAIL-seq workflow, the library generation was reattempted and 13-17 cycles of PCR was sufficient to successfully generate a library, with products corresponding to the library ranging from 100 bp to >1,000 bp (**Figure 3.10B**). The fact that products larger than 1,000 bp were amplified suggests that the RNase T1 digestion duration may need further optimisation.

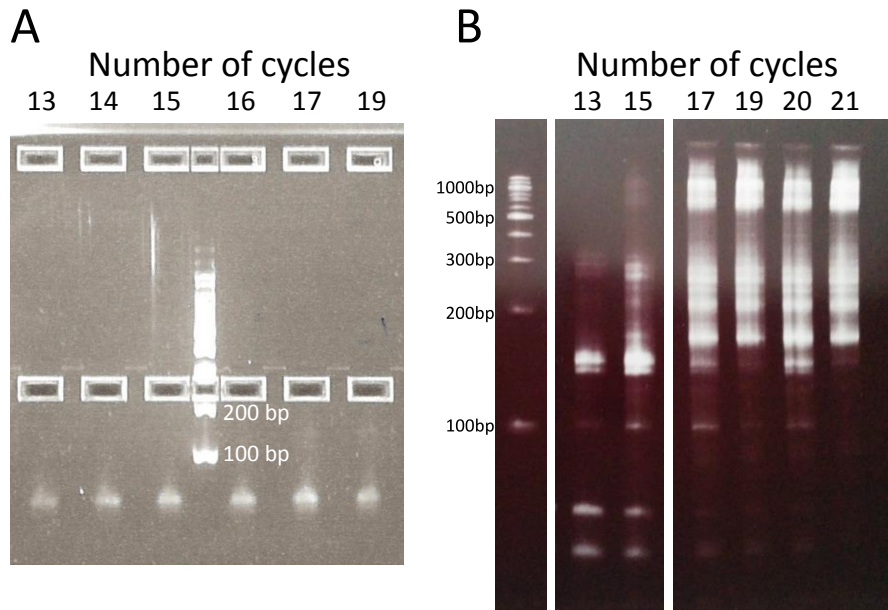


Figure 3.10. Changing the 3' adapter ligation strategy and increasing the RNase T1 digest duration resulted in successful amplification of a library.

(A) The original TAIL-seq workflow was followed with NIH 3T3 RNA, using the original protocol. 3' adapter ligation conditions: T4 RNA ligase 2 truncated, 10 pmol of the 3' adaptor, no PEG 8000, a 10 μ l reaction volume, 28°C for 1 hour, 25°C for 6 hours, 22°C for 6 hours, and then hold at 4°C. RNase T1 digest duration: 5 minutes. After the small scale PCR, samples were run on an agarose gel after completing the indicated number of PCR cycles to assess whether a library had been amplified. (B) As above except for 15 minute RNase T1 digest and altered 3' adapter ligation conditions: T4 RNA ligase 2 truncated KQ, 20 pmol of the adaptor, 15% PEG 8000 in a 20 μ l reaction volume, 16°C overnight. After the small scale PCR, samples were run on a TBE-urea PAGE gel after completing the indicated number of PCR cycles to assess whether a library had been amplified.

3.5 Discussion

Significant improvements were made to the PAT methodology through the identification of working deadenylation reaction conditions and use of the L2T ligation reaction in the RL2-PAT workflow. RL2-PAT was also superior to the sPAT method, even when it was combined with the L2T ligation. This is a beneficial outcome since sPAT is a longer and more expensive method than RL2-PAT, due to the need for an RNA oligo and DNase treatment step. RL2-PAT was implemented in the research group as the standard PAT method to use. Unless otherwise stated in the figure legends, all PAT presented in chapter 4 onwards is RL2-PAT and all products are run on agarose gels. Higher, unexpected bands that often appeared on PAT gels were identified as artefacts, and ways to remove them were found. It should be noted that the addition of oligo (dT) did not reliably and reproducibly remove these artefacts, but fully denaturing TBE-urea PAGE did. None of the PAT data in chapter 4 onwards use TBE-urea PAGE, however, as those data were all generated before TBE-urea PAGE was shown to remove artefacts. Progress was made on establishing TAIL-seq for use by our research group. We were unable to obtain usable data, so further adjustments to the workflow are necessary. However, a library was successfully created and data generated validated the technique in principle, which shows progress from the initial experience of not being able to even generate the library before steps in the workflow were altered. Further work should lead to the proper establishment of the technique, which would provide a means to analyse poly(A) tails on a genome-wide scale.

4 Inflammation and polyadenylation in RAW 264.7 cells

Our group previously reported that inhibiting polyadenylation results in a decrease in inflammatory gene expression (Kondrashov et al. 2012). Many mRNAs involved in inflammation are inherently unstable due to regulatory *cis* elements in their 3' UTRs, with AU-rich elements (AREs) being a well-studied example of such elements (P. Anderson 2010; Stumpo, Lai, and Blackshear 2010; Hao and Baltimore 2009). Part of ARE function includes recruitment of deadenylase machinery via *trans*-acting factors that removes the poly(A) tail. This is often regarded as the first and rate-limiting step of mRNA decay (C.-Y. A. Chen and Shyu 2011), and so a model can be conceived wherein the time taken to remove the poly(A) tail represents a delay before the mRNA can be degraded. Thus, regulation of poly(A) tail size could be particularly important for those mRNAs that are inherently unstable (like inflammatory mRNAs) and thus “depend” on the delay to exist long enough to be translated.

Previous experiments in our group studying polyadenylation and inflammation were done in human airway smooth muscle (ASM) cells, and we sought to further investigate the importance of polyadenylation in inflammatory gene induction using a macrophage-like cell type. I used the RAW 264.7 murine macrophage cell line and stimulated with lipopolysaccharide (LPS) to induce an inflammatory response. While primary macrophages may have been an ideal choice for being more representative of true macrophage biology, the RAW 264.7 cell line was chosen for two main reasons. Firstly, at the time of beginning the project, the poly(A) tail test (PAT) protocol required high input RNA quantities, especially if a deadenylated counterpart of a sample needed to be generated (in excess of 20 µg of RNA). Such high yields of RNA are more manageable and feasible with a cell line. Secondly, cell lines offer greater reproducibility across different types of experiments. When trying

to assemble and integrate data from multiple different experiments into an overall picture of how polyadenylation is important in the overall process of inflammation, and how cordycepin's effects are mediated (the subject of the next chapter), such reproducibility is very important.

Experiments in this chapter aimed to establish a working inflammatory system using LPS as a stimulus in the RAW 264.7 macrophage-like cell line. The inflammatory response would be assessed by RT-qPCR to monitor mRNA levels of inflammatory genes. Polyadenylation over the course of the inflammatory response was assessed by using the poly(A) tail test (PAT). This was done on both total RNA samples and also nuclear RNA, to examine whether the initial poly(A) tail size was the subject of regulation.

4.1 Developing the inflammatory system

I used the RAW 264.7 murine macrophage cell line and stimulated with lipopolysaccharide (LPS) to induce an inflammatory response. The cells were cultured in DMEM + 10% FBS, which contributes to growth factor signalling in the cells. In order to determine to what extent this signalling (and other effects of the serum) would have on the inflammatory dynamics, I performed LPS stimulations on cells still in the growth medium, and also on cells whose medium was changed to DMEM + 0.5% FBS. RT-qPCR data shows that serum starvation leads to a stronger degree of induction of the inflammatory genes by LPS compared to cells for which medium was not changed (**Figure 4.1**). The degree of induction refers to the difference in mRNA levels between unstimulated and stimulated conditions. This can result from either a lowering of mRNA levels in unstimulated conditions or an increase in mRNA levels in stimulated conditions (or some combination of the two). For *Tnf* mRNA, the greater degree of induction in serum-starved cells was mainly

due to a decrease of mRNA levels under unstimulated conditions. For *Cxcl2*, however, higher mRNA levels in stimulated conditions were the main contributor to the stronger induction in serum-starved cells. I decided to use the method involving serum starvation for subsequent experiments due to the stronger induction.

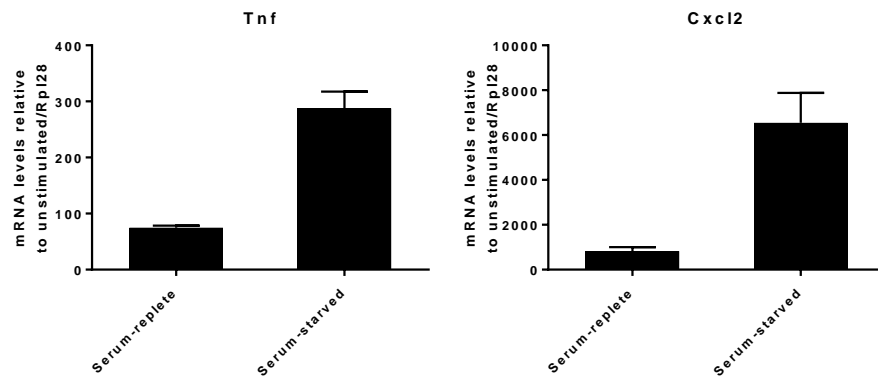


Figure 4.1. Serum withdrawal prior to LPS stimulation results in a more pronounced response. 24 hours after seeding RAW 264.7 cells, one set of cells was stimulated with LPS for 2 hours (serum-replete), while a second set of cells had medium changed to DMEM + 0.5% FBS (serum-starved). A further 24 hours later, serum-starved cells were stimulated with 1 $\mu\text{g}/\text{ml}$ LPS for 2 hours. RT-qPCR was done, error bars represent standard deviations across 3 technical replicates.

4.2 Time courses and poly(A) tails

With a working inflammatory system established, I then did time course experiments to observe the expression profiles of inflammatory genes over time, after induction with LPS. To this end, RT-qPCR was done on samples from the time course in addition to PAT to assess the distribution of poly(A) tails (**Figures 4.2 and 4.3**). Over a 2 hour period, all genes assessed showed an increase of 2-3 orders of magnitude in expression levels which remained elevated at the end of this period. RT-qPCR was also done for *Tnf* and *Acod1* using primers specific for unspliced mRNA in order to gauge pre-mRNA levels (and thereby estimate transcription levels). *Tnf* pre-mRNA levels appeared to increase and plateau by 30 minutes for the entire 2 hour period and mature mRNA levels followed a similar profile, with a slight decrease by 90 minutes. *Acod1* pre-mRNA levels, in contrast, rose to peak at 70 minutes and then declined greatly by 120 minutes. Although the *Acod1* pre-mRNA levels had decreased greatly by 90 minutes (and further still by 120 minutes) from the peak at 70 minutes, the levels of mature *Acod1* mRNA continued to increase throughout the whole 2 hour period. *Hprt* is shown as a control mRNA whose expression levels did not change, validating *Rpl28* as a reference mRNA.

Performing PAT on the RNA samples showed that *Cxcl2* and *Tnf* have relatively long poly(A) tails that coincide with their induction, and steadily get shorter over time (**Figure 4.3**). This could reflect a situation in which a pulse of transcription produces a population of mRNAs with long, freshly produced poly(A) tails which are gradually deadenylated over time. In the case of *Tnf*, the PAT data show the highest proportion of mRNAs with long poly(A) tails at 30 minutes, an approximately equal spread of mRNAs over a range of tail sizes at 50 minutes, and then most mRNAs are deadenylated from 70 minutes onwards. However, the *Tnf* pre-mRNA levels remain

elevated at these later timepoints, indicating that transcription is ongoing. This suggests that new *Tnf* transcripts produced at later timepoints may be made with shorter poly(A) tails.

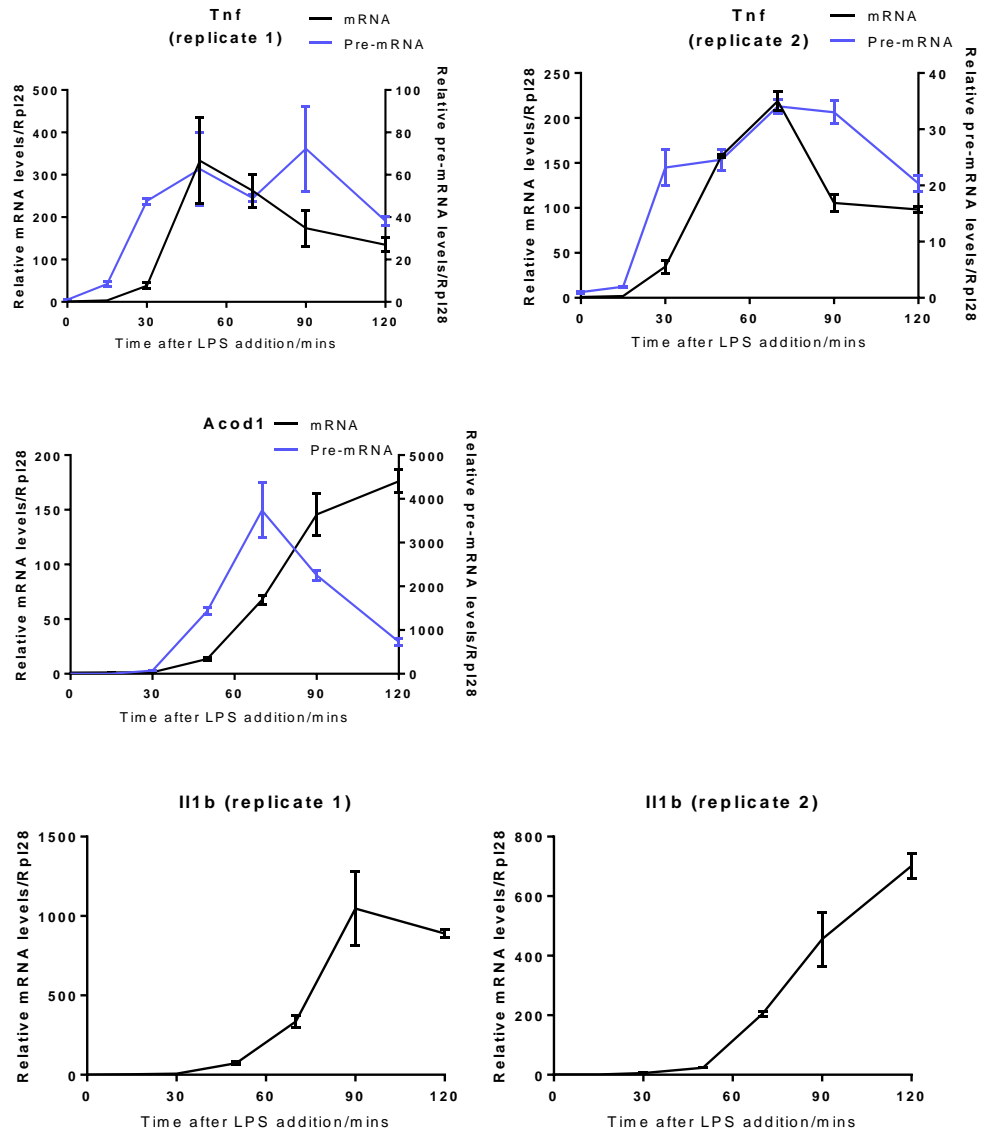


Figure 4.2. LPS stimulation of RAW 264.7 cells induces expression of inflammatory genes. RAW 264.7 cells were stimulated with 1 $\mu\text{g/ml}$ LPS for the indicated durations. RT-qPCR data obtained on the Qiagen Rotor-Gene Q platform show expression levels over the time course. Error bars represent standard deviations across 3 technical replicates. Data for 2 biological replicates are shown in separate graphs for each mRNA. *Acod1* data was only obtained for one biological replicate.

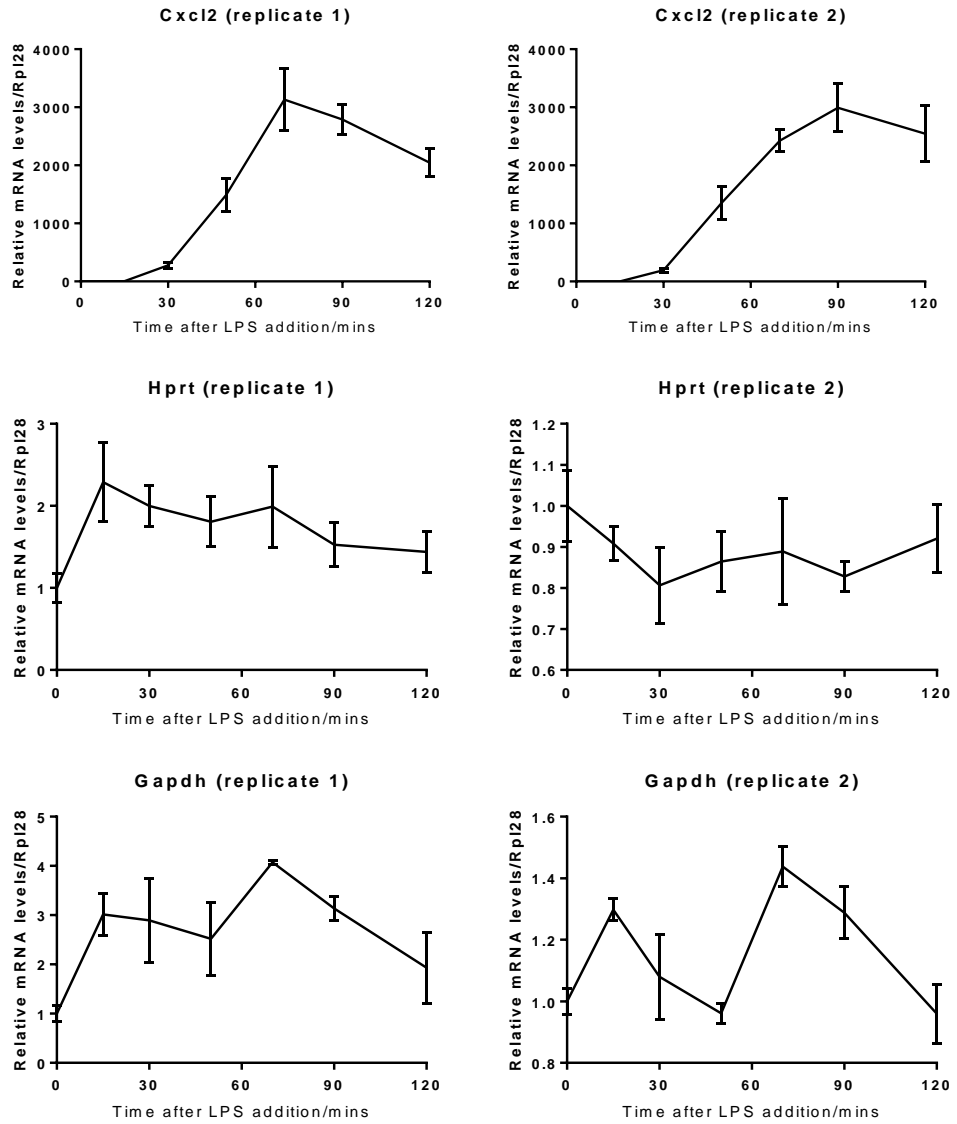


Figure 4.2. (cont) LPS stimulation of RAW 264.7 cells induces expression of inflammatory genes.

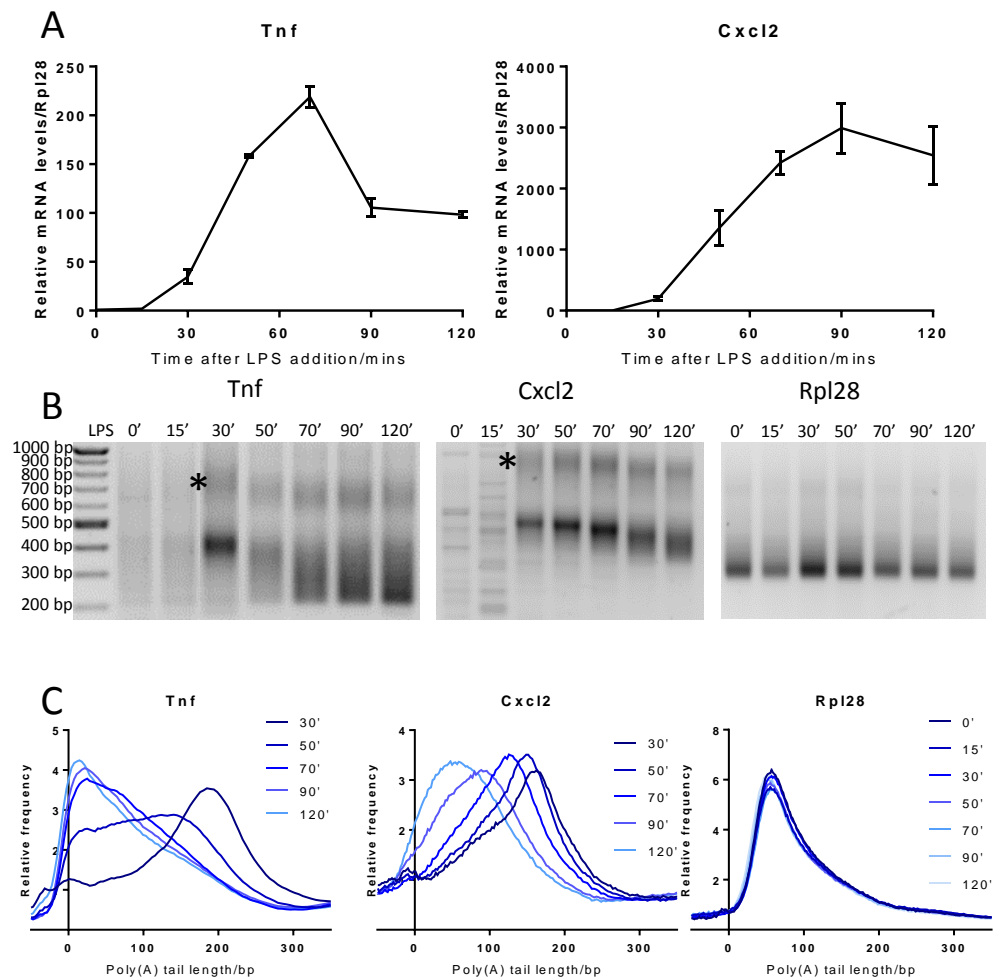


Figure 4.3. Tnf and Cxcl2 poly(A) tails change in size over the course of their inductions by LPS. RAW 264.7 cells were stimulated with 1 $\mu\text{g/ml}$ LPS for the indicated durations. RNA samples are the same as those analysed in **Figure 4.2** (replicate 2). (A) RT-qPCR data obtained on the Qiagen Rotor-Gene Q platform showing expression levels over the time course. These are the same data as those shown in **Figure 4.2**. (B) RNA samples were used for RL2-PAT, and products were run on an agarose gel. (C) Gel images were scanned using Quantity One software and profiles represented graphically. All data (including qPCR) are shown for a single biological replicate. qPCR error bars represent standard deviation across three technical replicates. * indicates artefactual bands.

Deadenylated product sizes – Tnf: 215 bp. Cxcl2: 339 bp. Rpl28: 259 bp.

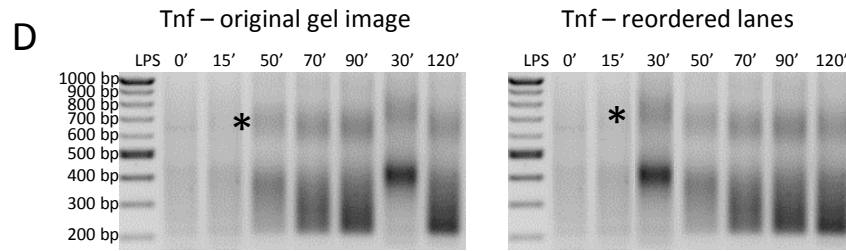


Figure 4.3. (cont) Tnf and Cxcl2 poly(A) tails change in size over the course of their inductions by LPS. (D) The Tnf PAT gel was loaded in the wrong order, so the image was altered to reorder the lanes. The original is shown alongside the altered image. * indicates artefactual bands.

To test whether initial poly(A) tail size was variable over the course of the inflammatory response, I performed another time course experiment but nuclear and cytoplasmic fractions were separated prior to RNA isolation. Doing PAT on nuclear RNA should show the poly(A) tail distribution of newly synthesised RNA. PAT for *Tnf* shows that the poly(A) tail of cytoplasmic RNA is longer at 30 minutes and shorter afterwards (**Figure 4.4**), as had been observed in total RNA (**Figure 4.3B** and **4.3C**). PAT done for *Tnf* on nuclear RNA appeared to generate very little product, leading to weak signal on the gel.

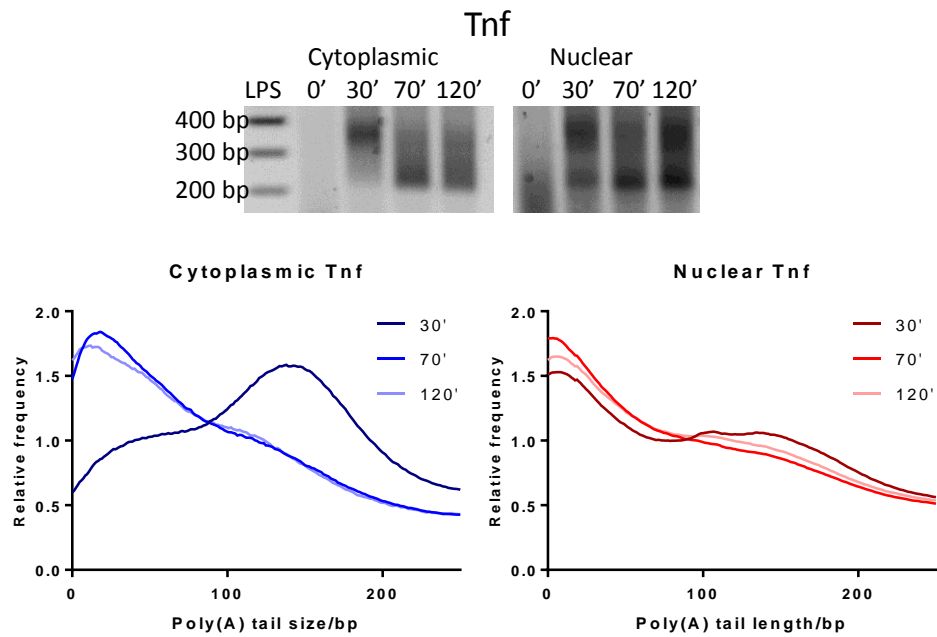


Figure 4.4. Initial *Tnf* poly(A) tail size is variable. RAW 264.7 cells were stimulated with 1 $\mu\text{g/ml}$ LPS for the indicated durations. Nuclear and cytoplasmic RNA was isolated from cells and RL2-PAT was done. PAT products were run on one agarose gel but different exposures were used for imaging cytoplasmic and nuclear lanes (images separated by a gap). PAT gel images were scanned using Quantity One software and profiles represented graphically.

Deadenylated *Tnf* product size: 215 bp.

Qualitatively, it appears that there is a band at 30 minutes corresponding to newly made RNA with a longer poly(A) tail compared to the PAT product for the 70 minute timepoint (**Figure 4.4**). This suggests that *Tnf* mRNA is made with a poly(A) tail whose length varies depending on what stage of the inflammatory response the cell is in. Notably, while PAT for cytoplasmic and total RNA samples shows that the poly(A) tail becomes shorter, and stays short, after 30 minutes of LPS treatment, this does not appear to be the case for nuclear RNA PAT. *Tnf* poly(A) tails of newly made mRNA appear to be long and short at 30 minutes, short only at 70 minutes, and long and short, again, at 120 minutes. This may indicate an oscillatory nature of the polyadenylation state of *Tnf* over the course of the inflammatory response.

4.3 Discussion

A working inflammatory model was established in the RAW 264.7 cells, as measured by levels of unspliced and mature mRNA of inflammatory genes. The poly(A) tails of *Tnf* and *Cxcl2* were shown to change over the course of their inductions. For *Tnf*, the fact that the poly(A) tail becomes progressively shorter after the 30' timepoint (**Figure 4.3**) even though unspliced levels of *Tnf* (i.e. pre-mRNA) remains elevated until at least 90' (**Figure 4.2**) suggests that the initial tail size is changing. Indeed, PAT done for *Tnf* on nuclear RNA (representing newly transcribed mRNA) showed that *Tnf* mRNA made at 30' had a greater proportion of long poly(A) tails than mRNA made at 70' (**Figure 4.4**). I was unable to obtain data for *Cxcl2* mRNA either for unspliced mRNA levels or nuclear PAT, and so there is insufficient data to make the same argument for *Cxcl2*. Additional replicates are needed for the nuclear PAT to confirm whether the initial *Tnf* poly(A) tail size is dynamic, and more mRNAs should be tested, particularly control mRNAs e.g. *Rpl28* to verify that their initial poly(A) tail size remains constant while that of *Tnf* (and perhaps also those of other inflammatory mRNAs) are dynamic.

However, the RAW 264.7 inflammatory system was successfully established and allowed reproducible inductions between replicates and measurement of poly(A) tails. While more data may be needed to validate the *Tnf* initial poly(A) tail size result, the idea that the initial poly(A) tail size varies is consistent with the qPCR data for mature and unspliced mRNA levels (which was shown across two biological replicates and validated against a control mRNA whose levels did not change). This represents a possibility of polyadenylation being involved in the regulation of such mRNAs.

5 Cordycepin and macrophages

The caterpillar fungi *Cordyceps* or *Ophiocordyceps* are prized in Far Eastern traditional medicine and are used for the treatment of many ailments including kidney and heart conditions (Winkler 2010). The adenosine analogue cordycepin is derived from *Cordyceps* fungi and has been shown to have clear biological activities, including anti-inflammatory properties (H. Kim et al. 2011; Kondrashov et al. 2012; Ying et al. 2014; Jeong et al. 2010b). See **section 1.3.3** for more detail.

Our group previously observed anti-inflammatory effects of cordycepin in human airway smooth muscle (ASM) cells (Kondrashov et al. 2012). Having established the inflammatory system in RAW 264.7 cells, we sought to test cordycepin in these cells. Time courses were done as in the previous chapter with and without cordycepin and the effects of cordycepin on mRNA levels and polyadenylation were both assessed. Proper cleavage and polyadenylation is needed for efficient transcription termination. In ASM cells, cordycepin was found to cause defective cleavage and transcription termination, consistent with a role in interfering with polyadenylation. We sought to test whether such effects were also present in the RAW 264.7 cells. Experiments were also done to gain insight into cordycepin's mechanism of action. In some studies, cordycepin has been reported to be active intracellularly (Kondrashov et al. 2012; Wong et al. 2010), while others report that effects of cordycepin on adenosine receptors are important. This was tested by assessing whether cordycepin's effects were altered by inhibiting its import into the cell. Another experiment was done in which, prior to LPS stimulation, cells were either preincubated with cordycepin for a given time or preincubated for part of that time and then had the medium replaced with cordycepin-free medium. In the event that cordycepin's effects are mediated extracellularly through adenosine receptors, any

effects of cordycepin should be lost or significantly reduced in cells for which the medium was replaced (whereas intracellular effects would persist). Cordycepin is metabolised by adenosine deaminase (ADA), resulting in its deamination to 3'-deoxyinosine. The ADA inhibitor pentostatin was used to see whether inhibition of deamination of cordycepin would potentiate its effects (which would imply that 3'-deoxyinosine is an inactive metabolite). LPS binding to Toll-like receptor 4 (TLR4) results in signalling that causes degradation of I κ B α (NFKBIA). This then allows nuclear translocation of NF- κ B, an important inflammatory transcription factor, and switching on of target genes (Lu, Yeh, and Ohashi 2008), as discussed in **section 1.3.2.1.3**. It has been reported by several groups that cordycepin interferes with this process, while the data of other groups (including our own ASM data) suggests that this does not happen. To assess this, the degradation of I κ B α was monitored in the presence and absence of cordycepin.

5.1 *Cordyceps* fungal extracts

Cordycepin is one of the metabolites present in *Cordyceps* fungi with a number of reported biological activities. We tested *Cordyceps militaris* and *Ophiocordyceps sinensis* ethanol extracts for anti-inflammatory potential, and also measured the concentration of cordycepin in the extracts. Both extracts were able to replicate the repressive effects of cordycepin on inflammatory gene expression in RAW 264.7 cells (**Figure 5.1A**) while control extracts from other fungi were not, with no reduction in *Tnf* or *Il1b* levels observed for treatments with *P. ostreatus*, *A. bisporus*, or *F. velutipes* extracts (**Figure 5.1B**). The level of cordycepin in the *C. militaris* extract was very similar to the stock concentration of cordycepin used for the cordycepin treatment, and both the cordycepin stock and *C. militaris* extract were used as 1000-fold concentrates (so the same volume of each was used in the respective cell

treatments). Taken together, these findings strongly imply that cordycepin is the bioactive component of *C. militaris*. Strikingly, however, the level of cordycepin in the *O. sinensis* extract was 5 orders of magnitude lower (**Table 5.1**), despite exhibiting repressive effects on inflammatory gene expression. This clearly demonstrates that cordycepin is not the sole component that contributes to the anti-inflammatory potential of at least one of these fungi.

Extract	[Cordycepin]	[3'-deoxyinosine]
<i>Coryceps militaris</i>	22.72 ± 1.59 mM	12.37 ± 1.57 μM
<i>Ophiocordyceps sinensis</i>	0.13 ± 0.01 μM	0.04 ± 0.003 μM

Table 5.1. *Cordyceps militaris* extract contains significant quantities of cordycepin while *Ophiocordyceps sinensis* extract does not.

Concentration of cordycepin and 3'-deoxyinosine was determined in the two fungal extracts by LC/MS.

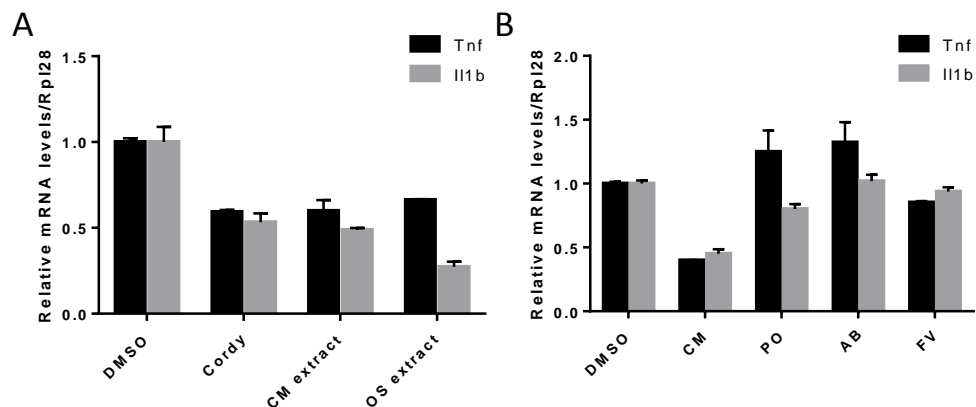


Figure 5.1. Ethanol extracts from *C. militaris* and *O. sinensis* exhibited similar repressive effects to those of cordycepin. RAW 264.7 cells were treated with the indicated compound or extract for 1 hour prior to stimulation with LPS at 1 μg/ml for 1 hour. RT-qPCR was performed, error bars represent standard deviations across 3 technical replicates. Extracts used: *Cordyceps militaris* (CM), *Ophiocordyceps sinensis* (OS), *Pleurotus ostreatus* (PO), *Agaricus bisporus* (AB), and *Flammulina velutipes* (FV).

5.2 Effects of purified cordycepin

Our lab group previously observed anti-inflammatory effects of cordycepin in airway smooth muscle cells (Kondrashov et al. 2012). To assess whether these effects were also present in macrophages, we incubated RAW 264.7 cells with DMSO (control) or cordycepin prior to stimulating the cells with LPS to provoke an inflammatory response. Expression of inflammatory genes was then measured by RT-qPCR at a number of timepoints over a course of 2 hours. Inflammatory gene expression of assessed genes was found to be repressed by cordycepin (**Figure 5.2**), while housekeeping gene expression (*Hprt* and *Gapdh*) was unaffected. A third set of cells was also used in which cordycepin was added 10 minutes after LPS stimulation, in order to assess how fast or slow the effects of cordycepin were (**Figure 5.3**). The repressive effects of cordycepin for cells pretreated with cordycepin and cells treated with cordycepin after LPS addition were identical. Cordycepin's observed effects are clearly very fast, and are thus likely to be primary in nature.

The previous work on ASM cells indicated that cordycepin did not affect the unspliced mRNA levels of most inflammatory mRNAs assessed (Kondrashov et al. 2012). In the RAW 264.7 cells, cordycepin was found to affect unspliced mRNA levels (**Figure 5.4**). Only two genes were assessed (*Tnf* and *Acod1*), but the result was observed over two replicates.

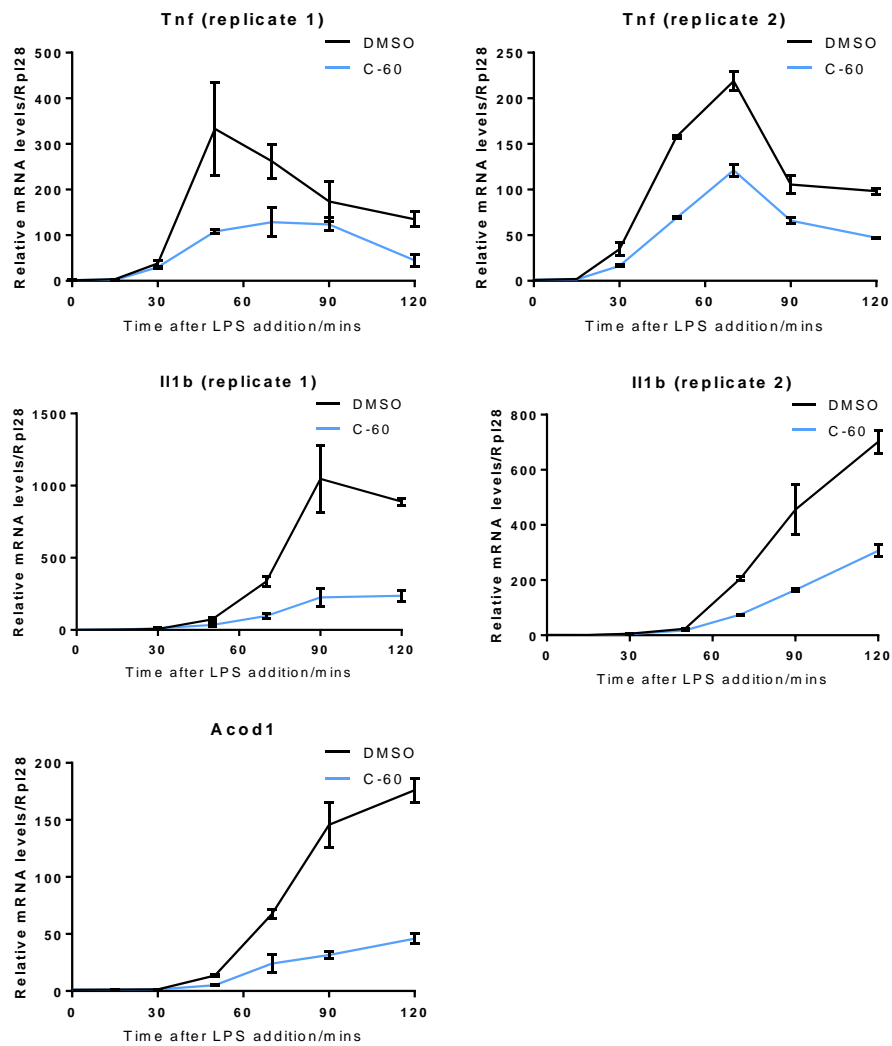


Figure 5.2. Cordycepin represses inflammatory gene expression. RAW 264.7 cells were treated with DMSO or 20 μ M cordycepin for an hour (DMSO and C-60 respectively) prior to 1 μ g/ml LPS addition for the indicated durations. Data for DMSO series are the same as those shown in **Figure 4.2**. RT-qPCR was performed, error bars represent standard deviations across 3 technical replicates. *Acod1* data was only obtained for one biological replicate.

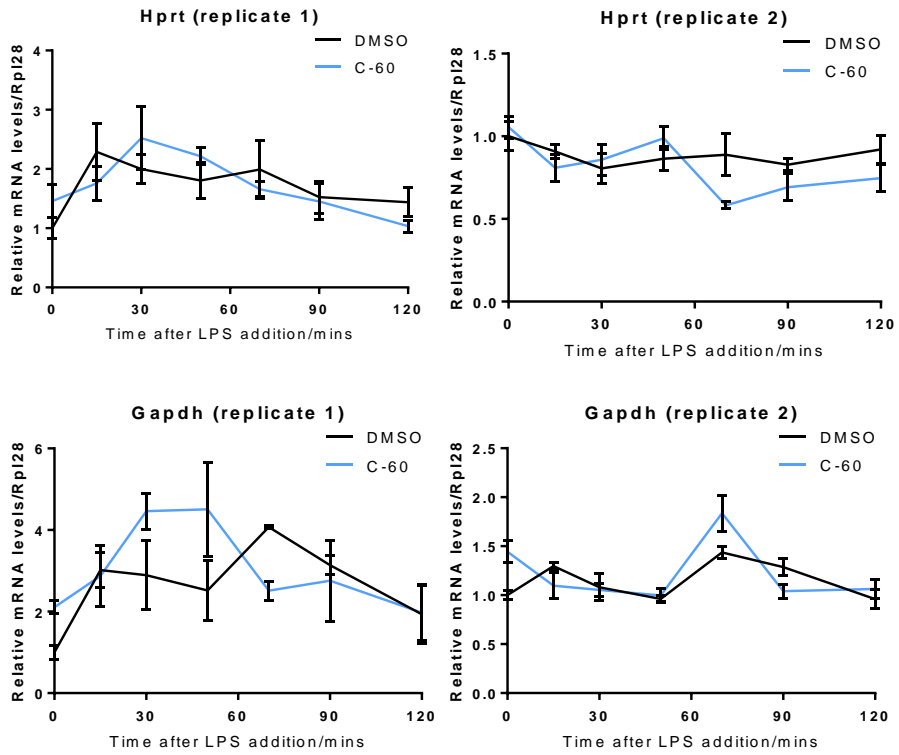


Figure 5.2. (cont) Cordycepin represses inflammatory gene expression.

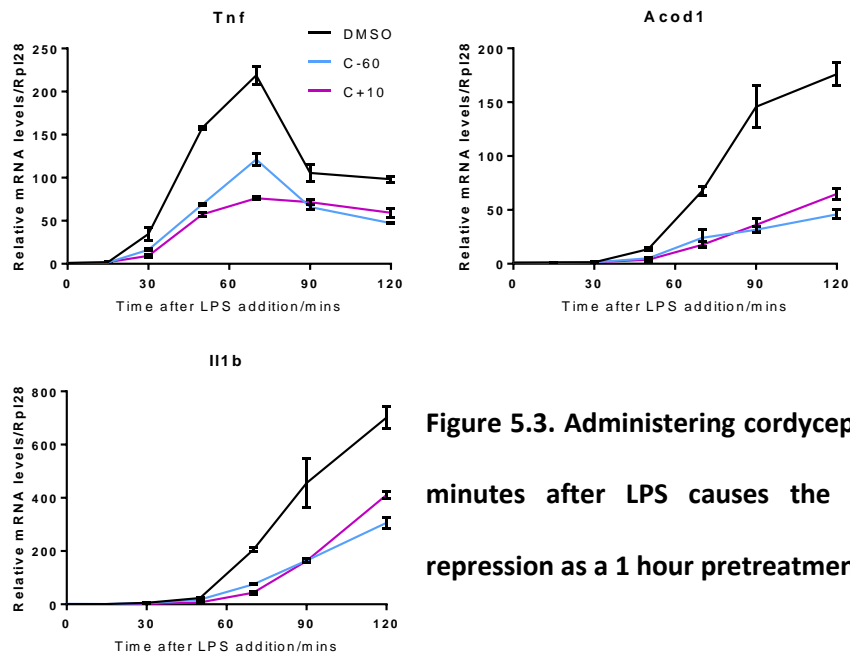


Figure 5.3. Administering cordycepin 10 minutes after LPS causes the same repression as a 1 hour pretreatment.

RAW 264.7 cells were treated with DMSO or 20 μ M cordycepin for an hour (DMSO and C-60 respectively) prior to 1 μ g/ml LPS addition for the indicated durations. Cells in the C+10 series had 20 μ M cordycepin added 10 minutes after addition of 1 μ g/ml LPS. The 0' timepoint for DMSO and C+10 was a single cell treatment, shared between both series. RT-qPCR was performed, error bars represent standard deviations across 3 technical replicates.

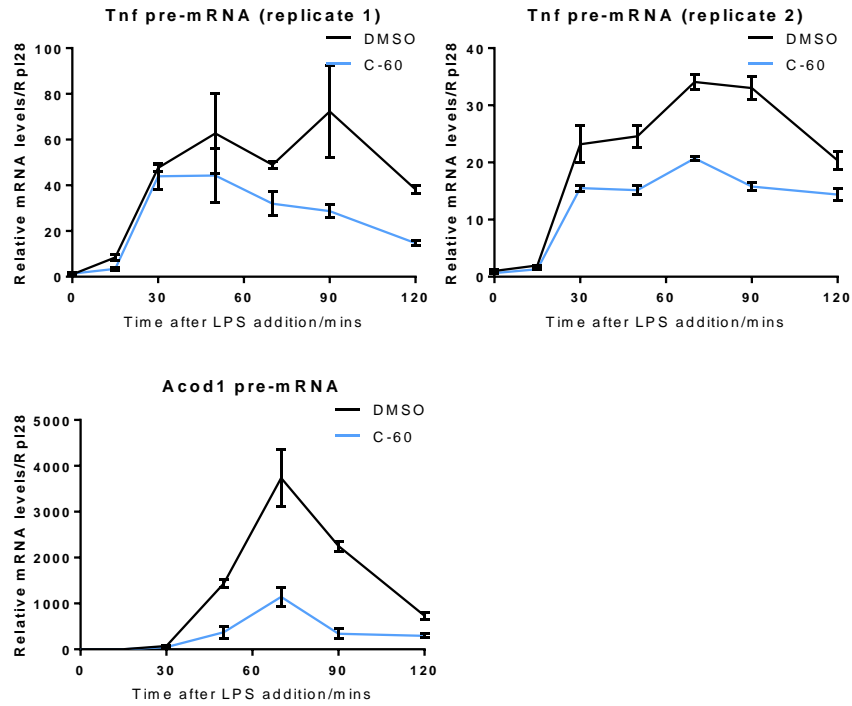


Figure 5.4. Cordycepin represses at the transcriptional level. See Figure 5.2 legend for experimental description. Error bars represent standard deviations across 3 technical replicates. Acod1 data are only available for 1 replicate.

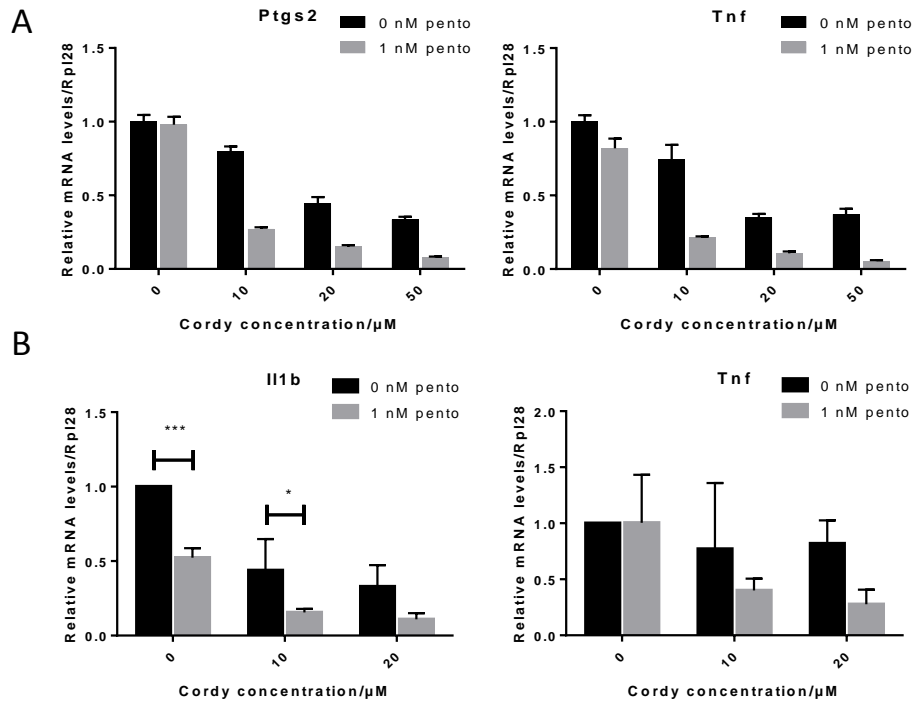


Figure 5.5. Pentostatin potentiates cordycepin's repressive effect on

inflammatory gene expression. (A) RAW 264.7 cells were seeded in DMEM + 10% FBS. After 24 hours, cells were treated with the indicated concentrations of cordycepin, with or without 1 nM pentostatin for 1 hour, at which point 1 μg/ml LPS was added to cells for a further 2 hours. RT-qPCR was performed, error bars represent standard deviations across 3 technical replicates.

(B) As above, but 24 hours after seeding, medium was changed to DMEM + 0.5% FBS. The experiment was then done 24 hours later. Error bars represent standard deviations across 3 biological replicates.

Significant differences assessed by 2-way ANOVA followed by Sidak's multiple comparisons test. * $p < 0.05$, ** $p < 0.01$, *** $p < 0.001$

The deamination of cordycepin by adenosine deaminase produces 3'-deoxyinosine as the breakdown product. To assess whether cordycepin (or a non-deaminated metabolite) was the active compound rather than 3'-deoxyinosine (or a metabolite of this compound), RAW 264.7 cells were incubated with cordycepin in the presence or absence of 1 nM pentostatin – an inhibitor of adenosine deaminase – prior to LPS stimulation. Pentostatin potentiated the repressive effects of cordycepin for all concentrations of cordycepin tested when cells were in DMEM + 10% FBS (**Figure 5.5A**), suggesting that deamination of cordycepin reduces or may even abolish its anti-inflammatory capacity. However, when this was repeated with biological replicates in cells for which serum was withdrawn (i.e. cells for which the medium was changed to DMEM + 0.5% FBS 24 hours after seeding cells in DMEM + 10% FBS, and 24 hours prior to the experiment), significant differences were only observed for Il1b and not for Tnf (**Figure 5.5B**). It should also be noted that a significant decrease in Il1b levels was observed when treating with pentostatin in the absence of cordycepin, suggesting possible additive, independent effects.

Stimulation of adenosine receptors with adenosine is known to cause anti-inflammatory effects in macrophages (Haskó and Cronstein 2013), and it has been reported that some of cordycepin's biological effects are also mediated through these receptors (Takahashi et al. 2012; Kadomatsu et al. 2012; Nakamura et al. 2006). As an adenosine analogue, it is conceivable that cordycepin can act extracellularly as an adenosine receptor agonist. Our group has previously shown that inhibiting cordycepin import into the cell, by using an inhibitor of the adenosine transporter, abrogates its anti-inflammatory effects in airway smooth muscle cells (Kondrashov et al. 2012). Work in the Centre for Bioanalytical Science (Nottingham) showed that cordycepin itself is short-lived intracellularly, while it persists as cordycepin triphosphate in tissue culture cells and liver (Wahyu Utami and David

Barrett, unpublished data). Moreover, inhibition of the phosphorylation of cordycepin through inhibition of adenosine kinase also abrogates its anti-inflammatory effects (Kondrashov et al. 2012). To address the question of whether cordycepin can act extracellularly, possibly through adenosine receptors, or whether it must be imported and phosphorylated, as is the case for airway smooth muscle cells, we performed similar experiments. RAW 264.7 cells were incubated with NBTI (adenosine transport inhibitor) or ITu (adenosine kinase inhibitor) or nothing (control) prior to addition of LPS together with DMSO, adenosine, or cordycepin. As had been the case with airway smooth muscle cells, it was found that NBTI or ITu treatment completely abolished cordycepin's repressive effects on inflammatory gene expression in RAW 264.7 cells (**Figure 5.6**). These data indicate that cordycepin must be imported and phosphorylated to have its effects, and does not act extracellularly.

The NBTI/ITu experiment also demonstrates distinct activities of cordycepin and adenosine. While adenosine was seen to repress *I1b* mRNA levels, its repression of other mRNAs was much less than that of cordycepin, if there was even any repression at all. The repression of *I1b* by adenosine was not relieved by NBTI or ITu, either. These data indicate that cordycepin and adenosine do not act in the same manner, and so cordycepin is unlikely to merely act as an adenosine analogue that mimics the effect of adenosine.

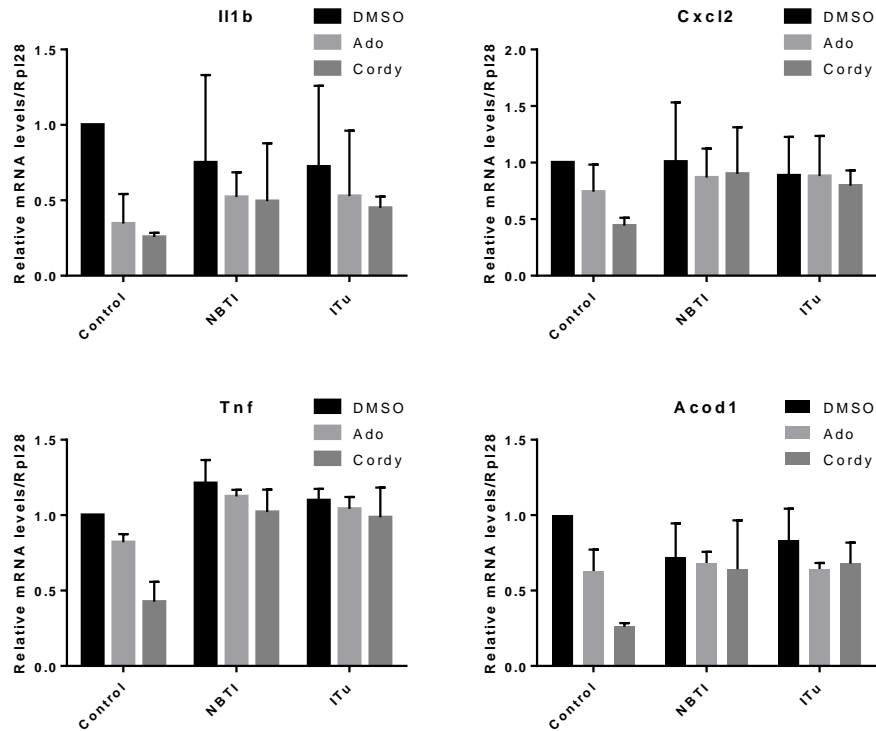


Figure 5.6. Inhibiting import of cordycepin or its phosphorylation abrogates its repression of inflammatory genes. RAW 264.7 cells were treated with nothing (control), 10 μ M NBTI, or 100 nM ITu for 15 minutes, then stimulated with LPS at 1 μ g/ml for 1 hour. RT-qPCR was performed, error bars represent standard deviations across 2 biological replicates.

To further distinguish the effects of cordycepin from those of adenosine, 2 sets of RAW 264.7 cells were briefly exposed to DMSO, adenosine, or cordycepin before being washed with PBS and having medium replaced. 1 set then had DMSO, adenosine, or cordycepin added back to the original concentration (non-washed) while the other set did not (washed). 2 hours after this point, cells were stimulated with LPS. Cordycepin that is intracellular and stable should still be able to exert its effects on the cells, while any extracellular action, e.g. that of adenosine on adenosine receptors, should be lost. While effects of adenosine were lost, the repressive effects of cordycepin were retained, albeit to a lesser degree, in the cases of *Acod1* and *Tnf*, but not for *Cxcl2* (Figure 5.7). These data show that the effects of

cordycepin are more persistent than those of adenosine, making effects through adenosine receptors even less likely. This experiment, alone, cannot rule out a distinct extracellular mode of action, since it could be the case that extracellular effects had already triggered long-acting signalling pathways within the cell by the time the washing was done. However, when taken together with the results of the inhibition of cordycepin import and phosphorylation experiment (**Figure 5.6**), an intracellular mechanism of action becomes likely. It is possible that washed cells had lower levels of intracellular cordycepin than non-washed cells, which may account for the loss of repression of *Cxcl2*, rather than because extracellular effects were lost. Adenosine did not display particularly strong repression of inflammatory gene expression, but for *Tnf* and *Cxcl2*, the modest repression observed in non-washed cells was lost in the washed counterparts. It should be noted that *Acod1* shows higher expression levels for DMSO treatment in washed cells than in non-washed cells. This highlights potential limitations of this experiment as a means for assessing changes in repressive capacity.

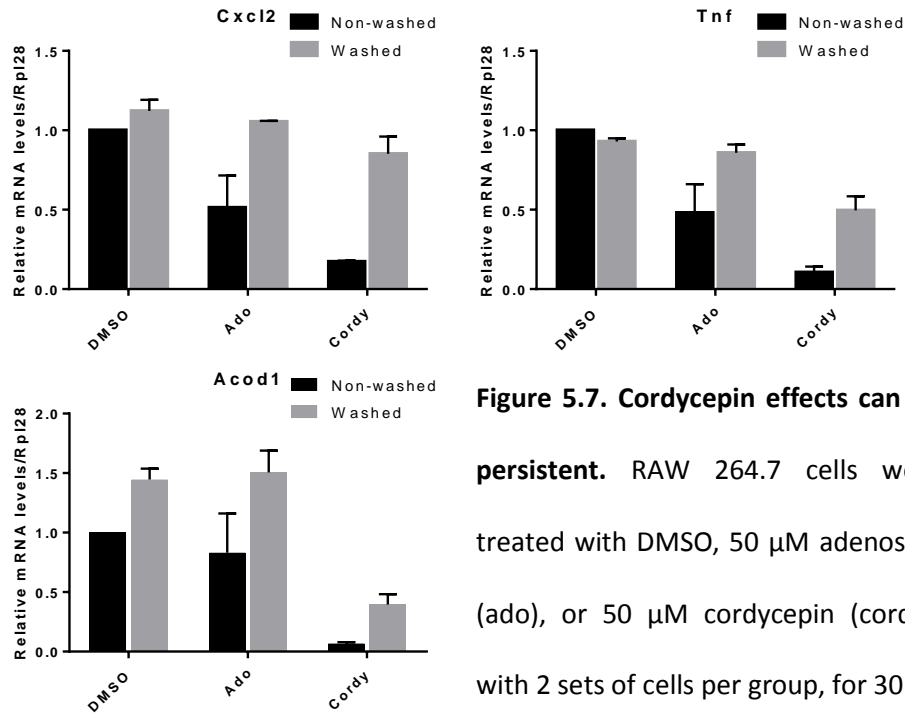


Figure 5.7. Cordycepin effects can be persistent. RAW 264.7 cells were treated with DMSO, 50 μ M adenosine (ado), or 50 μ M cordycepin (cordy), with 2 sets of cells per group, for 30

minutes. All cells then had medium removed and were washed with PBS. 1 set of cells had fresh DMEM + 0.5% FBS added (termed 'washed'), while the other set of cells also had the respective compound (DMSO, ado, or cordy) added at the original concentration (these cells were termed 'non-washed'). A further 2 hours later, cells were stimulated with LPS at 1 μ g/ml for 1 hour. RT-qPCR was performed, error bars represent standard deviations across 2 biological replicates.

It is known that cordycepin is a polyadenylation inhibitor, and so effects on polyadenylation must be considered when assessing its mechanism. For this reason, I did PAT for *Tnf* – an inflammatory gene whose poly(A) tail size changes over the inflammatory response, and whose expression is repressed by cordycepin – on samples from the LPS time course in the presence and absence of cordycepin. It was found that the poly(A) tail is, indeed, shortened by cordycepin (**Figure 5.8**). While this does not indicate causality, it is clear that the effects of cordycepin on polyadenylation are present.

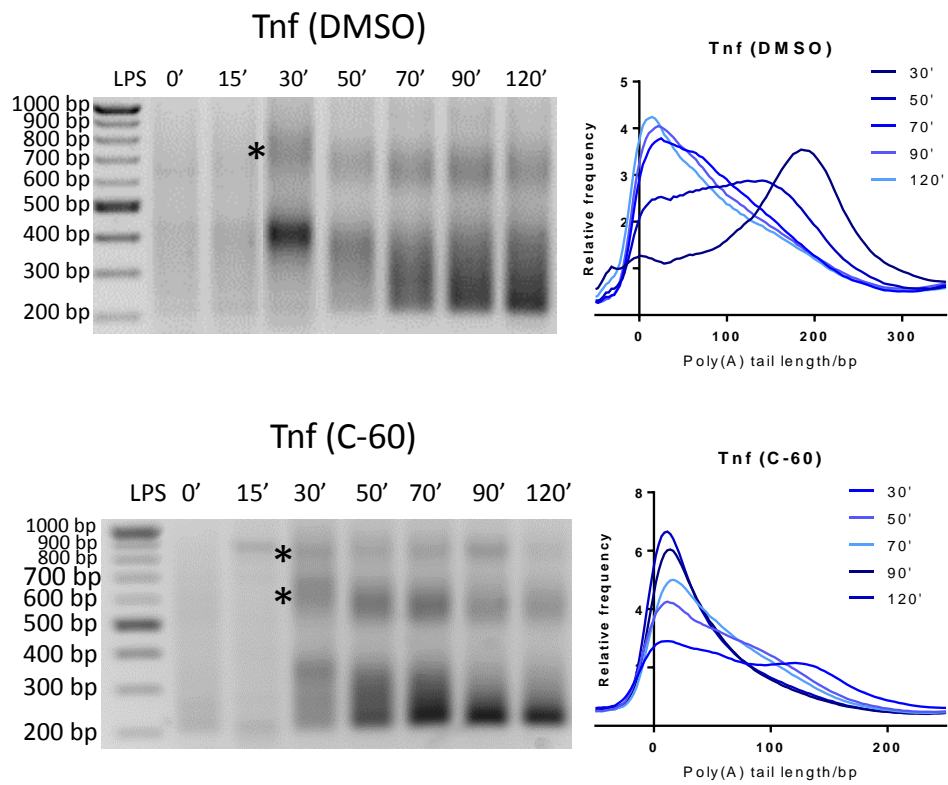


Figure 5.8. Cordycepin shortens the Tnf poly(A) tail. RAW 264.7 cells were treated either with DMSO or 20 μ M cordycepin (C-60) for 1 hour prior to addition of 1 μ g/ml LPS for the indicated durations. RNA was isolated and RL2 PAT performed to assess polyadenylation. Agarose gels were scanned in Quantity One and data presented graphically. N.B. Tnf (DMSO) gel image has been altered to reorder lanes – see **Fig 4.3D** for original image. * indicates artefactual bands.

Deadenylated Tnf product size: 215 bp.

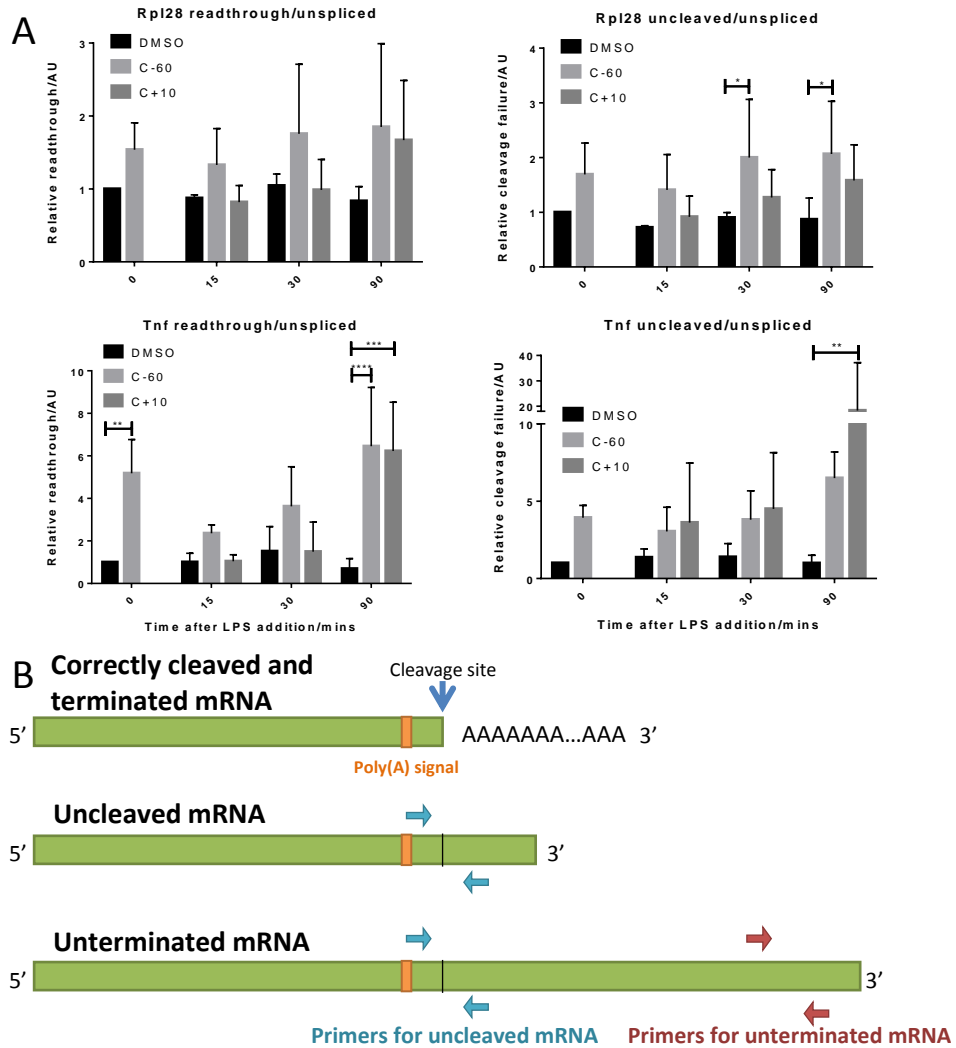


Figure 5.9. Cordycepin causes defects in transcription termination and mRNA

3' cleavage. (A) RAW 264.7 cells were treated with DMSO or 20 μ M cordycepin for an hour prior to 1 μ g/ml LPS addition for the indicated durations (DMSO and C-60 respectively), or 20 μ M cordycepin 10 minutes after 1 μ g/ml LPS addition for the indicated durations (C+10). The 0' timepoint for DMSO is used as the calibrator for both DMSO and C+10 series (the C+10 series does not have its own 0' timepoint). RNA was isolated and RT-qPCR performed. Error bars represent standard deviations across 3 biological replicates. Significant differences assessed by 2-way ANOVA followed by Dunnet's multiple comparisons test. * $p < 0.05$, ** $p < 0.01$, *** $p < 0.001$, **** $p < 0.0001$

(B) RT-qPCR primer locations for uncleaved and unterminated mRNA.

Proper mRNA 3' cleavage and polyadenylation is thought to be essential for efficient transcription termination (Luo, Johnson, and Bentley 2006; West, Proudfoot, and Dye 2008; Richard and Manley 2009). If cordycepin's effects on polyadenylation include interfering with mRNA 3' cleavage, it would be expected to lead to defective transcription termination. In order to measure this, we performed RT-qPCR using primers that amplified a region spanning the cleavage site, and primers that amplified a region 500-750 nt downstream of the cleavage site (**Figure 5.9**). These levels were then represented relative to the unspliced levels of the mRNA to gauge cleavage and termination efficiencies. Cordycepin caused an increase in the relative proportions of uncleaved transcripts for *Rpl28* and an increase in both uncleaved and unterminated transcripts for *Tnf* (**Figure 5.9**). These data support a model for an intracellular mode of action of cordycepin, involving impairment of and interference with mRNA 3' processing. The timepoints that were chosen (0', 15', 30', 90') allowed for assessment of both newly or recently made mRNA and also mRNA in the later stages of the induction.

Assessment of cleavage and termination efficiencies also showed differences in cordycepin and adenosine treatments (**Figure 5.10**). Adenosine treatment, whether in washed or non-washed cells, did not change measured cleavage and termination efficiency. Cordycepin treatment, however, caused a significant decrease in cleavage and termination efficiencies – an effect that was still clearly observed in washed cells. In the time course, cordycepin affected both cleavage and termination for *Tnf* but only cleavage for *Rpl28* (**Figure 5.9**). Data from the washing experiment, however, showed changes in both cleavage and termination efficiencies for both *Tnf* and *Rpl28* in cordycepin-treated cells. *Rpl28* expression levels are insensitive to cordycepin, but these data show that cordycepin, while having specific effects on final mRNA levels, may have more generalised effects on 3' processing and

transcription termination, as was previously observed in airway smooth muscle cells (Kondrashov et al. 2012).

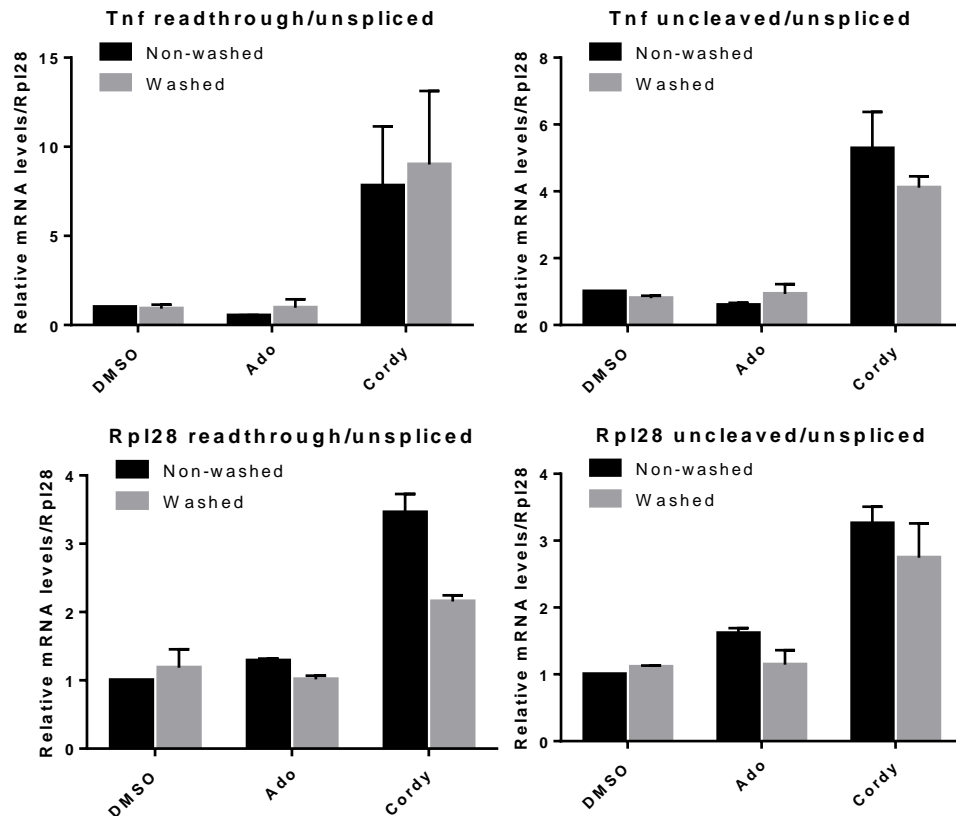


Figure 5.10. The effects of cordycepin on mRNA 3' processing are not shared by adenosine and are unlikely to be mediated extracellularly. RAW 264.7 cells were treated with DMSO, 50 μ M adenosine (ado), or 50 μ M cordycepin (cordy), with 2 sets of cells per group, for 30 minutes. All cells then had medium removed and were washed with PBS. 1 set of cells had fresh DMEM + 0.5% FBS added (termed 'washed'), while the other set of cells also had the respective compound (DMSO, ado, or cordy) added at the original concentration (these cells were termed 'non-washed'). A further 2 hours later, cells were stimulated with LPS at 1 μ g/ml for 1 hour. RT-qPCR was performed, error bars represent standard deviations across 2 biological replicates.

To test whether cordycepin affected NF- κ B signalling, an LPS time course was done in RAW 264.7 cells over a 30 minute period. Cells were treated with either DMSO or cordycepin for 1 hour prior to addition of LPS. Western blotting was then done on cell lysates for total I κ B α . The DMSO series shows a band for I κ B α in unstimulated cells and for a 5 minute LPS treatment (**Figure 5.11**). This band is almost completely lost, indicating degradation, in the 15 minute timepoint, and then reappeared in the 30 minute sample. The degradation of I κ B α was not at all prevented by cordycepin pretreatment. Further replicates are needed for verification, but these data suggest that cordycepin does not interfere with I κ B α degradation.

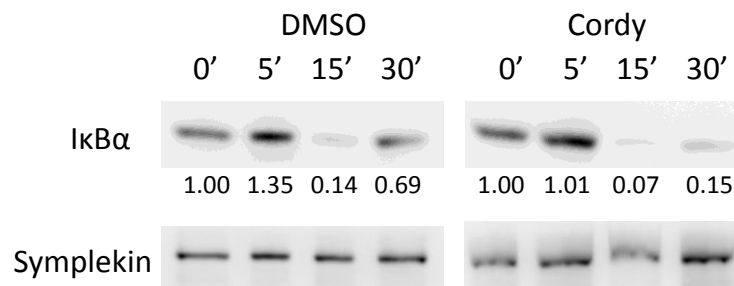


Figure 5.11. I κ B α degradation is not prevented by cordycepin. RAW 264.7 cells were treated with DMSO or cordycepin for an hour prior to LPS addition at 1 μ g/ml for the indicated durations. Cells were then lysed and Western Blot performed. Relative I κ B α levels for timepoints in each series (DMSO and cordy) are shown with the respective 0' timepoint set to 1. Symplekin was used as a loading control.

5.3 Discussion

Data in this chapter demonstrated the anti-inflammatory effects of cordycepin in RAW 264.7 cells. In general, more replicates are needed in order to be able to perform statistical analysis and confirm the conclusions that have (tentatively) been made here.

Cordycepin is likely to be the main bioactive component (as far as anti-inflammatory effects are concerned) of *C. militaris* ethanol extract. *O. sinensis* extract, however, contained 5 orders of magnitude less cordycepin than the concentration of cordycepin in the *C. militaris* extract or purified cordycepin stock in DMSO. This suggests that other metabolites are more important in *O. sinensis* for mediating its anti-inflammatory effects. Data in **Table 5.1** and **Figure 5.1** are only for one biological replicate, however. To confirm these findings and further investigate, more replicates would be needed, and perhaps fungal samples from multiple sources. Additionally, a treatment of pure cordycepin should be used that matches the low cordycepin concentration in the *O. sinensis* extract to show that the low level of cordycepin in *O. sinensis* alone cannot account for its anti-inflammatory properties.

Cordycepin decreased the expression of the assessed inflammatory genes and had identical effects when administered to cells ten minutes after addition of LPS rather than 1 hour beforehand (**Figures 5.2** and **5.3**). The fact that unspliced mRNA levels were decreased (**Figure 5.4**) suggests a transcriptional level of control by cordycepin. Since NF- κ B is a key inflammatory transcription factor whose activation is downstream of LPS/TLR4 signalling in macrophages (see **sections 1.3.2.1.1** and **1.3.2.1.2**), we assessed whether cordycepin interfered with the NF- κ B pathway, as

others have reported (H. G. Kim et al. 2006; Y. Li et al. 2016; Jie Peng et al. 2015; Ying et al. 2014). This was done by detecting I κ B α degradation following LPS stimulation in the presence and absence of cordycepin. Cordycepin did not impede the degradation of I κ B α (**Figure 5.11**). Further replicates are needed to confirm this finding, however.

Experiments with adenosine highlighted distinct activities of adenosine and cordycepin, showing that cordycepin is unlikely to simply act by mimicking the effect of adenosine. Cordycepin is likely to act intracellularly and require phosphorylation, since inhibition of the adenosine transporter and adenosine kinase abrogated its effects (**Figure 5.6**). The results of the washing experiment were entirely clear and seemed to sometimes contradict the results of the NBTI/ITu experiment. However, if cordycepin does act intracellularly, it is possible that non-washed cells accumulated more cordycepin within them than the washed cells. To monitor this variable, the experiment could be repeated with parallel sets of cells. At the end of the experiment, one set could be used for RT-qPCR (as we did), and the other set could be subjected to liquid chromatography-mass spectrometry analysis to determine cordycepin concentrations in washed and non-washed cells. Effects on polyadenylation by cordycepin were clearly observed (**Figure 5.8**), and were consistent with the observation that cordycepin caused defective mRNA cleavage and transcription termination (**Figures 5.9 and 5.10**). As such, valuable information was obtained for understanding molecular effects of cordycepin.

6 High-throughput analysis of cordycepin-treated RAW 264.7 cells

Having observed by RT-qPCR that cordycepin treatment in RAW 264.7 cells led to downregulation of a number of inflammatory mRNAs (see previous chapter), we elected to perform high-throughput analysis to reveal genome-wide changes brought about by cordycepin. To assess changes in gene expression, a microarray analysis was performed followed by cluster analysis on the lists of RNAs whose levels were changed by cordycepin. In order to see whether cordycepin sensitivity correlated with mRNA stability or transcription rates, RNA-seq was performed on newly transcribed RNA (generated by pulse labelling) from RAW 264.7 cells.

6.1 LPS and cordycepin treatments

With polyadenylation implicated in inflammatory gene expression, and cordycepin, as a polyadenylation inhibitor, shown to inhibit expression of a number of inflammatory genes, we sought to assess the effect of cordycepin in a genome-wide manner through microarray analysis. RAW 264.7 cells were either pre-treated with DMSO or 20 μ M cordycepin for an hour prior to either no further treatment or addition of 1 μ g/ml LPS for one hour. At the end of the two hour period (1 hour DMSO/cordycepin plus 1 hour LPS/no LPS) RNA was isolated from cells and analysed by microarray. Cell conditions were named 'D0', 'D60', 'C0', and 'C60' – D means DMSO pre-treated, C means cordycepin pre-treated, 0 means NOT stimulated with LPS, 60 means LPS-stimulated. We compared expression in D60 vs D0 (i.e. LPS-stimulated vs unstimulated, both without cordycepin) to show expression changes caused by LPS stimulation, and then compared C60 vs D60 (i.e. LPS-stimulated with cordycepin to LPS-stimulated without cordycepin) to show how those expression changes are affected. These two comparisons were then plotted against each other,

with genes whose expression levels were at least 2-fold changed in both comparisons considered, while other genes were disregarded (**Figure 6.1**). A Chi-squared test showed that LPS and cordycepin treatments are not independent ($p < 2.2 \times 10^{-16}$). Specifically, it appears that proportionately more RNAs that upregulated by LPS treatment are downregulated by cordycepin (94) than upregulated (30). Similarly, proportionately more RNAs that are downregulated by LPS treatment are upregulated by cordycepin (49) than downregulated (1). Additionally, performing gene ontology analysis on the list of genes most strongly downregulated in the LPS with cordycepin treatment compared to LPS alone revealed that immune and inflammatory gene clusters are the most significantly enriched (**Table 6.1**).

Gene Ontology Term	Count	Bonferroni-corrected P-value	Gene names	Fold Enrichment
mmu04060:Cytokine-cytokine receptor interaction	17	5.41E-08	CSF3, IL6, TNF, CCL2, PDGFB, TNFRSF12A, CSF1, CCL5, IL7R, CCL4, CCL7, CXCL10, OSM, LOC100045000, IL12RB1, LOC100044675, IFNB1, IL10RA, IL1B	7.0
cytokine	13	7.07E-06	CSF3, IL6, TNF, CCL2, CSF1, CCL5, CCL4, CCL7, CXCL10, OSM, LOC100045000, IFNB1, IL1B, CMTM5	8.4
GO:0005125~cytokine activity	13	2.16E-05	CSF3, IL6, TNF, CCL2, CSF1, CCL5, CCL4, CCL7, CXCL10, OSM, LOC100045000, IFNB1, IL1B, CMTM5	7.8
GO:0006955~immune response	22	4.56E-04	CSF3, IFIH1, IL6, CCL2, TNF, RSAD2, NLRP3, CCL5, IL7R, CCL4, CCL7, FOXP1, POLR3D, CXCL10, OSM, LOC100045000, ZGPAT, CLEC4E, SQSTM1, TICAM1, OASL1, IL1B, LIME1, CD300LB	3.7
GO:0006954~inflammatory response	14	8.83E-04	NFKBIZ, IL6, TNF, CCL2, CCL5, NLRP3, CCL4, CCL7, CXCL10, LOC100045000, CD44, TICAM1, IL1B, NOS2, PTAFR	5.8

Table 6.1. Immune and inflammatory GO terms are the most significantly enriched in genes downregulated by cordycepin.

RAW 264.7 cells were treated with 1 µg/ml LPS for 1 hour after a 1 hour pretreatment with DMSO or cordycepin (D60 and C60 respectively). Gene expression levels from microarray data were then compared between the two treatments. Those genes whose levels were >2-fold decreased in C60 compared to D60 were compiled into a list which was uploaded to DAVID for functional annotation. The 5 most significantly enriched GO terms are shown in the table.

Effects of LPS and cordycepin

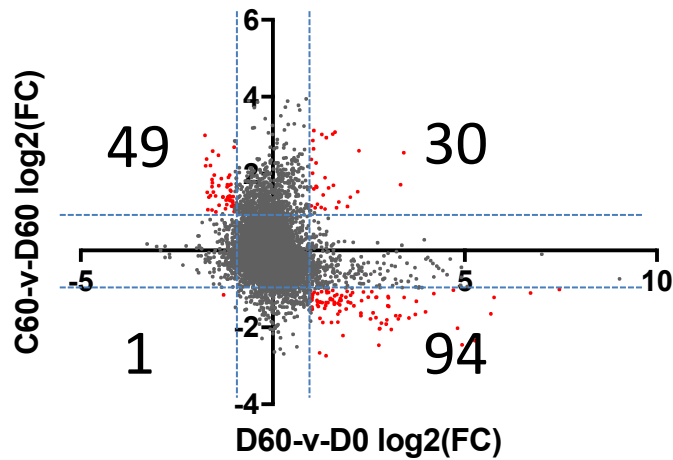


Figure 6.1. 94 RNAs with a >2-fold increase after LPS treatment are >2-fold downregulated by cordycepin. RAW 264.7 cells treated with DMSO for 2 hours (D0), or treated with 1 $\mu\text{g}/\text{ml}$ LPS for 1 hour after a 1 hour pretreatment with DMSO or cordycepin (D60 and C60 respectively). Gene expression levels from microarray analysis were compared between D60 and D0 (showing the effect of LPS) and between C60 and D60 (showing the effect of cordycepin in LPS-treated cells), and $\log_2(\text{fold change})$ values calculated. These values were then plotted against each other for all expressed genes. Grey dots indicate RNAs that did not show a significant >2-fold change in one or both comparisons. Red dots are RNAs that are >2-fold changed in both comparisons, with numbers indicating the number of such RNAs in each quadrant.

A Chi squared test showed that the two treatments are not independent ($p < 2.2 \times 10^{-16}$).

6.2 Cordycepin sensitivity and mRNA kinetics

Cordycepin inhibits both polyadenylation and transcription of inflammatory genes (**Figures 5.4** and **5.8**). In response to the inflammatory stimulus (LPS), inflammatory genes experience a large increase in transcription, and transcripts may be made with longer poly(A) tails for transient stabilisation of mRNAs that are otherwise unstable, as many inflammatory mRNAs are (P. Anderson 2010; Sanduja et al. 2012). If cordycepin's inhibitory effects on polyadenylation and transcription, possibly through defective termination and mRNA 3' processing, are responsible for its inhibition of inflammatory genes, then it may be the case that genes that have a high transcription rate and produce unstable mRNAs are sensitive to cordycepin. Information on which genes are cordycepin-sensitive is contained in the microarray data. RNA-seq data using 4-thiouridine-labelled RNA – i.e. RNA that was freshly transcribed within a short labelling period – from unstimulated RAW 264.7 cells (assumed to be at steady-state) was used to make inferences about mRNA transcription rates and stability. Consolidating the microarray and RNA-seq data allowed us to look for correlations between cordycepin-sensitivity and transcription rate or mRNA stability. No such correlation was observed, however (**Figure 6.2**).

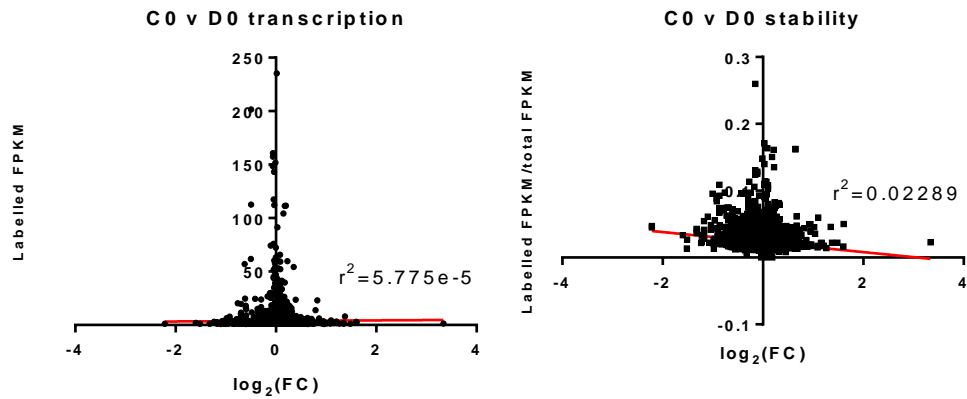


Figure 6.2. Cordycepin sensitivity is independent of mRNA stability and

transcription rate. RAW 264.7 cells treated with 20 μ M cordycepin (C0) or DMSO (D0) for 2 hours. Gene expression levels were compared between the two treatments and \log_2 (fold change) values calculated. In a separate experiment, untreated RAW 264.7 cells (in DMEM + 0.5% FBS) were exposed to a 15 minute 4-thiouridine labelling. RNA-seq was then performed and \log_2 (fold change) values from the microarray plotted against the 4SU-labelled FPKM (transcription rate) and 4SU-labelled FPKM/total FPKM values from the RNA-seq data. Linear regressions (red lines) were fitted to all plots, and r^2 values calculated. No significant correlation was observed.

6.3 Cordycepin and long noncoding RNAs

Long noncoding RNAs (lncRNAs) are RNAs longer than 200 nt that do not code for protein, but can have regulatory roles and implications for health and disease (Wapinski and Chang 2011; Kung, Colognori, and Lee 2013). It has been reported that there exists a class of lncRNAs whose turnover is promoted by PABPN1 in a polyadenylation-dependent manner (Beaulieu et al. 2012). If cordycepin inhibits polyadenylation, it would be expected to stabilise these lncRNAs, which should therefore be enriched in the set of RNAs upregulated by cordycepin. To test this hypothesis, I looked at the changes in RNA levels from the microarray data between

the cordycepin-treated and non-cordycepin-treated cells (both in the absence of LPS). The RNAs were categorised into 3 classes: significantly upregulated by cordycepin, significantly downregulated by cordycepin, and unchanged. Significantly upregulated and downregulated RNAs were those that were at least 2-fold changed in the appropriate direction, and had an adjusted p-value < 0.01. All other RNAs were placed in the 'unchanged' category. The vast majority of RNAs were in the unchanged category (>20,000), while the upregulated and downregulated categories had 547 and 146 RNAs, respectively. In order to perform the comparison between categories with similar numbers of RNAs, a random selection of 500 RNAs were taken from the unchanged category. The numbers of lncRNAs in each category was determined and a Chi-squared test done to see whether the proportion of lncRNAs in a category is independent of cordycepin treatment. The test revealed that lncRNA proportion and cordycepin treatment are not independent, with a much higher proportion of lncRNAs observed in the upregulated category (**Figure 6.3**). These data support the hypothesis that cordycepin stabilises a class of lncRNAs whose degradation is enhanced by polyadenylation. It may be that some or all of these RNAs are involved in mediating cordycepin's effects (i.e. they may regulate inflammation).

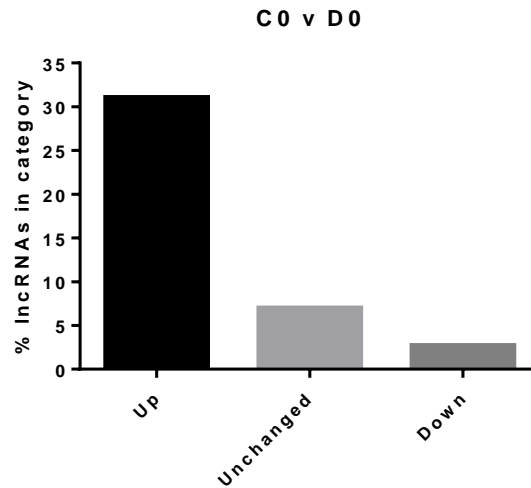


Figure 6.3. lncRNAs are enriched in RNAs that are upregulated by cordycepin treatment. RNA expression fold changes were calculated from microarray data between RAW 264.7 cells treated for 2 hours with 20 μ M cordycepin (C0) or DMSO (D0). RNAs that were >2-fold increased or decreased in expression, with an adjusted p value < 0.01, were placed in the up and down categories respectively. From the remaining RNAs, a random selection of 500 RNAs with a \log_2 (fold change) between -0.1 and 0.1 formed the unchanged category.

6.4 Discussion

Data in this chapter showed that cordycepin did indeed cause widespread repression of inflammatory mRNAs, as seen in the cluster analysis of the microarray data (**Table 6.1**). In **section 1.2.3.1**, some possible models by which cordycepin might act were proposed. One was that inherently unstable mRNAs may depend on a poly(A) tail more for the limited stability they do have, and that inhibition of polyadenylation would have a particularly strong destabilising effect on such mRNAs. The lack of a correlation between stability and cordycepin sensitivity, however (**Figure 6.2**), does not support this model. Another suggested possibility was that cordycepin may arrest the cleavage complex, as observed *in vitro* (Zarkower and Wickens 1987), thereby sequestering 3' processing factors. Genes for which transcription is taking place at a high rate (such as genes activated in the inflammatory response) would have high requirements for processing factors. A shortage of processing factors would affect transcription of such genes more than genes that are transcribed at a low rate (such that the availability of processing factors is not rate-limiting). However, the lack of a correlation between transcription rate and cordycepin (**Figure 6.2**) suggests this model does not apply. In the second model mentioned above, if a high need for processing factors arises through 'weaker' *cis* elements defining the poly(A) site rather than simply due to high rates of transcription, then cordycepin-sensitive genes may be enriched in such *cis* elements. This could be investigated through further bioinformatic analysis of the data sets.

Interestingly, lncRNAs are significantly enriched in RNAs upregulated by cordycepin treatment. There is a class of lncRNAs whose degradation is dependent on polyadenylation and whose levels are increased by PABPN1 knockdown (Beaulieu et

al. 2012). If cordycepin inhibits the polyadenylation of such lncRNAs, this would be expected to have a stabilising effect, which could account for the enrichment of lncRNAs in cordycepin-treated cells. If one or more of these lncRNAs affects the process of inflammation, cordycepin-mediated stabilisation of this/these lncRNA(s) could constitute part of the mechanism by which its anti-inflammatory effects are mediated. It would be interesting to assess whether the lncRNAs that are stabilised by cordycepin are the same as those whose levels are increased by PABPN1 knockdown, ostensibly through reduced polyadenylation-dependent degradation. This assessment was not carried out in this thesis as the work done by Beaulieu et al was performed in human cells while my data were generated from experiments in murine cells.

While data in this chapter did not support any of the proposed hypotheses to explain cordycepin's effects, a clear genome-wide anti-inflammatory effect of cordycepin was shown to exist in RAW 264.7 cells.

7 Cordycepin in a rat model of osteoarthritis

Osteoarthritis (OA) is a degenerative joint disease. While classically viewed as a non-inflammatory form of arthritis, evidence shows that inflammation can play a role in disease progression. Key features of the disease include remodelling of subchondral bone (bone under the cartilage) and degradation and loss of articular cartilage. As the previous two chapters show, cordycepin has widespread anti-inflammatory effects in RAW 264.7 cells. Furthermore, it has been reported that cordycepin shifts the balance of bone formation and degradation (F. Wang et al. 2015; Dou et al. 2016), and that it also reduced overactive cytokine production in chondrocytes from OA patients (Ying et al. 2014). For these reasons, cordycepin treatment was used in a rat model of osteoarthritis in order to see if it had any effect on pain behaviour in affected animals (this work was done by James Burston in Victoria Chapman's research group at the University of Nottingham). In order to see whether cordycepin affected mRNA levels of inflammatory genes or had effects on polyadenylation, RNA was isolated from the synovia of rats in the OA model and analysed by RT-qPCR and 3' end labelling.

7.1 Pain behaviour – work done by James Burston

Using the monosodium iodoacetate (MIA) chemically induced model of osteoarthritis in rats, cordycepin (administered orally) was assessed for its capacity to alter the pain behaviour of the animals. Animals had a saline (control) or MIA injection into the knee of a hind limb (day 0), and were then fed with DMSO (vehicle) or cordycepin every other day over the course of 14 days, during which time pain behaviour was assessed. Pain associated with the site of damage was measured through weight bearing asymmetry – animals were placed in a chamber that forced them to stand on their hind limbs, and the difference in weight borne by the leg with

the injury (ipsilateral) and the other leg (contralateral) was measured. Allodynia (pain caused by stimuli that do not normally cause pain) was measured by paw withdrawal threshold (PWT) – animals were placed in a cage in which the bottoms of their paws could have force applied by Von Frey filaments. The force applied was increased until the PWT was reached i.e. the force that caused the animal to withdraw its paw. The saline + vehicle group showed equal weight bearing over the course of the 14 days, while the MIA + vehicle group placed much more weight on their uninjured (contralateral) side (**Figure 7.1**). The MIA + cordycepin group also placed more weight on the contralateral limb than the saline + vehicle group, but placed significantly more weight on their ipsilateral side than the MIA + vehicle group in 3 of the 4 timepoints after day 0. The PWT of the saline + vehicle group remained constant over the 14 day period, while that of the MIA + vehicle group had dropped markedly by day 3, with no recovery observed over the remaining period. The MIA + cordycepin group experienced the same drop in PWT, with no differences between these groups at day 3 or day 7. At days 10 and 14, however, the PWT of the MIA + cordycepin group was significantly higher than that of the MIA + vehicle group. Together, these data show that cordycepin reduces pain behaviour in the MIA rat model of osteoarthritis.

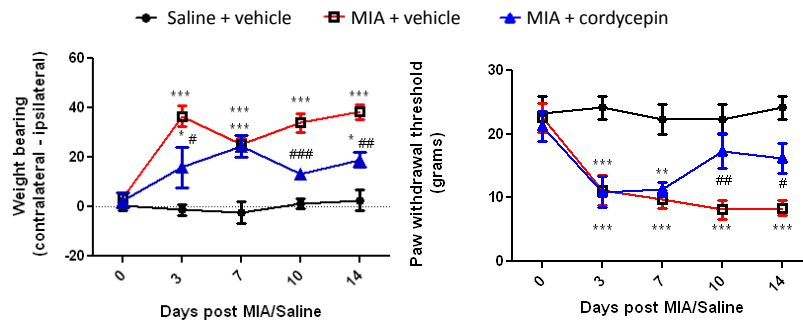


Figure 7.1. Cordycepin alters pain behaviour in a rat osteoarthritic model. MIA or saline was injected into the knee of one hind limb of rats on day 0. MIA rats were then fed 20 mg/kg cordycepin or DMSO (vehicle) every other day. Saline rats were fed DMSO every other day. Pain behaviour was then assessed through weight bearing asymmetry and paw withdrawal threshold upon application of pressure to the paw using Von Frey filaments.

$p < 0.05$, ** $p < 0.01$, *** $p < 0.001$ between MIA groups and saline control.

$p < 0.05$, ## $p < 0.01$, ### $p < 0.001$ Between MIA + vehicle group and MIA + cordycepin group.

N = 6-8 animals per group.

Data courtesy of James Burston and Victoria Chapman (University of Nottingham, School of Life Sciences)

7.2 Analysing rat RNA

At the end of the 14 day period over which the pain behaviour experiments were done, the rats were killed and tissues chilled. Since cordycepin affects RNA levels in cell culture, we sought to assess expression of inflammatory genes between the different treatment groups. In order to do this, we had to first isolate the RNA from the tissues. Using a column based kit was unsuccessful and resulted in the synovia being wasted. We therefore decided to use spare synovia from animals in other experiments (which would otherwise have been discarded) as our tissues on which to test different RNA isolation methods. Using TRIzol yielded enough RNA to work with, but, when run on a gel, it was found to be degraded. This may have occurred due to contaminating RNases in the workflow or degradation experienced in the lag time between killing the animal and chilling the tissue (in this case, the time was 19 minutes). Another possible explanation was that the decay occurred during the lysis procedure, with the denaturing reagents either being insufficient in quantity or not penetrating the tissue quickly enough. In the case of contaminating RNases being present, incubating the RNA at 37°C should further degrade the RNA. This was carried out, but no further degradation was observed (**Figure 7.2**). Upon repeating the entire RNA isolation process with a synovium that was chilled much sooner after killing the animal (2 minutes), the RNA was found to be intact, and incubation at 37°C did not lead to any degradation. The degradation that was originally observed was therefore probably due to the tissue not being chilled soon enough after the animal was killed. The amount of lysis reagent (TRIzol) was not changed, so this was unlikely to have been the cause of the problem before. RNA was then successfully isolated using TRIzol from the remaining ipsilateral synovia, and RT-qPCR was carried out to measure inflammatory gene expression in the synovia. No significant

differences were observed in the expression levels of the assessed genes between the three treatment groups (**Figure 7.3**).

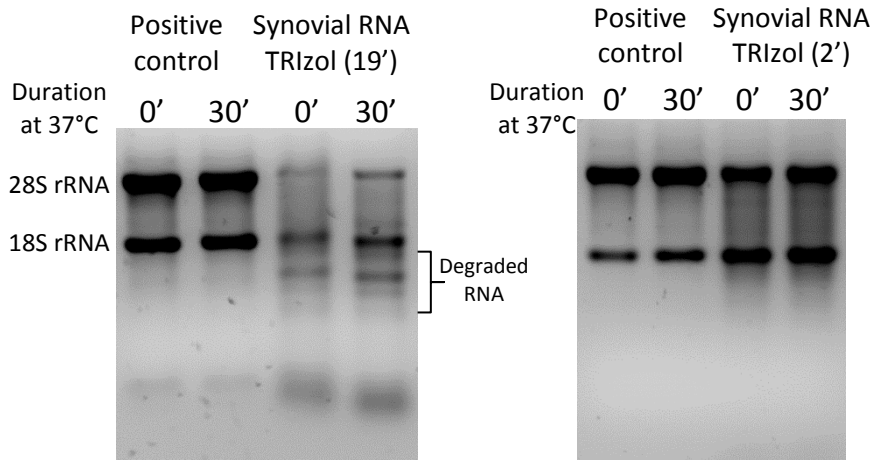


Figure 7.2. After killing the rat, the synovium must be quickly removed and chilled to avoid RNA degradation. RNA was isolated from the synovia of rats using TRIZOL. 19' and 2' refer to the time elapsed between killing the rat from which the synovium was taken and removing and chilling the synovium. Positive control is RNA isolated from RAW 264.7 cells known to be intact. RNA samples were then either incubated for 30' at 37°C or not to check for presence of RNases in the workflow. All RNA samples were then run on an agarose gel to assess integrity.

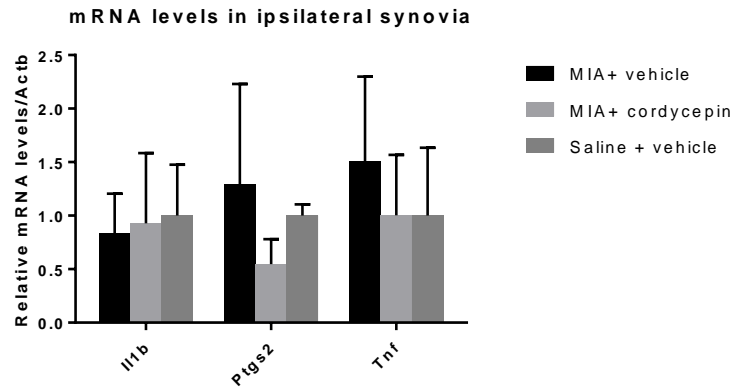


Figure 7.3. No significant differences observed in assessed inflammatory gene mRNA levels in rat ipsilateral synovia between treatment groups. MIA or saline was injected into the knee of one hind limb of rats on day 0. MIA rats were then fed 20 mg/kg cordycepin or DMSO (vehicle) every other day. Saline rats were fed DMSO every other day. RNA was extracted from rat ipsilateral synovia using TRIzol. RT-qPCR was performed, error bars represent standard deviations across 2 animals per group.

Since cordycepin is a polyadenylation inhibitor, and has been shown to shorten global poly(A) tails in a number of cell types (Kondrashov et al. 2012), we decided to determine whether cordycepin was having any such effect on the level of the entire tissue. Briefly, 5'-[³²P] pCp was ligated to the 3' end of RNA samples, a cocktail of RNases was added to digest all non-poly(A) RNA, and resulting RNA was run on a urea-TBE PAGE gel. A phosphor screen was then exposed to the gel and imaged on a phosphorimager. Doing so revealed no differences in global poly(A) tail lengths between the treatment groups (**Figure 7.4**). While cordycepin inhibits inflammatory gene expression in RAW 264.7 cells and inhibits global polyadenylation in a number of cell types, it appears that its effects on pain behaviour in the rat osteoarthritis model are not dependent on these phenomena occurring within the synovium, unless such effects already took place at an earlier, unobserved time.

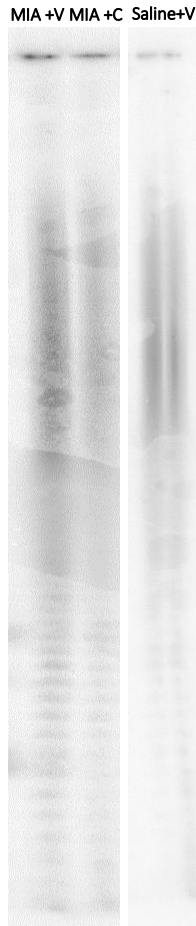


Figure 7.4. No global poly(A) tail length differences were observed between rat groups in ipsilateral synovial RNA samples. MIA or saline was injected into the knee of one hind limb of rats on day 0. MIA rats were then fed 20 mg/kg cordycepin or DMSO (vehicle) every other day. Saline rats were fed DMSO every other day. RNA was extracted from rat ipsilateral synovia using TRIzol. [5'-³²P]Cytidine 3',5'-bis(phosphate) was ligated to the 3' end of RNA samples, a cocktail of RNases was added to digest all non-poly(A) RNA, and resulting RNA was run on a urea-TBE PAGE gel. The gel was incubated at -80°C with a phosphor screen for > 5 days and then imaged on a GE Storm 825 phosphorimager.

7.3 Discussion

Data in this chapter show that OA pain behaviour in a rat model of the disease is significantly altered by orally administered cordycepin. When isolating RNA from animal tissues (or at least from the synovium), the tissue must be chilled very soon after killing the animal in order to prevent degradation of RNA. Analysis of RNA from rats in the OA study did not reveal any significant differences in mRNA levels of cytokines assessed, nor did it show any differences in total poly(A) tail sizes between rats in different treatment groups. However, the finding that pain behaviour in the OA rat model is altered by cordycepin is a very promising start to the investigation of cordycepin as a lead compound for new OA therapeutics.

8 Discussion and conclusions

During the course of this project, a working inflammatory model was established in the RAW 264.7 murine macrophage cell line. In this system, the poly(A) tail was found to be dynamic, with the initial poly(A) tail size of Tnf becoming longer following lipopolysaccharide (LPS) stimulation. Anti-inflammatory effects of cordycepin were observed in the system on a genome-wide scale, and mechanistic insight was gained into how cordycepin's effects are mediated. Pain-alleviating properties of cordycepin in a rat model of osteoarthritis (OA) warrant further investigation into its use as a therapeutic.

8.1 Advances in poly(A) tail measurements

Chapter 3 was concerned with method development and troubleshooting.

Previously, the method used for the poly(A) tail test (PAT) involved a high input RNA quantity, an unreliable deadenylation step, and an inefficient ligation. Optimisation was done that addressed all of these issues, resulting in a considerably improved method. In addition, higher PCR bands following PAT that often appeared on gels were identified as artefactual multimers. These could be removed by running the PAT products on a fully denaturing TBE-urea PAGE gel – a finding that should prove useful. Attempts to perform TAIL-seq were not ultimately successful in yielding usable data. Using the starting method, provided to us by the authors of the original TAIL-seq paper (Chang et al. 2014), we were unable to even generate a library. After further attempts and troubleshooting, the method was improved, most notably in the ligation efficiency, and a library was generated. Sequencing data from the library showed poly(A) tails and uridylation but 3' UTRs were too short (suggesting too great a degree of RNase T1 digestion) and counts were too low. As mentioned, however, considerable improvements were made, and further refinement should

yield usable data. Presently, work is being done in the group to develop an altered version of TAIL-seq termed quanTAIL-seq. The method aims to address inefficiencies in the TAIL-seq workflow that should yield libraries from which better quality data can be obtained. When quanTAIL seq is fully developed, usable poly(A) tail data should be obtainable.

8.2 Polyadenylation in the inflammatory response

An inflammatory system was successfully established in which LPS was used as a stimulus to induce an inflammatory response in RAW 264.7 cells. It was found that withdrawal of serum from the medium 24 hours prior to addition of LPS resulted in a greater degree of induction (**Figure 4.1**), and so this was done as standard in all experiments thereafter. It should be noted that many other groups do not withdraw serum prior to LPS induction (H. G. Kim et al. 2006; Y. Li et al. 2016; Shin, Lee, et al. 2009), and so the absence of growth factor signalling in our cells cf. the presence of it in theirs should be borne in mind when comparing data.

Once the system was established, the improved PAT procedure was applied to analyse poly(A) tail size changes over the inflammatory response. As can be seen in **Figure 4.3**, the *Tnf* and *Cxcl2* poly(A) tails change are variable while that of *Rpl28* remains constant. The *Tnf* poly(A) tail shortens much faster than that of *Cxcl2*. PAT performed on nuclear RNA (**Figure 4.4**) confirmed that the initial poly(A) tail of *Tnf* was variable in size at different timepoints. However, the change is relatively modest, only observed in one replicate, and data is needed to show that a control mRNA (e.g. *Rpl28* does not change). It should also be noted that the initial poly(A) tail size difference (**Figure 4.4**) was inferred from PAT performed on nuclear RNA, assumed to be newly synthesised. Using an independent method of isolating newly synthesised RNA, like 4-thiouridine labelling, followed by PAT would support the

idea that initial poly(A) tail size is variable. Also, nuclear PAT was only done for *Tnf*. PAT data to show that initial tail size does not change for a control mRNA is needed to confirm the validity of the finding. Since the poly(A) tail size of *Tnf* in total RNA changes so quickly, it may be that a greater proportion of *Tnf* mRNA is made with a longer poly(A) tail earlier on in the time course. Repeating the time course with more timepoints across multiple replicates and with control mRNAs for reference would be worthwhile. However, the indication that initial poly(A) tail size is variable is interesting and this may represent a means for regulation of the inflammatory response. Regulation at the level of polyadenylation is a phenomenon that we have observed in the serum response in NIH-3T3 mouse fibroblasts (Singhania et al, manuscript under review). A similar phenomenon may exist in the inflammatory response.

8.3 Mechanistic insight into cordycepin's mode of action

Anti-inflammatory effects of cordycepin are well documented, and a range of mechanisms have been proposed to explain its effects. This project confirms previous findings that cordycepin has anti-inflammatory effects. Given that the effects of *C. militaris* extract and cordycepin were very similar (**Figure 5.1**), and that the concentration of cordycepin in the *C. militaris* was almost the same as in the cordycepin stock (**Table 5.1**), it stands to reason that cordycepin is likely to be the active component of *C. militaris*. This was not the case for *O. sinensis* extract, in which the cordycepin concentration was 5 orders of magnitude lower, but anti-inflammatory effects were still observed, and so cordycepin is unlikely to be the active compound in this fungus.

Contrary to data obtained in ASM cells (Kondrashov et al. 2012), there appear to be effects at the transcriptional level (**Figure 5.4**). A decrease in transcription may be a

result of interfering with NF- κ B signalling, but cordycepin did not impede the degradation of I κ B α (**Figure 5.11**) suggesting that this is not the case. Other explanations include effects on polyadenylation causing decreased transcription termination efficiency (**Figure 5.9** and **5.10**) leading to inefficient recycling of transcriptional machinery (Mapendano et al. 2010), or that cordycepin may arrest the mRNA 3' cleavage complex as it does *in vitro* (Zarkower and Wickens 1987). If the cleavage complex is arrested, thus sequestering processing factors, generation of transcripts with high processing factor requirements could be limited by the availability of factors. In both cases (inefficient recycling of transcriptional machinery or lack of availability of processing factors), genes being transcribed at high rates would be expected to be most affected. However, the idea that cordycepin affects those mRNAs that are transcribed at high rates is inconsistent with the observation that no correlation was observed between transcription rate and cordycepin sensitivity (**Figure 6.2**). Alternatively (or additionally), cordycepin's mechanism may include effects on signal transduction – there is evidence that it inhibits AKT phosphorylation (H. G. Kim et al. 2006) which may decrease NF- κ B activation (Rajaram et al. 2006; Dan et al. 2008). Co-administration of cordycepin and pentostatin (inhibitor of adenosine deaminase) potentiated cordycepin's repressive effects on inflammatory mRNA levels (**Figure 5.5A**), suggesting that deamination of cordycepin reduces its activity. However, such effects were less clear in cells from which serum had been withdrawn (**Figure 5.5B**). This observation may have arisen due to the presence of adenosine deaminase in the serum, such that potentiation of cordycepin's effects through prevention of its deamination may become less pronounced in the absence of serum (since there would be less adenosine deaminase available to deaminate the cordycepin). The effects of cordycepin were abrogated by inhibiting either the adenosine transporter or adenosine kinase using

S-(4-Nitrobenzyl)-6-thioinosine (NBTI) or 5-Iodotubericidin (ITu) respectively (**Figure 5.6**). This outcome strongly suggests that cordycepin must be imported and phosphorylated in order to elicit its anti-inflammatory effects, and therefore that its effects are intracellular. Since effects of cordycepin on adenosine receptors have been reported (Kadomatsu et al. 2012; Kitamura et al. 2011; Nakamura et al. 2006), we sought to test whether extracellular effects of cordycepin in the RAW 264.7 system were present, although the NBTI/ITu experiment suggested that they were not. Repressive effects of adenosine were observed for *I11b*, but were much lower than those of cordycepin for other mRNAs (**Figure 5.6**), suggesting that the two compounds function in different ways. NBTI or ITu should not alter the effects of adenosine if it acts extracellularly, so repression of *I11b* mRNA should be maintained in the presence of either inhibitor. The data were too variable to confirm this, however.

To distinguish the effects of cordycepin and adenosine, we conducted the washing experiment (**Figure 5.7**), but the results were inconclusive. A different experiment could be done in which the effects of cordycepin are simply compared in the presence and absence of adenosine receptor antagonists. The ability or inability of adenosine receptor antagonists to relieve cordycepin-mediated repression of inflammatory gene expression would include or exclude adenosine receptors respectively in cordycepin's mode of action. The antagonists would need to have a higher affinity for the receptor(s) than cordycepin in order for the experiment to provide an answer, however.

The poly(A) tail size of *Tnf* was found to be elongated in response to LPS stimulation (**Figure 4.3**), and a size increase is present in the initial poly(A) tail size (**Figure 4.4**). Furthermore, cordycepin-treated cells display a much more modest increase in

poly(A) tail size after LPS stimulation. This shows that effects of cordycepin on polyadenylation are present, consistent with an intracellular mode of action. Further work would be required to establish whether the shorter poly(A) tail has a role in mediating cordycepin's effects, or whether it is merely a consequence of its effects.

Cordycepin was found to have no effect on the breakdown of I κ B α (**Figure 5.11**). This is at odds with findings from Peng et al (Jie Peng et al. 2015). This could be due to the differences in timings – they used a 24 hour incubation with LPS, while my observations of I κ B α levels were within a 30 minute window after addition of LPS, and so signalling events would be at different stages. Kim et al, who also used LPS as a stimulus in RAW 264.7 cells, reported that cordycepin treatment decreased phosphorylation of I κ B after 2.5 hours of LPS stimulation. Their paper does not show total I κ B α levels, which is what my data show, and so I cannot directly compare their data to mine. Also, without knowing total I κ B α levels, decreased signal of p-I κ B α could be explained either by decreased phosphorylation (as Kim et al conclude) or increased degradation of the protein entirely. My observation that I κ B α degradation is not prevented by cordycepin suggests that NF- κ B translocation into the nucleus would be unimpeded, while Kim et al show that NF- κ B translocation is inhibited by cordycepin (H. G. Kim et al. 2006). When measuring this, Kim et al used a longer LPS stimulation (2.5 hours). It would be interesting to repeat my experiments across a broader range of timepoints in order to better understand the timings of cordycepin's reported effects. It would also be informative to assess localisation of NF- κ B, as well as phosphorylation of I κ B α and activation of upstream members of the pathway including I κ B kinases (IKKs). In this way, a more complete picture would be obtained regarding the effects of cordycepin on NF- κ B signalling (none of which were detected in my experiment). It should be noted that the localisation of NF- κ B is not the only means to its regulation. Posttranslational mechanisms including

phosphorylation and acetylation of NF- κ B subunits also play roles (Karin and Ben-Neriah 2000; Christian, Smith, and Carmody 2016) which may be affected by cordycepin. Phosphorylation of p65 is an important activating modification in NF- κ B signalling (see **section 1.3.2.1.2** for more detail), and Li et al show this to be reduced by cordycepin (Y. Li et al. 2016). Such posttranslational modifications could also be assessed in a broader investigation into the effects of cordycepin on NF- κ B signalling.

8.4 High throughput analysis of cordycepin's effects

Genome-wide analysis by microarray showed that immune and inflammatory gene clusters are the most significantly enriched in the list of genes downregulated by cordycepin treatment compared to LPS alone. If intrinsically unstable mRNAs, which many inflammatory mRNAs are (P. Anderson 2010; Stumpo, Lai, and Blackshear 2010), were made with short poly(A) tails due to cordycepin treatment, this might explain why they are particularly sensitive to cordycepin. Since removal of the poly(A) tail is generally the first and rate-limiting step of mRNA decay (C.-Y. A. Chen and Shyu 2011), the loss of the poly(A) tail could leave unstable mRNAs susceptible to fast decay. However, no significant correlation was observed between mRNA stability and fold change after cordycepin treatment (**Figure 6.2**). If cordycepin arrests the cleavage complex as it has been shown to do *in vitro* (Zarkower and Wickens 1987), this could lead to a decreased availability of 3' processing factors to such an extent that they become rate-limiting for transcripts with high processing factor requirements. High processing factor requirements could arise from genes with such a high transcription rate that the sheer number of transcripts being made requires a correspondingly high number of processing factors. Alternatively, such a requirement could exist in mRNAs with inefficient poly(A) signals (PASs) due to suboptimal *cis* elements. **Figure 6.2** shows that no correlation was observed

between transcription rate and cordycepin sensitivity, and so this model does not fit either. To test whether there is a link between the efficiency or “strength” of poly(A) sites and cordycepin sensitivity from the microarray data, a bioinformatic approach could be used. However, preliminary analysis by project students of microarray data for cordycepin treatment in NIH-3T3 cells indicates that such a link is unlikely to exist. The arrested cleavage complex that forms the basis of the model has only been detected *in vitro*. It would be worthwhile investigating whether the stabilisation of the complex by cordycepin is a phenomenon that occurs in cordycepin-treated cells. Microarray analysis revealed an enrichment of long noncoding RNAs (lncRNAs) in cordycepin-treated cells (**Figure 6.3**). Given that there is a class of lncRNAs whose nuclear degradation is enhanced by polyadenylation (Beaulieu et al. 2012), this enrichment is consistent with a model in which cordycepin inhibits polyadenylation. If cordycepin inhibits polyadenylation of these lncRNAs, such RNAs would be expected to become stabilised (since their degradation is dependent upon polyadenylation). As mentioned previously, cordycepin causes repression of inflammatory genes at the transcriptional level, as inferred from unspliced mRNA levels (**Figure 5.4**). Cordycepin’s anti-inflammatory effects are very fast, since the addition of cordycepin 10 minutes after the addition of LPS or 60 minutes before led to virtually the same degree of repression of inflammatory mRNAs (**Figure 5.3**). This indicates that the anti-inflammatory effects are mediated very quickly, and unlikely to occur through a slow secondary process of altering transcription of a transcription factor. Rather, the effects are likely to be mediated either through a primary effect or through a fast secondary effect. This could be through effects on polyadenylation or effects on signal transduction e.g. AKT inhibition, as Kim et al claim is integral to cordycepin’s activities (H. G. Kim et al. 2006). The observation that a set of lncRNAs are stabilised by cordycepin presents

another explanation: if such lncRNAs regulate inflammation, whether by directly regulating inflammatory gene expression or modulating signal transduction, then their stabilisation by cordycepin could be responsible for the observed effects. Such a secondary effect could be quick enough to fit the data, since, in this model, cordycepin stabilises RNAs that have already been transcribed. Investigation into the potential involvement of the cordycepin-stabilised lncRNAs in mediating anti-inflammatory effects would be worthwhile.

To address the question of whether cordycepin's acts through effects on polyadenylation or not, inhibition of polyadenylation in other ways would be worth attempting to see whether this replicates cordycepin's effects. However, our attempts so far to perform knockdown of poly(A) polymerases (PAPs) in RAW 264.7 cells have been unsuccessful. Alternatively, other unrelated polyadenylation inhibitors could be used, or perhaps expression of a dominant negative PAP mutant.

8.5 Demonstrated therapeutic potential of cordycepin in osteoarthritis

Cordycepin has been successfully used as an anti-inflammatory compound in a number of animal models of disease and injury (X. Yang et al. 2015; M. Chen et al. 2012; H. Kim et al. 2011; Cheng et al. 2011). During this project, work done by James Burston (School of Life Sciences, University of Nottingham) showed that orally administered cordycepin alleviated pain behaviour in a rat model of osteoarthritis (**Figure 7.1**). No differences in poly(A) tail size between rat treatment groups were observed in synovial RNA, however (**Figure 7.4**), nor were there differences in the mRNA levels of cytokines that were assessed (**Figure 7.3**). If cordycepin has effects on polyadenylation *in vivo*, there are several possibilities that would account for our not detecting them. We may have been looking at the wrong time or in the wrong tissue. Also, it could be that total poly(A) tail size is unchanged but specific mRNAs

do experience changes. In this case, a more targeted approach of doing PAT on the rat RNA for specific mRNAs would be appropriate. *Tnf* may be one such mRNA, since its poly(A) tail was affected by cordycepin in RAW 264.7 cells (**Figure 5.8**).

Alternatively, a high throughput method like TAIL-seq could be used to observe genome-wide poly(A) landscape changes between animals, but at much greater expense. If RNA from multiple tissues and at multiple stages in the disease model were to be analysed, the expense of using TAIL-seq would certainly become prohibitive.

Limited data notwithstanding, the effects of cordycepin on pain behaviour in the rat OA model represent a promising start into an assessment of cordycepin's suitability as a lead compound for the development of new OA treatments. These findings are complemented by evidence of its anti-inflammatory effects in chondrocytes from OA patients (Ying et al. 2014). The ability of cordycepin to overcome impairment of osteogenesis and inhibit osteoclastogenesis (F. Wang et al. 2015; Dou et al. 2016) suggests a potential to shift the balance of bone destruction and formation. Changes in subchondral bone over the course of OA in the rat model may therefore be worth monitoring between cordycepin and non-cordycepin treated animals. Finally, as a compound with demonstrated anti-inflammatory effects, cordycepin would be worth testing in rheumatoid arthritis (RA) – a disease with a more inflammatory nature. Anti-TNF therapies have been highly successful in the treatment of RA (P. C. Taylor, Taylor, and Feldmann 2009; Brennan et al. 1989), and cordycepin represses TNF levels, both at the level of mRNA – as has been observed in this project – and protein (Shin, Lee, et al. 2009; Jie Peng et al. 2015). However, anti-TNF biologics have their shortcomings, including heightened risk of infections and loss of efficacy over time (Askling and Dixon 2008; Neovius et al. 2015; P. C. Taylor, Taylor, and

Feldmann 2009). Cordycepin's broad anti-inflammatory action may mean it has potential for the development of new RA treatment options.

In summary, this project provides insight into the effects of cordycepin, both at the transcriptomic and molecular level. In the context of inflammation, *Tnf* was found to have a dynamic poly(A) tail size in response to LPS stimulation, and this was true of the initial poly(A) tail size i.e. *Tnf* was made with a poly(A) tail of different size at different points in the inflammatory response. Cordycepin was shown to be anti-inflammatory and, in addition to reducing levels of inflammatory mRNAs, shortened the *Tnf* poly(A) tail. This effect, along with a stabilisation of lncRNAs, provide potential leads to be followed to discover the role of inhibiting polyadenylation in mediating cordycepin's observed effects. Improved and emerging poly(A) tail measurement techniques will doubtless play a role in such investigation. Lastly, promising animal data support further research into the potential use of cordycepin as a therapeutic agent.

9 Bibliography

- Akashi, Sachiko, Shin-ichiroh Saitoh, Yasutaka Wakabayashi, Takane Kikuchi, Noriaki Takamura, Yoshinori Nagai, Yutaka Kusumoto, et al. 2003. "Lipopolysaccharide Interaction with Cell Surface Toll-like Receptor 4-MD-2." *The Journal of Experimental Medicine* 198 (7). Rockefeller University Press: 1035–42. doi:10.1084/jem.20031076.
- Akkiraju, Hemanth, and Anja Nohe. 2015. "Role of Chondrocytes in Cartilage Formation, Progression of Osteoarthritis and Cartilage Regeneration." *Journal of Developmental Biology* 3 (4). Multidisciplinary Digital Publishing Institute: 177–92. doi:10.3390/jdb3040177.
- Aloe, Luigi, and Rita Levi-Montalcini. 1977. "Mast Cells Increase in Tissues of Neonatal Rats Injected with the Nerve Growth Factor." *Brain Research*. Vol. 133. doi:10.1016/0006-8993(77)90772-7.
- Ameur, Adam, Ammar Zaghlool, Jonatan Halvardson, Anna Wetterbom, Ulf Gyllensten, Lucia Cavelier, and Lars Feuk. 2011. "Total RNA Sequencing Reveals Nascent Transcription and Widespread Co-Transcriptional Splicing in the Human Brain." *Nature Structural & Molecular Biology* 18 (12). Nature Research: 1435–40. doi:10.1038/nsmb.2143.
- Anderson, Paul. 2008. "Post-Transcriptional Control of Cytokine Production." *Nature Immunology* 9 (4). Nature Publishing Group: 353–59. doi:10.1038/ni1584.
- . 2010. "Post-Transcriptional Regulons Coordinate the Initiation and Resolution of Inflammation." *Nature Reviews. Immunology* 10 (1). Nature Publishing Group: 24–35. doi:10.1038/nri2685.
- Anderson, S., A. T. Bankier, B. G. Barrell, M. H. L. de Bruijn, A. R. Coulson, J. Drouin, I. C. Eperon, et al. 1981. "Sequence and Organization of the Human Mitochondrial Genome." *Nature* 290 (5806). Nature Publishing Group: 457–65. doi:10.1038/290457a0.
- Askling, Johan, and Will Dixon. 2008. "The Safety of Anti-Tumour Necrosis Factor Therapy in Rheumatoid Arthritis." *Current Opinion in Rheumatology* 20 (2): 138–44. doi:10.1097/BOR.0b013e3282f4b392.
- Aurora, Arin B., Enzo R. Porrello, Wei Tan, Ahmed I. Mahmoud, Joseph A. Hill, Rhonda Bassel-Duby, Hesham A. Sadek, et al. 2014. "Macrophages Are Required for Neonatal Heart Regeneration." *Journal of Clinical Investigation* 124 (3). American Society for Clinical Investigation: 1382–92. doi:10.1172/JCI72181.
- Barnard, Daron C., Kevin Ryan, James L. Manley, and Joel D. Richter. 2004. "Symplekin and xGLD-2 Are Required for CPEB-Mediated Cytoplasmic Polyadenylation." *Cell* 119 (5). Elsevier: 641–51. doi:10.1016/j.cell.2004.10.029.
- Barnes, Peter J., M.R. Partridge, et al., J. Gamble, et al., P.J. Barnes, Q. Hamid, et al. 2010. "New Therapies for Asthma: Is There Any Progress?" *Trends in Pharmacological Sciences* 31 (7). Elsevier: 335–43. doi:10.1016/j.tips.2010.04.009.
- Beaulieu, Yves B., Claudia L. Kleinman, Anne-Marie Landry-Voyer, Jacek Majewski,

- François Bachand, E Wahle, U Kuhn, et al. 2012. "Polyadenylation-Dependent Control of Long Noncoding RNA Expression by the Poly(A)-Binding Protein Nuclear 1." Edited by Jeannie T. Lee. *PLoS Genetics* 8 (11). Public Library of Science: e1003078. doi:10.1371/journal.pgen.1003078.
- Ben-Neriah, Yinon, and Michael Karin. 2011. "Inflammation Meets Cancer, with NF- κ B as the Matchmaker." *Nature Immunology* 12 (8). Nature Research: 715–23. doi:10.1038/ni.2060.
- Benoit, Perrine, Catherine Papin, Jae Eun Kwak, Marvin Wickens, and Martine Simonelig. 2008. "PAP- and GLD-2-Type poly(A) Polymerases Are Required Sequentially in Cytoplasmic Polyadenylation and Oogenesis in *Drosophila*." *Development (Cambridge, England)* 135 (11). The Company of Biologists Ltd: 1969–79. doi:10.1242/dev.021444.
- Berenbaum, F. 2013. "Osteoarthritis as an Inflammatory Disease (Osteoarthritis Is Not Osteoarthrosis!)." *Osteoarthritis and Cartilage* 21 (1): 16–21. doi:10.1016/j.joca.2012.11.012.
- Berndt, H., C. Harnisch, C. Rammelt, N. Stohr, A. Zirkel, J. C. Dohm, H. Himmelbauer, J.-P. Tavanetz, S. Huttelmaier, and E. Wahle. 2012. "Maturation of Mammalian H/ACA Box snoRNAs: PAPD5-Dependent Adenylation and PARN-Dependent Trimming." *RNA* 18 (5). Cold Spring Harbor Laboratory Press: 958–72. doi:10.1261/rna.032292.112.
- Bernstein, P, S W Peltz, and J Ross. 1989. "The poly(A)-poly(A)-Binding Protein Complex Is a Major Determinant of mRNA Stability in Vitro." *Molecular and Cellular Biology* 9 (2). American Society for Microbiology: 659–70. doi:10.1128/MCB.9.2.659.
- Beyer, K., T. Dandekar, and W. Keller. 1997. "RNA Ligands Selected by Cleavage Stimulation Factor Contain Distinct Sequence Motifs That Function as Downstream Elements in 3'-End Processing of Pre-mRNA." *Journal of Biological Chemistry* 272 (42). American Society for Biochemistry and Molecular Biology: 26769–79. doi:10.1074/jbc.272.42.26769.
- Blom, Arjen B., Peter L.E.M. van Lent, Astrid E.M. Holthuysen, Peter M. van der Kraan, Johannes Roth, Nico van Rooijen, and Wim B. van den Berg. 2004. "Synovial Lining Macrophages Mediate Osteophyte Formation during Experimental Osteoarthritis." *Osteoarthritis and Cartilage* 12 (8): 627–35. doi:10.1016/j.joca.2004.03.003.
- Bohuslav, J, V V Kravchenko, G C Parry, J H Erlich, S Gerondakis, N Mackman, and R J Ulevitch. 1998. "Regulation of an Essential Innate Immune Response by the p50 Subunit of NF- κ B." *Journal of Clinical Investigation* 102 (9). American Society for Clinical Investigation: 1645–52. doi:10.1172/JCI3877.
- Bradley, JR. 2008. "TNF-Mediated Inflammatory Disease." *The Journal of Pathology* 214 (2). John Wiley & Sons, Ltd.: 149–60. doi:10.1002/path.2287.
- Brennan, Fionula M, Andrew Jackson, David Chantry, Ravinder Maini, and Marc Feldmann. 1989. "INHIBITORY EFFECT OF TNF?? ANTIBODIES ON SYNOVIAL CELL INTERLEUKIN-1 PRODUCTION IN RHEUMATOID ARTHRITIS." *The Lancet* 334 (8657). Elsevier: 244–47. doi:10.1016/S0140-6736(89)90430-3.
- Bresson, Stefan M., and Nicholas K. Conrad. 2013. "The Human Nuclear Poly(A)-

Binding Protein Promotes RNA Hyperadenylation and Decay." Edited by Gregory S. Barsh. *PLoS Genetics* 9 (10). Public Library of Science: e1003893. doi:10.1371/journal.pgen.1003893.

- Brook, M., C. R. Tchen, T. Santalucia, J. McIlrath, J. S. C. Arthur, J. Saklatvala, and A. R. Clark. 2006. "Posttranslational Regulation of Tristetraprolin Subcellular Localization and Protein Stability by p38 Mitogen-Activated Protein Kinase and Extracellular Signal-Regulated Kinase Pathways." *Molecular and Cellular Biology* 26 (6). American Society for Microbiology: 2408–18. doi:10.1128/MCB.26.6.2408-2418.2006.
- Brook, Matthew, and Nicola K Gray. 2012. "The Role of Mammalian poly(A)-Binding Proteins in Co-Ordinating mRNA Turnover." *Biochemical Society Transactions* 40 (4). Portland Press Ltd.: 856–64. doi:10.1042/BST20120100.
- Brooks, Seth A, and Perry J Blackshear. 2013. "Tristetraprolin (TTP): Interactions with mRNA and Proteins, and Current Thoughts on Mechanisms of Action." *Biochimica et Biophysica Acta* 1829 (6–7): 666–79. doi:10.1016/j.bbagr.2013.02.003.
- Bros, Matthias, Nadine Wiechmann, Verena Besche, Julia Art, Andrea Pautz, Stephan Grabbe, Hartmut Kleinert, and Angelika B. Reske-Kunz. 2010. "The RNA Binding Protein Tristetraprolin Influences the Activation State of Murine Dendritic Cells." *Molecular Immunology*. Vol. 47. doi:10.1016/j.molimm.2009.11.002.
- Burgess, Hannah M, Nicola K Gray, D.A. Mangus, M.C. Evans, A. Jacobson, B. Gorgoni, N.K. Gray, et al. 2010. "mRNA-Specific Regulation of Translation by poly(A)-Binding Proteins." *Biochemical Society Transactions* 38 (6). Portland Press Limited: 1517–22. doi:10.1042/BST0381517.
- Burns, D. M., and J. D. Richter. 2008. "CPEB Regulation of Human Cellular Senescence, Energy Metabolism, and p53 mRNA Translation." *Genes & Development* 22 (24). Cold Spring Harbor Laboratory Press: 3449–60. doi:10.1101/gad.1697808.
- Caput, D, B Beutler, K Hartog, R Thayer, S Brown-Shimer, and A Cerami. 1986. "Identification of a Common Nucleotide Sequence in the 3'-untranslated Region of mRNA Molecules Specifying Inflammatory Mediators." *Proceedings of the National Academy of Sciences of the United States of America* 83 (6). National Academy of Sciences: 1670–74. <http://www.ncbi.nlm.nih.gov/pubmed/2419912>.
- Carballo, E. 1998. "Feedback Inhibition of Macrophage Tumor Necrosis Factor-Production by Tristetraprolin." *Science* 281 (5379): 1001–5. doi:10.1126/science.281.5379.1001.
- Carrillo Oesterreich, Fernando, Stephan Preibisch, and Karla M. Neugebauer. 2010. "Global Analysis of Nascent RNA Reveals Transcriptional Pausing in Terminal Exons." *Molecular Cell* 40 (4): 571–81. doi:10.1016/j.molcel.2010.11.004.
- Cattaneo, Marco, Veena Chantarangkul, Emanuela Taioli, José Hermida Santos, and Liliana Tagliabue. 1999. "The G20210A Mutation of the Prothrombin Gene in Patients with Previous First Episodes of Deep-Vein Thrombosis: Prevalence and Association with Factor V G1691A, Methylenetetrahydrofolate Reductase C677T and Plasma Prothrombin Levels." *Thrombosis Research* 93 (1): 1–8. doi:10.1016/S0049-3848(98)00136-4.

- Chan, Serena L., Ina Huppertz, Chengguo Yao, Lingjie Weng, James J. Moresco, John R. Yates, Jernej Ule, James L. Manley, and Yongsheng Shi. 2014. "CPSF30 and Wdr33 Directly Bind to AAUAAA in Mammalian mRNA 3' Processing." *Genes & Development* 28 (21). Cold Spring Harbor Laboratory Press: 2370–80. doi:10.1101/gad.250993.114.
- Chang, Hyesik, Jaechul Lim, Minju Ha, and V Narry Kim. 2014. "TAIL-Seq: Genome-Wide Determination of poly(A) Tail Length and 3' End Modifications." *Molecular Cell* 53 (6): 1044–52. doi:10.1016/j.molcel.2014.02.007.
- Charlesworth, Amanda, Hedda A Meijer, and Cornelia H de Moor. 2013. "Specificity Factors in Cytoplasmic Polyadenylation." *Wiley Interdisciplinary Reviews. RNA* 4 (4): 437–61. doi:10.1002/wrna.1171.
- Chen, Chyi-Ying A, and Ann-Bin Shyu. 2011. "Mechanisms of Deadenylation-Dependent Decay." *Wiley Interdisciplinary Reviews. RNA* 2 (2). NIH Public Access: 167–83. doi:10.1002/wrna.40.
- Chen, Fan, Clinton C. MacDonald, and Jeffrey Wilusf. 1995. "Cleavage Site Determinants Min the Mammalian Polydenylation Signal." *Nucleic Acids Research* 23 (14). Oxford University Press: 2614–20. doi:10.1093/nar/23.14.2614.
- Chen, Grace Y., and Gabriel Nuñez. 2010. "Sterile Inflammation: Sensing and Reacting to Damage." *Nature Reviews Immunology* 10 (12). Nature Publishing Group: 826–37. doi:10.1038/nri2873.
- Chen, L.-F., S. A. Williams, Y. Mu, H. Nakano, J. M. Duerr, L. Buckbinder, and W. C. Greene. 2005. "NF- B RelA Phosphorylation Regulates RelA Acetylation." *Molecular and Cellular Biology* 25 (18). American Society for Microbiology: 7966–75. doi:10.1128/MCB.25.18.7966-7975.2005.
- Chen, Mengli, Florence W.K. Cheung, Ming Hung Chan, Pak Kwan Hui, Siu-Po Ip, Yick Hin Ling, Chun-Tao Che, and Wing Keung Liu. 2012. "Protective Roles of Cordyceps on Lung Fibrosis in Cellular and Rat Models." *Journal of Ethnopharmacology* 143 (2): 448–54. doi:10.1016/j.jep.2012.06.033.
- Cheng, Zhenyong, Wei He, Xiaoxia Zhou, Qing Lv, Xulin Xu, Shanshan Yang, Chenming Zhao, and Lianjun Guo. 2011. "Cordycepin Protects against Cerebral Ischemia/reperfusion Injury in Vivo and in Vitro." *European Journal of Pharmacology* 664 (1): 20–28. doi:10.1016/j.ejphar.2011.04.052.
- Cho, Hee-Jung, Sang-Yul Kim, Mae-Ja Park, Dong-Sun Kim, Jeong-Ki Kim, and Mi-Young Chu. 1997. "Expression of mRNA for Brain-Derived Neurotrophic Factor in the Dorsal Root Ganglion Following Peripheral Inflammation." *Brain Research*. Vol. 749. doi:10.1016/S0006-8993(97)00048-6.
- Chou, Chu-Fang, Alok Mulky, Sushmit Maitra, Wei-Jye Lin, Roberto Gherzi, John Kappes, and Ching-Yi Chen. 2006. "Tethering KSRP, a Decay-Promoting AU-Rich Element-Binding Protein, to mRNAs Elicits mRNA Decay." *Molecular and Cellular Biology* 26 (10). American Society for Microbiology: 3695–3706. doi:10.1128/MCB.26.10.3695-3706.2006.
- Chrestensen, C. A., M. J. Schroeder, J. Shabanowitz, D. F. Hunt, J. W. Pelo, M. T. Worthington, and T. W. Sturgill. 2004. "MAPKAP Kinase 2 Phosphorylates Tristetraprolin on in Vivo Sites Including Ser178, a Site Required for 14-3-3

- Binding." *Journal of Biological Chemistry* 279 (11). American Society for Biochemistry and Molecular Biology: 10176–84. doi:10.1074/jbc.M310486200.
- Christian, Frank, Emma L Smith, and Ruaidhrí J Carmody. 2016. "The Regulation of NF- κ B Subunits by Phosphorylation." *Cells* 5 (1). Multidisciplinary Digital Publishing Institute (MDPI). doi:10.3390/cells5010012.
- Clarke, L A, C S Rebelo, J Gonçalves, M G Boavida, and P Jordan. 2001. "PCR Amplification Introduces Errors into Mononucleotide and Dinucleotide Repeat Sequences." *Molecular Pathology* 54 (5). BMJ Publishing Group Ltd and Association of Clinical Pathologists: 351–53. doi:10.1136/mp.54.5.351.
- Cornett, Ashley L., and Carol S. Lutz. 2014. "Regulation of COX-2 Expression by miR-146a in Lung Cancer Cells." *RNA* 20 (9). Cold Spring Harbor Laboratory Press: 1419–30. doi:10.1261/rna.044149.113.
- Courtois, G, and T D Gilmore. 2006. "Mutations in the NF- κ B Signaling Pathway: Implications for Human Disease." *Oncogene* 25 (51). Nature Publishing Group: 6831–43. doi:10.1038/sj.onc.1209939.
- Cusson-Hermance, N., Smriti Khurana, Thomas H. Lee, Katherine A. Fitzgerald, and Michelle A. Kelliher. 2005. "Rip1 Mediates the Trif-Dependent Toll-like Receptor 3- and 4-Induced NF- κ B Activation but Does Not Contribute to Interferon Regulatory Factor 3 Activation." *Journal of Biological Chemistry* 280 (44). American Society for Biochemistry and Molecular Biology: 36560–66. doi:10.1074/jbc.M506831200.
- Dan, Han C, Matthew J Cooper, Patricia C Cogswell, Joseph A Duncan, Jenny P-Y Ting, and Albert S Baldwin. 2008. "Akt-Dependent Regulation of NF- κ B Is Controlled by mTOR and Raptor in Association with IKK." *Genes & Development* 22 (11). Cold Spring Harbor Laboratory Press: 1490–1500. doi:10.1101/gad.1662308.
- Danckwardt, Sven, Niels H Gehring, Gabriele Neu-Yilik, Patrick Hundsdoerfer, Margit Pforsich, Ute Frede, Matthias W Hentze, and Andreas E Kulozik. 2004. "The Prothrombin 3'end Formation Signal Reveals a Unique Architecture That Is Sensitive to Thrombophilic Gain-of-Function Mutations." *Blood* 104 (2). American Society of Hematology: 428–35. doi:10.1182/blood-2003-08-2894.
- Das Gupta, J, H Gu, E Chernokalskaya, X Gao, and D R Schoenberg. 1998. "Identification of Two Cis-Acting Elements That Independently Regulate the Length of poly(A) on Xenopus Albumin Pre-mRNA." *RNA (New York, N.Y.)* 4 (7). Cold Spring Harbor Laboratory Press: 766–76. <http://www.ncbi.nlm.nih.gov/pubmed/9671050>.
- de Moor, C. H., and Joel D. Richter. 1999. "Cytoplasmic Polyadenylation Elements Mediate Masking and Unmasking of Cyclin B1 mRNA." *The EMBO Journal* 18 (8). John Wiley & Sons, Ltd: 2294–2303. doi:10.1093/emboj/18.8.2294.
- de Vries, H., Ursula Rügsegger, Wolfgang Hübner, Arno Friedlein, Hanno Langen, Walter Keller, N. Amrani, et al. 2000. "Human Pre-mRNA Cleavage Factor IIm Contains Homologs of Yeast Proteins and Bridges Two Other Cleavage Factors." *The EMBO Journal* 19 (21). EMBO Press: 5895–5904. doi:10.1093/emboj/19.21.5895.
- De Wit, Dominique, Sandrine Tonon, Véronique Olislagers, Stanislas Goriely, Michaël

- Boutriaux, Michel Goldman, and Fabienne Willems. 2003. "Impaired Responses to Toll-like Receptor 4 and Toll-like Receptor 3 Ligands in Human Cord Blood." *Journal of Autoimmunity* 21 (3): 277–81. doi:10.1016/j.jaut.2003.08.003.
- Desrosiers, R C, F M Rottman, J A Boezi, and H C Towle. 1976. "The Sensitivity of RNA Polymerases I and II from Novikoff Hepatoma (N1S1) Cells to 3'-deoxyadenosine 5'-triphosphate." *Nucleic Acids Research* 3 (2): 325–41. <http://www.pubmedcentral.nih.gov/articlerender.fcgi?artid=342904&tool=pmcentrez&rendertype=abstract>.
- Dou, Ce, Zhen Cao, Ning Ding, Tianyong Hou, Fei Luo, Fei Kang, Xiaochao Yang, et al. 2016. "Cordycepin Prevents Bone Loss through Inhibiting Osteoclastogenesis by Scavenging ROS Generation." *Nutrients* 8 (4). Multidisciplinary Digital Publishing Institute: 231. doi:10.3390/nu8040231.
- Epelman, Slava, Kory J. Lavine, Anna E. Beaudin, Dorothy K. Sojka, Javier A. Carrero, Boris Calderon, Thaddeus Brija, et al. 2014. "Embryonic and Adult-Derived Resident Cardiac Macrophages Are Maintained through Distinct Mechanisms at Steady State and during Inflammation." *Immunity* 40 (1). Elsevier: 91–104. doi:10.1016/j.immuni.2013.11.019.
- Epelman, Slava, Kory J. Lavine, Gwendalyn J. Randolph, N. A-Gonzalez, J.A. Guillen, G. Gallardo, M. Diaz, et al. 2014. "Origin and Functions of Tissue Macrophages." *Immunity* 41 (1). Elsevier: 21–35. doi:10.1016/j.immuni.2014.06.013.
- Ezzeddine, N., C.-Y. A. Chen, and A.-B. Shyu. 2012. "Evidence Providing New Insights into TOB-Promoted Deadenylation and Supporting a Link between TOB's Deadenylation-Enhancing and Antiproliferative Activities." *Molecular and Cellular Biology* 32 (6). American Society for Microbiology: 1089–98. doi:10.1128/MCB.06370-11.
- Felson, D T, D R Gale, M Elon Gale, J Niu, D J Hunter, J Goggins, and M P Lavalley. 2005. "Osteophytes and Progression of Knee Osteoarthritis." *Rheumatology (Oxford, England)* 44 (1). Oxford University Press: 100–104. doi:10.1093/rheumatology/keh411.
- Ferrari, Luiz F, Oliver Bogen, David B Reichling, and Jon D Levine. 2015. "Accounting for the Delay in the Transition from Acute to Chronic Pain: Axonal and Nuclear Mechanisms." *The Journal of Neuroscience : The Official Journal of the Society for Neuroscience* 35 (2). Society for Neuroscience: 495–507. doi:10.1523/JNEUROSCI.5147-13.2015.
- Fox, C A, M D Sheets, and M P Wickens. 1989. "Poly(A) Addition during Maturation of Frog Oocytes: Distinct Nuclear and Cytoplasmic Activities and Regulation by the Sequence UUUUUAU." *Genes & Development* 3 (12b). Cold Spring Harbor Laboratory Press: 2151–62. doi:10.1101/gad.3.12b.2151.
- Frevel, Mathias A E, Tala Bakheet, Aristobolo M Silva, John G Hissong, Khalid S A Khabar, and Bryan R G Williams. 2003. "p38 Mitogen-Activated Protein Kinase-Dependent and -Independent Signaling of mRNA Stability of AU-Rich Element-Containing Transcripts." *Molecular and Cellular Biology* 23 (2). American Society for Microbiology: 425–36. doi:10.1128/MCB.23.2.425-436.2003.
- Gautier, Emmanuel L, Tal Shay, Jennifer Miller, Melanie Greter, Claudia Jakubzick, Stoyan Ivanov, Julie Helft, et al. 2012. "Gene-Expression Profiles and

Transcriptional Regulatory Pathways That Underlie the Identity and Diversity of Mouse Tissue Macrophages." *Nature Immunology* 13 (11). Nature Research: 1118–28. doi:10.1038/ni.2419.

Gehring, Niels H., Ute Frede, Gabriele Neu-Yilik, Patrick Hundsdoerfer, Barbara Vetter, Matthias W. Hentze, and Andreas E. Kulozik. 2001. "Increased Efficiency of mRNA 3' End Formation: A New Genetic Mechanism Contributing to Hereditary Thrombophilia." *Nature Genetics* 28 (4). Nature Publishing Group: 389–92. doi:10.1038/ng578.

Gehrmann, Jochen, Yoh Matsumoto, and Georg W. Kreutzberg. 1995. "Microglia: Intrinsic Immune Effector Cell of the Brain." *Brain Research Reviews* 20 (3): 269–87. doi:10.1016/0165-0173(94)00015-H.

González-Scarano, F., and Gordon Baltuch. 1999. "MICROGLIA AS MEDIATORS OF INFLAMMATORY AND DEGENERATIVE DISEASES." *Annual Review of Neuroscience* 22 (1). Annual Reviews 4139 El Camino Way, P.O. Box 10139, Palo Alto, CA 94303-0139, USA : 219–40. doi:10.1146/annurev.neuro.22.1.219.

Grenier St-Sauveur, V., S. Soucek, A. H. Corbett, and F. Bachand. 2013. "Poly(A) Tail-Mediated Gene Regulation by Opposing Roles of Nab2 and Pab2 Nuclear Poly(A)-Binding Proteins in Pre-mRNA Decay." *Molecular and Cellular Biology* 33 (23). American Society for Microbiology: 4718–31. doi:10.1128/MCB.00887-13.

Groisman, I., M. Ivshina, V. Marin, N. J. Kennedy, R. J. Davis, and J. D. Richter. 2006. "Control of Cellular Senescence by CPEB." *Genes & Development* 20 (19). Cold Spring Harbor Laboratory Press: 2701–12. doi:10.1101/gad.1438906.

Gruber, Andreas R., Georges Martin, Philipp Müller, Alexander Schmidt, Andreas J. Gruber, Rafal Gumienny, Nitish Mittal, et al. 2014. "Global 3' UTR Shortening Has a Limited Effect on Protein Abundance in Proliferating T Cells." *Nature Communications* 5 (November). Nature Publishing Group: 5465. doi:10.1038/ncomms6465.

Gu, H., and Daniel R. Schoenberg. 2003. "U2AF Modulates poly(A) Length Control by the poly(A)-Limiting Element." *Nucleic Acids Research* 31 (21). Oxford University Press: 6264–71. doi:10.1093/nar/gkg823.

Gu, H, J Das Gupta, and D R Schoenberg. 1999. "The poly(A)-Limiting Element Is a Conserved Cis-Acting Sequence That Regulates poly(A) Tail Length on Nuclear Pre-mRNAs." *Proceedings of the National Academy of Sciences of the United States of America* 96 (16). National Academy of Sciences: 8943–48. doi:10.1073/pnas.96.16.8943.

Guan, H., Shihe Hou, and Robert P. Ricciardi. 2005. "DNA Binding of Repressor Nuclear Factor- B p50/p50 Depends on Phosphorylation of Ser337 by the Protein Kinase A Catalytic Subunit." *Journal of Biological Chemistry* 280 (11). American Society for Biochemistry and Molecular Biology: 9957–62. doi:10.1074/jbc.M412180200.

Guha, Mausumee, and Nigel Mackman. 2001. "LPS Induction of Gene Expression in Human Monocytes." *Cellular Signalling* 13 (2): 85–94. doi:10.1016/S0898-6568(00)00149-2.

Hafer, Nathaniel, Shuwa Xu, Krishna Moorthi Bhat, Paul Schedl, J. M. Alarcon, R.

- Hodgman, M. Theis, et al. 2011. "The *Drosophila* CPEB Protein Orb2 Has a Novel Expression Pattern and Is Important for Asymmetric Cell Division and Nervous System Function." *Genetics* 189 (3). Genetics: 907–21. doi:10.1534/genetics.110.123646.
- Hall-Pogar, T., S. Liang, L. K. Hague, and C. S. Lutz. 2007. "Specific Trans-Acting Proteins Interact with Auxiliary RNA Polyadenylation Elements in the COX-2 3'-UTR." *RNA* 13 (7). Cold Spring Harbor Laboratory Press: 1103–15. doi:10.1261/rna.577707.
- Han, J., T Brown, and B Beutler. 1990. "Endotoxin-Responsive Sequences Control Cachectin/tumor Necrosis Factor Biosynthesis at the Translational Level [Published Erratum Appears in *J Exp Med* 1990 Mar 1;171(3):971-2]." *Journal of Experimental Medicine* 171 (2). Rockefeller University Press: 465–75. doi:10.1084/jem.171.2.465.
- Hao, Shengli, and David Baltimore. 2009. "The Stability of mRNA Influences the Temporal Order of the Induction of Genes Encoding Inflammatory Molecules." *Nature Immunology* 10 (3). Nature Publishing Group: 281–88. doi:10.1038/ni.1699.
- Harnisch, Christiane, Simona Cuzic-Feltens, Juliane C. Dohm, Michael Götze, Heinz Himmelbauer, and Elmar Wahle. 2016. "Oligoadenylation of 3' Decay Intermediates Promotes Cytoplasmic mRNA Degradation in *Drosophila* Cells." *RNA* 22 (3). Cold Spring Harbor Laboratory Press: 428–42. doi:10.1261/rna.053942.115.
- Harrison, P. F., D. R. Powell, J. L. Clancy, T. Preiss, P. R. Boag, A. Traven, T. Seemann, and T. H. Beilharz. 2015. "PAT-Seq: A Method to Study the Integration of 3'-UTR Dynamics with Gene Expression in the Eukaryotic Transcriptome." *RNA* 21 (8). Cold Spring Harbor Laboratory Press: 1502–10. doi:10.1261/rna.048355.114.
- Hashimoto, Daigo, Andrew Chow, Clara Noizat, Pearline Teo, Mary Beth Beasley, Marylene Leboeuf, Christian D. Becker, et al. 2013. "Tissue-Resident Macrophages Self-Maintain Locally throughout Adult Life with Minimal Contribution from Circulating Monocytes." *Immunity* 38 (4). Elsevier: 792–804. doi:10.1016/j.immuni.2013.04.004.
- Haskó, György, and Bruce Cronstein. 2013. "Regulation of Inflammation by Adenosine." *Frontiers in Immunology* 4. Frontiers: 85. doi:10.3389/fimmu.2013.00085.
- Hau, Heidi H, Richard J Walsh, Rachel L Ogilvie, Darlisha A Williams, Cavan S Reilly, and Paul R Bohjanen. 2007. "Tristetraprolin Recruits Functional mRNA Decay Complexes to ARE Sequences." *Journal of Cellular Biochemistry* 100 (6): 1477–92. doi:10.1002/jcb.21130.
- Hayden, M S, A P West, and S Ghosh. 2006. "NF-κB and the Immune Response." *Oncogene* 25 (51). Nature Publishing Group: 6758–80. doi:10.1038/sj.onc.1209943.
- Haywood, L., D. F. McWilliams, C. I. Pearson, S. E. Gill, A. Ganesan, D. Wilson, and D. A. Walsh. 2003. "Inflammation and Angiogenesis in Osteoarthritis." *Arthritis & Rheumatism* 48 (8). Wiley Subscription Services, Inc., A Wiley Company: 2173–77. doi:10.1002/art.11094.

- Haziot, Alain, Enza Ferrero, Frank Köntgen, Naoki Hijiya, Shunsuke Yamamoto, Jack Silver, Colin L Stewart, and Sanna M Goyert. 1996. "Resistance to Endotoxin Shock and Reduced Dissemination of Gram-Negative Bacteria in CD14-Deficient Mice." *Immunity* 4 (4): 407–14. doi:10.1016/S1074-7613(00)80254-X.
- Heneka, Michael T, Monica J Carson, Joseph El Khoury, Gary E Landreth, Frederic Brosseron, Douglas L Feinstein, Andreas H Jacobs, et al. 2015. "Neuroinflammation in Alzheimer's Disease." *The Lancet Neurology* 14 (4): 388–405. doi:10.1016/S1474-4422(15)70016-5.
- Ho, C. Kiong, Li Kai Wang, Christopher D. Lima, and Stewart Shuman. 2004. "Structure and Mechanism of RNA Ligase." *Structure* 12 (2): 327–39. doi:10.1016/j.str.2004.01.011.
- Ho, C Kiong, and Stewart Shuman. 2002. "Bacteriophage T4 RNA Ligase 2 (gp24.1) Exemplifies a Family of RNA Ligases Found in All Phylogenetic Domains." *Proceedings of the National Academy of Sciences of the United States of America* 99 (20). National Acad Sciences: 12709–14. doi:10.1073/pnas.192184699.
- Hörber, Sebastian, Dominic G. Hildebrand, Wolfgang S. Lieb, Sebastian Lorscheid, Stephan Hailfinger, Klaus Schulze-Osthoff, and Frank Essmann. 2016. "The Atypical Inhibitor of NF- κ B, I κ B ζ , Controls Macrophage Interleukin-10 Expression." *Journal of Biological Chemistry* 291 (24). American Society for Biochemistry and Molecular Biology: 12851–61. doi:10.1074/jbc.M116.718825.
- Huang, Jingxiang, and Brendan D. Manning. 2009. "A Complex Interplay between Akt, TSC2 and the Two mTOR Complexes." *Biochemical Society Transactions* 37 (1).
- Hume, David A. 2015. "The Many Alternative Faces of Macrophage Activation." *Frontiers in Immunology* 6 (July). Frontiers: 370. doi:10.3389/fimmu.2015.00370.
- Hummasti, S., and G. S. Hotamisligil. 2010. "Endoplasmic Reticulum Stress and Inflammation in Obesity and Diabetes." *Circulation Research* 107 (5). Lippincott Williams & Wilkins: 579–91. doi:10.1161/CIRCRESAHA.110.225698.
- Ioannidis, Panayotis, Nelly Courtis, Maria Havredaki, Emmanuel Michailakis, Chris M Tsiapalis, and Theoni Trangas. 1999. "The Polyadenylation Inhibitor Cordycepin (3'dA) Causes a Decline in c-MYC mRNA Levels without Affecting c-MYC Protein Levels." *Oncogene* 18 (1). Nature Publishing Group: 117–25. doi:10.1038/sj.onc.1202255.
- Italiani, Paola, and Diana Boraschi. 2014. "From Monocytes to M1/M2 Macrophages: Phenotypical vs. Functional Differentiation." *Frontiers in Immunology* 5 (October). Frontiers: 514. doi:10.3389/fimmu.2014.00514.
- Ivshina, Maria, Ilya M Alexandrov, Anastassiia Vertii, Stephen Doxsey, and Joel D Richter. 2015. "CPEB Regulation of TAK1 Synthesis Mediates Cytokine Production and the Inflammatory Immune Response." *Molecular and Cellular Biology* 35 (3). American Society for Microbiology: 610–18. doi:10.1128/MCB.00800-14.
- Jack, Robert S., Xiaolong Fan, Martin Bernheiden, Gabriele Rune, Monika Ehlers, Albert Weber, Gerhard Kirsch, et al. 1997. "Lipopolysaccharide-Binding Protein

- Is Required to Combat a Murine Gram-Negative Bacterial Infection." *Nature* 389 (6652). Nature Publishing Group: 742–45. doi:10.1038/39622.
- Jalkanen, Aimee L., Stephen J. Coleman, and Jeffrey Wilusz. 2014. "Determinants and Implications of mRNA poly(A) Tail Size – Does This Protein Make My Tail Look Big?" *Seminars in Cell & Developmental Biology* 34: 24–32. doi:10.1016/j.semcdb.2014.05.018.
- Jeong, Jin-Woo, Cheng-Yun Jin, Gi-Young Kim, Jae-Dong Lee, Cheol Park, Gun-Do Kim, Wun-Jae Kim, et al. 2010a. "Anti-Inflammatory Effects of Cordycepin via Suppression of Inflammatory Mediators in BV2 Microglial Cells." *International Immunopharmacology* 10 (12): 1580–86. doi:10.1016/j.intimp.2010.09.011.
- . 2010b. "Anti-Inflammatory Effects of Cordycepin via Suppression of Inflammatory Mediators in BV2 Microglial Cells." *International Immunopharmacology* 10 (12): 1580–86. doi:10.1016/j.intimp.2010.09.011.
- Jin, Chengcheng, Patrick Frayssinet, Richard Pelker, Diane Cwirka, Bo Hu, Agnès Vignery, Stephanie C. Eisenbarth, and Richard A. Flavell. 2011. "NLRP3 Inflammasome Plays a Critical Role in the Pathogenesis of Hydroxyapatite-Associated Arthropathy." *Proceedings of the National Academy of Sciences* 108 (36). National Academy of Sciences: 14867–72. doi:10.1073/PNAS.1111101108.
- Johnson, Barbra A, Justine R Stehn, Michael B Yaffe, and T Keith Blackwell. 2002. "Cytoplasmic Localization of Tristetraprolin Involves 14-3-3-Dependent and -Independent Mechanisms." *The Journal of Biological Chemistry* 277 (20): 18029–36. doi:10.1074/jbc.M110465200.
- Johnston, Spencer A. 1997. "Osteoarthritis: Joint Anatomy, Physiology, and Pathobiology." *Veterinary Clinics of North America: Small Animal Practice* 27 (4). Elsevier: 699–723. doi:10.1016/S0195-5616(97)50076-3.
- Kadomatsu, M, S Nakajima, H Kato, L Gu, Y Chi, J Yao, and M Kitamura. 2012. "Cordycepin as a Sensitizer to Tumour Necrosis Factor (TNF)- α -Induced Apoptosis through Eukaryotic Translation Initiation Factor 2 α (eIF2 α)- and Mammalian Target of Rapamycin Complex 1 (mTORC1)-Mediated Inhibition of Nuclear Factor (NF)- κ B." *Clinical and Experimental Immunology* 168 (3): 325–32. doi:10.1111/j.1365-2249.2012.04580.x.
- Kagan, Jonathan C, Tian Su, Tiffany Horng, Amy Chow, Shizuo Akira, and Ruslan Medzhitov. 2008. "TRAM Couples Endocytosis of Toll-like Receptor 4 to the Induction of Interferon- β ." *Nature Immunology* 9 (4). Nature Publishing Group: 361–68. doi:10.1038/ni1569.
- Kahvejian, A., Yuri V. Svitkin, Rami Sukarieh, Marie-Noël M'Boutchou, and Nahum Sonenberg. 2005. "Mammalian poly(A)-Binding Protein Is a Eukaryotic Translation Initiation Factor, Which Acts via Multiple Mechanisms." *Genes & Development* 19 (1). Cold Spring Harbor Laboratory Press: 104–13. doi:10.1101/gad.1262905.
- Kappel, Christian, Gerda Trost, Hjördis Czesnick, Anna Ramming, Benjamin Kolbe, Son Lang Vi, Cláudia Bispo, et al. 2015. "Genome-Wide Analysis of PAPS1-Dependent Polyadenylation Identifies Novel Roles for Functionally Specialized Poly(A) Polymerases in Arabidopsis Thaliana." Edited by Gregory P. Copenhaver. *PLoS Genetics* 11 (8). Public Library of Science: e1005474. doi:10.1371/journal.pgen.1005474.

- Karin, Michael. 2006. "NF- κ B and Cancer: Mechanisms and Targets." *Molecular Carcinogenesis* 45 (6). Wiley Subscription Services, Inc., A Wiley Company: 355–61. doi:10.1002/mc.20217.
- Karin, Michael, and Yinon Ben-Neriah. 2000. "Phosphorylation Meets Ubiquitination: The Control of NF- κ B Activity." *Annual Review of Immunology* 18 (1). Annual Reviews 4139 El Camino Way, P.O. Box 10139, Palo Alto, CA 94303-0139, USA : 621–63. doi:10.1146/annurev.immunol.18.1.621.
- Kaufmann, Isabelle, Georges Martin, Arno Friedlein, Hanno Langen, and Walter Keller. 2004. "Human Fip1 Is a Subunit of CPSF That Binds to U-Rich RNA Elements and Stimulates poly(A) Polymerase." *The EMBO Journal* 23 (3). EMBO Press: 616–26. doi:10.1038/sj.emboj.7600070.
- Kawai, T., O. Takeuchi, T. Fujita, J.-i. Inoue, P. F. Muhlradt, S. Sato, K. Hoshino, and S. Akira. 2001. "Lipopolysaccharide Stimulates the MyD88-Independent Pathway and Results in Activation of IFN-Regulatory Factor 3 and the Expression of a Subset of Lipopolysaccharide-Inducible Genes." *The Journal of Immunology* 167 (10). American Association of Immunologists: 5887–94. doi:10.4049/jimmunol.167.10.5887.
- Kawai, Taro, Osamu Adachi, Tomohiko Ogawa, Kiyoshi Takeda, and Shizuo Akira. 1999. "Unresponsiveness of MyD88-Deficient Mice to Endotoxin." *Immunity* 11 (1): 115–22. doi:10.1016/S1074-7613(00)80086-2.
- Kawai, Taro, and Shizuo Akira. 2007. "Signaling to NF- κ B by Toll-like Receptors." *Trends in Molecular Medicine* 13 (11): 460–69. doi:10.1016/j.molmed.2007.09.002.
- Keller, W, S Bienroth, K M Lang, and G Christofori. 1991. "Cleavage and Polyadenylation Factor CPF Specifically Interacts with the Pre-mRNA 3' Processing Signal AAUAAA." *The EMBO Journal* 10 (13). European Molecular Biology Organization: 4241–49. <http://www.ncbi.nlm.nih.gov/pubmed/1756731>.
- Kelly, S. M., S. W. Leung, C. Pak, A. Banerjee, K. H. Moberg, and A. H. Corbett. 2014. "A Conserved Role for the Zinc Finger Polyadenosine RNA Binding Protein, ZC3H14, in Control of poly(A) Tail Length." *RNA* 20 (5). Cold Spring Harbor Laboratory Press: 681–88. doi:10.1261/rna.043984.113.
- Kerr, B J, E J Bradbury, D L Bennett, P M Trivedi, P Dassan, J French, D B Shelton, S B McMahon, and S W Thompson. 1999. "Brain-Derived Neurotrophic Factor Modulates Nociceptive Sensory Inputs and NMDA-Evoked Responses in the Rat Spinal Cord." *The Journal of Neuroscience : The Official Journal of the Society for Neuroscience* 19 (12). Society for Neuroscience: 5138–48. <http://www.ncbi.nlm.nih.gov/pubmed/10366647>.
- Khabar, Khalid S. A. 2010. "Post-Transcriptional Control during Chronic Inflammation and Cancer: A Focus on AU-Rich Elements." *Cellular and Molecular Life Sciences* 67 (17). SP Birkhäuser Verlag Basel: 2937–55. doi:10.1007/s00018-010-0383-x.
- Khodor, Y. L., J. Rodriguez, K. C. Abruzzi, C.-H. A. Tang, M. T. Marr, and M. Rosbash. 2011. "Nascent-Seq Indicates Widespread Cotranscriptional Pre-mRNA Splicing in *Drosophila*." *Genes & Development* 25 (23). Cold Spring Harbor Laboratory Press: 2502–12. doi:10.1101/gad.178962.111.

- Kidd, B. L., and L. A. Urban. 2001. "Mechanisms of Inflammatory Pain." *British Journal of Anaesthesia* 87 (1). Oxford University Press: 3–11. doi:10.1093/bja/87.1.3.
- Kim, Ho Gyoung, Bhushan Shrestha, So Yeon Lim, Deok Hyo Yoon, Woo Chul Chang, Dong-Jik Shin, Sang Kuk Han, et al. 2006. "Cordycepin Inhibits Lipopolysaccharide-Induced Inflammation by the Suppression of NF-kappaB through Akt and p38 Inhibition in RAW 264.7 Macrophage Cells." *European Journal of Pharmacology* 545 (2–3): 192–99. doi:10.1016/j.ejphar.2006.06.047.
- Kim, Hogyoung, Amarjit S Naura, Youssef Errami, Jihang Ju, and A Hamid Boulares. 2011. "Cordycepin Blocks Lung Injury-Associated Inflammation and Promotes BRCA1-Deficient Breast Cancer Cell Killing by Effectively Inhibiting PARP." *Molecular Medicine (Cambridge, Mass.)* 17 (9–10): 893–900. doi:10.2119/molmed.2011.00032.
- Kim, Sodam, Sun Young Kim, John P Pribis, Michael Lotze, Kevin P Mollen, Richard Shapiro, Patricia Loughran, Melanie J Scott, and Timothy R Billiar. 2013. "Signaling of High Mobility Group Box 1 (HMGB1) through Toll-like Receptor 4 in Macrophages Requires CD14." *Molecular Medicine (Cambridge, Mass.)* 19 (1). The Feinstein Institute for Medical Research: 88–98. doi:10.2119/molmed.2012.00306.
- Kitamura, M, H Kato, Y Saito, S Nakajima, S Takahashi, H Johno, L Gu, and R Katoh. 2011. "Aberrant, Differential and Bidirectional Regulation of the Unfolded Protein Response towards Cell Survival by 3'-deoxyadenosine." *Cell Death and Differentiation* 18 (12). Macmillan Publishers Limited: 1876–88. doi:10.1038/cdd.2011.63.
- Kohda, Akira, Soh Yamazaki, and Hideki Sumimoto. 2016. "The Nuclear Protein IkbZ Forms a Transcriptionally Active Complex with Nuclear Factor-kB (NF-kB) p50 and *Lcn2* Promoter via the N- and C-Terminal Ankyrin Repeat Motifs." *Journal of Biological Chemistry*, August. American Society for Biochemistry and Molecular Biology, jbc.M116.719302. doi:10.1074/jbc.M116.719302.
- Kolev, Nikolay G, Therese A Yario, Eleni Benson, Joan A Steitz, L. Aravind, D. Baillat, MA. Hakimi, et al. 2008. "Conserved Motifs in Both CPSF73 and CPSF100 Are Required to Assemble the Active Endonuclease for Histone mRNA 3'-End Maturation." *EMBO Reports* 9 (10). EMBO Press: 1013–18. doi:10.1038/embor.2008.146.
- Kondrashov, Alexander, Hedda A Meijer, Adeline Barthet-Barateig, Hannah N Parker, Asma Khurshid, Sarah Tessier, Marie Sicard, Alan J Knox, Linhua Pang, and Cornelia H De Moor. 2012. "Inhibition of Polyadenylation Reduces Inflammatory Gene Induction." *RNA (New York, N.Y.)* 18 (12): 2236–50. doi:10.1261/rna.032391.112.
- Kontoyiannis, Dimitris, Manolis Pasparakis, Theresa T Pizarro, Fabio Cominelli, and George Kollias. 1999. "Impaired On/Off Regulation of TNF Biosynthesis in Mice Lacking TNF AU-Rich Elements: Implications for Joint and Gut-Associated Immunopathologies." *Immunity* 10 (3): 387–98. doi:10.1016/S1074-7613(00)80038-2.
- Kosmidou, I., J. P. Moore, M. Weber, and C. D. Searles. 2007. "Statin Treatment and 3' Polyadenylation of eNOS mRNA." *Arteriosclerosis, Thrombosis, and Vascular*

Biology 27 (12). Lippincott Williams & Wilkins: 2642–49.
doi:10.1161/ATVBAHA.107.154492.

Kuehner, Jason N., Erika L. Pearson, and Claire Moore. 2011. “Unravelling the Means to an End: RNA Polymerase II Transcription Termination.” *Nature Reviews Molecular Cell Biology* 12 (5). Nature Publishing Group: 283–94.
doi:10.1038/nrm3098.

Kuhn, U., M. Gundel, A. Knoth, Y. Kerwitz, S. Rudel, and E. Wahle. 2009. “Poly(A) Tail Length Is Controlled by the Nuclear Poly(A)-Binding Protein Regulating the Interaction between Poly(A) Polymerase and the Cleavage and Polyadenylation Specificity Factor.” *Journal of Biological Chemistry* 284 (34): 22803–14.
doi:10.1074/jbc.M109.018226.

Kung, Johnny T. Y., David Colognori, and Jeannie T. Lee. 2013. “Long Noncoding RNAs: Past, Present, and Future.” *Genetics* 193 (3).

Kuwahara, Mitsuhiro, Sumiko Kurachi, and Kotoku Kurachi. 2004. “Molecular Mechanism of Prothrombin G20210A Variant: Critical New Role of Exon Splicing Enhancer in Poly (A) Tailing.” *Blood* 104 (11). American Society of Hematology: 1944–1944.

Kwak, J. E., E. Drier, S. A. Barbee, M. Ramaswami, J. C. P. Yin, and M. Wickens. 2008. “GLD2 poly(A) Polymerase Is Required for Long-Term Memory.” *Proceedings of the National Academy of Sciences* 105 (38). National Academy of Sciences: 14644–49. doi:10.1073/pnas.0803185105.

Kwak, J. E., and M. Wickens. 2007. “A Family of poly(U) Polymerases.” *RNA* 13 (6). Cold Spring Harbor Laboratory Press: 860–67. doi:10.1261/rna.514007.

LaCava, John, Jonathan Houseley, Cosmin Saveanu, Elisabeth Petfalski, Elizabeth Thompson, Alain Jacquier, David Tollervey, et al. 2005. “RNA Degradation by the Exosome Is Promoted by a Nuclear Polyadenylation Complex.” *Cell* 121 (5). Elsevier: 713–24. doi:10.1016/j.cell.2005.04.029.

Laskin, Debra L. 2009. “Macrophages and Inflammatory Mediators in Chemical Toxicity: A Battle of Forces.” *Chemical Research in Toxicology* 22 (8): 1376–85.
doi:10.1021/tx900086v.

Lee, Na Kyung, Young Geum Choi, Ji Youn Baik, Song Yi Han, Dae-Won Jeong, Yun Soo Bae, Nacksung Kim, and Soo Young Lee. 2005. “A Crucial Role for Reactive Oxygen Species in RANKL-Induced Osteoclast Differentiation.” *Blood* 106 (3). American Society of Hematology: 852–59. doi:10.1182/blood-2004-09-3662.

Lee, Se-Jung, Gi-Seong Moon, Kyung-Hwan Jung, Wun-Jae Kim, and Sung-Kwon Moon. 2010. “C-Jun N-Terminal Kinase 1 Is Required for Cordycepin-Mediated Induction of G2/M Cell-Cycle Arrest via p21WAF1 Expression in Human Colon Cancer Cells.” *Food and Chemical Toxicology : An International Journal Published for the British Industrial Biological Research Association* 48 (1): 277–83. doi:10.1016/j.fct.2009.09.042.

Leppek, Kathrin, Johanna Schott, Sonja Reitter, Fabian Poetz, Ming C Hammond, and Georg Stoecklin. 2013. “Roquin Promotes Constitutive mRNA Decay via a Conserved Class of Stem-Loop Recognition Motifs.” *Cell* 153 (4). Elsevier: 869–81. doi:10.1016/j.cell.2013.04.016.

- Lewin, Gary R., Alain Rueff, and Lorne M. Mendell. 1994. "Peripheral and Central Mechanisms of NGF-Induced Hyperalgesia." *European Journal of Neuroscience* 6 (12). Blackwell Publishing Ltd: 1903–12. doi:10.1111/j.1460-9568.1994.tb00581.x.
- Li, Fei, and Joe Z. Tsien. 2009. "Memory and the NMDA Receptors." *New England Journal of Medicine* 361 (3). Massachusetts Medical Society : 302–3. doi:10.1056/NEJMcibr0902052.
- Li, Xuelin, Wei-Jye Lin, Ching-Yi Chen, Ying Si, Xiaowen Zhang, Liang Lu, Esther Suswam, Lei Zheng, and Peter H. King. 2012. "KSRP: A Checkpoint for Inflammatory Cytokine Production in Astrocytes." *Glia* 60 (11). Wiley Subscription Services, Inc., A Wiley Company: 1773–84. doi:10.1002/glia.22396.
- Li, Yan, Kang Li, Lu Mao, Xiuguo Han, Kai Zhang, Changqing Zhao, and Jie Zhao. 2016. "Cordycepin Inhibits LPS-Induced Inflammatory and Matrix Degradation in the Intervertebral Disc." *PeerJ* 4. PeerJ, Inc: e1992. doi:10.7717/peerj.1992.
- Lim, Jaechul, Minju Ha, Hyesik Chang, S. Chul Kwon, Dharendra K. Simanshu, Dinshaw J. Patel, and V. Narry Kim. 2014. "Uridylation by TUT4 and TUT7 Marks mRNA for Degradation." *Cell* 159 (6): 1365–76. doi:10.1016/j.cell.2014.10.055.
- Lim, Jaechul, Mihye Lee, Ahyeon Son, Hyesik Chang, and V. Narry Kim. 2016. "mTAIL-Seq Reveals Dynamic poly(A) Tail Regulation in Oocyte-to-Embryo Development." *Genes & Development* 30 (14). Cold Spring Harbor Laboratory Press: 1671–82. doi:10.1101/gad.284802.116.
- Liu, B., and Jau-Shyong Hong. 2003. "Role of Microglia in Inflammation-Mediated Neurodegenerative Diseases: Mechanisms and Strategies for Therapeutic Intervention." *Journal of Pharmacology and Experimental Therapeutics* 304 (1). American Society for Pharmacology and Experimental Therapeutics: 1–7. doi:10.1124/jpet.102.035048.
- Lu, Yong-Chen, Wen-Chen Yeh, and Pamela S. Ohashi. 2008. "LPS/TLR4 Signal Transduction Pathway." *Cytokine* 42 (2): 145–51. doi:10.1016/j.cyto.2008.01.006.
- Luitjens, C., Maria Gallegos, Brian Kraemer, Judith Kimble, and Marvin Wickens. 2000. "CPEB Proteins Control Two Key Steps in Spermatogenesis in *C. Elegans*." *Genes & Development* 14 (20). Cold Spring Harbor Laboratory Press: 2596–2609. doi:10.1101/gad.831700.
- Luo, Weifei, Arlen W Johnson, and David L Bentley. 2006. "The Role of Rat1 in Coupling mRNA 3'-end Processing to Transcription Termination: Implications for a Unified Allosteric-Torpedo Model." *Genes & Development* 20 (8): 954–65. doi:10.1101/gad.1409106.
- Mahtani, K R, M Brook, J L Dean, G Sully, J Saklatvala, and A R Clark. 2001. "Mitogen-Activated Protein Kinase p38 Controls the Expression and Posttranslational Modification of Tristetraprolin, a Regulator of Tumor Necrosis Factor Alpha mRNA Stability." *Molecular and Cellular Biology* 21 (19). American Society for Microbiology: 6461–69. doi:10.1128/MCB.21.9.6461-6469.2001.
- Malecki, Michal, Sandra C Viegas, Tiago Carneiro, Pawel Golik, Clémentine Dressaire, Miguel G Ferreira, Cecília M Arraiano, et al. 2013. "The Exoribonuclease Dis3L2

Defines a Novel Eukaryotic RNA Degradation Pathway." *The EMBO Journal* 32 (13). EMBO Press: 1842–54. doi:10.1038/emboj.2013.63.

Mandel, Corey R, Syuzo Kaneko, Hailong Zhang, Damara Gebauer, Vasupradha Vethantham, James L Manley, and Liang Tong. 2006. "Polyadenylation Factor CPSF-73 Is the Pre-mRNA 3'-end-Processing Endonuclease." *Nature* 444 (7121): 953–56. doi:10.1038/nature05363.

Mangus, David A, Matthew C Evans, Allan Jacobson, CG Burd, EL Matunis, G Dreyfuss, KC Kleene, et al. 2003. "Poly(A)-Binding Proteins: Multifunctional Scaffolds for the Post-Transcriptional Control of Gene Expression." *Genome Biology* 4 (7). BioMed Central: 223. doi:10.1186/gb-2003-4-7-223.

Mapendano, Christophe K, Søren Lykke-Andersen, Jørgen Kjems, Edouard Bertrand, and Torben Heick Jensen. 2010. "Crosstalk between mRNA 3' End Processing and Transcription Initiation." *Molecular Cell* 40 (3). Elsevier: 410–22. doi:10.1016/j.molcel.2010.10.012.

Marchese, F. P., A. Aubareda, C. Tudor, J. Saklatvala, A. R. Clark, and J. L. E. Dean. 2010. "MAPKAP Kinase 2 Blocks Tristetraprolin-Directed mRNA Decay by Inhibiting CAF1 Deadenylation Recruitment." *Journal of Biological Chemistry* 285 (36). American Society for Biochemistry and Molecular Biology: 27590–600. doi:10.1074/jbc.M110.136473.

Martin, G., and W. Keller. 2007. "RNA-Specific Ribonucleotidyl Transferases." *RNA* 13 (11). Cold Spring Harbor Laboratory Press: 1834–49. doi:10.1261/rna.652807.

Marzluff, William F. 2005. "Metazoan Replication-Dependent Histone mRNAs: A Distinct Set of RNA Polymerase II Transcripts." *Current Opinion in Cell Biology* 17 (3): 274–80. doi:10.1016/j.ceb.2005.04.010.

Marzluff, William F, Eric J Wagner, and Robert J Duronio. 2008. "Metabolism and Regulation of Canonical Histone mRNAs: Life without a poly(A) Tail." *Nature Reviews. Genetics* 9 (11). Nature Publishing Group: 843–54. doi:10.1038/nrg2438.

May, Michael J., and Sankar Ghosh. 1997. "Rel/NF- κ B and I κ B Proteins: An Overview." *Seminars in Cancer Biology* 8 (2). Academic Press: 63–73. doi:10.1006/scbi.1997.0057.

Mayer, C, and I Grummt. 2006. "Ribosome Biogenesis and Cell Growth: mTOR Coordinates Transcription by All Three Classes of Nuclear RNA Polymerases." *Oncogene* 25 (48). Nature Publishing Group: 6384–91. doi:10.1038/sj.onc.1209883.

Mayr, Christine, David P. Bartel, N. Amrani, S. Ghosh, D.A. Mangus, A. Jacobson, D.P. Bartel, et al. 2009. "Widespread Shortening of 3'UTRs by Alternative Cleavage and Polyadenylation Activates Oncogenes in Cancer Cells." *Cell* 138 (4). Elsevier: 673–84. doi:10.1016/j.cell.2009.06.016.

Memmott, Regan M., and Phillip A. Dennis. 2009. "Akt-Dependent and -Independent Mechanisms of mTOR Regulation in Cancer." *Cellular Signalling* 21 (5): 656–64. doi:10.1016/j.cellsig.2009.01.004.

Michels, A. A., A. M. Robitaille, D. Buczynski-Ruchonnet, W. Hodroj, J. H. Reina, M. N. Hall, and N. Hernandez. 2010. "mTORC1 Directly Phosphorylates and Regulates

- Human MAF1." *Molecular and Cellular Biology* 30 (15). American Society for Microbiology: 3749–57. doi:10.1128/MCB.00319-10.
- Minasaki, Ryuji, David Rudel, and Christian R Eckmann. 2014. "Increased Sensitivity and Accuracy of a Single-Stranded DNA Splint-Mediated Ligation Assay (sPAT) Reveals poly(A) Tail Length Dynamics of Developmentally Regulated mRNAs." *RNA Biology* 11 (2): 111–23. doi:10.4161/rna.27992.
- Minvielle-Sebastia, L, B Winsor, N Bonneaud, and F Lacroute. 1991. "Mutations in the Yeast RNA14 and RNA15 Genes Result in an Abnormal mRNA Decay Rate; Sequence Analysis Reveals an RNA-Binding Domain in the RNA15 Protein." *Mol. Cell. Biol.* 11 (6): 3075–87. doi:10.1128/MCB.11.6.3075.
- Moore, K. J., L. P. Andersson, R. R. Ingalls, B. G. Monks, R. Li, M. A. Arnaout, D. T. Golenbock, and M. W. Freeman. 2000. "Divergent Response to LPS and Bacteria in CD14-Deficient Murine Macrophages." *The Journal of Immunology* 165 (8). American Association of Immunologists: 4272–80. doi:10.4049/jimmunol.165.8.4272.
- Moynagh, Paul N. 2005. "TLR Signalling and Activation of IRFs: Revisiting Old Friends from the NF- κ B Pathway." *Trends in Immunology* 26 (9): 469–76. doi:10.1016/j.it.2005.06.009.
- Mullen, T. E., and W. F. Marzluff. 2008. "Degradation of Histone mRNA Requires Oligouridylation Followed by Decapping and Simultaneous Degradation of the mRNA Both 5' to 3' and 3' to 5'." *Genes & Development* 22 (1). Cold Spring Harbor Laboratory Press: 50–65. doi:10.1101/gad.1622708.
- Muniz, Lisa, Lee Davidson, and Steven West. 2015. "Poly(A) Polymerase and the Nuclear Poly(A) Binding Protein, PABPN1, Coordinate the Splicing and Degradation of a Subset of Human Pre-mRNAs." *Molecular and Cellular Biology* 35 (13). American Society for Microbiology: 2218–30. doi:10.1128/MCB.00123-15.
- Murray, Peter J., Judith E. Allen, Subhra K. Biswas, Edward A. Fisher, Derek W. Gilroy, Sergij Goerdt, Siamon Gordon, et al. 2014. "Macrophage Activation and Polarization: Nomenclature and Experimental Guidelines." *Immunity* 41 (1): 14–20. doi:10.1016/j.immuni.2014.06.008.
- Murthy, K G, and J L Manley. 1995. "The 160-kD Subunit of Human Cleavage-Polyadenylation Specificity Factor Coordinates Pre-mRNA 3'-end Formation." *Genes & Development* 9 (21). Cold Spring Harbor Laboratory Press: 2672–83. doi:10.1101/gad.9.21.2672.
- Nagaike, T., Tsutomu Suzuki, Takayuki Katoh, and Takuya Ueda. 2005. "Human Mitochondrial mRNAs Are Stabilized with Polyadenylation Regulated by Mitochondria-Specific Poly(A) Polymerase and Polynucleotide Phosphorylase." *Journal of Biological Chemistry* 280 (20). American Society for Biochemistry and Molecular Biology: 19721–27. doi:10.1074/jbc.M500804200.
- Nakamura, Kazuki, Noriko Yoshikawa, Yu Yamaguchi, Satomi Kagota, Kazumasa Shinozuka, and Masaru Kunitomo. 2006. "Antitumor Effect of Cordycepin (3'-deoxyadenosine) on Mouse Melanoma and Lung Carcinoma Cells Involves Adenosine A3 Receptor Stimulation." *Anticancer Research* 26 (1A): 43–47. <http://www.ncbi.nlm.nih.gov/pubmed/16475677>.

- Neovius, M, E V Arkema, H Olsson, J K Eriksson, L E Kristensen, J F Simard, J Askling, et al. 2015. "Drug Survival on TNF Inhibitors in Patients with Rheumatoid Arthritis Comparison of Adalimumab, Etanercept and Infliximab." *Annals of the Rheumatic Diseases* 74 (2). BMJ Publishing Group Ltd and European League Against Rheumatism: 354–60. doi:10.1136/annrheumdis-2013-204128.
- Novoa, Isabel, Javier Gallego, Pedro G. Ferreira, and Raul Mendez. 2010. "Mitotic Cell-Cycle Progression Is Regulated by CPEB1 and CPEB4-Dependent Translational Control." *Nature Cell Biology* 12 (5). Nature Publishing Group: 447–56. doi:10.1038/ncb2046.
- Oeckinghaus, A., and S. Ghosh. 2009. "The NF- κ B Family of Transcription Factors and Its Regulation." *Cold Spring Harbor Perspectives in Biology* 1 (4). Cold Spring Harbor Laboratory Press: a000034–a000034. doi:10.1101/cshperspect.a000034.
- Ofengeim, Dimitry, and Junying Yuan. 2013. "Regulation of RIP1 Kinase Signalling at the Crossroads of Inflammation and Cell Death." *Nature Reviews Molecular Cell Biology* 14 (11). Nature Research: 727–36. doi:10.1038/nrm3683.
- Oficjalska-Pham, Danuta, Olivier Harismendy, Wieslaw J Smagowicz, Anne Gonzalez de Peredo, Magdalena Boguta, André Sentenac, Olivier Lefebvre, et al. 2006. "General Repression of RNA Polymerase III Transcription Is Triggered by Protein Phosphatase Type 2A-Mediated Dephosphorylation of Maf1." *Molecular Cell* 22 (5). Elsevier: 623–32. doi:10.1016/j.molcel.2006.04.008.
- Oganesyan, Gagik, Supriya K. Saha, Beichu Guo, Jeannie Q. He, Arash Shahangian, Brian Zarnegar, Andrea Perry, and Genhong Cheng. 2006. "Critical Role of TRAF3 in the Toll-like Receptor-Dependent and -Independent Antiviral Response." *Nature* 439 (7073). Nature Publishing Group: 208–11. doi:10.1038/nature04374.
- Pak, ChangHui, Masoud Garshasbi, Kimia Kahrizi, Christina Gross, Luciano H. Apponi, John J. Noto, Seth M. Kelly, et al. 2011. "Mutation of the Conserved Polyadenosine RNA Binding Protein, ZC3H14/dNab2, Impairs Neural Function in *Drosophila* and Humans." *Proceedings of the National Academy of Sciences* 108 (30). National Academy of Sciences: 12390–95. doi:10.1073/PNAS.1107103108.
- Park, Beom Seok, Dong Hyun Song, Ho Min Kim, Byong-Seok Choi, Hayyoung Lee, and Jie-Oh Lee. 2009. "The Structural Basis of Lipopolysaccharide Recognition by the TLR4–MD-2 Complex." *Nature* 458 (7242). Nature Publishing Group: 1191–95. doi:10.1038/nature07830.
- Park, Jong-Eun, Hyerim Yi, Yoosik Kim, Hyesik Chang, V. Narry Kim, F. Amaldi, P. Pierandrei-Amaldi, et al. 2016. "Regulation of Poly(A) Tail and Translation during the Somatic Cell Cycle." *Molecular Cell* 62 (3). Elsevier: 462–71. doi:10.1016/j.molcel.2016.04.007.
- Peixeiro, Isabel, Ana Luísa Silva, Luísa Romão, J. Ross, AB. Sachs, P. Sarnow, MW. Hentze, et al. 2011. "Control of Human Beta-Globin mRNA Stability and Its Impact on Beta-Thalassemia Phenotype." *Haematologica* 96 (6). Haematologica: 905–13. doi:10.3324/haematol.2010.039206.
- Peng, J., Elizabeth L. Murray, and Daniel R. Schoenberg. 2005. "The poly(A)-Limiting Element Enhances mRNA Accumulation by Increasing the Efficiency of Pre-mRNA 3' Processing." *RNA* 11 (6). Cold Spring Harbor Laboratory Press: 958–

65. doi:10.1261/rna.2020805.

- Peng, Jie, Ping Wang, Hongshan Ge, Xianqin Qu, and Xingliang Jin. 2015. "Effects of Cordycepin on the Microglia-Overactivation-Induced Impairments of Growth and Development of Hippocampal Cultured Neurons." Edited by Michelle L. Block. *PLoS ONE* 10 (5). Public Library of Science: e0125902. doi:10.1371/journal.pone.0125902.
- Penman, S., M. Rosbash, and M. Penman. 1970. "Messenger and Heterogeneous Nuclear RNA in HeLa Cells: Differential Inhibition by Cordycepin." *Proceedings of the National Academy of Sciences* 67 (4): 1878–85. doi:10.1073/pnas.67.4.1878.
- Perez Canadillas, J. M., Gabriele Varani, FH-T. Allain, CC. Gubser, PWA. Howe, K. Nagai, D. Neuhaus, et al. 2003. "Recognition of GU-Rich Polyadenylation Regulatory Elements by Human CstF-64 Protein." *The EMBO Journal* 22 (11). EMBO Press: 2821–30. doi:10.1093/emboj/cdg259.
- Perry, A K, G Chen, D Zheng, H Tang, and G Cheng. 2005. "The Host Type I Interferon Response to Viral and Bacterial Infections." *Cell Res* 15 (6). Nature Publishing Group: 407–22. doi:10.1038/sj.cr.7290309.
- Philp, Ashleigh M, Edward T Davis, and Simon W Jones. 2016. "Developing Anti-Inflammatory Therapeutics for Patients with Osteoarthritis." *Rheumatology (Oxford, England)*, August. doi:10.1093/rheumatology/kew278.
- Piccinini, A M, K S Midwood, A. M. Piccinini, and K. S. Midwood. 2010. "DAMPening Inflammation by Modulating TLR Signalling." *Mediators of Inflammation* 2010. Hindawi Publishing Corporation. doi:10.1155/2010/672395.
- Poort, S R, F R Rosendaal, P H Reitsma, and R M Bertina. 1996. "A Common Genetic Variation in the 3'-untranslated Region of the Prothrombin Gene Is Associated with Elevated Plasma Prothrombin Levels and an Increase in Venous Thrombosis." *Blood* 88 (10). American Society of Hematology: 3698–3703. <http://www.ncbi.nlm.nih.gov/pubmed/8916933>.
- Proudfoot, N. J. 2011. "Ending the Message: poly(A) Signals Then and Now." *Genes & Development* 25 (17). Cold Spring Harbor Laboratory Press: 1770–82. doi:10.1101/gad.17268411.
- Puntmann, Valentina O, Peter C Taylor, and Manuel Mayr. 2011. "Coupling Vascular and Myocardial Inflammatory Injury into a Common Phenotype of Cardiovascular Dysfunction: Systemic Inflammation and Aging - a Mini-Review." *Gerontology* 57 (4): 295–303. doi:10.1159/000316577.
- Quail, Michael A, Harold Swerdlow, Daniel J Turner, and Harold Swerdlow. 2009. "Improved Protocols for the Illumina Genome Analyzer Sequencing System." *Current Protocols in Human Genetics* Chapter 18 (July). Europe PMC Funders: Unit 18.2. doi:10.1002/0471142905.hg1802s62.
- Rahmati, Maryam, Ali Mobasheri, and Masoud Mozafari. 2016. "Inflammatory Mediators in Osteoarthritis: A Critical Review of the State-of-the-Art, Current Prospects, and Future Challenges." *Bone* 85: 81–90. doi:10.1016/j.bone.2016.01.019.
- Rajaram, Murugesan V S, Latha P Ganesan, Kishore V L Parsa, Jonathan P Butchar,

- John S Gunn, and Susheela Tridandapani. 2006. "Akt/Protein Kinase B Modulates Macrophage Inflammatory Response to Francisella Infection and Confers a Survival Advantage in Mice." *Journal of Immunology (Baltimore, Md. : 1950)* 177 (9). American Association of Immunologists: 6317–24. doi:10.4049/JIMMUNOL.177.9.6317.
- Rassa, J C, G M Wilson, G A Brewer, and G D Parks. 2000. "Spacing Constraints on Reinitiation of Paramyxovirus Transcription: The Gene End U Tract Acts as a Spacer to Separate Gene End from Gene Start Sites." *Virology* 274 (2): 438–49. doi:10.1006/viro.2000.0494.
- Ren, Zhenghua, Jianhua Cui, Zeren Huo, Jinru Xue, Hao Cui, Bin Luo, Lanjin Jiang, and Rirong Yang. 2012. "Cordycepin Suppresses TNF- α -Induced NF- κ B Activation by Reducing p65 Transcriptional Activity, Inhibiting I κ B α Phosphorylation, and Blocking IKK γ Ubiquitination." *International Immunopharmacology* 14 (4): 698–703. doi:10.1016/j.intimp.2012.10.008.
- Richard, Patricia, and James L Manley. 2009. "Transcription Termination by Nuclear RNA Polymerases." *Genes & Development* 23 (11): 1247–69. doi:10.1101/gad.1792809.
- Rissland, O. S., A. Mikulasova, and C. J. Norbury. 2007. "Efficient RNA Polyuridylation by Noncanonical Poly(A) Polymerases." *Molecular and Cellular Biology* 27 (10). American Society for Microbiology: 3612–24. doi:10.1128/MCB.02209-06.
- Ritchie, M. E., B. Phipson, D. Wu, Y. Hu, C. W. Law, W. Shi, and G. K. Smyth. 2015. "Limma Powers Differential Expression Analyses for RNA-Sequencing and Microarray Studies." *Nucleic Acids Research* 43 (7). Oxford University Press: e47–e47. doi:10.1093/nar/gkv007.
- Rose, K M, L E Bell, and S T Jacob. 1977. "Specific Inhibition of Chromatin-Associated poly(A) Synthesis in Vitro by Cordycepin 5'-triphosphate." *Nature* 267 (5607): 178–80. doi:10.1038/267178a0.
- Rottenberg, Martin E, Willias Masocha, Marcela Ferella, Fabricio Petitto-Assis, Hiro Goto, Krister Kristensson, Ronald McCaffrey, and Hans Wigzell. 2005. "Treatment of African Trypanosomiasis with Cordycepin and Adenosine Deaminase Inhibitors in a Mouse Model." *The Journal of Infectious Diseases* 192 (9): 1658–65. doi:10.1086/496896.
- Rouhana, Labib, Liaoteng Wang, Natascha Buter, Jae Eun Kwak, Craig a Schiltz, Tania Gonzalez, Ann E Kelley, Charles F Landry, and Marvin Wickens. 2005. "Vertebrate GLD2 poly(A) Polymerases in the Germline and the Brain." *RNA (New York, N.Y.)* 11 (7). Cold Spring Harbor Laboratory Press: 1117–30. doi:10.1261/rna.2630205.
- Ryner, L C, and J L Manley. 1987. "Requirements for Accurate and Efficient mRNA 3' End Cleavage and Polyadenylation of a Simian Virus 40 Early Pre-RNA in Vitro." *Mol. Cell. Biol.* 7 (1): 495–503. doi:10.1128/MCB.7.1.495.
- Sagawa, Fumihiko, Hend Ibrahim, Angela L Morrison, Carol J Wilusz, and Jeffrey Wilusz. 2011. "Nucleophosmin Deposition during mRNA 3' End Processing Influences poly(A) Tail Length." *The EMBO Journal* 30 (19): 3994–4005. doi:10.1038/emboj.2011.272.
- Sandberg, Rickard, Joel R Neilson, Arup Sarma, Phillip A Sharp, and Christopher B

- Burge. 2008. "Proliferating Cells Express mRNAs with Shortened 3' Untranslated Regions and Fewer microRNA Target Sites." *Science (New York, N.Y.)* 320 (5883). American Association for the Advancement of Science: 1643–47. doi:10.1126/science.1155390.
- Sandler, Heike, Georg Stoecklin, G.A. Taylor, E. Carballo, D.M. Lee, W.S. Lai, M.J. Thompson, et al. 2008. "Control of mRNA Decay by Phosphorylation of Tristetraprolin." *Biochemical Society Transactions* 36 (Pt 3). Portland Press Limited: 491–96. doi:10.1042/BST0360491.
- Sanduja, Sandhya, Fernando F Blanco, Lisa E Young, Vimala Kaza, and Dan A Dixon. 2012. "The Role of Tristetraprolin in Cancer and Inflammation." *Frontiers in Bioscience (Landmark Edition)* 17 (January): 174–88. <http://www.pubmedcentral.nih.gov/articlerender.fcgi?artid=3461960&tool=pmcentrez&rendertype=abstract>.
- Sartain, Caroline V, Jun Cui, Richard P Meisel, Mariana F Wolfner, C. D. Allis, G. L. Waring, A. P. Mahowald, et al. 2011. "The poly(A) Polymerase GLD2 Is Required for Spermatogenesis in *Drosophila Melanogaster*." *Development (Cambridge, England)* 138 (8). Oxford University Press for The Company of Biologists Limited: 1619–29. doi:10.1242/dev.059618.
- Scherle, P A, E A Jones, M F Favata, A J Daulerio, M B Covington, S A Nurnberg, R L Magolda, and J M Trzaskos. 1998. "Inhibition of MAP Kinase Kinase Prevents Cytokine and Prostaglandin E2 Production in Lipopolysaccharide-Stimulated Monocytes." *Journal of Immunology (Baltimore, Md. : 1950)* 161 (10). American Association of Immunologists: 5681–86. <http://www.ncbi.nlm.nih.gov/pubmed/9820549>.
- Schoenberg, D R, J E Moskaitis, L H Smith, and R L Pastori. 1989. "Extranuclear Estrogen-Regulated Destabilization of *Xenopus Laevis* Serum Albumin mRNA." *Molecular Endocrinology (Baltimore, Md.)* 3 (5): 805–14. doi:10.1210/mend-3-5-805.
- Schönemann, Lars, Uwe Kühn, Georges Martin, Peter Schäfer, Andreas R. Gruber, Walter Keller, Mihaela Zavolan, and Elmar Wahle. 2014. "Reconstitution of CPSF Active in Polyadenylation: Recognition of the Polyadenylation Signal by WDR33." *Genes & Development* 28 (21). Cold Spring Harbor Laboratory Press: 2381–93. doi:10.1101/gad.250985.114.
- Sement, F. M., E. Ferrier, H. Zuber, R. Merret, M. Alioua, J.-M. Deragon, C. Bousquet-Antonelli, H. Lange, and D. Gagliardi. 2013. "Uridylation Prevents 3' Trimming of Oligoadenylated mRNAs." *Nucleic Acids Research* 41 (14). Oxford University Press: 7115–27. doi:10.1093/nar/gkt465.
- Shatkin, Aaron J., and James L. Manley. 2000. "The Ends of the Affair: Capping and Polyadenylation." *Nature Structural Biology* 7 (10). Nature Publishing Group: 838–42. doi:10.1038/79583.
- Shcherbik, Natalia, Minshi Wang, Yevgeniya R Lapik, Leena Srivastava, Dimitri G Pestov, C. Allmang, E. Petfalski, et al. 2010. "Polyadenylation and Degradation of Incomplete RNA Polymerase I Transcripts in Mammalian Cells." *EMBO Reports* 11 (2). EMBO Press: 106–11. doi:10.1038/embor.2009.271.
- Shell, S. A., Candice Hesse, Sidney M. Morris, and Christine Milcarek. 2005. "Elevated Levels of the 64-kDa Cleavage Stimulatory Factor (CstF-64) in

- Lipopolysaccharide-Stimulated Macrophages Influence Gene Expression and Induce Alternative Poly(A) Site Selection." *Journal of Biological Chemistry* 280 (48). American Society for Biochemistry and Molecular Biology: 39950–61. doi:10.1074/jbc.M508848200.
- Shen, Binzhang, and Howard M Goodman. 2004. "Uridine Addition after microRNA-Directed Cleavage." *Science (New York, N.Y.)* 306 (5698): 997. doi:10.1126/science.1103521.
- Shi, Yongsheng, Dafne Campigli Di Giammartino, Derek Taylor, Ali Sarkeshik, William J Rice, John R Yates, Joachim Frank, and James L Manley. 2009. "Molecular Architecture of the Human Pre-mRNA 3' Processing Complex." *Molecular Cell* 33 (3): 365–76. doi:10.1016/j.molcel.2008.12.028.
- Shigeura, Harold T., and George E. Boxer. 1964. "Incorporation of 3'-Deoxyadenosine-5'triphosphate into RNA by RNA Polymerase from *Micrococcus Lysodeikticus*." *Biochemical and Biophysical Research Communications* 17 (6): 758–63. doi:10.1016/0006-291X(64)90427-9.
- Shin, Seulmee, Sungwon Lee, Jeonghak Kwon, Sunhee Moon, Seungjeong Lee, Chong-Kil Lee, Kyunghae Cho, Nam-Joo Ha, and Kyungjae Kim. 2009. "Cordycepin Suppresses Expression of Diabetes Regulating Genes by Inhibition of Lipopolysaccharide-Induced Inflammation in Macrophages." *Immune Network* 9 (3): 98–105. doi:10.4110/in.2009.9.3.98.
- Shin, Seulmee, Sunhee Moon, Yoonhee Park, Jeonghak Kwon, Seungjeong Lee, Chong-Kil Lee, Kyunghae Cho, Nam-Joo Ha, and Kyungjae Kim. 2009. "Role of Cordycepin and Adenosine on the Phenotypic Switch of Macrophages via Induced Anti-Inflammatory Cytokines." *Immune Network* 9 (6): 255–64. doi:10.4110/in.2009.9.6.255.
- Shor, Boris, Jiang Wu, Quazi Shakey, Lourdes Toral-Barza, Celine Shi, Max Follettie, and Ker Yu. 2010. "Requirement of the mTOR Kinase for the Regulation of Maf1 Phosphorylation and Control of RNA Polymerase III-Dependent Transcription in Cancer Cells." *Journal of Biological Chemistry* 285 (20). American Society for Biochemistry and Molecular Biology: 15380–92. doi:10.1074/jbc.M109.071639.
- Siev, M, R Weinberg, and S Penman. 1969. "The Selective Interruption of Nucleolar RNA Synthesis in HeLa Cells by Cordycepin." *The Journal of Cell Biology* 41 (2): 510–20. <http://www.pubmedcentral.nih.gov/articlerender.fcgi?artid=2107749&tool=pmcentrez&rendertype=abstract>.
- Sizemore, Nywana, Stewart Leung, and George R. Stark. 1999. "Activation of Phosphatidylinositol 3-Kinase in Response to Interleukin-1 Leads to Phosphorylation and Activation of the NF- κ B p65/RelA Subunit." *Molecular and Cellular Biology* 19 (7). American Society for Microbiology: 4798–4805. doi:10.1128/MCB.19.7.4798.
- Slevin, Michael K., Stacie Meaux, Joshua D. Welch, Rebecca Bigler, Paula L. Miliiani de Marval, Wei Su, Robert E. Rhoads, Jan F. Prins, and William F. Marzluff. 2014. "Deep Sequencing Shows Multiple Oligouridylation Are Required for 3' to 5' Degradation of Histone mRNAs on Polyribosomes." *Molecular Cell*. Vol. 53. doi:10.1016/j.molcel.2014.02.027.

- Standart, Nancy, and Martin Dale. 1993. "Regulated Polyadenylation of Clam Maternal mRNAs in Vitro." *Developmental Genetics* 14 (6). Wiley Subscription Services, Inc., A Wiley Company: 492–99. doi:10.1002/dvg.1020140610.
- Stoecklin, Georg, Tiffany Stubbs, Nancy Kedersha, Stephen Wax, William F C Rigby, T Keith Blackwell, and Paul Anderson. 2004. "MK2-Induced tristetraprolin:14-3-3 Complexes Prevent Stress Granule Association and ARE-mRNA Decay." *The EMBO Journal* 23 (6). EMBO Press: 1313–24. doi:10.1038/sj.emboj.7600163.
- Stumpo, Deborah J, Wi S Lai, and Perry J Blackshear. 2010. "Inflammation: Cytokines and RNA-Based Regulation." *Wiley Interdisciplinary Reviews. RNA* 1 (1). NIH Public Access: 60–80. doi:10.1002/wrna.1.
- Subtelny, Alexander O., Stephen W. Eichhorn, Grace R. Chen, Hazel Sive, and David P. Bartel. 2014. "Poly(A)-Tail Profiling Reveals an Embryonic Switch in Translational Control." *Nature* 508 (7494). Nature Research: 66–71. doi:10.1038/nature13007.
- Sudo, Haruka, Aya Nozaki, Hideaki Uno, Yo-ichi Ishida, and Masami Nagahama. 2016. "Interaction Properties of Human TRAMP-like Proteins and Their Role in Pre-rRNA 5'ETS Turnover." *FEBS Letters*, August. doi:10.1002/1873-3468.12314.
- Sun, Antonia RuJia, Thor Friis, Sunderajhan Sekar, Ross Crawford, Yin Xiao, and Indira Prasadam. 2016. "Is Synovial Macrophage Activation the Inflammatory Link Between Obesity and Osteoarthritis?" *Current Rheumatology Reports* 18 (9): 57. doi:10.1007/s11926-016-0605-9.
- Sun, L., G. Stoecklin, S. Van Way, V. Hinkovska-Galcheva, R.-F. Guo, P. Anderson, and T. P. Shanley. 2006. "Tristetraprolin (TTP)-14-3-3 Complex Formation Protects TTP from Dephosphorylation by Protein Phosphatase 2a and Stabilizes Tumor Necrosis Factor- mRNA." *Journal of Biological Chemistry* 282 (6). American Society for Biochemistry and Molecular Biology: 3766–77. doi:10.1074/jbc.M607347200.
- Suri, S., S. E Gill, S. Massena de Camin, D. F McWilliams, D. Wilson, and D. A Walsh. 2007. "Neurovascular Invasion at the Osteochondral Junction and in Osteophytes in Osteoarthritis." *Annals of the Rheumatic Diseases* 66 (11). BMJ Publishing Group Ltd and European League Against Rheumatism: 1423–28. doi:10.1136/ard.2006.063354.
- Suri, Sunita, and David A. Walsh. 2012. "Osteochondral Alterations in Osteoarthritis." *Bone* 51 (2): 204–11. doi:10.1016/j.bone.2011.10.010.
- Suzuki, Akari, and Kazuhiko Yamamoto. 2015. "From Genetics to Functional Insights into Rheumatoid Arthritis." *Clinical and Experimental Rheumatology* 33 (4 Suppl 92): 40–43. <http://www.ncbi.nlm.nih.gov/pubmed/26457422>.
- Swantek, J L, M H Cobb, and T D Geppert. 1997. "Jun N-Terminal Kinase/stress-Activated Protein Kinase (JNK/SAPK) Is Required for Lipopolysaccharide Stimulation of Tumor Necrosis Factor Alpha (TNF-Alpha) Translation: Glucocorticoids Inhibit TNF-Alpha Translation by Blocking JNK/SAPK." *Molecular and Cellular Biology* 17 (11). American Society for Microbiology (ASM): 6274–82. <http://www.ncbi.nlm.nih.gov/pubmed/9343388>.
- Takagaki, Y., and J. L. Manley. 2000. "Complex Protein Interactions within the Human Polyadenylation Machinery Identify a Novel Component." *Molecular*

and Cellular Biology 20 (5). American Society for Microbiology: 1515–25. doi:10.1128/MCB.20.5.1515-1525.2000.

Takagaki, Y, and J L Manley. 1997. "RNA Recognition by the Human Polyadenylation Factor CstF." *Molecular and Cellular Biology* 17 (7). American Society for Microbiology: 3907–14. doi:10.1128/MCB.17.7.3907.

Takahashi, Shuhei, Minoru Tamai, Shotaro Nakajima, Hironori Kato, Hisashi Johno, Tomoyuki Nakamura, and Masanori Kitamura. 2012. "Blockade of Adipocyte Differentiation by Cordycepin." *British Journal of Pharmacology* 167 (3): 561–75. doi:10.1111/j.1476-5381.2012.02005.x.

Takaoka, Akinori, Hideyuki Yanai, Seiji Kondo, Gordon Duncan, Hideo Negishi, Tatsuaki Mizutani, Shin-ichi Kano, et al. 2005. "Integral Role of IRF-5 in the Gene Induction Programme Activated by Toll-like Receptors." *Nature* 434 (7030). Nature Publishing Group: 243–49. doi:10.1038/nature03308.

Tang, Daolin, Rui Kang, Carolyn B. Coyne, Herbert J. Zeh, and Michael T. Lotze. 2012. "PAMPs and DAMPs: Signal Os That Spur Autophagy and Immunity." *Immunological Reviews* 249 (1): 158–75. doi:10.1111/j.1600-065X.2012.01146.x.

Taylor, Gregory A, Ester Carballo, David M Lee, Wi S Lai, Michael J Thompson, Dhavalkumar D Patel, Daniel I Schenkman, et al. 1996. "A Pathogenetic Role for TNF α in the Syndrome of Cachexia, Arthritis, and Autoimmunity Resulting from Tristetraprolin (TTP) Deficiency." *Immunity* 4 (5): 445–54. doi:10.1016/S1074-7613(00)80411-2.

Taylor, P C, Peter C Taylor, and Marc Feldmann. 2009. "Anti-TNF Biologic Agents: Still the Therapy of Choice for Rheumatoid Arthritis." *Nature Reviews Rheumatology* 5 (10). doi:10.1038/nrrheum.2009.181.

Tian, Bin, and Joel H Graber. 2012. "Signals for Pre-mRNA Cleavage and Polyadenylation." *Wiley Interdisciplinary Reviews. RNA* 3 (3): 385–96. doi:10.1002/wrna.116.

Tilgner, H., D. G. Knowles, R. Johnson, C. A. Davis, S. Chakraborty, S. Djebali, J. Curado, M. Snyder, T. R. Gingeras, and R. Guigo. 2012. "Deep Sequencing of Subcellular RNA Fractions Shows Splicing to Be Predominantly Co-Transcriptional in the Human Genome but Inefficient for lncRNAs." *Genome Research* 22 (9). Cold Spring Harbor Laboratory Press: 1616–25. doi:10.1101/gr.134445.111.

Tudor, Corina, Francesco P. Marchese, Edward Hitti, Anna Aubareda, Lesley Rawlinson, Matthias Gaestel, Perry J. Blackshear, Andrew R. Clark, Jeremy Saklatvala, and Jonathan L.E. Dean. 2009. "The p38 MAPK Pathway Inhibits Tristetraprolin-Directed Decay of Interleukin-10 and pro-Inflammatory Mediator mRNAs in Murine Macrophages." *FEBS Letters* 583 (12): 1933–38. doi:10.1016/j.febslet.2009.04.039.

Utami Wahyu. 2015. "Ion Pairing LC-MS/MS Method for Analysis of Intracellular Phosphorylated Metabolites." PhD Thesis, University of Nottingham.

Vaňáčková, Štěpánka, Jeannette Wolf, Georges Martin, Diana Blank, Sabine Dettwiler, Arno Friedlein, Hanno Langen, Gérard Keith, and Walter Keller. 2005. "A New Yeast Poly(A) Polymerase Complex Involved in RNA Quality Control." Edited by

- Phillip Zamore. *PLoS Biology* 3 (6). Public Library of Science: e189.
doi:10.1371/journal.pbio.0030189.
- van der Kraan, P.M., and W.B. van den Berg. 2012. "Chondrocyte Hypertrophy and Osteoarthritis: Role in Initiation and Progression of Cartilage Degeneration?" *Osteoarthritis and Cartilage* 20 (3): 223–32. doi:10.1016/j.joca.2011.12.003.
- van Furth, R., and Zanvil A. Cohn. 1968. "THE ORIGIN AND KINETICS OF MONONUCLEAR PHAGOCYTES." *Journal of Experimental Medicine* 128 (3). Rockefeller University Press: 415–35. doi:10.1084/jem.128.3.415.
- Vassalli, J D, J Huarte, D Belin, P Gubler, A Vassalli, M L O'Connell, L A Parton, R J Rickles, and S Strickland. 1989. "Regulated Polyadenylation Controls mRNA Translation during Meiotic Maturation of Mouse Oocytes." *Genes & Development* 3 (12b). Cold Spring Harbor Laboratory Press: 2163–71. doi:10.1101/gad.3.12b.2163.
- Viguera, E., Danielle Canceill, S.Dusko Ehrlich, K. Baynton, RP. Fuchs, K. Bebenek, J. Abbotts, et al. 2001. "Replication Slippage Involves DNA Polymerase Pausing and Dissociation." *The EMBO Journal* 20 (10). EMBO Press: 2587–95. doi:10.1093/emboj/20.10.2587.
- Villalba, Ana, Olga Coll, and Fátima Gebauer. 2011. "Cytoplasmic Polyadenylation and Translational Control." *Current Opinion in Genetics & Development* 21 (4): 452–57. doi:10.1016/j.gde.2011.04.006.
- Vodnala, Suman K, Marcela Ferella, Hilda Lundén-Miguel, Evans Betha, Nick van Reet, Daniel Ndem Amin, Bo Oberg, et al. 2009. "Preclinical Assessment of the Treatment of Second-Stage African Trypanosomiasis with Cordycepin and Deoxycoformycin." *PLoS Neglected Tropical Diseases* 3 (8). Public Library of Science: e495. doi:10.1371/journal.pntd.0000495.
- Wajant, Harald, and Peter Scheurich. 2011. "TNFR1-Induced Activation of the Classical NF-κB Pathway." *The FEBS Journal* 278 (6): 862–76. doi:10.1111/j.1742-4658.2011.08015.x.
- Walsh, D. A., D. F. McWilliams, M. J. Turley, M. R. Dixon, R. E. Franses, P. I. Mapp, and D. Wilson. 2010. "Angiogenesis and Nerve Growth Factor at the Osteochondral Junction in Rheumatoid Arthritis and Osteoarthritis." *Rheumatology* 49 (10). Oxford University Press: 1852–61. doi:10.1093/rheumatology/keq188.
- Wang, Feng, Peipei Yin, Ye Lu, Zubin Zhou, Chaolai Jiang, Yingjie Liu, Xiaowei Yu, et al. 2015. "Cordycepin Prevents Oxidative Stress-Induced Inhibition of Osteogenesis." *Oncotarget* 6 (34). Impact Journals: 35496–508.
- Wang, H, O Bloom, M Zhang, J M Vishnubhakat, M Ombrellino, J Che, A Frazier, et al. 1999. "HMG-1 as a Late Mediator of Endotoxin Lethality in Mice." *Science (New York, N.Y.)* 285 (5425): 248–51. <http://www.ncbi.nlm.nih.gov/pubmed/10398600>.
- Wapinski, Orly, and Howard Y. Chang. 2011. "Long Noncoding RNAs and Human Disease." *Trends in Cell Biology* 21 (6): 354–61. doi:10.1016/j.tcb.2011.04.001.
- Weber, M., Curt H. Hagedorn, David G. Harrison, and Charles D. Searles. 2005. "Laminar Shear Stress and 3' Polyadenylation of eNOS mRNA." *Circulation*

- Research* 96 (11). Lippincott Williams & Wilkins: 1161–68.
doi:10.1161/01.RES.0000170651.72198.fa.
- Weill, Laure, Eulàlia Belloc, Felice-Alessio Bava, and Raúl Méndez. 2012. “Translational Control by Changes in poly(A) Tail Length: Recycling mRNAs.” *Nature Structural & Molecular Biology* 19 (6). Nature Research: 577–85.
doi:10.1038/nsmb.2311.
- Wenham, Claire Y J, and Philip G Conaghan. 2010. “The Role of Synovitis in Osteoarthritis.” *Therapeutic Advances in Musculoskeletal Disease* 2 (6). SAGE Publications: 349–59. doi:10.1177/1759720X10378373.
- West, Steven, Natalia Gromak, and Nick J. Proudfoot. 2004. “Human 5′ → 3′ Exonuclease Xrn2 Promotes Transcription Termination at Co-Transcriptional Cleavage Sites.” *Nature* 432 (7016). Nature Publishing Group: 522–25.
doi:10.1038/nature03035.
- West, Steven, and Nicholas J Proudfoot. 2008. “Human Pcf11 Enhances Degradation of RNA Polymerase II-Associated Nascent RNA and Transcriptional Termination.” *Nucleic Acids Research* 36 (3). Oxford University Press: 905–14.
doi:10.1093/nar/gkm1112.
- West, Steven, Nicholas J Proudfoot, and Michael J Dye. 2008. “Molecular Dissection of Mammalian RNA Polymerase II Transcriptional Termination.” *Molecular Cell* 29 (5): 600–610. doi:10.1016/j.molcel.2007.12.019.
- Whiteside, Simon T., and Alain Israël. 1997. “I κ B Proteins: Structure, Function and Regulation.” *Seminars in Cancer Biology* 8 (2). Academic Press: 75–82.
doi:10.1006/scbi.1997.0058.
- Wilson, William C, Hue-Tran Hornig-Do, Francesco Bruni, Jeong Ho Chang, Alexis A Jourdain, Jean-Claude Martinou, Maria Falkenberg, et al. 2014. “A Human Mitochondrial poly(A) Polymerase Mutation Reveals the Complexities of Post-Transcriptional Mitochondrial Gene Expression.” *Human Molecular Genetics* 23 (23). Oxford University Press: 6345–55. doi:10.1093/hmg/ddu352.
- Wilt, F H. 1973. “Polyadenylation of Maternal RNA of Sea Urchin Eggs after Fertilization.” *Proceedings of the National Academy of Sciences of the United States of America* 70 (8). National Academy of Sciences: 2345–49.
<http://www.ncbi.nlm.nih.gov/pubmed/4525169>.
- Winkler, Daniel. 2010. “CORDYCEPS SINENSIS.” *Field Mycology* 11 (2). Elsevier: 60–67. doi:10.1016/j.fldmyc.2010.04.009.
- Wong, Ying Ying, Alice Moon, Ruth Duffin, Adeline Barthet-Barateig, Hedda A Meijer, Michael J Clemens, and Cornelia H de Moor. 2010. “Cordycepin Inhibits Protein Synthesis and Cell Adhesion through Effects on Signal Transduction.” *The Journal of Biological Chemistry* 285 (4): 2610–21.
doi:10.1074/jbc.M109.071159.
- Woolf, C. J., A. Allchorne, B. Safieh-Garabedian, and S. Poole. 1997. “Cytokines, Nerve Growth Factor and Inflammatory Hyperalgesia: The Contribution of Tumour Necrosis Factor α .” *British Journal of Pharmacology* 121 (3). Blackwell Publishing Ltd: 417–24. doi:10.1038/sj.bjp.0701148.
- Wright, S D, R A Ramos, P S Tobias, R J Ulevitch, and J C Mathison. 1990. “CD14, a

Receptor for Complexes of Lipopolysaccharide (LPS) and LPS Binding Protein." *Science (New York, N.Y.)* 249 (4975). American Association for the Advancement of Science: 1431–33. doi:10.1126/science.1698311.

Wurfel, M M, and S D Wright. 1997. "Lipopolysaccharide-Binding Protein and Soluble CD14 Transfer Lipopolysaccharide to Phospholipid Bilayers: Preferential Interaction with Particular Classes of Lipid." *Journal of Immunology (Baltimore, Md. : 1950)* 158 (8). American Association of Immunologists: 3925–34. <http://www.ncbi.nlm.nih.gov/pubmed/9103463>.

Wyers, Françoise, Mathieu Rougemaille, Gwenaël Badis, Jean-Claude Rousselle, Marie-Elisabeth Dufour, Jocelyne Boulay, Béatrice Régnault, et al. 2005. "Cryptic Pol II Transcripts Are Degraded by a Nuclear Quality Control Pathway Involving a New poly(A) Polymerase." *Cell* 121 (5). Elsevier: 725–37. doi:10.1016/j.cell.2005.04.030.

Wynn, Thomas A., Ajay Chawla, and Jeffrey W. Pollard. 2013. "Macrophage Biology in Development, Homeostasis and Disease." *Nature* 496 (7446). Nature Research: 445–55. doi:10.1038/nature12034.

Xia, Zheng, Lawrence A. Donehower, Thomas A. Cooper, Joel R. Neilson, David A. Wheeler, Eric J. Wagner, Wei Li, et al. 2014. "Dynamic Analyses of Alternative Polyadenylation from RNA-Seq Reveal a 3'-UTR Landscape across Seven Tumour Types." *Nature Communications* 5 (November). Nature Publishing Group: 5274. doi:10.1038/ncomms6274.

Yamamoto, Masahiro, Soh Yamazaki, Satoshi Uematsu, Shintaro Sato, Hiroaki Hemmi, Katsuaki Hoshino, Tsuneyasu Kaisho, et al. 2004. "Regulation of Toll/IL-1-Receptor-Mediated Gene Expression by the Inducible Nuclear Protein I κ B ζ ." *Nature* 430 (6996). Nature Publishing Group: 218–22. doi:10.1038/nature02738.

Yang, Qin, Gregory M. Gilmartin, and Sylvie Doublé. 2011. "The Structure of Human Cleavage Factor I_m Hints at Functions beyond UGUA-Specific RNA Binding." *RNA Biology* 8 (5). Taylor & Francis: 748–53. doi:10.4161/rna.8.5.16040.

Yang, Xiaofeng, Yanxiang Li, Yanhao He, Tingting Li, Weirong Wang, Jiye Zhang, Jingyuan Wei, Yanhong Deng, and Rong Lin. 2015. "Cordycepin Alleviates Airway Hyperreactivity in a Murine Model of Asthma by Attenuating the Inflammatory Process." *International Immunopharmacology* 26 (2): 401–8. doi:10.1016/j.intimp.2015.04.017.

Ying, Xiaozhou, Lei Peng, Hua Chen, Yue Shen, Kehe Yu, and Shaowen Cheng. 2014. "Cordycepin Prevented IL- β -Induced Expression of Inflammatory Mediators in Human Osteoarthritis Chondrocytes." *International Orthopaedics* 38 (7). Springer Berlin Heidelberg: 1519–26. doi:10.1007/s00264-013-2219-4.

Zaragoza, Dean, Ataollah Ghavidel, Joseph Heitman, and Michael C. Schultz. 1998. "Rapamycin Induces the G0 Program of Transcriptional Repression in Yeast by Interfering with the TOR Signaling Pathway." *Molecular and Cellular Biology* 18 (8). American Society for Microbiology: 4463–70. doi:10.1128/MCB.18.8.4463.

Zarkower, D, P Stephenson, M Sheets, and M Wickens. 1986. "The AAUAAA Sequence Is Required Both for Cleavage and for Polyadenylation of Simian Virus 40 Pre-mRNA in Vitro." *Molecular and Cellular Biology* 6 (7): 2317–23. <http://www.pubmedcentral.nih.gov/articlerender.fcgi?artid=367784&tool=pm>

centrez&rendertype=abstract.

Zarkower, D, and M Wickens. 1987. "Formation of mRNA 3' Termini: Stability and Dissociation of a Complex Involving the AAUAAA Sequence." *The EMBO Journal* 6 (1): 177–86.

<http://www.pubmedcentral.nih.gov/articlerender.fcgi?artid=553374&tool=pmcentrez&rendertype=abstract>.

Zhang, F, and C N Cole. 1987. "Identification of a Complex Associated with Processing and Polyadenylation in Vitro of Herpes Simplex Virus Type 1 Thymidine Kinase Precursor RNA." *Molecular and Cellular Biology* 7 (9): 3277–86.

<http://www.pubmedcentral.nih.gov/articlerender.fcgi?artid=367965&tool=pmcentrez&rendertype=abstract>.

Zhao, J, L Hyman, and C Moore. 1999. "Formation of mRNA 3' Ends in Eukaryotes: Mechanism, Regulation, and Interrelationships with Other Steps in mRNA Synthesis." *Microbiology and Molecular Biology Reviews : MMBR* 63 (2).

American Society for Microbiology: 405–45.

<http://www.ncbi.nlm.nih.gov/pubmed/10357856>.

Zhong, Haihong, Helena SuYang, Hediye Erdjument-Bromage, Paul Tempst, and Sankar Ghosh. 1997. "The Transcriptional Activity of NF- κ B Is Regulated by the I κ B-Associated PKAc Subunit through a Cyclic AMP–Independent Mechanism." *Cell* 89 (3): 413–24. doi:10.1016/S0092-8674(00)80222-6.

Zhong, Haihong, Reinhard E Voll, Sankar Ghosh, M.L Avantaggiati, V Ogryzko, K Gardner, A Giordano, et al. 1998. "Phosphorylation of NF- κ B p65 by PKA Stimulates Transcriptional Activity by Promoting a Novel Bivalent Interaction with the Coactivator CBP/p300." *Molecular Cell* 1 (5). Elsevier: 661–71. doi:10.1016/S1097-2765(00)80066-0.